



UNIVERSITÀ  
DEGLI STUDI  
DI PADOVA

Sede Amministrativa: Università degli Studi di Padova  
Dipartimento di Fisica e Astronomia "Galileo Galilei"

---

CORSO DI DOTTORATO DI RICERCA IN PHYSICS  
CICLO XXXIV

## Scattering amplitudes calculation and intersection theory

Tesi redatta con il contributo finanziario dell'Istituto Nazionale di Fisica Nucleare (INFN)

**Coordinatore:** Ch.mo Prof. Franco Simonetto  
**Supervisore:** Ch.mo Prof. Pierpaolo Mastrolia

**Dottorando :** Luca Mattiazzi



# Abstract

In this thesis, we present new developments for the analytic calculation of multi-loop level amplitudes. Similarly, we study the underlying mathematical structure of such key objects for modern high energy physics research.

In this thesis we elaborate on the new and powerful tools provided by intersection theory. This mathematical tool sheds new light on the algebraic structure of Feynman integrals, paving a new way to perform multi-loop precision computation. Specifically, multi-loop scattering amplitudes for state of the art calculations are built upon a large number of scalar multi-loop integrals, whose reduction in terms of a smaller set of Master Integrals (MIs) can be a bottleneck in amplitudes computation. Such reduction is possible thanks to the Integration By Parts Identities (IBPs), which consist in linear relations among Feynman integrals generated by the vanishing of a total derivative under the integral sign. The reduction is usually achieved thanks to the Laporta algorithm by solving a huge system of such relations which, depending on the number of scales involved, can require very demanding algebraic manipulations. In a different approach, intersection theory allows us to embed Feynman integrals in a vector space, defining a scalar product between them: the intersection number. In this way, obtaining the coefficients that multiplies a MI in the reduction of a Feynman integral is equivalent to finding the decomposition of a vector in terms of its basis vector in a vector space. It consists of using simple linear algebra methods to project the multi-loop integrals directly on the MIs basis, bypassing the system-solving procedure otherwise required in the standard approach to multi-loop calculations. In the first part of the thesis, we describe the main features of the multi-loop calculations. We briefly overview the adaptive integrand decomposition (AID), a variant of the standard integrand reduction algorithm. AID exploits the decomposition of the space-time dimension in parallel and orthogonal subspaces. We then proceed to introduce IBPs and the Differential Equation method for the computation of master integrals, finally outlining the key steps that allowed the computation of the two-loop four-fermion scattering amplitude in QED, with one massive fermion.

We then elaborate on the properties of intersection theory and how to apply it in relation with Feynman Integrals.

After showing its successful application to a wide variety of Feynman integrals admitting a univariate integral representation, we present the implementation of a recursive algorithm for multivariate intersection number to extend this method to generic Feynman integrals. We also present alternative algorithms for the application of multivariate intersection number to Feynman integrals decomposition, showing the flexibility of this powerful tool, combining the advantages of the decomposition by intersection numbers with the subtraction algorithm traditionally used in methods of integrand decomposition. Aside from the reduction to MIs, we apply intersection theory for the derivation of contiguity relations and of differential equations for MIs, as first steps towards potential applications to generic multi-loop integrals.



# Publication list

This thesis is based on the author’s work conducted at the Department of Physics and Astronomy “Galileo Galilei” of the Padova University. Parts of this work have already appeared in the following publications:

## Journal papers

- [1] H. Frellesvig, F. Gasparotto, S. Laporta, M. K. Mandal, P. Mastrolia, L. Mattiazzi, and S. Mizera, *Decomposition of Feynman Integrals on the Maximal Cut by Intersection Numbers*, JHEP **05** (2019) 153, [arXiv:1901.11510]
- [2] H. Frellesvig, F. Gasparotto, M. K. Mandal, P. Mastrolia, L. Mattiazzi, and S. Mizera, *Vector Space of Feynman Integrals and Multivariate Intersection Numbers*, Phys. Rev. Lett. **123** (2019), no. 20 201602, [arXiv:1907.02000].
- [3] H. Frellesvig, F. Gasparotto, S. Laporta, M. K. Mandal, P. Mastrolia, L. Mattiazzi, and S. Mizera, *Decomposition of Feynman Integrals by Multivariate Intersection Numbers*, JHEP **03** (2021) 027, [arXiv:2008.04823].
- [4] R. Bonciani et al., *Two-Loop Four-Fermion Scattering Amplitude in QED*, Phys. Rev. Lett. **128** (2022), no. 2 022002, [arXiv:2106.13179]

## Conference proceedings

- [5] H. A. Frellesvig and L. Mattiazzi, *On the Application of Intersection Theory to Feynman Integrals: the univariate case*, PoS **MA2019** (2022) 017, [arXiv:2102.01576].
- [6] D. D. Canko, F. Gasparotto, L. Mattiazzi, C. G. Papadopoulos, and N. Syrrakos,  *$N^3LO$  calculations for  $2 \rightarrow 2$  processes using simplified differential equations*, SciPost Phys. Proc. **7** (2022) 028, [arXiv:2110.08110].
- [7] M. K. Mandal, L. Mattiazzi, J. Ronca, and W. J. Bobadilla Torres, *Analytic Evaluation of the NNLO virtual corrections to Muon–Electron scattering*, PoS (2022) in [8].



# Contents

<b>1 Introduction</b>	<b>9</b>
<b>2 Multiloop Feynman Integrals</b>	<b>15</b>
2.1 Definition	15
2.1.1 Baikov representation	16
2.1.2 Parallel and orthogonal space	20
2.2 Properties	22
2.2.1 IBPs	22
2.2.2 Differential and Difference Equations for Feynman Integrals	23
2.2.3 Differential Equations	23
2.2.4 Difference Equations	26
2.2.5 Initial Conditions	27
2.2.6 Numerical Integration	28
2.3 Adaptive integrand decomposition	28
2.3.1 Polynomial division	28
2.3.2 The Divide, Integrate, Divide algorithm	29
2.3.3 Example: muon-electron scattering	31
<b>3 Muon Electron scattering</b>	<b>35</b>
3.1 Introduction	35
3.1.1 The QED cross section	39
3.2 The Amplitude analytical evaluation	40
3.2.1 Renormalization	42
3.2.2 Results	47
3.2.3 Additional tests	48
<b>4 Intersection theory and Feynman integrals</b>	<b>51</b>
4.1 Introduction	51
4.1.1 Twisted Cohomology group	52
4.1.2 Twisted Homology group	53
4.1.3 Feynman Integrals and their duals	56
4.1.4 Dimension of twisted cohomology groups	56
4.2 Intersection Numbers and IBPs	58
4.2.1 Differential equation for forms and dual forms	59
4.2.2 Dimensional Recurrence Relation	60
4.2.3 Intersection number definition and its properties	61
4.3 Univariate intersection number	62
4.4 Univariate application of twisted intersection theory	64
4.4.1 Euler Beta Integrals	64
4.4.2 Gauss ${}_2F_1$ Hypergeometric Function	67
4.4.3 Two-Loop Pentabox	69

4.4.4	Multileg and Massive Cases	74
4.4.5	Arbitrary Loop Examples	77
4.5	Multivariate intersection number	88
4.5.1	2-variable intersection number	89
4.5.2	$n$ -variable intersection number	93
4.5.3	An explicit example in two variables	95
4.5.4	Intersection numbers of logarithmic forms	96
4.6	Feynman integrals decomposition	97
4.6.1	Straight decomposition	98
4.6.2	Bottom-up decomposition	99
4.6.3	Top-down decomposition	100
4.7	Multivariate examples	101
4.7.1	The one-loop massless box	101
4.8	Further Examples	106
<b>5</b>	<b>Conclusions</b>	<b>113</b>
<b>Appendices</b>		
<b>A</b>	<b>Infrared Structure</b>	<b>121</b>
<b>B</b>	<b>Intersection numbers for the multivariate example</b>	<b>123</b>



# Chapter 1

## Introduction

Scattering amplitudes are a key instrument in testing our understanding of the laws of nature, being one of the expressions of our theoretical model which is closest to the experimental measurements.

They represent the scattering among particles described within the Quantum Field Theory (QFT) framework, which embodies the principles of Quantum Mechanics and those of Special Relativity. Currently, the best model to describe the interactions among these quantum mechanical objects, or fields, is the Standard Model (SM). It details three out of the four fundamental forces of nature: the strong interaction described by the Quantum Chromodynamics (QCD) through the  $SU(3)_c$  symmetry group, and the weak and electromagnetic interaction of Quantum Electro-Dynamics (QED) based on the symmetry group  $U(1)_Y \times SU(2)_W$ . The latter electro-weak symmetry group is expected to be broken spontaneously via the Brout-Englert-Higgs mechanism that predicts the existence of the Higgs particle.

Its detection at CMS and ATLAS at the Large Hadron Collider (LHC) [9,10], marked the final validation of the SM of particles as the model that describes the fundamental interactions, aside gravity.

Although its great successes, the SM fails to explain many known phenomenon, as the dark matter, the dark energy, or the mass of neutrinos. For this reasons, it is believed that there should be a bigger theory that contains the SM and accommodates a description for said effects. Hence new directions to investigate physics beyond the Standard Model (BSM) have been considered. Evidences for this new physics may arise from the production of a new heavy particle, or a slight deviation of the measures from the expected SM parameters. Thus increasing the precision with which the physical observables are measured, together with the precision of their theoretical expectation values, is an interesting path to follow in order to achieve a better understanding of nature.

Among the quantities that could be measured at modern colliders, the anomalous magnetic dipole moment of the muon ( $a_\mu$ ), exhibits a tension between its theoretical expectation value [11] and its measured one [12] which could signal the presence of yet to be discovered BSM effects. This possibility is further motivated by the fact that  $a_\mu$  appear to be more sensible to beyond the standard model effects than the electric anomalous magnetic dipole moment  $a_e$ , due to the higher mass of the muon.

The existence of such tension thus requires deeper investigation for this physical observable, both experimentally and theoretically. The uncertainties for the latter are dominated by the contribution involving hadronic interactions ( $a_\mu^{HAD}$ ), due to the nature of the strong force for which perturbative theory alone is not enough to obtain sensible estimates in this case.

The MUonE proposal [13,14] aims to lower the uncertainty of the leading contribution to  $a_\mu^{HAD}$  by extracting it from the measurements of the cross section of the  $\mu e \rightarrow \mu e$  scattering. In this thesis we discuss the precise evaluation of the QED next to next to leading order (NNLO) scattering amplitude required in order to achieve the precision expected from MUonE, which is

the first fully analytic evaluation of the two-loop amplitude for the scattering of a mass-less into a massive pair of fermions in Quantum Electrodynamics.

Scattering amplitudes can be expressed in terms of Feynman integrals. Furthermore, when the theory grants it, they can be arranged in a perturbative expansions in the coupling constant, allowing us to compute it up to the desired accuracy. On the other hand this implies that in order to enhance the precision of a known theoretical estimate, we need to compute terms further down in the expansion, which are characterised by exponentially more Feynman integrals that become harder to compute the further the term is in the expansion. Integrals appearing at higher order, are characterized by Feynman graphs with higher number of loops.

These difficulties that arise from seeking higher accuracy in the value of the scattering amplitudes require to systematize the computation of such quantities. This is achieved in three steps: first the amplitudes is reduced to a combination of scalar (Lorentz invariant) integrals, then it is expressed in terms of a minimal basis of independent functions which finally are evaluated.

The decomposition of a one-loop amplitude in terms of a basis of scalar integrals was first demonstrated by Passarino and Veltman [15]. This, together with *generalized unitarity* techniques that allowed to directly obtain the coefficients in front of the basis integral, triggered the development of the *integrand decomposition method*, firstly defined in four dimensions [16, 17] and later extended to accomodate the effects of dimensional regularization [18–21]. Its efficient numerical implementation [22–24] and its insertion in automated frameworks for one-loop computations [25–34] was of fundamental importance for the so called *NLO revolution*, that brought a great number of next to leading order predictions for a series of processes of phenomenological interest for LHC. Within this method, the integrand in consideration was reduced to a combination of integrand that contains at denominator, a subset of the denominators of the initial set of propagators, and as numerators the remainders of the corresponding divisions. After the integrand decomposition, the integral sign is recovered, introducing spurious terms which vanish upon integration. At one loop these terms were taken care of by the lorentz invariance, without representing any real issue.

This approach was later studied beyond one loop [35, 36] and formalized by means of algebraic geometry methods as a multivariate polynomial division modulo Gröbner bases [37, 38].

The jump in difficulty of the computation going from one to two loop due to the introduction of *irreducible scalar products* which cannot be expressed in terms of denominators, the fact that it was non trivial to detect spurious terms, and additionally that the results from the integrand reduction were not independent but needed further integral-level reduction to get to a minimal basis, prevented the integrand decomposition method to be as effective as it was in the one loop case.

Nonetheless these techniques were embedded in the *adaptive integrand decomposition method* [39–42]. Here the loop momenta are split between their component parallel to the external momenta, and orthogonal to them, so this method systematically *adapts* to the integrand in consideration. This makes apparent the polynomial dependence of the integral with respect to the transverse components which can then be integrated out by expressing them in terms of Gegenbauer polynomials allowing us to take care of the integration by applying iteratively the orthogonality conditions proper of these polynomials. This integration has also the advantage of removing eventual spurious term that could arise after the integrand decomposition.

The polynomial division, together with the systematic integration over the transverse variables, yields a new reduction procedure called the *divide-integrate-divide* algorithm, which has an outcome free of spurious terms and contains integrals whose integrand is expressed in terms of scalar products between loop and external momenta. Hence, through this powerful tool is possible to express the Feynman integrals appearing in the multi-loop amplitude in consideration as a combination of scalar integral, achieving the first step in our framework for multi-loop scattering amplitude evaluation.

The second step requires an integral-level reduction, where our amplitude is expressed in term of a *minimal* basis of Master Integrals (MIs). This is achieved by the *integration-by-parts* (IBP) decomposition described in the Laporta’s algorithm [43]. Exploiting the fact that the total derivative of a Feynman integral in dimensional regularization vanishes, it is possible to draw a system of equation among them, which can then be solved in order to express our scattering amplitude in terms of a set of independent functions called MI.

The last step left is the evaluation of the MI. Considering them as analytical function of the external kinematics, it is possible to build a coupled differential equation system by means of IBPs. The integral is then evaluated by solving the differential equations (DeQ) rather than integrating it. This procedure was firstly proposed by Kotikov [44] for internal masses and later extended by Remiddi [45] and Gehrmann and Remiddi [46] to external invariants (see [47] for a review on the topic).

Nevertheless, in physical cases we are interested in the value of Feynman integrals around 4 dimension, hence Laurent expanded in the parameter  $\epsilon = (d - 4)/2$ . When possible, it is convenient then to pick a MI basis in such a way that the  $\epsilon$  dependence in the system of differential equation is factorised from the kinematical ones, and the latter can be expressed as the differential of a logarithm. This approach was firstly proposed by [48], allowing to easily solve the system order by order in  $\epsilon$  expressing the Feynman integrals as *generalised polylogarithm* [49] making the evaluation of the integral completely algorithmic. Alternatively, it is possible to choose a basis of master integrals such that the system of differential equations is at most linear in  $\epsilon$ . In this case, by means of the Magnus method [50] one can evaluate the similarity transformation that puts the system into canonical form.

In this thesis, we apply this complete framework for multiloop scattering amplitude computation to the case of the 2–loops QED amplitude for the process  $\mu e \rightarrow \mu e$  [4], which is crucial for the MUonE experiment. In this specific case, although analytical expressions of the MI are already available [51,52], the generation of the amplitude, its reduction to a minimal basis and their use within the structure previously mentioned were still missing. In this thesis, we discuss these steps carried out via an in house code, together with the mixed renormalization scheme required by this multi-loop amplitudes (partly on-shell, partly  $\overline{\text{MS}}$ ). We also outline the numerical checks needed for a computation of this complexity.

The results of this endeavor, other than being useful for the evaluation of observables directly related to the process considered, are helpful also in processes characterized by initial and final particles kinematically similar to the one considered here, such as the heavy-quark pair production through light-quark annihilation process in QCD [53].

Even in light of the general framework aforementioned, state of the art computations represent a formidable challenge to complete. In particular, the solution to the system of IBPs in multi-loop multi-particles case turns out to be quite challenging. This has motivated multiple refinements of the system solving strategies [54–67].

Recently, the problem of the reduction of Feynman integrals to a minimal basis has been studied under a new perspective firstly proposed in [68]. Considering Feynman integrals in parametric representations such as the Baikov representation, which exposes their nature as Aomoto-Gel’fand integrals, enables a novel approach to the investigation of their algebraic structure by means of intersection theory of twisted de Rham (co)homology for general hypergeometric functions [69–80]. This allows us to define the *twisted intersection number* between forms (which represent Feynman integrals), that acts as a scalar product in a vector space characterized by multivalued integrals. We can then project multiloop integrals into MI basis in the same way in which vectors are decomposed into a basis of the vector space, providing an alternative to the system solution required by the standard IBP approach. While integrals were connected by identities derived from the vanishing of a total derivative within the standard IBP method, in this new approach we exploit the quotient group structure proper of the cohomology

group which identifies integrals that differ by a vanishing piece that could be written as a total derivative.

This connection between mathematics and physics, entails a deeper study of this topic in relation to Feynman integrals, never before considered together, as well as the development of an efficient algorithm for the computation of intersection numbers relevant for multi-loop amplitudes and its implementation in an automatic software.

As a first result, this novel point of view reveals a correspondence between the number of MI and the topological properties of the integration domain, giving us the ability to know the number of independent functions that characterize our problem a priori.

The application of this method, together with generalized unitarity, allows to study firstly multi-loop integral decomposition by means of twisted intersection theory in the univariate case [1,68], addressing the decomposition of integrals on the maximal cut. In this thesis, we apply this framework in multiple relevant cases, providing example of differential equation computation on top of regular multi-loop integral reduction on the MI basis for high number of loop and high multiplicity cases. We also studied multiple basis choice and how these affects the computation. In order to achieve the complete decomposition of a multivalued integral into its integral basis, we extended this approach to the multivariate case [2,3], exploiting the iterative application of univariate intersection, performing computation in the general case with an arbitrary number of variables [81]. In particular, in this work, by the joint use of *integrand decomposition*, *generalized unitarity* and twisted intersection theory, multiple algorithms for Feynman integrals reduction are proposed: the *top-down*, *bottom-up* and straight decomposition. We also provide examples in which these methods are applied successfully by means of an in-house code we developed, paving the way to a new strategy for integral reduction and differential equations computation for Feynman integrals.

This thesis is organised as follows. In chapter 2 we will review modern method for the computation of multi-loop Feynman amplitudes. Firstly we introduce parametric representation of Feynman integrals such as the Baikov representation, discussing its main properties, from its derivation to the expression of its boundary. We will also address integrals in parallel and orthogonal space  $d = d_{\perp} + d_{\parallel}$ . Then we will present the main tool for multiloop integral computation: from IBPs, to possible techniques for the evaluation of Feynman integrals, discussing the properties of difference and differential equations, the canonical basis and the generalised polylogarithm. Lastly, we will address the adaptive integrand decomposition, describing the polynomial division, the integration of the transverse component and the divide-integrate-divide algorithm, briefly showcasing the outcome of its application to a one loop case.

In chapter 3 we discuss the application of the framework outlined in chapter 2 to the case of the two-loop QED amplitude for the process  $\mu e \rightarrow \mu e$ . After introducing the motivation behind this computation, briefly discussing the muon anomalous dipol magnetic moment and the MUonE proposal, we will outline the key step of the computation. From the evaluation of the bare amplitude by means of adaptive integrand decomposition, IBPs and differential equations, to the renormalization procedure. Finally, we present the result of the computation in a specific phase space point.

In chapter 4 we discuss the application of intersection theory to Feynman integrals. Firstly, we will motivate its introduction and the basic objects that characterizes it. Then, after introducing a novel algorithm for Feynman integral decomposition by means of intersection number, we will proceed to outline the algorithm behind the computation of such objects. Firstly we will address the univariate case, starting from simple special function cases such as the Beta function and the Hypergeometric function, arriving to apply this powerful tool to multi loop and multi particles Feynman integrals. Afterwards, we discuss the extension of the algorithm for the computation of intersection number to the multivariate case, presenting different ways of performing the decomposition and applying them to Feynman integrals. Finally, chapter 5

contains our conclusions.



## Chapter 2

# Multiloop Feynman Integrals

Feynman integrals are ubiquitous in precision computation for high-energy physics. Given their crucial role, let us outline their definition and properties.

### 2.1 Definition

Let us start by introducing them in dimensional regularization, hence writing them in their  $d$ -dimensional generalization. We will discuss their properties in finite dimensions later on in this work.

We define a  $l$ -loop Feynman integral with  $n$  external legs and  $t$  internal propagators as integrals over the momentum space

$$I_{x_1, \dots, x_t}^{[d](l, n)}[\mathcal{N}] = \int \prod_{i=1}^l \frac{d^d q_i}{(2\pi)^d} \frac{\mathcal{N}(q_j)}{D_1^{x_1} \dots D_t^{x_t}} \quad (2.1)$$

with  $\mathcal{N}(q_j)$  a generic tensor numerator that may depend on the loop momenta, while the denominators  $D_i$  are

$$D_i = l_i^2 + m_i^2 \quad (2.2)$$

where

$$l_i^\alpha = \sum_j \alpha_{ij} q_j^\alpha + \sum_j \beta_{ij} p_j^\alpha \quad (2.3)$$

with  $p_j^\alpha$  being the external momenta that satisfies momentum conservation

$$p_1 + p_2 + \dots + p_{n-1} + p_n = 0 \quad (2.4)$$

while  $\alpha$  and  $\beta$  are matrices which entries take values in  $(0, \pm 1)$ . From now on, the normalization factor of  $(2\pi)^D$  will be omitted.

It is possible to further simplify the integrand of our Feynman integral, writing it as a Lorentz-invariant function of the scalar products between the momenta appearing in the integral. This is achieved through tensor reduction or integrand decomposition by breaking up the numerator into fundamental objects called Irreducible Scalar Products (ISP). In this way, we can express the integral in eq. (2.1) in the form

$$I_{x_1, \dots, x_s}^{[d]} = \int \prod_{i=1}^l d^d q_i \frac{1}{D_1^{x_1} \dots D_s^{x_s}} \quad (2.5)$$

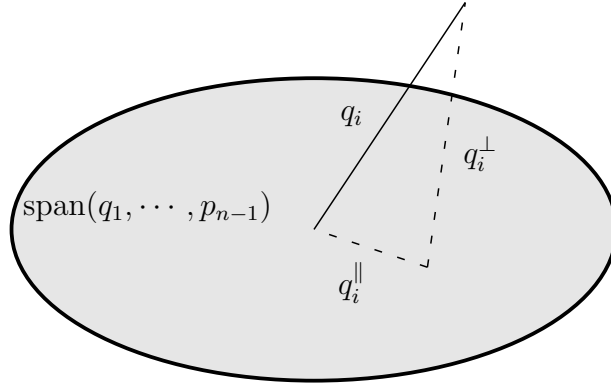
where we treated the ISPs as denominators with negative power  $x_i$ , making  $s$  the total number of internal lines plus the number of Irreducible Scalar Products.

### 2.1.1 Baikov representation

In equation (2.5) we have presented Feynman integrals in momentum space representation. Through suitable change of variables, it is possible to alter their appearance in order to take advantages of properties made apparent by the new choice of variables. We will be particularly interested in the so called *Baikov* representation [82,83], which allows to study the topological structure of Feynman integrals as Aomoto Gel'Fand integrals [68]. In this representation, rather than integrating over the loop momenta, the integration spans over the scalar products containing  $q_i$ . Defining  $l$  as the number of loops and  $n$  as the number of external legs, with  $n-1$  independent momenta, we label  $m = l + n - 1$  as the total number of independent momenta. Then, it is possible to cast the integration measure in the following form:

$$d^d q_1 \cdots d^d q_l = d^{m-1} q_{i\parallel} d^{d-m+1} q_{i\perp} \cdots d^{m-l} q_{l\parallel} d^{d-m+l} q_{l\perp}, \quad (2.6)$$

where  $q_{i\parallel}$  lies in the space spanned by  $\{q_{i+1} \dots q_l, p_1 \dots p_{n-1}\}$ , while  $q_{i\perp}$  lies in the orthogonal space. To better explain this factorization of the integration measure, it is represented in the figure below.



Introducing  $k = (q_1 \dots q_l, p_1 \dots p_{n-1})$ , where for  $i \leq l$  we have  $k_i = q_i$ , while for  $i > l$ , we have  $k_i = p_{i-l}$  we can define

$$G(q_1, \dots, q_l, p_1, \dots, p_{n-1}) = \det(k_i \cdot k_j) = \det(s_{ij}), \quad (2.7)$$

which is the determinant of the Gram matrix  $\mathbf{G}(q_1, \dots, q_l, p_1, \dots, p_{n-1})$ , the matrix that takes as entries the scalar product between all the momenta appearing in the amplitude:

$$\mathbf{G} = \begin{pmatrix} s_{11} & \cdots & s_{1m} \\ \vdots & \ddots & \vdots \\ s_{m1} & \cdots & s_{mm} \end{pmatrix}. \quad (2.8)$$

The Gram determinant could be interpreted as a volume in the momentum space, since  $G^{1/2}$  corresponds to the volume of the parallelotope spanned by the vectors  $q_1, \dots, q_l, p_1, \dots, p_{n-1}$ . Then, by geometric considerations, the volume elements  $d^{m-i} q_{i\parallel}$  are

$$d^{m-i} q_{i\parallel} = \frac{ds_{i,i+1} ds_{i,i+2} \cdots ds_{i,m}}{G^{1/2}(q_i, q_{i+1}, \dots, q_l, p_1, \dots, p_{n-1})}, \quad (2.9)$$

in which Gram determinants appear at the denominator; hence, they correspond to the volumes of the parallelogram formed by the momenta  $(q_i, q_{i+1}, \dots, q_l, p_1, \dots, p_{n-1})$ .

In the case of the orthogonal components of the measure, we have

$$d^{d-m+i} q_{i\perp} = \Omega_{d-m+i-1} |q_{i\perp}|^{d-m+i-1} d|q_{i\perp}| = \frac{1}{2} \Omega_{d-r+i-1} (|q_{i\perp}|)^{d-m+i-2} dq_{i\perp}^2, \quad (2.10)$$



where  $|q_{i\perp}|$  is the height of the parallelogram with the base formed by  $q_i, q_{i+1}, \dots, q_l, p_1, \dots, p_{n-1}$ , while  $\Omega_d$  is the  $d$ -dimensional solid angle. If we reinterpret  $|q_{i\perp}|$  as the volume of the whole parallelogram divided by the area of its base, and we replace  $dq_{i\perp}^2$  with  $ds_{ii}$ , we arrive at

$$d^{d-m+i}q_{i\perp} = \frac{1}{2}\Omega_{d-m+i-1} \left( \frac{G(q_i+1, q_{i+2}, \dots, q_l, p_1, \dots, p_{n-1})}{G(q_{i+1}, q_{i+2}, \dots, q_l, p_1, \dots, p_{n-1})} \right)^{\frac{d-m+i-2}{2}} ds_{ii}. \quad (2.11)$$

After all these considerations, putting everything back together yields

$$\int_{\mathcal{C}} \prod_1^l \frac{d^d q_i}{(2\pi)^d} \frac{1}{D_1^{x_1} \dots D_r^{x_r}} = \frac{1}{(2\pi)^d} \frac{\pi^{dl/2-l(l-1)/4-l(n-1)/2}}{\prod_{i=1}^l \Gamma(\frac{d-m+i}{2})} G(p_1, \dots, p_{n-1})^{\frac{-d+n}{2}} \int_{\mathcal{C}} \prod_{i=1}^l \prod_{j>i}^r ds_{ij} B^{\frac{d-m-1}{2}} \frac{1}{D_1^{x_1} \dots D_r^{x_r}}, \quad (2.12)$$

with  $\mathcal{C}$  being the region of integration, while  $B = G(q_1, q_2, \dots, q_l, p_1, \dots, p_{n-1})$ .  $\mathcal{C}$  can be rather complicate, nevertheless as proven in [84] its boundaries are determined by the brunch cat of the integrand. Considering that the integrand contains the Gram determinant raised to a non integer power, this condition can be translated to the vanishing of the Gram determinant on  $\partial\mathcal{C}$ .

### Integration Boundaries

Let us analyze how to derive the explicit boundaries of integration for this representation of Feynman integrals. We will start by fixing all the boundaries of  $s_{ii}$  by their positivity condition, and then we fix the boundaries of  $s_{ij}$  with  $i \neq j$  by  $G(q, \dots, p_{n-1}) \geq 0$ . Considering the remaining scalar products, we can set greater and greater minors of the Gram determinant to 0 until we impose this condition on the Gram determinant built with all the momenta appearing in the amplitude, in order to determine the boundaries for the last scalar product. In this way, one can determine the whole integration domain. This idea leads to the following expression, with the integration domain written explicitly:

$$\int_{\mathcal{C}} \prod_1^l \frac{d^d q_i}{(2\pi)^d} \frac{1}{D_1^{x_1} \dots D_r^{x_r}} = K \int_0^{+\infty} ds_{11} \dots \int_0^{+\infty} ds_{ll} \int_{G(q_1, p_1) \geq 0} ds_{1, l+1} \dots \int_{G(q_1, p_1, \dots, p_{n-1}) \geq 0} ds_{1m} \dots \int_{G(q_l, p_1, \dots, p_{n-1}) \geq 0} ds_{lm} \int_{G(q_1, q_2, p_1, \dots, p_{n-1}) \geq 0} ds_{12} \dots \int_{G(q_1, q_l, p_1, \dots, p_{n-1}) \geq 0} ds_{1l} \int_{G(q_1, q_2, q_3, \dots, p_{n-1}) \geq 0} ds_{23} \dots \int_{G(q_1, \dots, q_l, p_1, \dots, p_{n-1}) \geq 0} ds_{l-1, l} \frac{B^{\frac{d-m-1}{2}}}{D_1^{x_1} \dots D_r^{x_r}}. \quad (2.13)$$

where we have labelled the prefactor appearing in eq. (2.12)  $K$ . Alternatively we can write it as a multiplication of productoria,

$$\int_{\mathcal{C}} \prod_1^l \frac{d^d q_i}{(2\pi)^d} \frac{1}{D_1^{x_1} \dots D_r^{x_r}} = K \prod_{i=1}^l \left[ \int_0^{+\infty} ds_{ii} \right] \prod_{i=1}^l \prod_{j=1}^{n-1} \left[ \int_{G(q_i, p_1, \dots, p_j) \geq 0} ds_{i, l+j} \right] \prod_{i=1}^{l-1} \prod_{j=i+1}^l \left[ \int_{G(q_1, \dots, q_i, q_j, p_1, \dots, p_{n-1}) \geq 0} ds_{ij} \right] \frac{B^{\frac{d-m-1}{2}}}{D_1^{x_1} \dots D_r^{x_r}}. \quad (2.14)$$

The advantage of using this formula is that the 0 of a generic Gram determinant is known. In fact, using Laplace's formula to expand the determinant, one finds

$$G(q_1, q_2, \dots, q_L, p_1, \dots, p_E) = (s_{ij})^2 a + s_{ij} b_{ij} + c_{ij}, \quad (2.15)$$

with

$$\begin{aligned} a_{ij} &= \frac{1}{2} \frac{\partial^2 G}{\partial s_{ij}^2}, \\ b_{ij} &= \left. \frac{\partial G}{\partial s_{ij}} \right|_{s_{ij}=0}, \\ c_{ij} &= G|_{s_{ij}=0}. \end{aligned} \quad (2.16)$$

Hence to evaluate explicitly the integration boundaries, one needs to solve a second-order equation, obtaining

$$G = 0 \Rightarrow s_{ij} = \frac{b_{ij} \pm \sqrt{G_i^i G_j^j}}{G_{ij}^{ij}}, \quad (2.17)$$

with

$$G_i^j = \det \begin{pmatrix} s_{11} & \cdots & s_{1,j-1} & s_{1,j+1} & \cdots & s_{1M} \\ \vdots & \ddots & \vdots & \vdots & & \vdots \\ s_{i-1,1} & \cdots & s_{i-1,j-1} & s_{i-1,j+1} & \cdots & s_{i-1,M} \\ s_{i+1,1} & \cdots & s_{i+1,j-1} & s_{i+1,j+1} & \cdots & s_{i+1,M} \\ \vdots & & \vdots & \vdots & \ddots & \vdots \\ s_{M1} & \cdots & s_{M,j-1} & s_{M,j+1} & \cdots & s_{MM} \end{pmatrix}, \quad (2.18)$$

the determinant of the Gram matrix without the  $i$ -th row and  $j$ -th column, while

$$b_{ij} = (-1)^{i+j} 2 \det \left[ G_i^j \right] \Big|_{s_{ij}=0}. \quad (2.19)$$

Further details on the derivation of this result can be found in [\[85\]](#)

### Denominators as variables

Thanks to the auxiliary numerators defined in [\(2.5\)](#), multi-loop integrals have the same number of denominators and of scalar products. Moreover, naming the formers as  $z_a$ , there exists a linear transformation  $A_a^{ij}$  such that we can write

$$z_a = \sum_{i=1}^l \sum_{j=i}^m A_a^{ij} s_{ij} + m_a^2, \quad (2.20)$$

where the mass has a positive sign in front of it due to the Euclidean prescription, otherwise the sign would be the opposite. At one-loop,  $A_a^{ij}$  is always invertible, since the number of scalar products and denominators are equal, while at higher loop this is not granted because we can have irreducible scalar products. In that case, we introduce new variables  $z_a$ , or new denominators that depend on ISPs, and write them with a positive exponent.

This allows to define an  $A_a^{ij}$  which is always invertible (considering  $ij$  as a single index spanning from 1 to  $r$ , as does the index  $a$ ). Hence, we can write:

$$s_{ij} = \sum_{a=1}^r A_{ij}^a (z_a - m_a^2). \quad (2.21)$$

Given the above relation, we can perform a change of variables integrating now over the denominators  $z_a$  instead of the scalar products.

Applying this change of variables to eq. (2.12) yields

$$I = \frac{\pi^{Dl/2-l(l-1)/4-l(n-1)/2}}{(2\pi)^d \prod_{i=1}^l \Gamma(\frac{D-m+i}{2})} G(p_1, \dots, p_{n-1})^{-\frac{D+n}{2}} \det A_{ij}^a \int \frac{\prod_{a=1}^N dz_a}{z_1^{\alpha_1} \dots z_r^{\alpha_r}} B(\mathbf{z})^{\frac{D-m-1}{2}}, \quad (2.22)$$

where the couple (ij) in  $\det A_{ij}^a$  is considered as a single index and  $B(z_1 - m_1^2, \dots, z_r - m_r^2)$  is the Gram determinant written as a function of the denominators, also labeled *Baikov Polynomial*. In general, we will refer to integrals in parametric representation as [1, 3, 68]

$$I = K \int u \varphi \quad (2.23)$$

where

$$u = B^\gamma, \quad \gamma \equiv \frac{d-m-1}{2} \quad (2.24)$$

and

$$\varphi \equiv \hat{\varphi} d^r \mathbf{z}, \quad \hat{\varphi} \equiv \frac{f(\mathbf{z})}{z_1^{a_1} z_2^{a_2} \dots z_r^{a_r}}, \quad d^r \mathbf{z} \equiv dz_1 \wedge dz_2 \wedge \dots \wedge dz_r, \quad (2.25)$$

in order to ease the notation. In this form,  $u$  represents the multivalued component of the integrands encoded in  $B^\gamma$ ,  $\varphi$  contains the measure of integration and the denominators raised to their respective powers,  $f$  is a rational function of the  $z_i$ , and  $K$  is a constant pre-factor (independent of the integration variables), which may depend on the external kinematic invariants and on the dimensional regulator  $d$ , as one can observe from eq. (2.22). Let us stress that we will omit the prefactor  $K$  when it doesn't play any role in the computation considered.

### Loop-by-Loop Baikov representation

An alternative version of this representation considers a more efficient approach in order to minimize the number of integration variables that we are left with in the final integral. Indeed there could be integration variables that appear only in  $B(\mathbf{z})$  and not in our integral. In such cases we would like to find an automatic way to have the least possible amount of them, integrating out as many as possible of such variables.

To achieve this, the loop-by-loop Baikov representation [86] applies the variable changes outlined in eq. (2.6) one-loop momentum at a time, instead of changing the integration variables all together. This leads to an integral characterized by multiple Baikov polynomial

$$I = K \int \prod_i B_i^{\gamma_i} \varphi, \quad (2.26)$$

where the prefactor  $K$ , the Baikov polynomial and its exponents  $\gamma_i$  heavily depends on the order with which the loop-by-loop parametrization has been applied. In this way we are left with an integral which in most cases has a smaller (and never larger) number of variables than the parametrization in eq. (2.22).

### Cuts in Baikov representation

Within the Baikov representation, the *generalized cut* conditions in which propagators are set on-shell ( $D_i = 0$ ) are most naturally expressed as a contour integration. Any multiple  $n$ -cut integral, with  $D_1 = D_2 = \dots = D_n = 0$ , becomes

$$I_{a_1, a_2, \dots, a_N} \Big|_{n\text{-cut}} \equiv K \int_{\mathcal{C}_{n\text{-cut}}} u \varphi \quad (2.27)$$

where the deformed contour is defined as

$$\mathcal{C}_{n\text{-cut}} = \mathcal{O}_1 \wedge \mathcal{O}_2 \wedge \dots \wedge \mathcal{O}_n \wedge \mathcal{C}' \quad (2.28)$$

with the  $\mathcal{O}_i$ -contours denoting a small loop in the complex plane around the pole at  $z_i = 0$ . The integration domain of the cut-integral is given accordingly by the geometric intersection of  $\mathcal{C}$  with the planes  $z_i = 0$ , ( $i = 1, 2, \dots, n$ ) defining the on-shell conditions,

$$\mathcal{C}' \equiv \bigcap_{i=1}^n \{z_i = 0\} \cap \mathcal{C}. \quad (2.29)$$

After integrating over the cut variables, the remaining integral becomes

$$I_{a_1, a_2, \dots, a_r} \Big|_{n\text{-cut}} = K' \int_{\mathcal{C}'} u' \varphi' , \quad (2.30)$$

with

$$K' u' = (K u) \Big|_{z_1 = \dots = z_n = 0} , \quad \varphi' \equiv \hat{\varphi}' d^{r-n} \mathbf{z}' , \quad (2.31)$$

$$\hat{\varphi}' \equiv \frac{f(z_{n+1}, \dots, z_r)}{z_{n+1}^{a_{n+1}} \dots z_r^{a_r}} \left( \frac{\mathcal{D}_n(u)}{u} \right) \Big|_{z_1 = \dots = z_n = 0} , \quad (2.32)$$

$$\mathcal{D}_n \equiv \prod_{i=1}^n \frac{\partial_{z_i}^{(a_i-1)}}{(a_i-1)!} , \quad (2.33)$$

$$d^{r-n} \mathbf{z}' \equiv dz_{n+1} \wedge \dots \wedge dz_r , \quad (2.34)$$

with  $u'$  that vanishes on the boundary  $\mathcal{C}'$ , and  $f$  is a rational function (see eqs. (2.25)).

**Notation.** In the following thesis, for ease of notation, when considering integral on the cut we drop the prime symbol  $'$ , in favor of using directly  $K$ ,  $u$ ,  $\varphi$  and  $z$  to express the various quantities on the cut. Moreover, when integrals on the maximal cut are characterized by a single ISP, we use the notation  $I_{a_1, a_2, \dots, a_r} \Big|_{n\text{-cut}} \equiv I_{a_1, \dots, a_r; a_{n+1}}$ , where  $a_{n+1}$  is the power of the remaining irreducible scalar product.

### 2.1.2 Parallel and orthogonal space

As outlined in Section (2.1.1), the Baikov representation is very versatile and allows for a simple implementation of the generalized cut approach. Let us consider it in the case in which the loop momenta is split in two components, one parallel to physical four dimensions, and the other orthogonal to it.

The loop momenta in this case becomes

$$q_i^\alpha = q_{[4]i}^\alpha + \mu_i^\alpha \quad q_i \cdot q_j = q_{[4]i} \cdot q_{[4]j} + \mu_{ij} \quad (\mu_{ij} = \mu_i \cdot \mu_j) . \quad (2.35)$$

Substituting such decomposition into the expression of multiloop denominators (2.2), one obtains

$$D_i = l^2 + m_i^2 = l_{[4]i}^2 + \sum_{j,k} \alpha_{ij} \alpha_{ik} \mu_{jk} + m_i^2 , \quad (2.36)$$

where

$$l_{[4]i}^\alpha = \sum_j \alpha_{ij} q_{[4]j}^\alpha + \sum_j \beta_{ij} p_j^\alpha . \quad (2.37)$$

With this choice of parameterization for the loop momenta, both the numerator and the denominators will depend on the scalar products  $\mu_{ij}$  and the components of  $q_{[4]i}$  with respect to

a four-dimensional basis of vectors  $\{e_i^\alpha\}$ , such that  $q_{[4]i}^\alpha = \sum_j x_{ij} e_j^\alpha$ . It is then possible to apply the Baikov parameterization seen in Section 2.1.1 to the extra dimensional component of the integration measure, writing a generic multiloop integral as

$$I^{[d](\ell,n)}[\mathcal{N}] = \Omega_d^{(\ell)} \int \prod_{i=1}^{\ell} d^4 q_{[4]i} \int \prod_{1 \leq i \leq j \leq \ell} d\mu_{ij} G(\mu_{ij})^{\frac{d-5-\ell}{2}} \frac{\mathcal{N}(q_{[4]i}, \mu_{ij})}{\prod_j D_j(q_{[4]i}, \mu_{ij})}, \quad (2.38)$$

with  $G(\mu_{ij})$  the Gram determinant as defined in (2.7), hence  $G(\mu_{ij}) = \det(\mu_i \cdot \mu_j)$ . The prefactor  $\Omega_d^{(\ell)}$  is the result of the angular integration over the angular directions.

In the same sense, it is always possible to split the loop momenta into orthogonal components, choosing the directions that one prefers to perform the splitting. Let us discuss a more convenient choice of directions for this procedure. Consider splitting the loop variables along the space parallel to the external momenta and the space orthogonal to them. This parameterization in the case of  $n \geq 5$  external leg coincides with the previous case, while in the other cases it is different, but nonetheless ease the calculation of the integral.

Defining  $d_{\parallel}$  as the dimension of the space spanned by the external momenta, one finds that it is possible to choose  $4 - d_{\parallel}$  of the vectors that belong to the basis  $\{e_i^\alpha\}$  to lie into the subspace orthogonal to the external kinematics, i.e., such that

$$e_i \cdot p_j = 0 \quad \text{for } i > d_{\parallel}, \forall j \quad (2.39)$$

and

$$e_i \cdot e_j = \delta_{ij}. \quad (2.40)$$

In this way, the loop momenta can be written in its  $d = d_{\parallel} + d_{\perp}$  component as

$$q_i^\alpha = q_{\parallel}^\alpha + \lambda_i^\alpha, \quad (2.41)$$

where

$$q_{\parallel}^\alpha = \sum_{j=1}^{d_{\parallel}} x_{ij} e_j^\alpha \quad \lambda_i^\alpha = \sum_{j=d_{\parallel}+1}^4 x_{ij} e_j^\alpha + \mu_i^\alpha, \quad (2.42)$$

with  $q_{\parallel}$  that lies in the  $d_{\parallel}$  space, while  $\lambda_i$  belongs to the orthogonal  $d_{\perp}$  dimensional one. In this parameterization all the denominators become independent from the single orthogonal component of the transverse loop momenta and they depend only on the scalar products between them. In fact, the denominators appear as

$$D_i = l_{\parallel i}^2 + \sum_{j,k} \alpha_{ij} \alpha_{ik} \lambda_{jk} + m_i^2, \quad (2.43)$$

with

$$l_{\parallel i}^\alpha = \sum_j \alpha_{ij} q_{\parallel j}^\alpha + \sum_j \beta_{ij} p_j^\alpha \quad (2.44)$$

and

$$\lambda_{jk} = \sum_{l=d_{\parallel}+1}^4 x_{jl} x_{lk} + \mu_{jk}. \quad (2.45)$$

In light of these manipulations, the integral becomes

$$I^{d(\ell,n)}[\mathcal{N}] = \Omega_d^{(\ell)} \int \prod_{i=1}^{\ell} d^{n-1} q_{\parallel i} \int \prod_{1 \leq i \leq j}^{\ell} d\lambda_{ij} G(\lambda_{ij})^{\frac{d_{\perp}-1-\ell}{2}} \int d^{(4-d_{\parallel})\ell} \Theta_{\perp} \frac{\mathcal{N}(q_{\parallel i}, \lambda_{ij}, \Theta_{\perp})}{\prod_j D_j(q_{\parallel i}, \lambda_{ij})}, \quad (2.46)$$

where  $\Theta_{\perp}$  parameterizes the integral over the single orthogonal component  $\lambda_i$  that lies in the four dimensional space.

## 2.2 Properties

### 2.2.1 IBPs

Feynman integrals enjoy many properties which can be exploited in order to ease the computation of scattering amplitudes. One of which comes from the symmetry of the integrals  $I^d(x_1, \dots, x_s)$  with respect to the linear shift of loop momenta

$$q_i^\alpha \rightarrow q_i^\alpha + \delta b_{ij} k_j^\alpha, \quad (2.47)$$

where  $k_j \in \{q_1, \dots, q_l, p_1, \dots, p_n\}$  and  $\delta b_{ij}$  is an infinitesimal parameter. Exploiting this symmetry, it is possible to derive a large set of identities as shown in [83], linking complex Feynman integrals to a set of building blocks, effectively breaking them down into a basis of integrals. Such identities are called *Integration-by-Part-Identities* or IBPs.

Alternatively, one can study these relations by means of Gauss theorem in  $d$  dimensions.

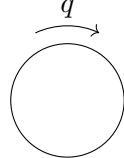
Considering Feynman integrals in dimensional regularization,  $d$  is considered as a continuous parameter and hence we can assume that the integral (2.5) is well defined and convergent. This means that the integrand must vanish rapidly enough at the boundary of the integration domain. This implies that when applying the Gauss theorem to the total derivative of any Feynman integral, no boundary terms are generated, implying the vanishing of such integral

$$\int \prod_{i=1}^l d^D q_i \frac{\partial}{\partial q_j^\alpha} \left( \frac{v^\alpha}{D_1^{x_1} \dots D_r^{x_r}} \right) = 0, \quad (2.48)$$

where  $v^\alpha$  is a vector such that  $v \in \{q_1, \dots, q_l, p_1, \dots, p_n\}$ . Choosing to differentiate over any loop momenta and by changing the vector  $v^\alpha$  over all its possible values, it is possible to produce many independent IBPs for each integral.

### Example

Let us briefly discuss the application of this method to the simplest example possible: the one-loop integral without any external leg:

$$\int \frac{d^D q}{(2\pi)^D} \frac{1}{q^2 + m^2} = \int \frac{d^D q}{(2\pi)^D} \frac{1}{D_0} = \text{Diagram} \quad (2.49)$$


As a convention, the integral will be portrayed as a graph which has momentum conservation applied at each vertex, and its internal lines will correspond to its denominators. If an internal line has dots over it, it means that the denominator corresponding to that line is raised to the power  $a - 1$ , with  $a$  being the number of dots appearing over it.

Applying the total derivative with respect to the loop momenta in this case, one obtains  $\partial_\mu D_0 = 2q_\mu$ . Therefore, choosing  $v^\mu = q^\mu$ , in the IBP equation (2.48) we have:

$$0 = \int \frac{d^D q}{(2\pi)^D} \partial_\mu \left( \frac{q^\mu}{D_0} \right) = \int \frac{d^D q}{(2\pi)^D} \left( \frac{D}{D_0} - 2 \frac{q^2}{D_0^2} \right) = \int \frac{d^D q}{(2\pi)^D} \left( \frac{D-2}{D_0} + \frac{2m^2}{D_0^2} \right). \quad (2.50)$$

This yields

$$\int \frac{d^D q}{(2\pi)^D} \frac{1}{D_0^2} = -\frac{D-2}{2m^2} \int \frac{d^D q}{(2\pi)^D} \frac{1}{D_0} \quad (2.51)$$

and can be portrayed as

$$\text{Diagram with a circle and a dot on top} = -\frac{D-2}{2m^2} \text{Diagram with a circle} . \quad (2.52)$$

Let us stress that this can be derived recursively for integrals of this kind with arbitrary power of the denominator, linking many different objects to a common element. ■

The systematic application of this method to general multiloop integrals, allows to build a system of identities of this kind, which, upon solution, allows to express Feynman integrals in terms of a common basis of independent functions labeled *master integrals* by means of the *Laporta's algorithm* [87] and represent a crucial component of multi-loop amplitude computation. Automatic software for generating and solving IBPs are publicly available, such as REDUZE [61], LITERED [88], KIRA [89].

### 2.2.2 Differential and Difference Equations for Feynman Integrals

Linear relations as the IBPs discussed above are useful to express the scattering amplitude in terms of MIs. In order to complete such computation the missing piece is the evaluation of the latter. For this goal IBPs play a key role, because they can be used to build differential equations as well as finite difference equations obeyed by the MIs.

Such functional relations for the MIs can be generated from the action of special differential operators and polynomials, say  $Q$  acting on the integrand of the MIs, say  $\mathbf{I}$ . Generically, one obtains an equation of the type:

$$Q \cdot \mathbf{I} = \mathbb{A} \cdot \mathbf{I} , \quad (2.53)$$

where the right hand side is obtained after applying the IBPs to the result of the l.h.s, namely after applying  $Q$  to the vector of MIs  $\mathbf{I}$ . The matrix  $\mathbb{A} = \mathbb{A}(d, \vec{s}, m^2)$  has rational entries depending on the external kinematic invariants  $\vec{s}$ ,  $m^2$  and the dimensional parameter  $d$ .

### 2.2.3 Differential Equations

Let us consider the case in which  $Q$  is a differential operator. Starting from a Feynman integral where the  $i$ -th internal line has a non-degenerate mass  $m_i$  (hence this parameter appears only in the  $i$ -th propagator), we have

$$\partial_{m_i^2} I_{x_1, \dots, x_i, \dots, x_s}^{[d]} = I_{x_1, \dots, x_{i+1}, \dots, x_s}^{[d]} \quad (2.54)$$

as follows from the definition of the denominators  $D_i = l_i^2 + m_i^2$ , notice that in Minkowsky there would be a different sign. In the case where the mass is degenerate, the only difference is that on the right hand side more terms would appear.

As we can notice, the integral on the right hand side is the starting integral, plus a dot. As we have shown, such integral can be reduced by means of IBPs to a linear combination of the starting integral, plus some simpler one having

$$\partial_{m_i^2} I_{x_1, \dots, x_i, \dots, x_s}^{[d]} = A_{m_i^2} I_{x_1, \dots, x_{i+1}, \dots, x_s}^{[d]} + \text{non homogeneous terms} , \quad (2.55)$$

where  $A_{m_i^2}$  is a rational coefficient in the space-time dimension and the kinematic invariants due to the properties of IBPs. The same goes for the coefficient multiplying integrals with lower number of denominators.

This approach can be systematized, applying the derivative to a vector of suitably chosen Master Integrals  $\mathbf{I}(d, \vec{s}, m_j^2)$ , yielding

$$\partial_{m_i^2} \mathbf{I}(d, \vec{s}, m_j^2) = \mathbb{A}_{m_i^2}(d, \vec{s}, m_j^2) \mathbf{I}(d, \vec{s}, m_j^2) . \quad (2.56)$$

Similar systems of differential equation are obtained by deriving w.r.t. the external kinematical parameter. Although Feynman integrals in momentum space retain a dependence on single  $p_i$  rather than the  $\vec{s}$  parameters, it is possible to link the differential operators corresponding to this two different set of variables. Knowing that

$$\frac{\partial}{\partial p_i^\alpha} = \sum_j \frac{\partial s_j}{\partial p_i^\alpha} \frac{\partial}{\partial s_j} . \quad (2.57)$$

It is possible to build a set of independent scalar relation by contracting the above identity with external momenta

$$p_k^\alpha \frac{\partial}{\partial p_i^\alpha} = \sum_j \frac{\partial s_j}{\partial p_i^\alpha} \frac{\partial}{\partial s_j} , \quad (2.58)$$

which allows us to express the derivative w.r.t. the  $s_i$  in to a combination of derivative w.r.t. the external momenta.

Applying such operators to Feynman integrals yields a result analogous to what is shown in (2.56), therefore including  $m_i^2$  in the vector  $\vec{s}$  we can write the system of DEQs satisfied by MIs in any kinematical variables  $s_i \in \vec{s}$

$$\partial_{s_i} \mathbf{I}(d, \vec{s}) = \mathbb{A}_{s_i}(d, \vec{s}) \mathbf{I}(d, \vec{s}) , \quad (2.59)$$

where  $\mathbb{A}_{s_i}$  is a block triangular matrix with rational coefficients in  $x_i$  and  $d$ .

It is often convenient to express our system of differential equations in terms of dimensionless variables by choosing one of the variables  $\vec{s}$ , say  $s_1$  (which is usually picked to be the mass) and by building the ratios

$$\hat{s} = \frac{s_i}{s_1} \quad \text{for } i \neq 1 . \quad (2.60)$$

The system of DEQ then is equivalent to consider the system w.r.t.  $\vec{\hat{s}}$  and the DEQ in  $s_1$ . In this way, after solving the DEQ in the single dimensionful parameter  $s_1$ , the dependence of the MIs on it can be removed by a suitable rescaling of the MIs to deal with a basis of dimensionless integrals  $\mathbf{I}$ .

The resulting system can be solved one variable at a time, by adding to the solution an integration constant that depends on the remaining variables. The convergence of the integration procedure is granted by the Schwartz integrability condition

$$\partial_{\hat{s}_i} \partial_{\hat{s}_j} \mathbf{I}(d, \vec{\hat{s}}) = \partial_{\hat{s}_j} \partial_{\hat{s}_i} \mathbf{I}(d, \vec{\hat{s}}) , \quad (2.61)$$

which applied to (2.59), gives

$$\partial_{\hat{s}_i} \mathbb{A}_{\hat{s}_j} - \partial_{\hat{s}_j} \mathbb{A}_{\hat{s}_i} + [\mathbb{A}_{\hat{s}_i}, \mathbb{A}_{\hat{s}_j}] = 0 . \quad (2.62)$$

After these passages, we are left with a residual integration constant which is independent from the kinematics and must be fixed with suitable *boundary conditions*. This can be achieved by the analytic evaluation of the MIs at some specific kinematic points, although it may be quite a demanding task. A possible alternative is to impose regularity or finiteness of the MIs at kinematic pseudo-thresholds.

### Canonical system of differential equations

In the case of Feynman integrals, according to the physical problem, which, in general, can be characterized by a critical number of dimensions, say  $d_0$ , one might be interested in the evaluation of the scattering amplitudes, hence of Feynman integrals in  $d \rightarrow d_0$  limit. Therefore, we introduce the dimensional parameter,  $\epsilon$  defined as

$$d = d_0 - 2\epsilon . \quad (2.63)$$



Singular behaviors, arising from loop integrations, are parameterized as poles in  $\epsilon$ . For the same reason, knowing the full dependence of the integral under consideration w.r.t. the dimensional parameter may be unnecessary when not prohibitive. Therefore, we are interested in the Laurent series expansions of Feynman integrals around  $\epsilon = 0$ ,

$$\mathbf{I}(\epsilon, \vec{x}) = \sum_{j=j_{min}}^{\infty} \epsilon^j \mathbf{I}^{(j)}(\vec{x}), \quad (2.64)$$

which can be obtained by solving the system of DEQs,

$$d\mathbf{I}(\epsilon, \vec{x}) = d\mathbb{A}(\epsilon, \vec{x}) \cdot \mathbf{I}(\epsilon, \vec{x}), \quad \text{with} \quad d\mathbb{A} \equiv \sum_i \mathbb{A}_{x_i} dx_i, \quad \mathbb{A}_{x_i} \equiv \frac{\partial \mathbb{A}}{\partial x_i}. \quad (2.65)$$

Let us stress that in general the value  $k_{min}$  from which the Laurent expansion starts can be negative and depends on the convergence properties of  $I^{(j)}(\vec{x})$ . However, it might be convenient to identify an alternative basis of MIs, say  $\mathbf{J} = \mathbb{R} \cdot \mathbf{I}$ , related to the original basis  $\mathbf{I}$  through a rotation matrix  $\mathbb{R}$ , obeying a DEQ system, of the form [90],

$$d\mathbf{J}(\epsilon, x) = \epsilon d\hat{\mathbb{A}}(\vec{x}) \cdot \mathbf{J}(\epsilon, \vec{x}), \quad (2.66)$$

with

$$d\hat{\mathbb{A}} = \mathbb{R}^{-1}(\vec{x}) \cdot d\mathbb{A}(\epsilon, \vec{x}) \cdot \mathbb{R}(\vec{x}) - \mathbb{R}^{-1}(\vec{x}) \cdot d\mathbb{R}(\vec{x}), \quad (2.67)$$

where the  $\epsilon$  dependence of the matrix is factorized from the kinematic dependence.

In this case, the solution  $\mathbf{J}$  admits a Taylor series expansion in  $\epsilon$ ,

$$\mathbf{J}(\epsilon, \vec{x}) = \sum_{j=0}^{\infty} \epsilon^j \mathbf{J}^{(j)}(\vec{x}). \quad (2.68)$$

In particular, the coefficient of the series  $\mathbf{J}^{(j)}$ , can be determined by repeated integration as

$$\mathbf{J}(\epsilon, \vec{x}) = \mathcal{P} \exp \left\{ \epsilon \int_{\gamma} d\hat{\mathbb{A}} \right\} \cdot \mathbf{J}(\epsilon, \vec{x}_0) \quad (2.69)$$

like a Dyson series, or equivalently Magnus series [50], where the integration path is defined as

$$\gamma(t) = \gamma(\vec{x}(t)), \quad t \in [0, 1]: \quad \gamma(0) = \vec{x}_0, \gamma(1) = \vec{x}. \quad (2.70)$$

When  $d\hat{\mathbb{A}}$  is a differential logarithmic (dlog) form, *i.e.*

$$d\hat{\mathbb{A}}(x) = \sum_i M_i d \log(\eta_i), \quad (2.71)$$

with rational  $\eta_i = \eta_i(x)$ , the basis  $\mathbf{J}$  is called *canonical bases*, and the coefficients of the Dyson series have the property of uniform weight,

$$\mathbf{J}(\epsilon, \vec{x}) = \left( \mathbb{1} + \epsilon \int_{\gamma} d\hat{\mathbb{A}}(t_1) + \frac{1}{2} \epsilon^2 \int_{\gamma} \int_{\gamma} d\hat{\mathbb{A}}(t_1) d\hat{\mathbb{A}}(t_2) + \dots \right) \mathbf{J}(\epsilon, \vec{x}_0). \quad (2.72)$$

### Generalized Polylogarithms

The repeated integration appearing in the Dyson series of MIs, can be conveniently carried out in terms of Generalized Polylogarithms (GPLs) [49, 91, 92]. In particular they become useful, when the entries of the matrix differential  $d\hat{A}$  are rational functions of the variables of our SDE. After introducing a linear parameterization of the letters  $\eta_i$ , in terms of the integration variable  $t$  and the weight  $\omega_i$  as,

$$\eta_i = t - \omega_i, \quad (2.73)$$

GPLs can be defined through the recursive formula,

$$G(\vec{\omega}_n, x_i) = \int_0^{x_i} dt \frac{1}{t - \omega_1} G(\vec{\omega}_{n-1}, t) \quad n > 0, \quad (2.74)$$

$$G(\vec{0}_n, x_i) = \frac{1}{n!} \log^n(x_i). \quad (2.75)$$

The following properties can be derived directly from the definition:

- *Derivative:*

$$\frac{\partial}{\partial x_i} G(\vec{\omega}_n, x_i) = \frac{1}{x_i - \omega_1} G(\vec{\omega}_{n-1}, x_i); \quad (2.76)$$

- *Identical weights:*

$$G(\vec{\omega}_n, x_i) = \frac{1}{n!} \log^n\left(1 - \frac{x_i}{\omega}\right), \quad \vec{\omega}_n = \underbrace{\{\omega, \dots, \omega\}}_{n \text{ times}}; \quad (2.77)$$

- *Rescaling:*

$$G(\vec{\omega}_n, x_i) = G(z\vec{\omega}_n, zx_i), \quad \omega_n \neq 0. \quad (2.78)$$

- *Conversion formula:*

$$\int_{\gamma} d\log(x_i - \omega_n) \cdots d\log(x_i - \omega_1) = G\left(\frac{x_{0,i} - \omega_n}{x_{0,i} - x_i}, \dots, \frac{x_{0,i} - \omega_1}{x_{0,i} - x_i}, 1\right), \quad (2.79)$$

- *Shuffle algebra:*

$$G(\vec{m}, x_i) G(\vec{n}, x_i) = G(\vec{m}, x_i) \sqcup G(\vec{n}, x_i) \sum_{\vec{r}=\vec{m} \sqcup \vec{n}} G(\vec{r}, x_i), \quad (2.80)$$

where  $\sqcup$  denotes the shuffle products and  $\vec{\omega}_{r=m \sqcup n}$  represents all possible merges between the two vectors  $\vec{\omega}_m$  and  $\vec{\omega}_n$  which preserves their internal ordering.

#### 2.2.4 Difference Equations

Let us consider now eq. (2.53), and mention how it can be used to build finite difference equations for (FDE) MIs. We can distinguish two paradigmatic cases of FDE, namely when the recursion is built on the space-time dimensions [93, 94] and when it is built in the power of a single denominator.

- **Dimensional Recurrence Relations.**

Let us consider the  $i$ -th MI in  $d$ -dimensions  $\mathbf{I}_i^{[d]} \in \mathbf{I}^{[d]}$ , generically defined as

$$\mathbf{I}_i^{[d]} \equiv \int \prod_{\ell=1}^L \frac{d^d q_{\ell}}{(2\pi)^d} \frac{1}{\prod_{j=1}^n D_j^{a_{i,j}}}, \quad \text{with } a_{i,j} \in \mathbb{Z}, \quad (2.81)$$

where the vector of exponents  $\vec{a}_i \equiv \{a_{i,1}, \dots, a_{i,n}\}$  stands for a list of integer powers, which is characteristic of the integral itself. The integrals in  $d + 2$ -dimensions [93,95] are defined by inserting (powers of)  $Q$ , which is proportional to  $G(p_i, q_i)$ , that is, the Gram determinant introduced in eq. (2.7), in the numerator of any integral. In particular, if one power of  $Q$  is inserted in the integrand of a MI, originally defined in  $d$ -dimensions, one gets the same MIs in  $(d + 2)$ -dimensions, as

$$\mathbf{I}_i^{[d+2]} \equiv \int \prod_{\ell=1}^L \frac{d^d q_\ell}{(2\pi)^d} \frac{Q}{\prod_{j=1}^n D_j^{a_{i,j}}} , \quad (2.82)$$

The new born integral can be interpreted as an integral in  $d$ -dimensions, and decomposed in terms of MIs in  $d$ -dimensions. Therefore, by applying it to all MIs, one derives a system of equations like

$$\mathbf{I}^{[d+2]} = \mathbb{M}(d, \vec{x}) \cdot \mathbf{I}^{[d]} \quad (2.83)$$

that relate the MIs in shifted dimensions, where the entries of the matrix  $\mathbb{M}$  arise from IBPs. Like any system of the 1st ODE for  $n$  MIs is equivalent to a single  $n$ -th ODE just for one MI, this system is equivalent to single finite difference equations in  $d$  just for one of the MIs.

Using a different operator  $Q$  (built out of differential operators, rather than as a polynomial in the scalar products) [93,95], it is also possible to generate an alternative, yet equivalent system

$$\mathbf{I}^{[d-2]} = \mathbb{N}(d, \vec{x}) \cdot \mathbf{I}^{[d]} , \quad (2.84)$$

where MIs in  $(d - 2)$ -dimension are expressed in terms of MIs in  $d$ -dimensions. From this system one can also build a single finite difference equation in  $d$ .

- **Recurrence Relations in the denominator powers.**

An alternative type of finite difference equation can be built by considering the definition in eq. (2.81) for a given MIs, in  $d$ -dimension, and keeping one of the exponents in the denominator, say  $a_{i,k}$  as arbitrary, while all the other powers,  $a_{i,j} \equiv z$  ( $j \neq k$ ) are set to explicit integer values [96],

$$\mathbf{I}_i^{[d]}[z] \equiv \int \prod_{\ell=1}^L \frac{d^d q_\ell}{(2\pi)^d} \frac{1}{\prod_{j=1}^n D_j^{a_{i,j}}} , \quad \text{with } \forall j \neq k, a_{i,j} \in \mathbb{Z} , \quad (2.85)$$

In this case, IBP identities can be used to write a recurrence relation for integrals of the  $\mathbf{I}_i^{[d]}$ -type, having shifted values of the exponent  $z$ , as

$$\sum_h p_{i,h}(z) \mathbf{I}_i^{[d]}[z + h] = \text{known term} , \quad (2.86)$$

where  $p_{i,h}(z)$  are polynomials in  $z$  and the "known term" is a non-homogeneous contribution coming from integrals belonging to sub-diagrams, which can be considered known in a bottom-up approach (namely, evaluating integrals starting from the simpler diagrams).

### 2.2.5 Initial Conditions

To solve differential and difference equations obeyed by the MIs, boundary values are needed too, and they have to be provided as independent information, independent input. These initial conditions correspond to the knowledge of the MIs at special values of the parameters: a given point in the space of kinematic variables  $\vec{x} = \vec{x}_0$ , for the case of the differential equation; a given

value  $d = d^*$  of the space-time dimension, or a given denominator power  $z = z_0$ , for the case of the difference equation. In general, the initial conditions are simpler integrals, related to the subdiagrams/subsectors, generally integrals with fewer denominators, or with a reduced number of scales, which are considered as easier to determine.

### 2.2.6 Numerical Integration

However, the analytic determination of the MIs may become prohibitive as the number of loops and of scales increases. Numerical methods become of fundamental importance in these cases: direct integration techniques, applied to Feynman parametrized integrals (or similar parametrisations); Sector Decomposition Methods [97], implemented in public software like SECDEC [98] and FIESTA [99]; numerical solution of differential equations, of which [100][101] are an example; numerical solutions of difference equation, see, for instance, [96][102].

In many cases, the combination of analytic and numerical evaluation methods are employed. Often, boundary conditions for functional equations are provided numerically. Alternatively, the use of functional equations can be exploited to identify bases of MIs which are more suitable (free of singularities) for the numerical integration. Therefore, in the case of cutting edge calculation, these techniques are used in tandem, allowing for a semi-analytic determination of MIs.

## 2.3 Adaptive integrand decomposition

In general, scattering amplitudes are expressed in terms of a sum of tensor integrals, whereas the joint use of IBPs and Differential equation give a clear framework that helps in computing it, once this is expressed in terms of scalar integrals. This demands for a procedure to simplify the numerator and write it either as an object which is independent from the loop momenta or as a combination of Irreducible Scalar Products. On top of that, one can be interested in simplifying the Feynman integrals appearing in the amplitude before applying IBPs. Both this goals are achievable thanks to the *Adaptive integrand decomposition* method [39,41,42]. In this framework, one exploits the advantages of splitting the loop momenta between the space parallel to the external momenta that characterizes the integral in consideration and its orthogonal space. This technique *adapts* to the diagram to which it is applied, reducing at minimum the number of variables appearing at the denominator, enabling the direct integration of the variables that appear only at the numerator and simplifying the use of integrand reduction techniques such as the polynomial division.

### 2.3.1 Polynomial division

The integrand of a general Feynman integral is a rational function of the momenta and the masses of the particles flowing in it, as shown in [2.1]. It is therefore possible to apply polynomial division until we are left with irreducible polynomials in order to simplify it. Defining

$$I_{i_1, \dots, i_a}^{d(\ell, n)}[\mathcal{N}] = \int \frac{d^D q_1}{(2\pi)^D} \cdots \frac{d^D q_\ell}{(2\pi)^D} \mathcal{I}_{i_1, \dots, i_a}, \quad \mathcal{I}_{i_1, \dots, i_a} \equiv \frac{\mathcal{N}_{i_1, \dots, i_a}}{D_{i_1} \cdots D_{i_a}}, \quad (2.87)$$

through such technique it is possible to write the numerator as a quotient  $\mathcal{Q}_{i_1, \dots, i_a}$ , that depends on the denominators, plus a remainder  $\Delta_{i_1, \dots, i_a}$  that is :

$$\begin{aligned} \mathcal{N}_{i_1, \dots, i_a} &= \mathcal{Q}_{i_1, \dots, i_a} + \Delta_{i_1, \dots, i_a} \\ &= \sum_{k=1}^a \mathcal{N}_{i_1, \dots, i_{k-1}, i_{k+1}, \dots, i_a} D_k + \Delta_{i_1, \dots, i_a}. \end{aligned} \quad (2.88)$$

In this way it is possible to *reduce* the integrand, in fact substituting (2.88) back into  $\mathcal{I}_{i_1, \dots, i_a}$  one finds that

$$\mathcal{I}_{i_1, \dots, i_a} = \sum_{k=1}^a \mathcal{I}_{i_1, \dots, i_{k-1}, i_{k+1}, \dots, i_a} + \frac{\Delta_{i_1, \dots, i_a}}{D_{i_1} \cdots D_{i_a}}. \quad (2.89)$$

Iterating such procedure on the resulting  $\mathcal{I}_{i_1, \dots, i_{k-1}, i_{k+1}, \dots, i_a}$  it is possible to write the integrand as a combination of irreducible remainder, arriving to the final form

$$\mathcal{I}_{i_1, \dots, i_a} \equiv \frac{\mathcal{N}_{i_1, \dots, i_a}}{D_{i_1} \cdots D_{i_a}} = \sum_{k=1}^a \sum_{\{j_1 \cdots j_k\}} \frac{\Delta_{j_1 \cdots j_k}}{D_{j_1} \cdots D_{j_k}}. \quad (2.90)$$

This procedure finds a natural description in mathematics through the use of *ideals*. Let us label the integration variables to be  $z_i$ . Defining  $P[z_i]$  as the ring of all polynomials in the  $z_i$  variables, every set of indices  $i_1, \dots, i_a$  defines the ideal

$$\mathcal{I}_{i_1 \dots i_a} \equiv \langle D_{i_1}, \dots, D_{i_a} \rangle = \left\{ \sum_{k=1}^a h_k(z_i) D_{i_k}(z_i) : h_k(z_i) \in P[z_i] \right\}. \quad (2.91)$$

With that definition in mind, the goal of the integrand reduction can be expressed as to write the integrand as a contribution of *irreducible* polynomials  $\Delta_{j_1 \cdots j_k}$ , i.e. polynomials which contain no contribution belonging in the corresponding ideal  $\mathcal{I}_{j_1 \cdots j_k}$ .

### 2.3.2 The Divide, Integrate, Divide algorithm

In order to apply this machinery to our integrals, let us consider the parallel and perpendicular parametrization of the integration variables seen in Section 2.1.2, namely integrating over the set of variables

$$z = \{x_{\parallel i}, x_{\perp i}, \lambda_{ij}\}, \quad i, j = 1, \dots, l, \quad (2.92)$$

where  $x_{\parallel i}$  describes the components of the loop momenta parallel to the external momenta

$$x_{\parallel i} = \{x_{ji}\} \quad \text{where } j \leq d_{\parallel}, \quad (2.93)$$

whereas  $x_{\perp i}$  parametrize the four dimension orthogonal components

$$x_{\perp i} = \{x_{ji}\} \quad \text{where } d_{\parallel} < j \leq 4. \quad (2.94)$$

In this parametrization we have

$$\mathcal{I}_{i_1, \dots, i_a} \equiv \frac{\mathcal{N}_{i_1, \dots, i_a}(x_{\parallel i}, x_{\perp i}, \lambda_{ij})}{\prod_k D_{i_k}(x_{\parallel i}, \lambda_{ij})} \quad (2.95)$$

and as we can see it is possible to perform the polynomial division with respect to the smaller set of variables  $\{x_{\parallel i}, \lambda_{ij}\}$  rather than applying it with respect to the full set of integration variables. Moreover, in this parametrization, it is possible to perform the polynomial division bypassing the computation of the Groebner basis. As proved in [41], it is possible to build a linear system in order to replace a subset of the  $x_{\parallel i}$  integration variables which we will call  $x_{\parallel i}^{RSP}$  since they corresponds to the Reducible Scalar Products, with a combination of denominator. The same can be done with the  $\lambda_{ij}$  variables using the same definition of a subset of denominators:

$$\begin{cases} x_{\parallel i}^{RSP} \rightarrow P \left[ D_{i_k}, x_{\parallel i}^{ISP} \right] \\ \lambda_{ij} \rightarrow P \left[ D_{i_k}, x_{\parallel i}^{ISP} \right] \end{cases}. \quad (2.96)$$

Thanks to this substitution, we can express the numerator as follows

$$\mathcal{N}_{i_1 \dots i_r} (x_{\parallel i}, x_{\perp i}, \lambda_{ij}) = \sum_{k=1}^r \mathcal{N}_{i_1 \dots i_{k-1} i_{k+1} \dots i_r} (x_{\parallel i}^{ISP}, x_{\perp i}) D_{i_k} + \Delta_{i_1 \dots i_r} (x_{\parallel i}^{ISP}, x_{\perp i}) , \quad (2.97)$$

where  $x_{\parallel i}^{ISP}$  are the parallel components which are connected to the ISPs.

From a mathematical standpoint, performing the polynomial division requires to select a monomial ordering to obtain a unique result. In this case, this would correspond to perform it in terms of the lexicographical order  $\lambda_{ij} \prec x_{\parallel i}$ .

The integral can then be further parametrized, mapping the orthogonal components  $x_{\perp i}$  into the angles characterizing our problem and the length of the loop momenta:

$$x_{\perp i} \rightarrow P \left[ \sqrt{\lambda_{ii}}, \sin \Theta_{\perp}, \cos \Theta_{\perp} \right] . \quad (2.98)$$

In this way, the polynomial dependence on  $x_{\perp i}$  of any integrand is converted in to a polynomial dependence on  $\sin [\Theta_{\perp, \Lambda}]$  and  $\cos [\Theta_{\perp, \Lambda}]$ , enabling us to systematically perform the left over angular integration through the properties of the *Gegenbauer polynomial*. Indeed, after mapping our numerator in to such objects, one can carry out the integration using the orthogonality condition proper of such objects:

$$\int_{-1}^1 d \cos \theta (\sin \theta)^{2\alpha-1} C_n^{(\alpha)} (\cos \theta) C_m^{(\alpha)} (\cos \theta) = \delta_{mn} \frac{2^{1-2\alpha} \pi \Gamma (n+2\alpha)}{n! (n+\alpha) \Gamma^2 (\alpha)} , \quad (2.99)$$

where the  $C_n^{(\alpha)} (\cos \theta)$  are the Gegenbauer polynomial. In this way we obtain

$$\Delta_{i_1 \dots i_r}^{int} (x_{\parallel}^{ISP}, \lambda_{ij}) = \int \prod_{i=1}^l dx_{\perp i} \Delta_{i_1 \dots i_r} (x_{\parallel}^{ISP}, x_{\perp i}) \quad (2.100)$$

$$\propto \int d^{(4-d_{\parallel})l} \Theta_{\perp} \Delta_{i_1 \dots i_r}^{n-sp} (x^{ISP}, \lambda_{ij}, \Theta_{\perp}) . \quad (2.101)$$

The residues  $\Delta_{i_1 \dots i_r}^{int} (x_{\parallel}^{ISP}, \lambda_{ij})$  can be still reduced by rewriting again the  $\lambda_{ij}$  through eq. (2.96):

$$\Delta_{i_1 \dots i_r}^{int} (x_{\parallel}^{ISP}, \lambda_{ij}) = \sum_{k=1}^r \mathcal{N}_{i_1 \dots i_{k-1} i_{k+1} \dots i_r} (x_{\parallel}^{ISP}) + \Delta'_{i_1 \dots i_r} (x_{\parallel}^{ISP}) . \quad (2.102)$$

In this way, we were able to simplify the Feynman integral and to rewrite it as a combination of scalar integral with a numerator that contains components of the loop momenta only through ISPs, writing it as

$$I_{i_1, \dots, i_a}^{[d]\ell} = \sum_{k=0}^r \sum_{\{j_1 \dots j_k\}} \int \prod_{j=1}^{\ell} \frac{d^d q_j}{(2\pi)^d} \frac{\Delta'_{j_1 \dots j_k}}{D_{j_1} \dots D_{j_k}} , \quad (2.103)$$

ready to undergo the IBP reduction.

This approach has been applied in many cases. In particular the variables remaining after each step of the algorithm in few two-loop cases are shown in Figures [2.1](#), [2.2](#), [2.3](#), [2.4](#).

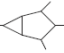
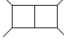






$\mathcal{I}_{i_1 \dots i_r}$	$\Delta_{i_1 \dots i_r}$	$\Delta_{i_1 \dots i_r}^{\text{int}}$	$\Delta'_{i_1 \dots i_r}$
$\mathcal{I}_{156791011}^P$ 	94 {1, $x_{21}, x_{31}, x_{41}, x_{42}$ }	53 {1, $x_{21}, x_{31}, \lambda_{11}, \lambda_{22}, \lambda_{12}$ }	10 {1, $x_{21}, x_{31}$ }
$\mathcal{I}_{1225691011}^P$ 	160 {1, $x_{31}, x_{41}, x_{32}, x_{42}$ }	93 {1, $x_{31}, x_{32}, \lambda_{11}, \lambda_{22}, \lambda_{12}$ }	22 {1, $x_{31}, x_{32}$ }
$\mathcal{I}_{135691011}^{\text{NP1}}$ 	184 {1, $x_{31}, x_{42}, x_{32}, x_{42}$ }	105 {1, $x_{31}, x_{32}, \lambda_{11}, \lambda_{22}, \lambda_{12}$ }	25 {1, $x_{31}, x_{32}$ }
$\mathcal{I}_{1356811}^P$ 	180 {1, $x_{31}, x_{41}, x_{22}, x_{32}, x_{42}$ }	101 {1, $x_{31}, x_{22}, x_{32}, \lambda_{11}, \lambda_{22}, \lambda_{12}$ }	39 {1, $x_{31}, x_{22}, x_{32}$ }
$\mathcal{I}_{16891011}^P$ 	66 {1, $x_{11}, x_{21}, x_{31}, x_{41}, x_{42}$ }	35 {1, $x_{11}, x_{21}, x_{31}, \lambda_{11}, \lambda_{22}, \lambda_{12}$ }	10 {1, $x_{11}, x_{21}, x_{31}$ }
$\mathcal{I}_{24691011}^{\text{NP1}}$ 	245 {1, $x_{31}, x_{41}, x_{21}, x_{32}, x_{42}$ }	137 {1, $x_{31}, x_{22}, x_{32}, \lambda_{11}, \lambda_{22}, \lambda_{12}$ }	55 {1, $x_{31}, x_{22}, x_{32}$ }
$\mathcal{I}_{3681011}^P$ 	115 {1, $x_{31}, x_{41}, x_{12}, x_{22}, x_{32}, x_{42}$ }	66 {1, $x_{31}, x_{12}, x_{22}, x_{32}, \lambda_{11}, \lambda_{22}, \lambda_{12}$ }	35 {1, $x_{31}, x_{12}, x_{22}, x_{32}$ }
$\mathcal{I}_{136811}^P$ 	180 {1, $x_{11}, x_{31}, x_{41}, x_{22}, x_{32}, x_{42}$ }	103 {1, $x_{11}, x_{31}, x_{22}, x_{32}, \lambda_{11}, \lambda_{22}, \lambda_{12}$ }	60 {1, $x_{11}, x_{31}, x_{22}, x_{32}$ }

Figure 2.1: Universal irreducible numerators for two-loop four-point topologies. For each of the residues,  $\Delta_{i_1 \dots i_n}$ ,  $\Delta_{i_1 \dots i_n}^{\text{int}}$  and  $\Delta'_{i_1 \dots i_n}$  we indicate the number of monomials and the list of their variables.


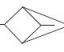
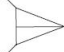
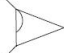

$\mathcal{I}_{i_1 \dots i_r}$	$\Delta_{i_1 \dots i_r}$	$\Delta_{i_1 \dots i_r}^{\text{int}}$	$\Delta'_{i_1 \dots i_r}$
$\mathcal{I}_{1356911}^P$ 	180 {1, $x_{31}, x_{41}, x_{22}, x_{32}, x_{42}$ }	22 {1, $x_{22}, \lambda_{11}, \lambda_{22}, \lambda_{12}$ }	4 {1, $x_{22}$ }
$\mathcal{I}_{15691011}^{\text{NP1}}$ 	240 {1, $x_{31}, x_{41}, x_{22}, x_{32}, x_{42}$ }	30 {1, $x_{22}, \lambda_{11}, \lambda_{22}, \lambda_{12}$ }	6 {1, $x_{22}$ }
$\mathcal{I}_{1571011}^P$ 	180 {1, $x_{21}, x_{31}, x_{41}, x_{12}, x_{32}, x_{42}$ }	33 {1, $x_{21}, x_{12}, \lambda_{11}, \lambda_{22}, \lambda_{12}$ }	13 {1, $x_{21}, x_{12}$ }
$\mathcal{I}_{1691011}^P$ 	115 {1, $x_{31}, x_{41}, x_{12}, x_{22}, x_{32}, x_{42}$ }	20 {1, $x_{11}, x_{22}, \lambda_{11}, \lambda_{22}, \lambda_{12}$ }	6 {1, $x_{12}, x_{22}$ }
$\mathcal{I}_{361011}^P$ 	100 {1, $x_{11}, x_{21}, x_{31}, x_{41}, x_{22}, x_{32}, x_{42}$ }	26 {1, $x_{11}, x_{21}, x_{22}, \lambda_{11}, \lambda_{22}, \lambda_{12}$ }	16 { $x_{11}, x_{21}, x_{22}$ }

Figure 2.2: Universal irreducible numerators for two-loop three-point topologies. For each of the residues,  $\Delta_{i_1 \dots i_n}$ ,  $\Delta_{i_1 \dots i_n}^{\text{int}}$  and  $\Delta'_{i_1 \dots i_n}$  we indicate the number of monomials and the list of their variables.

### 2.3.3 Example: muon-electron scattering

The amplitude of the muon electron scattering at one-loop is described by the 6 diagram presented in Figure 2.5

In particular, we will take a look at the virtual contribution to the  $\sigma_{NLO}$  which can be written as

$$2\text{Re}\mathcal{A}_b^{(0)*} \mathcal{A}_b^{(1)} = \int \frac{d^d q}{(2\pi)^d} \sum_{j=1}^6 \mathcal{I}_j. \quad (2.104)$$

The integrand that will be used as an input for the Adaptive Integrand Decomposition Algorithm (AIDA) can be organized organized in to three groups

$$G_1 = \{\mathcal{I}_1, \mathcal{I}_6\}, \quad G_2 = \{\mathcal{I}_3, \mathcal{I}_2, \mathcal{I}_5\}, \quad G_3 = \{\mathcal{I}_4\}, \quad (2.105)$$

$\mathcal{I}_{i_1 \dots i_r}$	$\Delta_{i_1 \dots i_r}$	$\Delta_{i_1 \dots i_r}^{\text{int}}$	$\Delta'_{i_1 \dots i_r}$
$\mathcal{I}_{1561011}^{\text{P}}$	180 $\{1, x_{21}, x_{31}, x_{41}, x_{22}, x_{32}, x_{42}\}$	8 $\{1, \lambda_{11}, \lambda_{22}, \lambda_{12}\}$	1 $\{1\}$
$\mathcal{I}_{161011}^{\text{P}}$	100 $\{1, x_{11}, x_{21}, x_{31}, x_4, x_{22}, y_3, x_{42}\}$	8 $\{1, x_{11}, \lambda_{11}, \lambda_{22}, \lambda_{12}\}$	3 $\{1, x_{11}\}$
$\mathcal{I}_{131011}^{\text{P}}$	100 $\{1, x_{11}, x_{21}, x_{31}, x_{41}, x_{12}, x_{32}, x_{42}\}$	26 $\{1, x_{11}, x_{21}, x_{12}, \lambda_{11}, \lambda_{22}, \lambda_{12}\}$	16 $\{1, x_{11}, x_{21}, x_{12}\}$
$\mathcal{I}_{21011}^{\text{P}}$	45 $\{1, x_{11}, x_{21}, x_{31}, x_{41}, x_{12}, x_{22}, x_{32}, x_{42}\}$	9 $\{1, x_{11}, x_{12}, \lambda_{11}, \lambda_{22}, \lambda_{12}\}$	6 $\{1, x_{11}, x_{12}\}$
$\mathcal{I}_{21011}^{\text{P}}$	45 $\{1, x_{11}, x_{21}, x_{31}, x_{41}, x_{12}, x_{22}, x_{32}, x_{42}\}$	18 $\{1, x_{11}, x_{21}, x_{12}, x_{22}, \lambda_{11}, \lambda_{22}, \lambda_{12}\}$	15 $\{1, x_{11}, x_{22}, x_{21}, x_{22}\}$

Figure 2.3: Universal irreducible numerators for two-loop two-point topologies. For each of the residues,  $\Delta_{i_1 \dots i_n}$ ,  $\Delta_{i_1 \dots i_n}^{\text{int}}$  and  $\Delta'_{i_1 \dots i_n}$  we indicate the number of monomials and the list of their variables.

$\mathcal{I}_{i_1 \dots i_r}$	$\Delta_{i_1 \dots i_r}$	$\Delta_{i_1 \dots i_r}^{\text{int}}$	$\Delta'_{i_1 \dots i_r}$
$\mathcal{I}_{11011}^{\text{P}}$	45 $\{1, x_{11}, x_{21}, x_{31}, x_{41}, x_{12}, x_{22}, x_{32}, x_{42}\}$	4 $\{1, \lambda_{11}, \lambda_{22}, \lambda_{12}\}$	1 $\{1\}$

Figure 2.4: Universal irreducible numerators for two-loop one-point topologies. For each of the residues,  $\Delta_{i_1 \dots i_n}$ ,  $\Delta_{i_1 \dots i_n}^{\text{int}}$  and  $\Delta'_{i_1 \dots i_n}$  we indicate the number of monomials and the list of their variables.

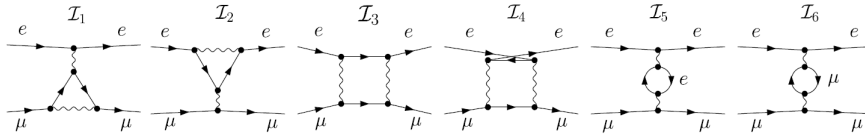


Figure 2.5: Feynman diagrams for the  $\mu e$  scattering at one-loop.

characterized by the following set of denominators

$$\begin{aligned}
G_1 : \quad & D_1 = q^2 - m^2, \\
& D_2 = (q + p_1)^2, \\
& D_3 = (q + p_1 - p_4)^2 - m^2, \\
G_2 : \quad & D_1 = q^2, \\
& D_2 = (q + p_1)^2 - m^2, \\
& D_3 = (q + p_1 - p_4)^2, \\
& D_4 = (q + p_1 - p_4 - p_3)^2, \\
G_3 : \quad & D_1 = q^2, \\
& D_2 = (q + p_2)^2, \\
& D_3 = (q + p_2 - p_4)^2 - m^2, \\
& D_4 = (q + p_1 + p_2 - p_4)^2
\end{aligned}$$

Through the use of AIDA, we can then express this contribution as

$$2\text{Re}\mathcal{A}_b^{(0)} * \mathcal{A}_b^{(1)} = \int \frac{d^d q}{(2\pi)^d} \left[ \frac{c_1}{D_1 D_3} + \frac{c_2}{D_1 D_2 D_3} \right]_{G_1} + \left[ \frac{c_3}{D_2} + \frac{c_4}{D_1 D_2} + \frac{c_5}{D_2 D_4} + \right.$$



$$\begin{aligned}
& + \frac{c_6}{D_1 D_3} + \frac{c_7}{D_1 D_3 D_4} + \frac{c_8}{D_2 D_3 D_4} + \frac{c_9}{D_1 D_2 D_3} + \frac{c_{10}}{D_1 D_2 D_3 D_4} \Big]_{G_2} + \\
& + \left[ \frac{c_{11}}{D_2 D_4} + \frac{c_{12}}{D_1 D_3 D_4} + \frac{c_{13}}{D_1 D_2 D_3 D_4} \right]_{G_3} \quad (2.106)
\end{aligned}$$



# Chapter 3

## Muon Electron scattering

### 3.1 Introduction

#### Magnetic moments

The magnetic dipole momentum is an observable enjoyed by particles, together with the charge, spin and mass, which is currently under investigation in the case of the muon due to a tension between its expected value in the Standard Model and the measured one. Defining as  $\vec{l} = m\vec{r} \times \vec{v}$  the angular momentum of a particle spinning around an axis, we can define the magnetic dipole momentum as

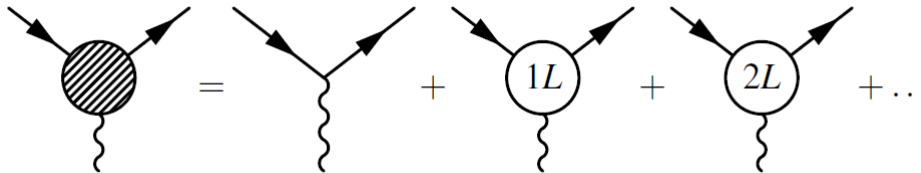
$$\vec{\mu}_l = \frac{q}{2m} \vec{l}. \tag{3.1}$$

Indeed, particles also enjoy an intrinsic quantized angular momentum, the *spin*, represented by the spin- $\frac{1}{2}$  operator  $\vec{\Sigma}$  (built on the Pauli matrices  $\sigma_i, i = 1, 2, 3$ ). Replacing the angular momentum with the spin, we can define the magnetic dipole momentum of a particle as

$$\vec{\mu}_s = \frac{q}{2m} g \vec{\Sigma}, \tag{3.2}$$

where  $g$  is a proportionality constant.

The anomalous magnetic dipole moment is computed considering the interaction of a particle, a *lepton* in the case we are treating, with an external electromagnetic field. In the framework of quantum field theory, this interaction is described by a graph with 3 external lines, computed in a perturbative series:



The tree-level diagram corresponds to the "classical" limit, the result obtained by taking the non-relativistic limit of the interaction between the particle described by the Dirac equation and the external 4-potential. At the first order in the perturbative expansion in QFT, the computation of  $\mu_s$  yields  $g = 2$ , whereas the loop correction amounts to smaller deviation from this value as one goes further in the perturbative expansion. Therefore, it is more convenient to work with

$$a_l = \frac{(g_l - 2)}{2}, \tag{3.3}$$

where  $l$  is the lepton we are considering ( $l = e, \mu, \tau$ ). This quantity that encodes the discrepancy from the "classical" limit is known as *anomaly*. Radiative corrections contain richer interactions than the tree-level counterpart, involving also processes proper of the Electro-Weak and Strong interaction. Thus, the match between measurements and prediction is either a verification of the validity of the Standard Model (SM) or an evidence for new physics still unexplored.

Historically, the first anomaly factor observed was  $a_e$ . Its accurate measurement was performed in 1948 by Kusch and Foley [103], producing  $g_e = 2,00238(6)$ . Its theoretical prediction at the lowest order in the radiative correction was first calculated by Schwinger [104] in QED

$$g_e = 2 \left( 1 + \frac{\alpha}{2\pi} \right) \approx 2.00232 \quad (3.4)$$

$$\rightarrow a_e = \frac{\alpha}{2\pi} \approx 0.00116, \quad (3.5)$$

yielding the first compelling evidence of the validity of the QFT framework. Since then,  $a_e$  has been evaluated up to 5 loop order of precision [105] and is in agreement with the state of the art measurement [106].

In this work, we will address the anomalous magnetic moment of another lepton, the muon. Given the difference in mass with its lighter counterpart,  $a_\mu$  appears to be more sensitive beyond the standard-model effects. This is because the sensitivity of some leptonic g-factor to unknown short-range interaction ought to scale as

$$\frac{\delta a_l}{a_l} \sim \frac{m_l^2}{\Lambda^2} \quad (3.6)$$

taking into account that  $(m_\mu/m_e)^2 \sim 10^4$ ,  $a_\mu$  is expected to be 40000 times more sensible than  $a_e$  to beyond the standard model physics, making it a very good "monitor for new physics". Completing the overview of all the leptonic anomalous momentum,  $a_\tau$  would be even more sensible to this new short range interaction if we could measure it with comparable precision. However, this is beyond our experimental possibilities due to the very short lifetime of  $\tau$ . The up to date experimental value for  $a_\mu$ , obtained after the run-1 of Fermilab  $g - 2$  experiment [107], is

$$a_\mu^{exp} = 116592061(41) \times 10^{-11}, \quad (3.7)$$

whereas the best Standard Model prediction for this observable adds up to [11]

$$a_\mu^{SM} = 116591810(43) \times 10^{-11}, \quad (3.8)$$

displaying a discrepancy of  $\sim 4.2\sigma$  with its experimental measurement.

This tension demands a deeper investigation for this physical observable, both theoretically and experimentally.

From the theoretical point of view, the anomalous magnetic dipole moment receives contribution from different sectors of the standard model, in particular, we can write

$$a_\mu^{SM} = a_\mu^{QED} + a_\mu^{EW} + a_\mu^{HAD}. \quad (3.9)$$

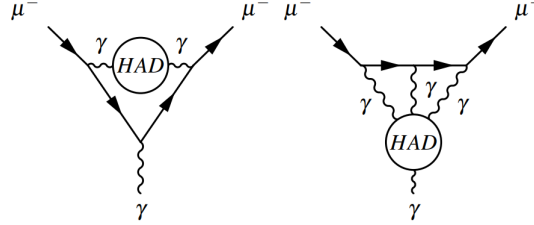
The QED and the EW contribution [11] are, respectively,

$$a_\mu^{QED} = 116584718.931(0.104) \times 10^{-11} \quad (3.10)$$

$$a_\mu^{EW} = 153.6(1.0) \times 10^{-11} \quad (3.11)$$

and, as we can see, are known with good precision compared to the final theoretical estimate of eq. [3.8]. In fact, the major contribution to the uncertainty of the total estimate comes from the strong sector, and thus  $a_\mu^{HAD}$  requires an enhancement of the precision of its estimated value.

Hadrons appear in the anomalous magnetic moment only at higher loop order, mainly through a Vacuum Polarization insertion or as a Light by Light (LbL) scattering as depicted below.



The up-to-date estimates for these components of  $a_\mu$  are

$$a_\mu^{HLbL} = 92(18) \times 10^{-11} \quad (3.12)$$

$$a_\mu^{HVP} = 6845(40) \times 10^{-11}, \quad (3.13)$$

showcasing how their uncertainties are dominant with respect to  $a_\mu^{QED}$  and  $a_\mu^{EW}$ .

Given the nature of strong interactions, perturbative quantum mechanics alone is not enough to obtain sensible estimates of  $a_\mu^{HAD}$ , therefore many techniques such as lattice calculation and data-driven method are used.

A comparison of published result regarding HVP and HLbL is shown in Figure 3.1

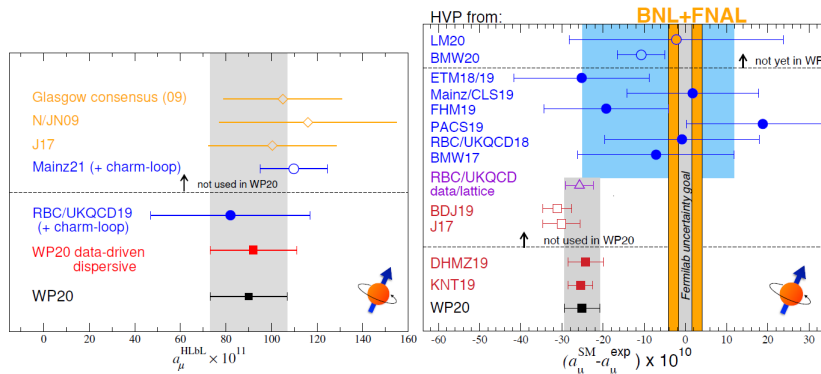


Figure 3.1: **Left:** Comparison of HLbL evaluations to earlier estimates (orange)[CITAZIONI da aggiungere] and more recent lattice calculation (open blue). **Right:** Comparison of theoretical predictions of  $a_\mu$  with experiment (orange band). Each data point represents a different evaluation of leading-order HVP, to which the remaining SM contributions have been added. Red squares show data driven results; filled blue circles indicate lattice-QCD calculations that were taken into account in the WP20 lattice average, while the open ones show results published after the deadline for conclusion in the average; the purple triangle give a hybrid of the two. The SM prediction is shown as the black square and gray band.

We will focus on  $a_\mu^{HVP}$ , the leading hadronic contribution to  $a_\mu^{HAD}$ , and a more precise estimate of its value will be the subject of the following chapter.

### MUonE experiment

Starting from the corresponding Feynman diagram, after due manipulation and rewriting the Vacuum Polarization  $\Pi_{HAD}$  through a dispersion relation, the integral describing  $a_\mu^{HVP}$  is written

as

$$a_\mu^{HVP} = \frac{\alpha}{\pi} \int_{4m_\pi^2}^{\infty} \frac{ds}{s} \int_0^1 dx \frac{x^2(1-x)}{x^2 + \frac{s}{m_\mu^2}(1-x)} \frac{1}{\pi} \text{Im} [\Pi_h(s)] . \quad (3.14)$$

In the range of energies where QCD becomes non-perturbative, we can evaluate the hadronic VP through the experimental measure of the electron annihilation cross section thanks to the optical theorem, since they are related by the following identity:

$$\sigma(s)_{[e^+e^- \rightarrow \text{Hadrons}]} = \frac{4\pi^2\alpha}{s} \frac{1}{\pi} \text{Im} [\Pi_h(s)] . \quad (3.15)$$

However, this measure presents a series of challenges, such as the selection of the desired hadronic states that need to be measured separately, the systematic uncertainty and the use of different experimental techniques, which prevent us from reaching the desired precision in determining  $a_\mu^{HVP}$ .

An alternative to this data-driven method is proposed in [13], in which one observes that by exchanging the integration order between the variables  $x$  and  $t$  the integration over  $dt$  can be carried out as a dispersion relation, yielding

$$a_\mu^{HVP} = \frac{\alpha}{\pi} \int_0^1 dx (1-x) \int_{4m_\pi^2}^{\infty} \frac{ds}{s} \frac{\frac{x^2}{1-x} m_\mu^2}{s + \frac{x^2}{1-x} m_\mu^2} \frac{1}{\pi} \text{Im} [\Pi_h(s)] \quad (3.16)$$

$$= -\frac{\alpha}{\pi} \int_0^1 dx (1-x) \Pi_h[t(x)] , \quad (3.17)$$

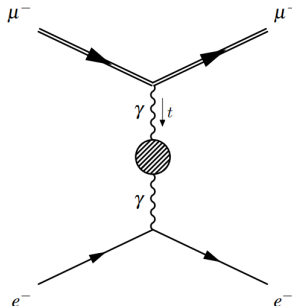
where  $t(x) = \frac{x^2 m_\mu^2}{1-x} < 0$ , thus the VP is evaluated in the space-like region.

Given that  $\Delta\alpha_h(t)$  is related to the running of the QED coupling by  $\Pi_h(t) = -\Delta\alpha_h(t)$ , it is possible to formulate a procedure to measure the Hadronic VP correction to  $a_\mu$  by actually measuring the hadronic contribution to the running of  $\alpha$ . One first measure  $\Delta\alpha$  in the space-like region, subtract the known QED contribution and the result is then substituted into

$$a_\mu^{HVP} = \frac{\alpha}{\pi} \int_0^1 dx (1-x) \Delta\alpha_h[t(x)] . \quad (3.18)$$

This would provide an independent cross-check to the previous, more standard approach. Moreover, this procedure avoids measures of processes with hadronic final states, keeping them completely virtual, and working in the space-like region prevents us from encountering spikes and throats in the VP function, which appear in the time-like region due to phenomena such as pair-production of particles and threshold behavior.

In conclusion, the estimate of  $a_\mu^{HVP}$  involves the evaluation of the running of  $\alpha$  from the cross section of a physical process. The MUonE proposal [14] aims to obtain  $\Delta\alpha_h(t)$  from the measure of the scattering  $\mu^\pm(p_1) e^-(p_2) \rightarrow \mu^\pm(p_3) e^-(p_4)$ , with the focus on the precise estimate of the leading order contribution to  $a_\mu^{HVP}$ :



As a final remark, let us stress that, in this measure, hadronic next to leading order contributions need to be considered since they alter the final result by a relevant amount [108]. This is achieved by evaluating them in an analogous way to what has been done in eq. 3.14 using-time like measurement of  $\sigma(s)_{[e^+e^- \rightarrow \text{Hadrons}]}$ . Then these quantities have to be subtracted from the data together with the QED contribution to the running of alpha, as portrayed in the following equation:

$$\begin{aligned}
 & \text{NLO-hadronic} = \text{data} - \text{QED-Leptonic [analytic]} - \text{NNLO-hadronic [semi-numerical]} - \text{NNLO-hadronic [semi-numerical]} + \text{higher order terms} . \quad (3.19)
 \end{aligned}$$

### 3.1.1 The QED cross section

The precise estimate of  $a_\mu^{HVP}$  is intertwined with the accurate determination of all the components of eq. 3.19. For what concerns the quantities coming from a purely theoretical scope, the evaluation of the QED cross section up to the required accuracy is still a problem under investigation. In this case, given the properties of the electromagnetic interaction, the computation for this quantity can be arranged in a perturbative expansion

$$d\sigma = d\sigma^{(0)} + d\sigma^{(1)} + d\sigma^{(2)} + O(\alpha^{2+n}) , \quad (3.20)$$

in which the apex  $n$  of  $d\sigma^{(n)}$  represents the power of  $\alpha^{2+n}$  to which the said cross-section component is proportional to. These elements are computed through the squared amplitude integrated over the phase space  $\Phi_n$  of the  $n$  particles appearing in it, in this case  $n = 2$ . The Leading Order (LO) contribution  $d\sigma^{(0)}$  is

$$d\sigma^{(0)} = \int d\Phi_n \mathcal{M}_n^{(0)} = \int d\Phi_n \left| \mathcal{A}_n^{(0)} \right|^2 . \quad (3.21)$$

In the Next to Leading Order (NLO) case represented by  $d\sigma^{(1)}$  other than the amplitude  $\mathcal{M}_n^{(1)} = \mathcal{M}^{(1)}(e^- \mu^\pm \rightarrow e^- \mu^\pm)$ , denominated as the *virtual* contribution, we have to consider an additional squared amplitude, the *real* component of the cross section  $d\sigma^{(r)}$ :

$$d\sigma^{(1)} = d\sigma^{(v)} + d\sigma^{(r)} = \int d\Phi_n \mathcal{M}_n^{(1)} + \int d\Phi_{n+1} \mathcal{M}_{n+1}^{(0)} , \quad (3.22)$$

where

$$\mathcal{M}_{n+1}^{(0)} = \left| \mathcal{A}_{n+1}^{(0)} \right|^2 \quad (3.23)$$

$$\mathcal{M}_n^{(1)} = 2 \text{Re} \left[ \mathcal{A}_n^{(1)} \times \left( \mathcal{A}_n^{(0)} \right)^* \right] . \quad (3.24)$$

The *real* cross section is integrated over the  $n + 1$ 's particle phase space, and describes the scattering of the same particles, but has an additional photon between the final states of the reaction:  $\mathcal{M}_{n+1}^{(0)} = \mathcal{M}^{(0)}(e^- \mu^\pm \rightarrow e^- \mu^\pm \gamma)$ .

Although the LO and NLO contribution to the cross section are known [109,110], the evaluation of  $d\sigma^{(2)}$  represents a crucial, yet challenging, computation that has yet to be completed.

At Next to Next to Leading Order (NNLO) the complexity of the calculation grows even further:

$$d\sigma^{(2)} = d\sigma^{(vv)} + d\sigma^{(vr)} + d\sigma^{(rr)} \quad (3.25)$$

$$= \int d\Phi_n \mathcal{M}_n^{(2)} + \int d\Phi_{n+1} \mathcal{M}_{n+1}^{(1)} + \int d\Phi_{n+2} \mathcal{M}_{n+2}^{(0)}, \quad (3.26)$$

where

$$\mathcal{M}_{n+2}^{(0)} = \left| \mathcal{A}_{n+2}^{(0)} \right|^2 \quad (3.27)$$

$$\mathcal{M}_{n+1}^{(1)} = 2 \operatorname{Re} \left[ \mathcal{A}_{n+1}^{(1)} \times \left( \mathcal{A}_{n+1}^{(0)} \right)^* \right] \quad (3.28)$$

$$\mathcal{M}_n^{(2)} = 2 \operatorname{Re} \left[ \mathcal{A}_n^{(2)} \times \left( \mathcal{A}_n^{(0)} \right)^* \right], \quad (3.29)$$

involving real and double real (hence, with two additional photons in the final states) contributions.

Among all the components of the NNLO cross section required for the MUonE experiment, we will discuss the calculation of the two-loop amplitude  $\mathcal{M}_n^{(2)}$  [4], essential for the evaluation of  $d\sigma^{(vv)}$ .

### 3.2 The Amplitude analytical evaluation

Let us consider the annihilation reaction between a massless fermion  $f$  ( $m_f = 0$ ) and its antiparticle, producing a particle-antiparticle couple of heavier fermions  $F$  that have a non-zero mass ( $m_F = M$ ):

$$f^-(p_1) + f^+(p_2) \rightarrow F^-(p_3) + F^+(p_4). \quad (3.30)$$

This scattering is parameterized by the mandelstam invariants

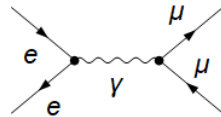
$$s = (p_1 + p_2)^2, \quad t = (p_1 - p_3)^2, \quad \text{and} \quad u = (p_2 - p_3)^2, \quad (3.31)$$

satisfying the condition  $s + t + u = 2M^2$ . This amplitude is linked to the scattering required for the MUonE experiment through a crossing relation, a substitution rule for the mandelstam invariant, with the advantage of easing the cross-check of the result.

The four-point unrenormalized or bare amplitude  $\mathcal{A}_b$  for this process admits a perturbative expansion in the bare coupling constant  $\alpha_b \equiv e_b^2/4\pi$ , which up to the inclusion of second-order corrections reads as

$$\begin{aligned} \mathcal{A}_b(\alpha_b) &= 4\pi\alpha_b S_\epsilon \mu^{-2\epsilon} \\ &\times \left[ \mathcal{A}_b^{(0)} + \left( \frac{\alpha_b}{\pi} \right) \mathcal{A}_b^{(1)} + \left( \frac{\alpha_b}{\pi} \right)^2 \mathcal{A}_b^{(2)} \right], \end{aligned} \quad (3.32)$$

where  $\mathcal{A}_b^{(n)}$  indicates the  $n$ -loop bare amplitude,  $S_\epsilon \equiv (4\pi e^{-\gamma_E})^\epsilon$  and  $\mu$  is the 't Hooft mass scale. The leading order (LO) term  $\mathcal{A}_b^{(0)}$ , referred to as *Born term*, receives contribution from a single tree-level Feynman diagram,



and its squared LO amplitude, summed over the final spins and averaged over the initial states, reads

$$\mathcal{M}_b^{(0)} = \frac{1}{4} \sum_{\text{spins}} |\mathcal{A}_b^{(0)}|^2$$



$$= \frac{1}{s^2} [2(1 - \epsilon)s^2 + 4(t - M^2)^2 + 4st], \quad (3.33)$$

for external states treated in  $d = 4 - 2\epsilon$  space-time dimensions according to the conventional dimensional regularization (CDR) scheme [111], which we use throughout the whole computation. The analytic evaluation of  $\mathcal{M}_b^{(1)}$  and  $\mathcal{M}_b^{(2)}$  has been completely automated, within an in-house software, which can be applied to generic one- and two-loop amplitudes. As a first step, the Feynman diagrams contributing to the NLO and NNLO corrections to the scattering amplitudes are generated through the MATHEMATICA package FEYNARTS [112], and they are depicted in Fig. 3.2 and Fig. 3.3 respectively. The algebraic manipulation to simplify the Dirac- $\gamma$  algebra

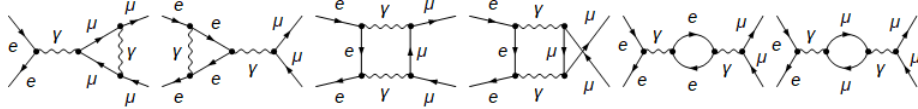


Figure 3.2: One-loop diagrams for the  $e^+ e^- \rightarrow \mu^+ \mu^-$  scattering

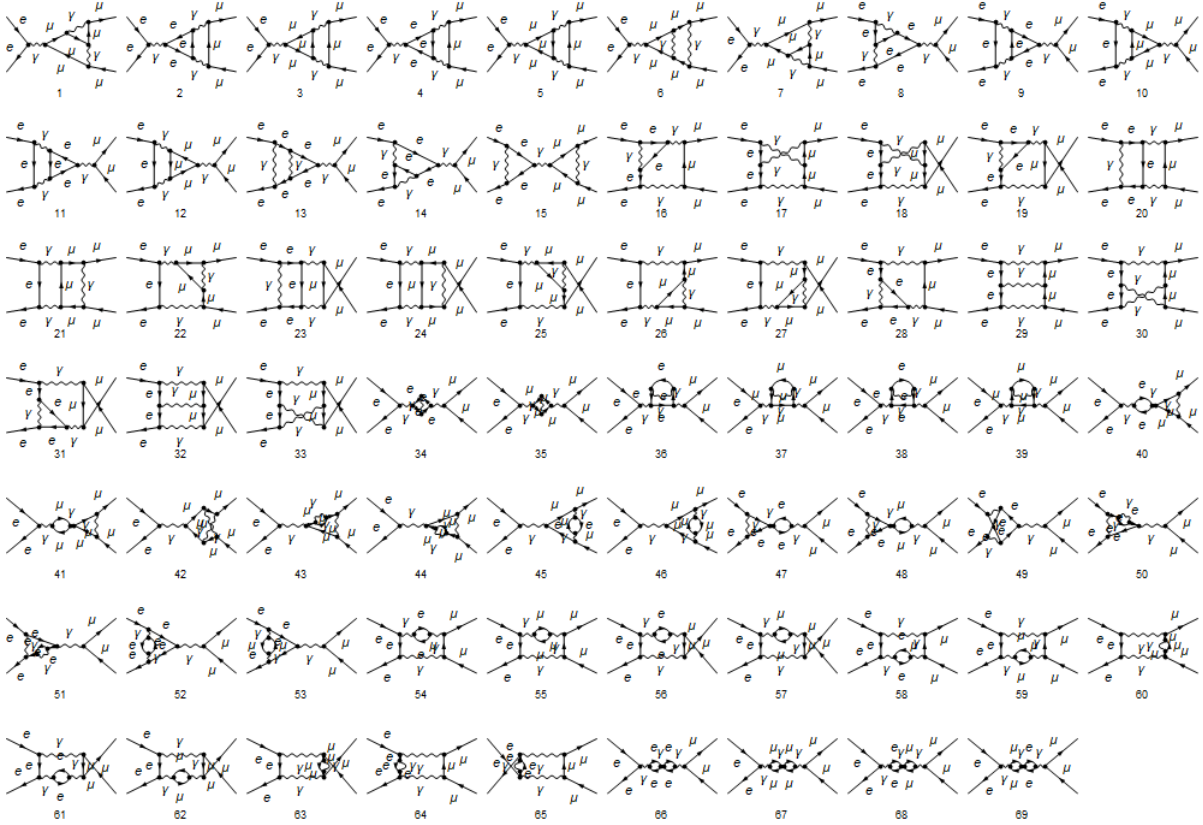


Figure 3.3: Diagrams appearing in the two loop amplitude for  $e^+ e^- \rightarrow \mu^+ \mu^-$  scattering

and the spin sum are carried out by means of the FEYNCALC [113–115] package. Each  $n$ -loop graph  $G$  (interfered with the Born amplitude) corresponds to an integrand written in terms of scalar products between external,  $p_i^\nu$ , and internal,  $k_i^\nu$ , momenta. Therefore, the  $\ell$  loop bare amplitude can be written in general as [can be generically written as,

$$\mathcal{M}_b^{(\ell)} = (S_\epsilon)^\ell \int \prod_{i=1}^{\ell} \frac{d^d q_i}{(2\pi)^d} \sum_G \frac{N_G}{\prod_{\sigma \in G} D_\sigma} \quad , \quad (3.34)$$

where:  $N_G = N_G(p_i, k_i)$  indicates the numerator, and  $D_\sigma = D_\sigma(p_i, k_i, M)$  are the denominators corresponding to the internal lines of the integral family  $G$ .

Integrands are simplified by employing the *adaptive integrand decomposition method*, implemented in the AIDA framework [116] to

$$\mathcal{M}_b^{(\ell)} = (S_\epsilon)^\ell \int \prod_{i=1}^{\ell} \frac{d^d q_i}{(2\pi)^d} \sum_G \sum_{k=0}^r \sum_{\{i_1 \dots i_k\}} \frac{\Delta'_{i_1 \dots i_k; G}}{D_{i_1} \dots D_{i_k}}. \quad (3.35)$$

At this point, the intermediate results emerging from the integrand decomposition can be further simplified by means of IBP identities [87, 117]. Our software is interfaced with the publicly available codes REDUZE [61] and KIRA [64], and, for each diagram, it produces the files for the automatic generation of the IBP relations.

After the decomposition phase, the interference terms  $\mathcal{M}_b^{(\ell)}$  become linear combinations of a set of Master Integrals  $\mathbf{I}^{(\ell)}$ ,

$$\mathcal{M}_b^{(\ell)} = \mathbb{C}^{(\ell)} \cdot \mathbf{I}^{(\ell)}, \quad (3.36)$$

where  $\mathbb{C}^{(\ell)}$  is a vector of coefficients that are rational functions of  $\epsilon$  and the kinematic variables,  $s, t, M^2$ . In particular,  $\mathcal{M}_b^{(1)}$  and  $\mathcal{M}_b^{(2)}$  are conveniently expressed in terms of 12 and 264 MIs respectively, which have been already analytically computed. Two- and three-point functions have been known since long [46, 118, 119], while planar and non-planar four-point integrals were computed in [51, 52], using the differential equation method by the Magnus exponential, and independently in [120–122] and are depicted in Fig 3.4.

Lastly, the analytic expressions of  $\mathcal{M}_b^{(n)}$  can be written as a Laurent series around  $d = 4$  space-time dimensions ( $\epsilon = 0$ )

$$\mathcal{M}_b^{(n)} = \sum_i b_i \epsilon^i, \quad (3.37)$$

with the coefficients  $b_i$  that contain Generalized Polylogarithms (GPLs) [49], iterated integrals defined in eq. (2.74).

Specifically, in our case the two-loop interference term contains 4063 GPLs with up to weight four, whose arguments are written in terms of 18 letters,  $w_i = w_i(x, y, z)$ , which depend on the Mandelstam variables through the relations,

$$-\frac{s}{M^2} = x, \quad -\frac{t}{M^2} = \frac{(1-y)^2}{y}, \quad -\frac{u-M^2}{s-M^2} = \frac{z^2}{y}. \quad (3.38)$$

(see [51, 52] for more details). For the numerical evaluation of GPLs, we use public libraries as GiNAC [92] and HANDYG [123]. The flow chart of the entire algorithm is shown in Fig. 3.5.

### 3.2.1 Renormalization

The one- and two-loop diagrams contributing to  $\mathcal{M}_b^{(1)}$  and  $\mathcal{M}_b^{(2)}$  contain infrared (IR) and ultraviolet (UV) divergences, the latter of which needs to be removed to compute the cross section. To do so, the bare lepton fields ( $\psi_l$ , with  $l = f, F$ , for massless and massive leptons, respectively) and the photon field ( $A^\mu$ ), as well as the bare mass of the massive lepton are renormalized as follows,

$$\psi_b = \sqrt{Z_2} \psi, \quad A_b^\mu = \sqrt{Z_3} A^\mu, \quad M_b = Z_M M, \quad (3.39)$$

where, to simplify the notation, the label  $l$  in the lepton fields is understood and restored when required. The renormalization of the QED interaction vertex,

$$\mathcal{L}_{\text{int}} = e_b \bar{\psi}_b A_b \psi_b = e Z_1 \bar{\psi} A \psi, \quad (3.40)$$

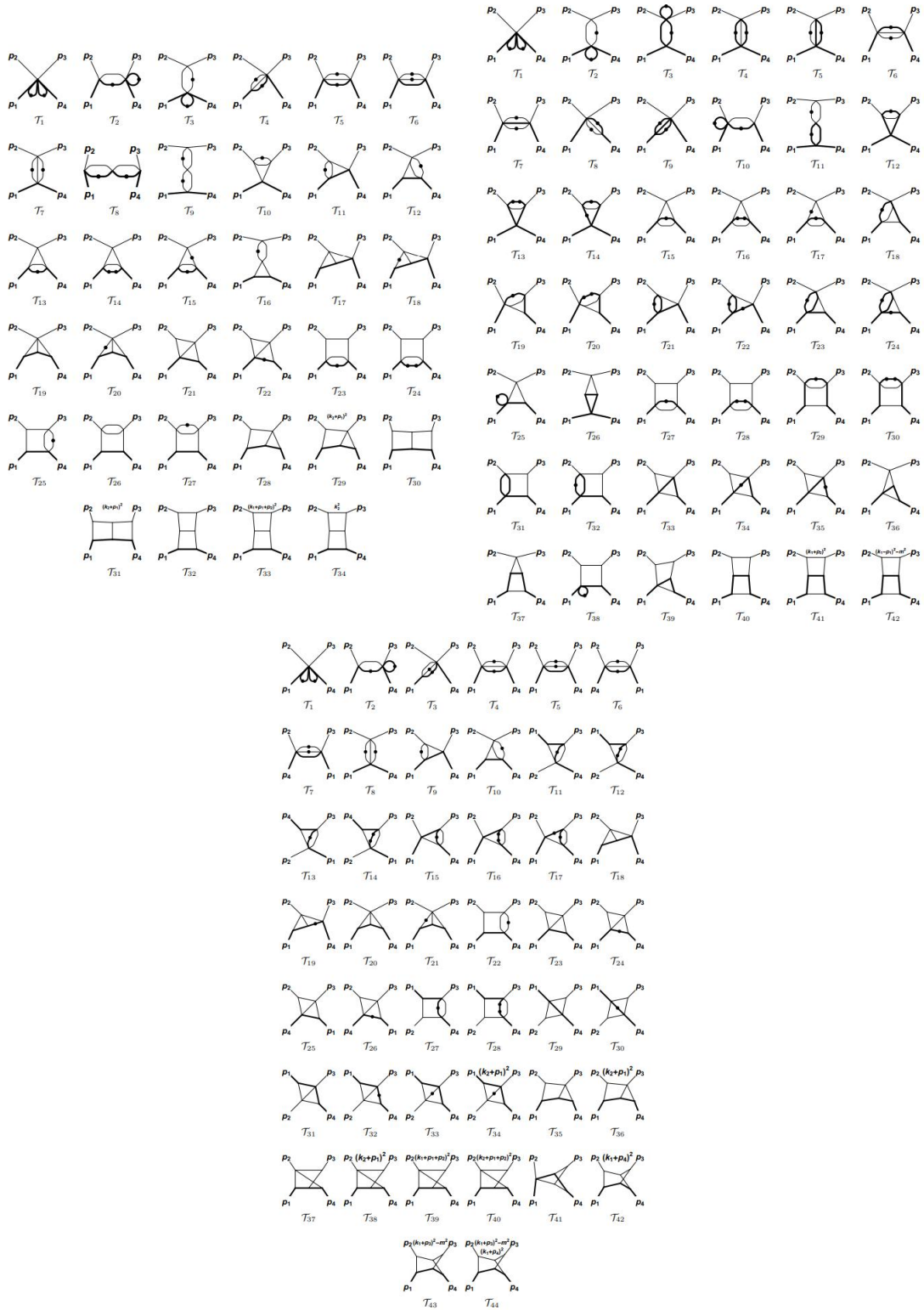


Figure 3.4: Two-loop 4-particles MI required for the computation of the two-loop Amplitude. The thicker lines indicate massive particles.

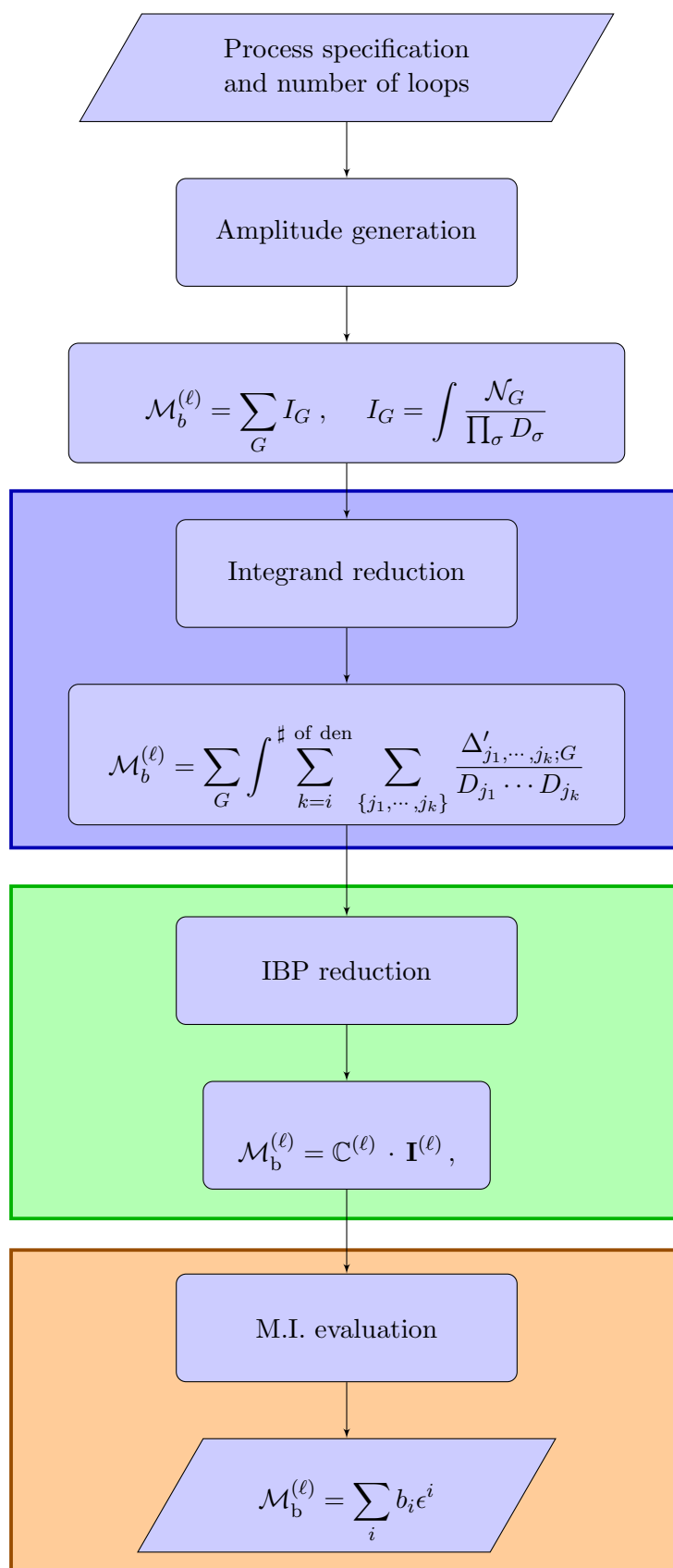


Figure 3.5: Flow chart of the algorithm for the evaluation of scattering amplitude

can then be entirely fixed using the QED Ward identity, which implies  $Z_1 = Z_2$ . This leads to a simple relation between the renormalized charge and the bare charge (obtained by applying Eq. (3.39) to the bare interaction term and comparing the two renormalized expressions)  $e Z_1 = e_b Z_2 \sqrt{Z_3}$ , yielding  $e = e_b \sqrt{Z_3}$ . The lepton wave functions and the mass of the massive lepton are renormalized in the on-shell scheme, namely,  $Z_{2,f} = Z_{2,f}^{\text{OS}}$ ,  $Z_{2,F} = Z_{2,F}^{\text{OS}}$ ,  $Z_M = Z_M^{\text{OS}}$ . The coupling constant is renormalized in the  $\overline{\text{MS}}$  scheme at the scale  $\mu^2$ ,

$$\alpha_b S_\epsilon = \alpha(\mu^2) \mu^{2\epsilon} Z_\alpha^{\overline{\text{MS}}}, \quad (3.41)$$

with  $Z_\alpha^{\overline{\text{MS}}} = 1/Z_3^{\overline{\text{MS}}}$ . In this way, the renormalized amplitude is obtained by multiplying the bare amplitude by a factor  $\sqrt{Z_{2,l}}$  for any external lepton  $l$ , hence,

$$\mathcal{A} = Z_{2,f} Z_{2,F} \hat{\mathcal{A}}_b, \quad (3.42)$$

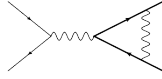
where  $\hat{\mathcal{A}}_b = \mathcal{A}_b(\alpha_b = \alpha_b(\alpha), M_b = M_b(M))$ , namely expressing the bare coupling and mass in terms of their renormalized counterparts.

Let us observe that  $\mathcal{A}$  depends on four renormalization constants, namely  $Z_\alpha^{\overline{\text{MS}}}, Z_{2,f}^{\text{OS}}, Z_{2,F}^{\text{OS}}, Z_M^{\text{OS}}$ . They are simply indicated as  $Z_j$ , with  $j = \{\alpha, f, F, M\}$  respectively, and admit a perturbative expansions in  $\alpha$ ,

$$Z_j = 1 + \left(\frac{\alpha}{\pi}\right) \delta Z_j^{(1)} + \left(\frac{\alpha}{\pi}\right)^2 \delta Z_j^{(2)} + \mathcal{O}(\alpha^3). \quad (3.43)$$

They are computed from a subset of one- and two-loop integrals appearing in the amplitude and their derivation can be summarized as follows:

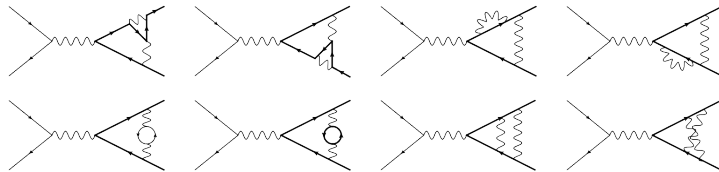
- $Z_F$  receives contribution both at one- and two-loops in the form of  $\delta Z_F^{(1)}$  and  $\delta Z_F^{(2)}$  respectively. In the first case, the counterterm is evaluated from the one-loop diagram



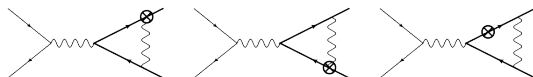
in the  $s = 0$  limit, yielding

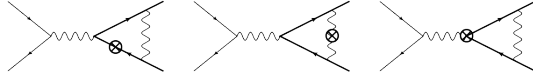
$$\begin{aligned} \delta Z_F^{(1)} = & -\frac{3}{4\epsilon} - \frac{3L_\mu}{4} - 1 \\ & + \epsilon \left( -\frac{3L_\mu^2}{8} - L_\mu - \frac{\pi^2}{16} - 2 \right) \\ & + \epsilon^2 \left( -\frac{L_\mu^3}{8} - \frac{L_\mu^2}{2} - \frac{\pi^2 L_\mu}{16} - 2L_\mu + \frac{\zeta_3}{4} - \frac{\pi^2}{12} - 4 \right), \end{aligned} \quad (3.44)$$

with  $L_\mu \equiv \ln(\mu^2/M^2)$ . In the second case, instead, the following two-loop diagrams need to be considered



Combining them with the one-loop counterterm diagrams

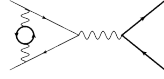




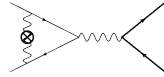
and taking the  $s = 0$  limit yields the second-order component of the counterterm:

$$\begin{aligned} \delta Z_F^{(2)} = & n_h \left( \frac{1}{\epsilon} \left( \frac{L_\mu}{4} + \frac{1}{16} \right) + \frac{3L_\mu^2}{8} + \frac{11L_\mu}{24} - \frac{5\pi^2}{16} + \frac{947}{288} \right) \\ & + n_l \left( -\frac{1}{8\epsilon^2} + \frac{11}{48\epsilon} + \frac{L_\mu^2}{8} + \frac{19L_\mu}{24} + \frac{\pi^2}{12} + \frac{113}{96} \right); \end{aligned}$$

- $Z_f$  receives a contribution only at two-loop. This is because the Feynman integral that should contribute to  $\delta Z_f^{(1)}$  results in a scaleless integral once we evaluate it in the kinematical limit needed for the on shell counterterm. For the same reason, at two-loop the only integral contributing to  $\delta Z_f^{(2)}$  is



which, combined with its one-loop counterterm



gives

$$\delta Z_f^{(2)} = n_h \left( \frac{L_\mu}{8} + \frac{1}{16\epsilon} - \frac{5}{96} \right), \quad (3.45)$$

in the  $s = 0$  limit.

- $Z_M$  is completely determined from the counterterm for the massive fermion  $F$  with

$$\delta Z_M^{(1)} = \delta Z_F^{(1)}; \quad (3.46)$$

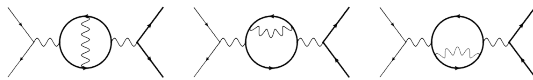
- $Z_\alpha$  receives contribution both at the one- and two-loop level. At one-loop the diagram contributing to it are



Since this counterterm is computed in  $\overline{\text{MS}}$  scheme, its value is obtained from the epsilon divergent part of such diagrams, yielding

$$\delta Z_\alpha^{(1)} = \frac{(n_h + n_l)}{3\epsilon}. \quad (3.47)$$

At two-loop, the diagram involved are:



that combined with the one-loop counterterm diagrams



together with their electronic counterparts (identical diagrams where the fermionic loop has an electron flowing into it) that yields

$$\delta Z_\alpha^{(2)} = \frac{(n_h + n_l)^2}{9\epsilon^2} + \frac{(n_h + n_l)}{8\epsilon}. \quad (3.48)$$

After substituting the expansions of the bare amplitude given in eq. (3.32) and the renormalization constants likewise expanded in in Eq. (3.43) inside of eq. (3.42), the UV renormalized two-loop amplitude reads

$$\mathcal{A}(\alpha) = 4\pi\alpha \left[ \mathcal{A}^{(0)} + \left(\frac{\alpha}{\pi}\right) \mathcal{A}^{(1)} + \left(\frac{\alpha}{\pi}\right)^2 \mathcal{A}^{(2)} \right], \quad (3.49)$$

up to second-order corrections in  $\alpha$ . Expressing  $n$ -loop coefficients  $\mathcal{A}^{(n)}$  in terms of those appearing in the bare amplitude, yields

$$\mathcal{A}^{(0)} = \mathcal{A}_b^{(0)}, \quad (3.50a)$$

$$\mathcal{A}^{(1)} = \mathcal{A}_b^{(1)} + \left(\delta Z_\alpha^{(1)} + \delta Z_F^{(1)}\right) \mathcal{A}_b^{(0)}, \quad (3.50b)$$

$$\begin{aligned} \mathcal{A}^{(2)} = & \mathcal{A}_b^{(2)} + \left(2\delta Z_\alpha^{(1)} + \delta Z_F^{(1)}\right) \mathcal{A}_b^{(1)} \\ & + \left(\delta Z_\alpha^{(2)} + \delta Z_F^{(2)} + \delta Z_f^{(2)} + \delta Z_F^{(1)} \delta Z_\alpha^{(1)}\right) \mathcal{A}_b^{(0)} \\ & + \delta Z_M^{(1)} \mathcal{A}_b^{(1, \text{mass CT})}. \end{aligned} \quad (3.50c)$$

Let us stress that the last term in eq. (3.50c) contains the extra one-loop contribution of diagrams that have an insertion of the mass counterterm in the massive propagators in all possible ways, as depicted in Fig. 3.6.

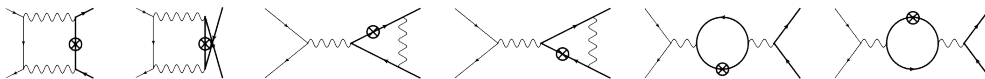


Figure 3.6: Counterterm diagrams for mass renormalization.

### 3.2.2 Results

The renormalized amplitudes  $\mathcal{A}^{(n)}$  ( $n = 0, 1, 2$ ) and the renormalized coupling  $\alpha_b$  obtained in this way allow us to compute the Born term,  $\mathcal{M}^{(0)}$ , and the renormalized interference terms, at one-loop,  $\mathcal{M}^{(1)}$ , and at two-loop,  $\mathcal{M}^{(2)}$ .

The latter two quantities are the main results of this thesis. They are expressed in a Laurent series in  $\epsilon$

$$\mathcal{M}^{(1)} = \frac{\mathcal{M}_{-2}^{(1)}}{\epsilon^2} + \frac{\mathcal{M}_{-1}^{(1)}}{\epsilon} + \mathcal{M}_0^{(1)} + \mathcal{M}_1^{(1)} \epsilon + \mathcal{O}(\epsilon^2), \quad (3.51a)$$

$$\mathcal{M}^{(2)} = \frac{\mathcal{M}_{-4}^{(2)}}{\epsilon^4} + \dots + \frac{\mathcal{M}_{-1}^{(2)}}{\epsilon} + \mathcal{M}_0^{(2)} + \mathcal{O}(\epsilon). \quad (3.51b)$$

$\mathcal{M}^{(1)}$  is computed analytically both in the pair-production region,  $s > 4M^2$ ,  $t < 0$ , and the non-physical region. The former can be used to predict the IR poles of  $\mathcal{M}^{(2)}$  directly in the production region, as discussed in Appendix A.  $\mathcal{M}^{(2)}$  is computed analytically in the non-physical region,  $s < 0$ ,  $t < 0$ , and its analytic continuation is performed numerically. The renormalized one- and the two-loop interference terms are conveniently decomposed in gauge-invariant components,

characterized by the numbers of closed fermion loops, indicated by  $n_l$  and  $n_h$ , separating the contribution coming from diagrams containing massless and massive lepton loops, as

$$\mathcal{M}^{(1)} = A^{(1)} + n_l B_l^{(1)} + n_h C_h^{(1)}, \quad (3.52a)$$

$$\begin{aligned} \mathcal{M}^{(2)} = & A^{(2)} + n_l B_l^{(2)} + n_h C_h^{(2)} + n_l^2 D_l^{(2)} \\ & + n_h n_l E_{hl}^{(2)} + n_h^2 F_h^{(2)}. \end{aligned} \quad (3.52b)$$

In Table 3.1, we show the numerical values of the coefficients  $A, B, C, D, E, F$ , at a particular phase-space point, in the massive fermion pair-production region.

### 3.2.3 Additional tests

In order to check the validity of our expression, several checks have been performed. In particular, the master integral for the diagrams in QED can be used to build the analytic expressions for some of the gauge-invariant components of the two-loop amplitude of the process  $q\bar{q} \rightarrow t\bar{t}$  in QCD [120, 121, 124, 125]: specifically, our results (after properly accounting for the color factor and evaluating it in the region of heavy lepton pair-production) agree with the numerical coefficients  $E_l^q, E_h^q, F_l^q, F_{lh}^q, F_h^q$  provided in the Table 1 of Ref. [120, 124, 125], which receive contributions only from Abelian diagrams; moreover, the agreement on the coefficients of the poles at other phase-space points of the color coefficients mentioned above has been compared against the formula for the IR poles of amplitudes at two-loop in QCD, given in Ref. [126], and are in perfect agreement with it.



	$\epsilon^{-4}$	$\epsilon^{-3}$	$\epsilon^{-2}$	$\epsilon^{-1}$	$\epsilon^0$	$\epsilon$
$\mathcal{M}^{(0)}$	-	-	-	-	$\frac{181}{100}$	-2
$A^{(1)}$	-	-	$-\frac{181}{100}$	1.99877525	22.0079572	-11.7311017
$B_l^{(1)}$	-	-	-	-	-0.069056030	4.94328573
$C_h^{(1)}$	-	-	-	-	-2.24934027	2.54943566
$A^{(2)}$	$\frac{181}{400}$	-0.499387626	-35.4922919	19.4997261	49.0559119	-
$B_l^{(2)}$	-	$-\frac{181}{400}$	0.785712779	-16.1576674	-3.75247701	-
$C_h^{(2)}$	-	-	1.12467013	-9.50785825	-25.8771503	-
$D_l^{(2)}$	-	-	-	-	-3.96845688	-
$E_{h_l}^{(2)}$	-	-	-	-	-4.88512563	-
$F_h^{(2)}$	-	-	-	-	-0.158490810	-

Table 3.1: Numerical values of the leading order squared amplitude, in eq. (3.33), and of the coefficients appearing in the decomposition of the renormalized one- and two-loop amplitudes in Eqs. (3.52), evaluated at the phase space point  $s/M^2 = 5$ ,  $t/M^2 = -5/4$ ,  $\mu = M$ .



## Chapter 4

# Intersection theory and Feynman integrals

### 4.1 Introduction

The evaluation of the theoretical expectation values for the observables measured at modern colliders through the calculation of scattering amplitude is indeed a very challenging task. As we have seen in previous chapters, many mathematical tools have been developed and exploited to simplify and automatize the demanding step required to complete such an endeavor. Among all of them, indeed IBPs play a key role in multiple parts of the computation, both reducing the number of integrals that need to be evaluated in order to obtain the scattering amplitude, and computing the differential equation required for the MIs computation. Although integration by parts identities have been studied since a couple of decades now and a lot of effort has been put in improving and refining such powerful instrument, for multi-loop and multiscale scattering amplitudes solving the system of IBP relation may still represent a formidable task. On top of that, IBP decomposition is a very simple instrument from the mathematical point of view, but suggests the existence of a deeper and more complex mathematical structure behind Feynman integrals, which is not fully exploited in such framework.

Recently, a new perspective on the problem of the reduction of Feynman integrals to a minimal basis has been proposed in [68]. Using a novel mathematical tool borrowed from intersection theory [69–81] it was suggested that Feynman integrals actually belonged to a vector space, and it was possible to define an operation to directly project any integral on the MI basis, effectively bypassing the system solution required by the more standard approach given by IBPs. We elaborated on this very promising proposal consolidating its applicability to Feynman integrals and extending it to a much wider set of cases, effectively obtaining the complete decomposition of Feynman integrals in terms of MIs by means of intersection theory [1–3], as well as developing and automating a general algorithm for the evaluation of such decomposition which has been implemented in an in-house code. As a result, several relevant contributions have been triggered by these novel results [127–135] paving the way for a bright future for this newly discovered approach.

This new approach is better understood by looking at Feynman integrals in parametric representation rather than in the usual momentum space one. Therefore, we will focus on Baikov representation from here on, which was presented in section 2.1.1. Let us briefly recall the shape taken by Feynman integrals under this reparametrization, as defined in eq. (2.23)

$$I = \int_{\mathcal{C}} u(\mathbf{z}) \varphi(\mathbf{z}) , \quad (4.1)$$

where  $u(\mathbf{z})$  is a multivalued function of  $\mathbf{z} = \{z_1, z_2, \dots, z_n\}$  described by the Baikov polynomial

$$u(\mathbf{z}) = B(\mathbf{z})^\gamma \quad (4.2)$$

( $u(\mathbf{z}) = \prod_i B_i(\mathbf{z})^{\gamma_i}$  in more general cases) with  $\gamma \notin \mathbb{Z}$  which depends on the dimensions and the number of loops. Intuitively, this function holds the information regarding the Feynman graph we are considering: the number of external legs, loops and the denominators describing the process under study.

On the other hand,  $\varphi(\mathbf{z})$  is an  $n$ -form with poles at the zeros of  $B$  that retains information regarding the specific integral in consideration, such as the powers to which the denominators are risen and what the numerator is.

$$\varphi(\mathbf{z}) = \hat{\varphi}(\mathbf{z})d\mathbf{z} \quad \hat{\varphi}(\mathbf{z}) = \frac{f(\mathbf{z})}{z_1^{x_1} z_2^{x_2} \dots z_n^{x_n}}, \quad (4.3)$$

with  $\hat{\varphi}(\mathbf{z})$  its differential stripped version, while  $f(\mathbf{z})$  is a rational function and  $x_i$  are integer exponents,  $x_i \notin \mathbb{Z}$ .

These objects are considered in the affine variety  $X$ , defined by

$$X = \mathbb{C}\mathbb{P}^n \setminus D \quad \text{with} \quad D = \{\mathbf{z} \in \mathbb{C}^n \mid B(\mathbf{z}) = 0\}, \quad (4.4)$$

with  $D = \bigcup D_i$  with  $D_i = \{\mathbf{z} \in \mathbb{C}^n \mid B_i(\mathbf{z}) = 0\}$  in the case of Baikov loop-by-loop.

Lastly  $\mathcal{C}$  is the path of integration which in Baikov representation satisfies

$$B(\partial\mathcal{C}) = 0, \quad (4.5)$$

hence the baikov polynomial vanishes on its boundaries.

IBPs as we know are identities linking integral with different powers of denominators, and are derived by the vanishing of a total derivative. With this parameterization, it translates to

$$I = \int_{\mathcal{C}} d(u\xi) = 0. \quad (4.6)$$

Let us stress that this identity holds in absence of boundary terms which is granted by the property outlined in eq. (4.2), a characteristic feature of Baikov representation.

As said, these relation links integrals with different integrands, which would amount to different  $\hat{\xi}(\mathbf{z})$ . Let us manipulate eq. (4.5) in order to highlight the effect of the total derivative on this term of our expression:

$$0 = \int_{\mathcal{C}} d(u\xi) = \int_{\mathcal{C}} (du \wedge \xi + u d\xi) = \int_{\mathcal{C}} u \left( \frac{du}{u} \wedge + d \right) \xi \equiv \int_{\mathcal{C}} u \nabla_{\omega} \xi, \quad (4.7)$$

where

$$\nabla_{\omega} = d + \omega \wedge \quad \omega = \frac{du}{u} \wedge. \quad (4.8)$$

Since the expression above integrates to zero, we can state that

$$\int_{\mathcal{C}} u(\mathbf{z}) \varphi(\mathbf{z}) = \int_{\mathcal{C}} u(\mathbf{z}) (\varphi(\mathbf{z}) + \nabla_{\omega} \xi(\mathbf{z})), \quad (4.9)$$

hence, the forms  $\varphi$  and  $\varphi + \nabla_{\omega} \xi$  describe Feynman integrals which are equal upon integration and which are *equivalent* through IBPs decomposition. This suggests the definition of an equivalence class.

#### 4.1.1 Twisted Cohomology group

Let us consider a natural equivalence class between forms: the *de Rham Cohomology*. This mathematical object is characterized by an operator, the full differential operator  $d$ , which acts on the group of  $n$ -forms defined on an  $m$ -dimensional manifold  $X$ :  $\Omega^n(X)$ . Its action sends an

$n$ -form to an  $(n + 1)$ -form, linking their respective groups. In fact, it defines a *cochain complex* through its reiterated application

$$0 \xrightarrow{d} \Omega^0(X) \xrightarrow{d} \Omega^1(X) \xrightarrow{d} \dots \xrightarrow{d} \Omega^n(X) \xrightarrow{d} 0. \quad (4.10)$$

The second key property that allows us to define a Cohomology group is the property of  $d$  to be nihil potent:

$$d^2 = 0, \quad (4.11)$$

which follows from *Schwartz Lemma*. Recalling that an exact form is an  $n$ -form generated by the action of a total derivative on a  $(n - 1)$ -form ( $\varphi = d\xi$ ), whereas a closed one is a form that satisfies  $d\varphi = 0$ , from eq. [4.11](#) it follows that the group of exact form is contained in to the group of closed one. Hence, we can define the quotient group

$$H_{dR}^n(X) = \frac{\{ \varphi \in \Omega^n(X) \mid d\varphi = 0 \}}{\{ \varphi \in \Omega^{n-1}(X) \mid \varphi = d\xi \}}, \quad (4.12)$$

in which the forms  $\varphi$  and  $\varphi + d\xi$  are identified and considered equivalent.

Therefore, the structure given by Cohomology seems appropriate to describe the equivalence shown in eq. [4.9](#), though it slightly differs from  $H_{dR}^n$  in the operator characterizing it: instead of solely the total differential, we need to consider  $\nabla_\omega$  in order to describe IBP identities, taking into account also  $\omega$ . Therefore, we can define the *twisted Cohomology group* [69](#)

$$H_\omega^n = \frac{\{ \varphi \in \Omega^n(X) \mid \nabla_\omega \varphi = 0 \}}{\{ \varphi \in \Omega^n(X) \mid \varphi = \nabla_\omega \xi \}}, \quad (4.13)$$

which elements will be represented as  $\langle \varphi |$ .

### 4.1.2 Twisted Homology group

The definition of a twisted cohomology group of forms relies on the identity portrayed in eq. [4.5](#) which allows us to define an equivalence class between integrals that differ by a total derivative. After fixing a specific branch  $u_C$  of the multivalued function  $u$  on the path  $\mathcal{C}$ , it is possible to use Stokes theorem to trade the total differential appearing in the integral with a boundary operator acting on the integration region

$$0 = \int_{\mathcal{C}} d(u_C \xi) = \int_{\partial \mathcal{C}} u_C \xi. \quad (4.14)$$

This highlights the possibility of constructing an equivalence class between contour of integration, and consequentially allowing us to define a structure analogous to the one presented in eq. [4.13](#) but for cycles  $\mathcal{C}$ : the twisted Homology group [69](#).

Let us first address single-valued integrals. In this case, we consider integration regions that are defined as linear combination of *singular  $n$ -simplices*. While  $n$ -simplices are  $n$ -dimensional generalizations of triangles and tetrahedrons defined as

$$\Delta^n = \left\{ \sum_{i=0}^n t_i v_i \mid 0 \leq t_i \leq 1, \sum_{i=0}^n t_i = 1 \right\}, \quad (4.15)$$

where  $\{v_0, \dots, v_n\}$  are  $n + 1$  affinely independent points in  $\mathbb{R}^n$ , singular simplices are their images through the action of a continuous map  $\sigma : \Delta^n \rightarrow X$ . Thus, we can define the path of integration  $\gamma$  of a single-valued integral as a *singular chain*

$$\gamma = \sum_i c_i \sigma_i, \quad c_i \in \mathbb{Z}. \quad (4.16)$$

We will call  $C_n(X)$  the group generated by singular chains of degree  $n$ .

It is possible to define a boundary operator  $\partial_n$  that acts on the elements of such a group by decomposing singular simplices in a combination of their  $(n - 1)$  dimensional faces

$$\partial_n \sigma = \sum_{i=0}^n (-1)^i \sigma_{[v_0, v_1, \dots, v_{i-1}, v_{i+1}, \dots, v_n]}, \quad (4.17)$$

with  $\sigma_{[v_0, v_1, \dots, v_{i-1}, v_{i+1}, \dots, v_n]}$  the restriction of  $\sigma$  to its boundary face with vertices  $\{v_0, v_1, \dots, v_{i-1}, v_{i+1}, \dots, v_n\}$ , mapping  $C_n(X)$  into  $C_{n-1}$ , where for any  $\partial_m$  with  $m > n$  or  $m < 0$  the boundary operator is defined as the zero map.

As it follows from its definition, this operator is nihil potent and satisfies the identity

$$\partial_{n-1}(\partial_n(\sigma)) = 0. \quad (4.18)$$

This implies that  $\text{Im } \partial_{n+1} \subset \text{Ker } \partial_n$  thus allowing us to define the singular Homology group as the quotient space

$$H_n^{\text{sing}}(X) = \frac{\{\gamma \in C_n(X) \mid \partial_n \gamma = 0\}}{\{\gamma \in C_n(X) \mid \gamma = \partial_{n+1} \delta\}}. \quad (4.19)$$

In order to determine an integral of a multivalued function such as  $u \varphi$  on  $\gamma$ , we have to fix a branch of  $u$  on  $\gamma$ . This is achieved using *twisted* chains as integration regions that, given singular simplices  $\gamma$  and a multivalued function  $u$ , are defined as

$$\gamma' = \gamma \otimes u. \quad (4.20)$$

They are integration paths *loaded* with the multivalued function appearing in the integral, keeping track of the phase factor that could arise in the integrand from crossing a branch cut of  $u$  when moving along the path  $\gamma$ . Formally, they are chains with coefficients in the local system  $\mathcal{L}_\omega$  of which  $u(z)$  is a section (for more details, see [69, 81, 136]) and forms the group of twisted chains  $C_n(X, \mathcal{L}_\omega)$ .

We introduce a *twisted* boundary operator  $\partial_\omega$  that acts on  $\gamma'$  by substituting  $\gamma$  with its boundary evaluated as shown in eq. (4.17), and  $u$  with its value at the boundary. Through the twisted version of the Stokes theorem, one can show that two integrals differing by a boundary term in the integration region are equal

$$\int_{\mathcal{C}} u(\mathbf{z}) \varphi(\mathbf{z}) = \int_{\mathcal{C} + \partial_\omega \gamma} u(\mathbf{z}) \varphi(\mathbf{z}). \quad (4.21)$$

similarly to eq. (4.9), making apparent the existence of an equivalence class among cycles. Analogously to the single-valued case, one can show that the twisted boundary operator satisfies  $\partial_\omega \circ \partial_\omega = 0$ , allowing us to define the quotient space

$$H_n^\omega(X, \mathcal{L}_\omega) = \frac{\{\gamma \in C_n(X, \mathcal{L}_\omega) \mid \partial_\omega \gamma = 0\}}{\{\gamma \in C_n(X, \mathcal{L}_\omega) \mid \gamma = \partial_\omega \delta\}}. \quad (4.22)$$

which is linked to its cohomological counterpart  $H_\omega^n$  through the *Poincarée duality* and have the same dimensions as the latter. An equivalence class of the Homology group with representative the cycle  $\mathcal{C}$  will be written as  $[\mathcal{C}]$ . Lastly, let us remark that  $H_\omega^n$  and  $H_n^\omega$  are linked through *Poincarée duality* and have the same dimensions.

### An example: the regularized beta function

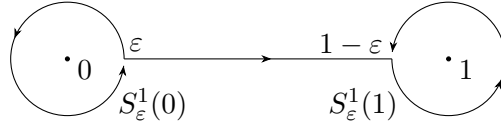
Let us briefly give an example of what the twisted cycle is and how the twisted boundary operator  $\partial_\omega$  acts on it. We will consider the analytic continuation of the Beta function defined

as  $\square$

$$B_\varepsilon(p, q) = \frac{1}{e^{2\pi ip} - 1} \int_{S_\varepsilon^1(0)} u(z)\varphi + \int_\varepsilon^{1-\varepsilon} u(z)\varphi - \frac{1}{e^{2\pi iq} - 1} \int_{S_\varepsilon^1(1)} u(z)\varphi, \quad (4.23)$$

where  $u(z) = z^p(1 - z)^q$  and is defined for  $p, q \notin \mathbb{Z}$ , instead of the classic definition valid for  $p, q > 0$ .

This version of the beta function has the path that has been manipulated, instead of terminating at 0 and 1 it takes the form depicted in the following figure:



with  $S_\varepsilon^1(z_0)$  is a circle of radius  $\varepsilon$  centered in  $z_0$  and  $\varepsilon$  is a sufficiently small positive number. This is a proper analytic continuation of the beta function given that  $\lim_{\varepsilon \rightarrow 0} B_\varepsilon(p, q) = B(p, q)$  for  $p, q > 0$ , since the integration along the circles  $S_\varepsilon^1(0)$  and  $S_\varepsilon^1(1)$  vanishes while the integration along the central path becomes the classic beta function, and it does not depend on the value of  $\varepsilon$ .

The latter statement can be proven by considering

$$B_\varepsilon(p, q) - B_\delta(p, q) \quad (4.24)$$

and observing that, assuming without loss of generality that  $\delta < \varepsilon$ , we have

$$\begin{aligned} B_\varepsilon(p, q) - B_\delta(p, q) &= \text{Diagram 1} - \text{Diagram 2} \\ &= \text{Diagram 3} - \text{Diagram 4} = 0, \end{aligned} \quad (4.25)$$

by Cauchy's integral theorem.

**Twisted chain** The twisted chain in consideration, which will be labeled  $\gamma$ , is defined as

$$\gamma = \frac{1}{e^{2\pi ip} - 1} S_\varepsilon^1(0) \otimes u(t) + [\varepsilon, 1 - \varepsilon] \otimes u(t) - \frac{1}{e^{2\pi iq} - 1} S_\varepsilon^1(1) \otimes u(t). \quad (4.26)$$

As we can see, the definition of a twisted cycle requires to specify the multivalued function appearing in the integral. This allows us to keep track of the phase factor arising from encircling the branch points 0 or 1: indeed the effect of moving along the path  $S_\varepsilon^1(0)$ , is taken into account by multiplying  $u(z)$  by the phase  $e^{2\pi ip}$  every time a revolution is completed.

**Twisted boundary operator** The action of the twisted boundary operator  $\partial_\omega$  associates to a given path of integration its boundary taking into account the effects of the multivaluedness of  $u(z)$  as in the following example:

$$\partial_\omega S_\varepsilon^1(0) = [z]_{z=\varepsilon} \otimes e^{2\pi ip} u(\varepsilon) - [z]_{z=\varepsilon} \otimes u(\varepsilon). \quad (4.27)$$

<sup>1</sup>We wish to acknowledge professor K.Matsumoto and Y.Goto for the lectures they held in Padova, from which this example is based on.

Applying it to the twisted chain  $\gamma$  in eq. eq:twistedchain one obtains

$$\begin{aligned} \partial_\omega \gamma = & \frac{1}{e^{2\pi ip} - 1} ([z]_{z=\varepsilon} \otimes e^{2\pi ip} u(\varepsilon) - [z]_{z=\varepsilon} \otimes u(\varepsilon)) + \\ & + ([z]_{z=1-\varepsilon} \otimes u(1-\varepsilon) - [z]_{z=\varepsilon} \otimes u(\varepsilon)) - \\ & - \frac{1}{e^{2\pi iq} - 1} ([z]_{z=\varepsilon} \otimes e^{2\pi iq} u(\varepsilon) - [z]_{z=\varepsilon} \otimes u(\varepsilon)) = 0, \end{aligned}$$

proving that, indeed,  $\gamma$  is a twisted cycle.

### 4.1.3 Feynman Integrals and their duals

The natural way to pair a form (which consists of an integrand and its measure) and a cycle is indeed through integration. In this way, as originally proposed in [68], we can look at the Feynman integral in eq. (4.1) as a pairing between an equivalence class of cycles and one of cocycles:

$$I = \int_{\mathcal{C}} u(\mathbf{z}) \varphi(\mathbf{z}) = \langle \varphi | \mathcal{C} \rangle. \quad (4.28)$$

Let us also consider an integral containing  $u^{-1}$  instead of  $u$ . We will refer to it as *dual* integral:

$$I^\vee = \int_{\mathcal{C}} u^{-1} \varphi. \quad (4.29)$$

In this case, the covariant derivative is

$$\nabla_{-\omega} = d - \omega \wedge, \quad \omega = d \log u = \sum_{i=1}^n \hat{\omega}_i dz_i \quad (4.30)$$

and an equivalence relation similar to the one inferred from eq. (4.9) is drawn between dual forms:

$$\varphi \sim \varphi + \nabla_{-\omega} \xi \quad (4.31)$$

Applying the same argument presented in Section 4.1.1 one formalizes this equivalence class through the definition of the dual twisted Cohomology group  $H_{-\omega}^n$ . The equivalence class will be denoted as  $|\varphi\rangle$  in order to differentiate it from the one defined by ordinary Feynman integrals. Analogously, an equivalence class of dual twisted cycles characterized by the operator  $\partial_{-\omega}$  is defined, and will be represented as  $[\mathcal{C}]$ . This equivalence class defines a dual twisted Homology group  $H_n^{-\omega}$ , completing the picture of dual Feynman integrals that now can be represented as a pairing between dual twisted cocycles and the corresponding cycle indicated as

$$I^\vee = [\mathcal{C} | \varphi]. \quad (4.32)$$

### 4.1.4 Dimension of twisted cohomology groups

Rephrasing Feynman integrals in terms of a pairing between elements of the twisted cohomology and homology groups links the number of MIs to the dimension of the cohomology and homology groups

$$\nu = \dim H_{\pm\omega}^n = \dim H_n^{\pm\omega}. \quad (4.33)$$



Using the fact that the Euler characteristic  $\chi$  of  $X$  is related to the twisted Betti numbers through

$$\chi(X) = \sum_{k=0}^{2n} (-1)^k \dim H_{\omega}^k(X), \quad (4.34)$$

where  $n = \dim_{\mathbb{C}} X$ , together with the fact that under the assumptions given in [69] the only non-trivial twisted cohomology group is the one of dimensions  $n$ ,

$$\dim H_{\omega}^k = 0 \quad \text{for } k \neq n, \quad (4.35)$$

we can compute the number of MIs by means of algebraic topology, since

$$\chi(X) = (-1)^n \dim H_{\pm\omega}^n. \quad (4.36)$$

In ref. [2], we recall that  $\nu$  can be computed using one of the many ways of evaluating the topological invariant Euler characteristics  $\chi(X)$ :  $X = \mathbb{CP}^n - \mathcal{P}_{\omega}$ , where  $\mathcal{P}_{\omega} \equiv \{\text{set of poles of } \omega\}$  in projective space, the above relation can be written as

$$\nu = (-1)^n \chi(X) = (-1)^n (n+1 - \chi(\mathcal{P}_{\omega})), \quad (4.37)$$

where we used  $\chi(\mathbb{CP}^n) = n+1$  together with the inclusion-exclusion principle for the Euler characteristics. In other words, to compute  $\nu$ , it is sufficient to evaluate  $\chi(\mathcal{P}_{\omega})$  of the projective variety  $\mathcal{P}_{\omega}$  (see also refs. [137–139]).

Alternatively, in ref. [140], the number of MIs within the IBP decomposition was related to the number of independent ‘‘contours’’ of integration, generating no surface terms. In particular, by means of the complex Morse (Picard-Lefschetz) theory, it is possible to relate the basis of cycles and the critical points of the graph-polynomial of the considered integral parameterization, the number of MIs was related to the rank of the homology groups  $H_n^{\pm\omega}$ .

Let us consider  $\log(u)$  as a Morse function (a function with non-degenerate critical points). We define the Morse index of a critical point  $p$  as the number of independent directions in which the Morse function decreases in a neighborhood of  $p$ . Through the strong Morse inequality we can then express  $\chi$  in function of the number of critical points of  $\log(u)$

$$\chi(X) = \sum_{k=0}^{2n} (-1)^k M_k, \quad (4.38)$$

with  $M_k$  the number of critical points of the Morse index  $k$ . Moreover, in our case, the Morse index for the critical points of the Morse function considered is  $n$  [81], implying that  $M_k = 0$  for  $k \neq n$ . This leads to

$$\chi(X) = (-1)^n M_n, \quad (4.39)$$

allowing us to compute the number of independent master integrals from the number of critical points of  $\log(u)$ .

This is given by the number of solutions of the (zero-dimensional) system.

$$\hat{\omega}_i \equiv \partial_{z_i} \log u(\mathbf{z}) = 0, \quad i = 1, \dots, n \quad (4.40)$$

and can be determined without explicitly computing its zeros [140]. In our applications, the function  $u(\mathbf{z})$  always takes the form  $u(\mathbf{z}) = \prod_j \mathcal{B}_j^{\gamma_j}(\mathbf{z})$ , which gives the equations:

$$\hat{\omega}_i = \sum_j \gamma_j \frac{\partial_{z_i} \mathcal{B}_j}{\mathcal{B}_j}, \quad i = 1, \dots, n. \quad (4.41)$$

In the absence of critical points at infinity, the number of solutions of (4.40) is equal to the dimension of the quotient space for the ideal<sup>2</sup>

$$\mathcal{I} = \left\langle \beta_1, \dots, \beta_n, z_0 \prod_j \mathcal{B}_j - 1 \right\rangle \quad \text{with} \quad \beta_k \equiv \sum_i \gamma_i (\partial_{z_k} \mathcal{B}_i) \prod_{j \neq i} \mathcal{B}_j. \quad (4.42)$$

In the special case where  $u(\mathbf{z}) = \mathcal{B}^\gamma(\mathbf{z})$ , it becomes simply (140)

$$\mathcal{I} = \langle \partial_{z_1} \mathcal{B}, \dots, \partial_{z_n} \mathcal{B}, z_0 \mathcal{B} - 1 \rangle. \quad (4.43)$$

Considering a Gröbner basis  $\mathcal{G}$  generating  $\mathcal{I}$ , the Shape Lemma (see, e.g. (141), and (38) for an application to physics) ensures that the number  $\nu$  of zeros of  $\mathcal{I}$ , and hence the number of solutions of the system (4.40), is the dimension of the quotient ring,

$$\nu = \dim(\mathbb{C}[\mathbf{z}]/\langle \mathcal{G} \rangle), \quad (4.44)$$

where  $\mathbb{C}[\mathbf{z}]$  is the set of all polynomials that vanish on the zeros of  $\mathcal{I}$  (they identify a discrete variety,  $V \subset \mathbb{C}^\nu$ ). In particular, the lemma ensures that the degree of the remainder of the polynomial division modulo  $\mathcal{G}$  is  $\nu + 1$ .

In the following, we will compute the dimension of the cohomology groups to determine the size of the basis of differential forms for different choices of  $H_{\pm\omega}^n$ , each characterized by  $\omega$ , or correspondingly by  $u$ .

## 4.2 Intersection Numbers and IBPs

The vectorial structure of the twisted cohomology group allows us to reinterpret IBPs decomposition in this new language. IBPs let us reduce an integral in terms of a *basis* of  $\nu$  MIs

$$I = \sum_{i=1}^{\nu} c_i J_i, \quad (4.45)$$

or, in terms of equivalence classes

$$I = \langle \varphi | \mathcal{C} \rangle = \sum_{i=1}^{\nu} c_i \langle e_i | \mathcal{C} \rangle. \quad (4.46)$$

Since all paths of integration are the same, this corresponds to a decomposition of an element of the twisted Cohomology group in terms of a basis of such vector space

$$\langle \varphi | = \sum_{i=1}^{\nu} c_i \langle e_i |. \quad (4.47)$$

The same remains valid for the decomposition of a dual integral  $I^\vee = [\mathcal{C} | \varphi]$  in terms of  $\nu$  dual MIs:

$$I^\vee = \sum_{i=1}^{\nu} c_i^\vee J_i^\vee, \quad (4.48)$$

becomes

$$|\varphi \rangle = \sum_{i=1}^{\nu} c_i^\vee |e_i \rangle. \quad (4.49)$$

---

<sup>2</sup>We introduce an extra variable  $z_0$  in order to prevent the case when  $\mathcal{B}_j = 0$  for either  $j$ .

The final goal is to determine the reduction coefficient  $c_i$ . This is achieved by means of the *intersection number* between cocycles. This new object is a pairing different from the kind already presented between cycles and cocycles relative to the same integral: it is built as a pairing between cocycles  $\langle \varphi_L |$  and dual cocycles  $| \varphi_R \rangle$ . Taking into account the twisted cocycle basis  $\{ \langle e_i | \} \in H_{\omega}^n$  and its dual counterpart  $\{ | e_i \rangle \} \in H_{-\omega}^n$  it is possible to define the corresponding identity operator in both spaces

$$\mathbb{I} = \sum_{i=1}^{\nu} | e_i \rangle \langle e_i | , \quad \mathbb{I}^{\vee} = \sum_{j=1}^{\nu} | h_j \rangle \langle h_j | , \quad (4.50)$$

which combined together lead to

$$\mathbb{I}_c = \sum_{i,j=1}^{\nu} | h_j \rangle (\mathbf{C})_{ji}^{-1} \langle e_i | , \quad (4.51)$$

where  $\mathbf{C}$  is the matrix built out of all the possible intersection number between the basis  $\{ \langle e_i | \}$  and its dual

$$\mathbf{C}_{ij} = \langle e_i | h_j \rangle . \quad (4.52)$$

Inserting this operator on the right hand side of eq. [4.47](#) leads to

$$\langle \varphi | = \langle \varphi | \mathbb{I}_c = \sum_{i,j=1}^{\nu} \langle \varphi | h_j \rangle (\mathbf{C})_{ji}^{-1} \langle e_i | . \quad (4.53)$$

We have thus obtained a new way of obtaining the coefficient of the reduction, bypassing the system solution procedure required by classic IBPs through the *master decomposition formula*:

$$c_i \equiv \sum_{j=1}^{\nu} \langle \varphi | h_j \rangle (\mathbf{C}^{-1})_{ji} . \quad (4.54)$$

Analogously for dual integral we have

$$c_i^{\vee} \equiv \sum_{j=1}^{\nu} (\mathbf{C}^{-1})_{ij} \langle e_j | \varphi \rangle . \quad (4.55)$$

### 4.2.1 Differential equation for forms and dual forms

Differentiating a loop integral by an external kinematical variable gives us an object that can still be reduced in terms of master integrals. Thus, we can exploit the same algorithm to write down the system of differential equations, using the univariate intersection number. Let us discuss this procedure more in details.

Taking into account the system of differential equations in an external variable  $x$  for the basis  $\langle e_i |$  and the dual basis  $| h_i \rangle$ ,

$$\partial_x \langle e_i | = \Omega_{ij} \langle e_j | , \quad (4.56)$$

$$\partial_x | h_i \rangle = - | h_j \rangle \Omega_{ji}^{\vee} , \quad (4.57)$$

where the matrices  $\Omega$  and  $\Omega^{\vee}$  generally depend on the space-time dimension  $d$  and external variables including  $x$ . Let us consider the *l.h.s.* of eqs. [\(4.56\)](#) and [\(4.57\)](#), after taking the derivative in  $x$ ,

$$\partial_x \langle e_i | = \langle (\partial_x + \sigma) e_i | \equiv \langle \Phi_i | , \quad (4.58)$$

$$\partial_x |h_i\rangle = |(\partial_x - \sigma)h_i\rangle \equiv |\Phi_i^\vee\rangle, \quad (4.59)$$

where  $\sigma = \partial_x \log u$ . Here  $\langle \Phi_i |$  and  $|\Phi_i^\vee\rangle$  can be decomposed in terms of  $\langle e_j |$ , and  $|h_j\rangle$  respectively, by means of intersection numbers using eq. (4.53),

$$\langle \Phi_i | = \underbrace{\langle \Phi_i | h_k \rangle}_{\Omega_{ij}} (\mathbf{C}^{-1})_{kj} \langle e_j | \quad (4.60)$$

and similarly

$$|\Phi_i^\vee\rangle = |h_j\rangle \underbrace{(\mathbf{C}^{-1})_{jk}}_{-\Omega_{ji}^\vee} \langle e_k | \Phi_i^\vee \rangle \quad (4.61)$$

where summation over indices  $j, k$  is implied. Using the above ingredients, one can relate the matrices  $\Omega$  and  $\Omega^\vee$  through the identity

$$\partial_x \langle e_i | h_j \rangle = (\partial_x \langle e_i |) |h_j\rangle + \langle e_i | (\partial_x |h_j\rangle) = \Omega_{ik} \langle e_k | h_j \rangle - \langle e_i | h_k \rangle \Omega_{kj}^\vee, \quad (4.62)$$

or in the matrix notation

$$\partial_x \mathbf{C} = \Omega \mathbf{C} - \mathbf{C} \Omega^\vee. \quad (4.63)$$

In particular, if the bases were orthonormal such that  $\mathbf{C} = \mathbb{I}$  then  $\Omega = \Omega^\vee$ .

### 4.2.2 Dimensional Recurrence Relation

In the standard Baikov representation, the  $d$  dependence of Feynman integrals is carried only by the prefactor  $K$  and by the exponent  $\gamma$  of the Baikov polynomial  $B$ . Let us write the MIs in  $d + 2n$  dimensions as,

$$J_i^{(d+2n)} \equiv K(d+2n) E_i^{(d+2n)}, \quad (4.64)$$

with  $K(d+2n)$  the kinematical prefactor appearing in front of the integral as defined in eq. (2.22), while

$$E_i^{(d+2n)} \equiv \langle B^n e_i | \mathcal{C} \rangle = \int_{\mathcal{C}} u (B^n e_i), \quad i = 1, 2, \dots, \nu, \quad (4.65)$$

and consider the decomposition of  $\langle B^n e_i |$  in terms of the basis  $\langle e_j |$ ,

$$\langle B^n e_i | = (\mathbf{R}_n)_{ij} \langle e_j |, \quad n = 0, 1, \dots, \nu - 1. \quad (4.66)$$

This equation can be interpreted as a basis change, from  $\langle e_i |$  with  $(i = 1, 2, \dots, \nu)$  to  $\langle B^n e_i |$  with  $(n = 0, 1, \dots, \nu - 1)$ . Therefore, we can decompose  $\langle B^\nu e_i |$  in terms of the new basis  $\langle B^n e_i |$ , as

$$\langle B^\nu e_i | = \sum_{n=0}^{\nu-1} c_n \langle B^n e_i |, \quad (4.67)$$

which can be written as

$$\sum_{n=0}^{\nu} c_n \langle B^n e_i | = 0, \quad (4.68)$$

with  $c_\nu \equiv -1$ . Upon the pairing with  $|\mathcal{C}\rangle$ , it yields the recursion formula for the integral  $E_i$ ,

$$\sum_{n=0}^{\nu} c_n E_i^{(d+2n)} = 0, \quad (4.69)$$

where the coefficients  $c_n$ , calculated by means of the master decomposition formula eq. (4.53), may depend on  $d$  and on the kinematics. Finally, by redefining the coefficients, the dimensional recurrence relation for the MIs  $J_i$  arises,

$$\sum_{n=0}^{\nu} \alpha_n J_i^{(d+2n)} = 0, \quad (4.70)$$

with  $\alpha_n \equiv c_n/K(d+2n)$ .

### 4.2.3 Intersection number definition and its properties

#### Definition

The pairing between twisted cocycles and their dual counterpart plays a pivotal role in the derivation of the *master decomposition formula* and thus in translating the IBP decomposition in this novel language.

Similarly to the pairing between cycles and cocycles defined in eq. (4.28), one could consider defining it as the integration among the two forms

$$\int_{\mathcal{X}} \varphi_L \wedge \varphi_R, \quad (4.71)$$

however, this integral is not well defined because of two major reasons.

Firstly,  $\varphi_L$  and  $\varphi_R$  are both holomorphic  $n$ -forms, which means that they depend on the same variables  $\mathbf{z}$ . This gives an integrand which is identically 0, while when wedging two forms only the mixed term  $d\mathbf{z} \wedge d\bar{\mathbf{z}}$  containing both the holomorphic and anti-holomorphic components survives.

Secondly, these forms are integrated over the space  $X$ , which is  $\mathbb{C}^n$  without hyperplanes where  $\omega$  is singular. This is a non-compact space. For these reasons, we introduce the function  $\iota_\omega$ , which maps a form  $\varphi \in H_\omega^n$  into a form with compact support  $\iota_\omega(\varphi) \in H_{\omega,c}^n$  while introducing non-holomorphicities in the integrand, effectively solving both the issues that the definition in eq. (4.71) has.

Thus, we define the intersection number between twisted forms as

$$\langle \varphi_L | \varphi_R \rangle_\omega = \frac{1}{(2\pi i)^n} \int_X \iota_\omega(\varphi_L) \wedge \varphi_R. \quad (4.72)$$

#### Properties

From the definition in eq. (4.72), one can prove that the intersection number between cocycles and their duals satisfies the symmetry relation

$$\langle \varphi_L | \varphi_R \rangle_\omega = (-1)^n \langle \varphi_R | \varphi_L \rangle_{-\omega}, \quad (4.73)$$

where on the right hand side the intersection number is evaluated using  $-\omega$  instead of  $\omega$ . As a final remark, let us stress that the twisted intersection number is not affected by total derivative terms by definition

$$\langle \varphi_L + \nabla_\omega \xi | \varphi_R \rangle_\omega = \langle \varphi_L | \varphi_R + \nabla_{-\omega} \xi \rangle_\omega = \langle \varphi_L | \varphi_R \rangle_\omega, \quad (4.74)$$

thus naturally embodying IBP identities.

### 4.3 Univariate intersection number

In order to gain intuition in to the action of  $\iota_\omega$  and to explicitly compute the intersection number, let us consider it in the univariate case. Let also be  $z_i \in \mathbb{C}$  the poles of the 1-form  $\varphi_L(z)$ . In order to build its counterpart with compact support, we need to define two discs  $U_i$  and  $V_i$  centered in  $z_i$ , such that  $V_i \subset U_i$  and  $U_i \cap U_j$  and a step function for each  $z_i$ ,  $h_i$  such that:

$$h_i(z) = \begin{cases} 1 & \text{on } V_i \\ 0 \leq h_i \leq 1 & \text{smooth interpolation on } U_i \setminus V_i \\ 0 & \text{out of } U_i \end{cases} \quad (4.75)$$

We then define the action of  $\iota_\omega$  as

$$\iota_\omega(\varphi_L) = \varphi_L - \sum_i \nabla_\omega(h_i \psi_i) , \quad (4.76)$$

where

$$\nabla_\omega \psi_i = \varphi_L \quad \text{on } U_i \setminus z_i . \quad (4.77)$$

In this way, replacing  $\varphi_L$  with  $\iota_\omega \varphi_L$  does not alter the value of the intersection number as shown in eq. (4.74). Another relevant fact to note is that this manipulation of  $\varphi_L$  leaves the form unaltered outside of  $U_i$  while  $\iota_\omega(\varphi_L) = 0$  inside  $V_i$ , since  $h_i = 1$  and  $\varphi_L$  gets fully subtracted, making  $\iota_\omega(\varphi_L)$  a form with compact support. Lastly, the term  $dh_i \varphi_L$  that comes from the action of the covariant derivative on the additional term introduced by  $\iota_\omega$  gives a non-holomorphic contribution to the form in consideration.  $\iota_\omega$  thus satisfies all the required properties needed to define a proper intersection number.

Substituting the explicit definition of eq. (4.76) inside eq. (4.72) we have

$$\langle \varphi_L | \varphi_R \rangle_\omega = \frac{1}{(2\pi i)^n} \int_X \left[ \varphi_L - \sum_i (dh_i \psi_i - h_i \psi_i \omega - h_i \nabla_\omega \psi_i) \right] \wedge \varphi_R \quad (4.78)$$

$$= \frac{1}{(2\pi i)^n} \sum_i \int_{U_i \setminus V_i} dh_i \psi_i \wedge \varphi_R , \quad (4.79)$$

where the last equality is a consequence of the fact that all the other contribution except  $dh_i \psi_i$  contains the wedge product of two holomorphic forms which is zero ( $dz \wedge dz = 0$ ), and that  $dh_i \neq 0$  only in  $U_i \setminus V_i$ .

Considering that both  $d\psi_i \wedge \varphi_R$  and  $d\varphi_R$  vanish, we can rewrite

$$dh_i \psi_i \wedge \varphi_R = d(h_i \psi_i \varphi_R) . \quad (4.80)$$

Using Stokes theorem we can rewrite

$$\langle \varphi_L | \varphi_R \rangle_\omega = \frac{1}{(2\pi i)^n} \sum_i \int_{U_i \setminus V_i} d(h_i \psi_i \varphi_R) = \frac{1}{(2\pi i)^n} \sum_i \int_{\partial(U_i \setminus V_i)} h_i \psi_i \varphi_R \quad (4.81)$$

$$= \frac{1}{(2\pi i)^n} \sum_i \int_{\partial(U_i \setminus V_i)} \psi_i \varphi_R . \quad (4.82)$$

$$(4.83)$$

Using the fact that  $\partial V_i$  is a closed path we can rewrite the integrals as residues, yielding

$$\langle \varphi_L | \varphi_R \rangle_\omega = \sum_{i=1}^k \text{Res}_{z=z_i} (\psi_i \varphi_R) . \quad (4.84)$$

**Univariate algorithm** Define  $\mathcal{P}$  as the set of *poles* of  $\omega$ ,

$$\mathcal{P} \equiv \{ z \mid z \text{ is a pole of } \omega \}. \quad (4.85)$$

Note that, if  $\text{Res}_{z=\infty}(\omega) \neq 0$ ,  $\mathcal{P}$  also includes the pole at infinity.

Given two (univariate) 1-forms  $\varphi_L$  and  $\varphi_R$ , we define the *intersection number* as [72](#),[142](#)

$$\langle \varphi_L | \varphi_R \rangle_\omega = \sum_{p \in \mathcal{P}} \text{Res}_{z=p}(\psi_p \varphi_R), \quad (4.86)$$

where,  $\psi_p$  is a function (0-form), solution to the differential equation  $\nabla_\omega \psi = \varphi_L$ , around  $p$ , *i.e.*,

$$\nabla_{\omega_p} \psi_p = \varphi_{L,p}, \quad (4.87)$$

(the notation  $f_p$  indicates the Laurent expansion of  $f$  around  $z = p$ ). The above equation can be also solved globally, however only a handful of terms in the Laurent expansion around  $z = p$  are needed to evaluate the residue in [\(4.86\)](#). In particular, after defining  $\tau \equiv z - p$ , and the *ansatz*,

$$\psi_p = \sum_{j=\min}^{\max} \psi_p^{(j)} \tau^j + \mathcal{O}(\tau^{\max+1}), \quad (4.88)$$

$$\min = \text{ord}_p(\varphi_L) + 1, \quad \max = -\text{ord}_p(\varphi_R) - 1, \quad (4.89)$$

the differential equation in eq. [\(4.87\)](#) freezes all unknown coefficients  $\psi_p^{(j)}$ . In other words, the Laurent expansion of  $\psi_p$  around each  $p$ , is determined by the Laurent expansion of  $\varphi_{L,R}$  and of  $\omega$ . A given point  $p$  contributes only if the condition  $\min \leq \max$  is satisfied, and the above expansion exists only if  $\text{Res}_{z=p}(\omega)$  is not a non-positive integer.

**Logarithmic Forms.** When both  $\varphi_L$  and  $\varphi_R$  are logarithmic, meaning that  $\text{ord}_p(\varphi_{L/R}) \geq -1$  for all points  $p \in \mathcal{P}$ , then the formula [\(4.86\)](#) simplifies to

$$\langle \varphi_L | \varphi_R \rangle_\omega = \sum_{p \in \mathcal{P}} \frac{\text{Res}_{z=p}(\varphi_L) \text{Res}_{z=p}(\varphi_R)}{\text{Res}_{z=p}(\omega)}. \quad (4.90)$$

Note that in this case the intersection number becomes symmetric in  $\varphi_L$  and  $\varphi_R$ , *i.e.*,

$$\langle \varphi_L | \varphi_R \rangle_\omega = \langle \varphi_R | \varphi_L \rangle_\omega, \quad (4.91)$$

while [\(4.73\)](#) still holds.

**Choices of Bases.** The bases  $|h_i\rangle$  and  $|e_i\rangle$  can be different from each other, but  $|h_i\rangle = |e_i\rangle$  is a possible choice too. We decompose 1-form employing either a *monomial basis*

$$\langle e_i | = \langle \phi_i | \equiv z^{i-1} dz, \quad (4.92)$$

or a *dlog-basis*, of the type,

$$\langle e_i | = \langle \varphi_i | \equiv \frac{dz}{z - z_i}, \quad (4.93)$$

where  $z_i$  are *poles* of  $\omega$ .

Alternatively, *orthonormal bases* for twisted cocycles can be chosen as follows. Out of the set of poles  $\mathcal{P} = \{z_1, z_2, \dots, z_{\nu+1}, z_{\nu+2}\}$  pick two special ones, say  $z_{\nu+1}$  and  $z_{\nu+2}$ . Then construct bases of  $\nu$  one-forms using:

$$\langle e_i | \equiv d \log \frac{z - z_i}{z - z_{\nu+1}}, \quad |h_i\rangle \equiv \text{Res}_{z=z_i}(\omega) d \log \frac{z - z_i}{z - z_{\nu+2}} \quad (4.94)$$

for  $i = 1, 2, \dots, \nu$ . With this choice, the intersection matrix  $\mathbf{C}$  becomes the identity matrix,

$$\mathbf{C}_{ij} = \delta_{ij} \quad (4.95)$$

as can be shown directly using the residue prescription (4.86), and therefore the basis decomposition formula simplifies to

$$\langle \varphi | = \sum_{i=1}^{\nu} \langle \varphi | h_i \rangle \langle e_i | . \quad (4.96)$$

## 4.4 Univariate application of twisted intersection theory

### 4.4.1 Euler Beta Integrals

Let us start by discussing integral relations for a simple class of integrals such as the Euler *beta function*, defined as

$$\beta(a, b) \equiv \int_0^1 dz z^{a-1} (1-z)^{b-1} = \frac{\Gamma(a)\Gamma(b)}{\Gamma(a+b)} . \quad (4.97)$$

#### Direct Integration

We will consider integrals of the type

$$I_n \equiv \int_{\mathcal{C}} u z^n dz , \quad u \equiv B^\gamma , \quad B \equiv z(1-z) , \quad \mathcal{C} \equiv [0, 1] . \quad (4.98)$$

These integrals admit a closed-form expression in terms of  $\Gamma$  functions,

$$I_n = \frac{\Gamma(1+\gamma)\Gamma(1+\gamma+n)}{\Gamma(2+2\gamma+n)} , \quad (4.99)$$

from which it is possible to derive a relation between  $I_n$  and  $I_0$ ,

$$I_n = \frac{\Gamma(1+\gamma+n)\Gamma(2+2\gamma)}{\Gamma(1+\gamma)\Gamma(2+2\gamma+n)} I_0 . \quad (4.100)$$

For instance, when  $n = 1$ , it reads

$$I_1 = \frac{1}{2} I_0 . \quad (4.101)$$

#### Integration-by-Parts Identities

Let us recover the same relation from integration by parts identities. With the choice of  $\mathcal{C}$  as above, the following integration-by-parts identity holds

$$\int_{\mathcal{C}} d(B^{\gamma+1} z^{n-1}) = 0 . \quad (4.102)$$

The action of the differential operator under the integral sign yields the following equation,

$$(\gamma+n)I_{n-1} - (1+2\gamma+n)I_n = 0 . \quad (4.103)$$

Therefore we obtain the recurrence relation

$$I_n = \frac{(\gamma+n)}{(1+2\gamma+n)} I_{n-1} , \quad (4.104)$$

which, for  $n = 1$ , gives

$$I_1 = \frac{1}{2} I_0 . \quad (4.105)$$



### Intersections

We are going to (re)derive, once more, the relations between Euler beta integrals using intersection numbers. We consider integrals defined as,

$$I_n \equiv \int_{\mathcal{C}} u \phi_{n+1} \equiv \omega \langle \phi_{n+1} | \mathcal{C} \rangle, \quad \phi_{n+1} \equiv z^n dz, \quad (4.106)$$

with

$$u = B^\gamma \quad B = z(1-z), \quad \omega = d \log u = \gamma \left( \frac{1}{z} + \frac{1}{z-1} \right) dz, \quad (4.107)$$

$$\nu = 1, \quad \mathcal{P} = \{0, 1, \infty\}. \quad (4.108)$$

**Monomial Basis.**  $\nu = 1$  implies the existence of 1 master integral, which we choose as  $I_0 = \omega \langle \phi_1 | \mathcal{C} \rangle$ . The goal of this calculation is to derive the relation between  $I_1$  and  $I_0$ ,

$$I_1 = c_1 I_0 \quad \iff \quad \omega \langle \phi_2 | \mathcal{C} \rangle = c_1 \omega \langle \phi_1 | \mathcal{C} \rangle \quad (4.109)$$

which can be derived by decomposing  $\langle \phi_2 |$  in terms of  $\langle \phi_1 |$ ,

$$\langle \phi_2 | = c_1 \langle \phi_1 |, \quad c_1 = \langle \phi_2 | \phi_1 \rangle \langle \phi_1 | \phi_1 \rangle^{-1} \quad (4.110)$$

Notice that since  $\nu = 1$ , the intersection matrix  $\mathbf{C}_{ij}$  has just one element  $\mathbf{C}_{11} = \langle \phi_1 | \phi_1 \rangle$ .

We need to evaluate the intersection numbers  $\langle \phi_1 | \phi_1 \rangle$ , and  $\langle \phi_2 | \phi_1 \rangle$ .

For each pole  $p \in \mathcal{P}$ , we identify  $\phi_{i,p}$  (the series expansion of  $\phi_i$  around  $z = p$ ), and determine the associated function  $\psi_{i,p}$  (the series expansion of  $\psi_i$  around  $z = p$ ), by solving the following differential equation,

$$\nabla_\omega \psi_{i,p} = \phi_{i,p}. \quad (4.111)$$

After inserting the series expansion of  $\phi_{i,p}$  and an ansatz for  $\psi_{i,p}$  in the above equation, we get an equation at each order on  $p$ , which together determines the coefficients in the ansatz for  $\psi_{i,p}$ . In practice, we introduce a local coordinate  $\tau$ , defined as  $\tau = z - p$ , for finite poles, or  $\tau = 1/z$  for the pole at infinity, and consider the Laurent expansions around  $\tau \rightarrow 0$  of,

$$\phi_{i,p} = \sum_{k=\min-1} \phi_{i,p}^{(k)} \tau^k, \quad \omega_p = \sum_{k=-1} \omega_p^{(k)} \tau^k, \quad (\text{known}) \quad (4.112)$$

and the ansatz,

$$\psi_p = \sum_{k=\min}^{\max} \alpha_k \tau^k, \quad (\alpha_k \text{ unknown}) \quad (4.113)$$

to solve the following differential equation,

$$\frac{d}{d\tau} \psi_p + \omega_p \psi_p - \phi_{i,p} = 0. \quad (4.114)$$

In our case we have,

- For  $\varphi_L = \phi_1 = dz$ ,  $\varphi_R = \phi_1 = dz$ :

$p$	min	max	$\varphi_{L,p}$	$\psi_p$
0	1	-1	$d\tau$	-
1	1	-1	$d\tau$	-
$\infty$	-1	1	$-d\tau/\tau^2$	$\sum_{i=-1}^1 \alpha_i \tau^i$

with

$$\alpha_{-1} = \frac{1}{2\gamma + 1}, \quad \alpha_0 = -\frac{1}{2(2\gamma + 1)}, \quad \alpha_1 = -\frac{\gamma}{2(2\gamma - 1)(2\gamma + 1)}. \quad (4.115)$$

Around  $p = 0, 1$ , the solution  $\psi_p$  does not exist (owing to the values of min and max), therefore

$$\langle \phi_1 | \phi_1 \rangle = \text{Res}_{z=\infty}(\psi_\infty \phi_1) = \frac{\gamma}{2(2\gamma - 1)(2\gamma + 1)}. \quad (4.116)$$

- For  $\varphi_L = \phi_2 = z dz$ ,  $\varphi_R = \phi_1 = dz$ :

$p$	min	max	$\varphi_{L,p}$	$\psi_p$
0	2	-1	$\tau d\tau$	-
1	1	-1	$d\tau$	-
$\infty$	-2	1	$-d\tau/\tau^3$	$\sum_{i=-2}^1 \alpha_i \tau^i$

with

$$\alpha_{-2} = \frac{1}{2(\gamma + 1)}, \quad \alpha_{-1} = -\frac{\gamma}{2(\gamma + 1)(2\gamma + 1)}, \quad (4.117)$$

$$\alpha_0 = -\frac{1}{4(2\gamma + 1)}, \quad \alpha_1 = -\frac{\gamma}{4(2\gamma - 1)(2\gamma + 1)}. \quad (4.118)$$

Around  $p = 0, 1$ , the solution  $\psi_p$  does not exist, therefore

$$\langle \phi_2 | \phi_1 \rangle = \text{Res}_{z=\infty}(\psi_\infty \phi_1) = \frac{\gamma}{4(2\gamma - 1)(2\gamma + 1)}. \quad (4.119)$$

Notice that in the above formulas only the  $p = \infty$  gave a non-trivial contribution. In general, the situation depends on the form of the integrands, and in particular on the values of min and max, which are dictated by the Laurent series expansions around  $p$  of  $\varphi_L$  and  $\varphi_R$  paired in the intersection number  $\langle \varphi_L | \varphi_R \rangle$ .

Finally, we get the decomposition of  $I_1$  in terms of  $I_0$ ,

$$I_1 = c_1 I_0, \quad (4.120)$$

$$c_1 = \langle \phi_2 | \phi_1 \rangle \langle \phi_1 | \phi_1 \rangle^{-1} = \frac{1}{2}, \quad (4.121)$$

in agreement with eq. (4.101).

**dlog-basis.** Consider the master integral associated to the form

$$\varphi_1 = d \log \frac{z}{z-1} = \left( \frac{1}{z} - \frac{1}{z-1} \right) dz, \quad (4.122)$$

and let us decompose both  $\langle \phi_1 |$  and  $\langle \phi_2 |$  in the basis of  $\langle \varphi_1 |$ ,

$$\langle \phi_1 | = \langle \phi_1 | \varphi_1 \rangle \langle \varphi_1 | \varphi_1 \rangle^{-1} \langle \varphi_1 |, \quad (4.123)$$

$$\langle \phi_2 | = \langle \phi_2 | \varphi_1 \rangle \langle \varphi_1 | \varphi_1 \rangle^{-1} \langle \varphi_1 |. \quad (4.124)$$

We need the intersection numbers,

$$\langle \varphi_1 | \varphi_1 \rangle = \frac{2}{\gamma}, \quad \langle \phi_1 | \varphi_1 \rangle = \frac{1}{2\gamma + 1}, \quad \langle \phi_2 | \varphi_1 \rangle = \frac{1}{2(2\gamma + 1)}. \quad (4.125)$$

Therefore

$$\langle \phi_1 | = \frac{\gamma}{2(2\gamma + 1)} \langle \varphi_1 |, \quad \langle \phi_2 | = \frac{\gamma}{4(2\gamma + 1)} \langle \varphi_1 | \quad (4.126)$$

from which one can also deduce  $\langle \phi_2 | = 1/2 \langle \phi_1 |$ .

Please note, that in this basis the metric term  $\langle \varphi_1 | \varphi_1 \rangle$  is very simple, and that  $\langle \varphi_1 | \varphi_1 \rangle^{-1} = \gamma/2$ , has  $\gamma$  factorizing out.

This simple example contains all the relevant ingredients for the decomposition of Feynman integrals in terms of master integrals. It corresponds to a case with 1 master integral. We now consider two other cases, with respectively 2 and 3 master integrals, in order to show the algorithmic procedure of the decomposition by intersection numbers.

#### 4.4.2 Gauss ${}_2F_1$ Hypergeometric Function

Gauss  ${}_2F_1$  Hypergeometric function is defined as

$$\beta(b, c-b) {}_2F_1(a, b, c; x) = \int_0^1 z^{b-1} (1-z)^{c-b-1} (1-xz)^{-a} dz \quad (4.127)$$

The integration contour  $\mathcal{C}$  is  $[0, 1]$ , which is the twisted cycle.  $\beta(b, c-b)$  is the Euler beta function defined in eq. (4.97). In order to use intersection theory, we re-express this integral in terms of the pairing of the twisted cycle and the twisted cocycle:

$$\beta(b, c-b) {}_2F_1(a, b, c; x) = \int_{\mathcal{C}} u \varphi = \omega \langle \varphi | \mathcal{C} \rangle, \quad (4.128)$$

where

$$u = z^{b-1} (1-xz)^{-a} (1-z)^{-b+c-1}, \quad (4.129)$$

$$\omega = d \log u = \frac{xz^2(c-a-2) + z(ax-c+x+2) - bxz + b-1}{(z-1)z(xz-1)} dz, \quad (4.130)$$

$$\varphi = dz. \quad (4.131)$$

In this case, we have

$$\nu = 2, \quad \mathcal{P} = \{0, 1, \frac{1}{x}, \infty\} \quad (4.132)$$

indicating the existence of 2 independent integrals. Contiguity relations for Gauss Hypergeometric functions can be obtained through intersection theory, *via* the master decomposition formula in eq. (4.53), requiring the knowledge of the (inverse of the) matrix  $\mathbf{C}$ . We build this matrix for various different choices of the integral basis.

**Monomial Basis.** We choose the basis as  $\{\langle \phi_i | \}_{i=1,2}$ , we build the metric matrix  $\mathbf{C}$ ,

$$\mathbf{C} = \begin{pmatrix} \langle \phi_1 | \phi_1 \rangle & \langle \phi_1 | \phi_2 \rangle \\ \langle \phi_2 | \phi_1 \rangle & \langle \phi_1 | \phi_2 \rangle \end{pmatrix} \quad (4.133)$$

whose entries are

$$\langle \phi_1 | \phi_1 \rangle = \left( x^2(-a-b+1)(b-c+1) - 2ax(-b+c-1) + a(c-2) \right) / \left( x^2(a-c+1)(a-c+2)(a-c+3) \right), \quad (4.134)$$

$$\langle \phi_1 | \phi_2 \rangle = \left( x^3(-a-b+1)(a-b+2)(b-c+1) - ax^2(-b+c-1)(2a-3b) \right)$$

$$+ c + 2) + ax(a + 2c - 5)(-b + c - 1) - a(c - 3)(c - 2) \Big) / \left( x^3(a - c + 1)(a - c + 2)(a - c + 3)(a - c + 4) \right), \quad (4.135)$$

$$\langle \phi_2 | \phi_1 \rangle = \left( x^3(-(a - b))(a - b + 1)(b - c + 1) - ax^2(-b + c - 1)(2a - 3b + c) + ax(a + 2c - 3)(-b + c - 1) - a(c - 2)(c - 1) \right) / \left( x^3(a - c)(a - c + 1)(a - c + 2)(a - c + 3) \right), \quad (4.136)$$

$$\langle \phi_2 | \phi_2 \rangle = \left( -ax^2(a^2b - a^2c + a^2 - 3ab^2 + 7abc - 8ab - 4ac^2 + 9ac - 5a - 3b^2c + 6b^2 + 4bc^2 - 10bc + 6b - c^3 + 2c^2 - c) + x^4(-(a^3 - 3a^2b + 3a^2 + 3ab^2 - 6ab + 2a - b^3 + 3b^2 - 2b))(b - c + 1) + 2ax^3(a - b + 1)(ab - ac + a - 2b^2 + 3bc - 2b - c^2 + c) + 2a(c - 2)x(a + c - 2)(b - c + 1) + a(c^3 - 6c^2 + 11c - 6) \right) / \left( x^4(a - c)(a - c + 1)(a - c + 2)(a - c + 3)(a - c + 4) \right). \quad (4.137)$$

Now, we can derive any functional relation using the following decomposition.

$$\langle \phi_n | = \sum_{i,j=1}^2 \langle \phi_n | \phi_j \rangle (\mathbf{C}^{-1})_{ji} \langle \phi_i |. \quad (4.138)$$

Let us consider the decomposition of  $\beta(b + 2, c - b)_2F_1(a, b + 2, c + 2; x) \equiv \langle \phi_3 | \mathcal{C}$  in terms of  $\beta(b, c - b)_2F_1(a, b, c; x)$  and  $\beta(b + 1, c - b)_2F_1(a, b + 1, c + 1; x)$ . Using the eq. (4.138) we obtain

$$\beta(b + 2, c - b)_2F_1(a, b + 2, c + 2; x) = \left( \frac{b}{x(a - c - 1)} \right) \beta(b, c - b)_2F_1(a, b, c; x) + \left( \frac{(b - a + 1)x + c}{x(c - a + 1)} \right) \beta(b + 1, c - b)_2F_1(a, b + 1, c + 1; x) \quad (4.139)$$

or correspondingly

$${}_2F_1(a, b + 2, c + 2; x) = \frac{(c + 1)}{x(b + 1)(c - a + 1)} \times \left( ((b - a + 1)x + c) {}_2F_1(a, b + 1, c + 1; x) - c {}_2F_1(a, b, c; x) \right), \quad (4.140)$$

as verified using MATHEMATICA.

**dlog-basis.** Let us consider the following dlog-basis.

$$\varphi_1 = \left( \frac{1}{z} - \frac{1}{z - 1} \right) dz \quad (4.141)$$

$$\varphi_2 = \left( \frac{1}{z - 1} - \frac{x}{xz - 1} \right) dz. \quad (4.142)$$

The  $\mathbf{C}$  matrix with entries  $\mathbf{C}_{ij} = \langle \varphi_i | \varphi_j \rangle$  for this case is as follows

$$\mathbf{C} = \frac{1}{c - b - 1} \begin{pmatrix} \frac{c-2}{b-1} & -1 \\ -1 & \frac{a+b-c+1}{a} \end{pmatrix}. \quad (4.143)$$

The above relations between hypergeometric functions can be obtained using the dlog-basis as well. The  $\mathbf{C}$  matrix in this case takes a very simple form and it is factorized. If we consider the powers of all the factors to be equal, for example  $a = -\gamma$ ,  $b = \gamma + 1$ ,  $c = 2(\gamma + 1)$ , then  $\gamma$  factorizes out, and as a result the system of differential equations for  $\varphi_i$  is canonical.

In particular, let us introduce the prefactor

$$K = \frac{(c-b-1)(b-1)}{(c-1)(c-2)\beta(b, c-b)}, \quad (4.144)$$

and consider the two integrals,

$$I_1 = \langle \varphi_1 | \mathcal{C} \rangle = {}_2F_1(a, b-1, c-2; x), \quad (4.145)$$

$$I_2 = \langle \varphi_2 | \mathcal{C} \rangle = \frac{(b-1)(x-1)}{c-2} {}_2F_1(a+1, b, c-1; x), \quad (4.146)$$

which, for  $a = -\gamma$ ,  $b = \gamma+1$ ,  $c = 2(\gamma+1)$ , read,

$$I_1 = {}_2F_1(-\gamma, \gamma, 2\gamma; x), \quad I_2 = \frac{x-1}{2} {}_2F_1(1-\gamma, 1+\gamma, 1+2\gamma; x). \quad (4.147)$$

Following the method of Sec. [4.2.1](#), we derive the system of differential equations with respect to  $x$ ,

$$\partial_x I_i = \mathbf{A}_{ij} I_j, \quad \text{with} \quad \mathbf{A} = \gamma \begin{pmatrix} 0 & \frac{-1}{x-1} \\ \frac{-1}{x} & \frac{2}{x-1} - \frac{2}{x} \end{pmatrix}, \quad (4.148)$$

which is *canonical*, namely it is fuchsian and  $\gamma$ -factorised. It is easily seen that the system can be integrated up order-by-order in  $\gamma$ , yielding a result where the coefficient at order  $\gamma^n$  can be expressed in terms of harmonic polylogarithms (HPLs) [\[91\]](#) of weight  $n$ , therefore making explicit the relation between HPLs and the series expansion of  ${}_2F_1$  around  $\gamma = 0$ .

**Mixed bases.** By using mixed bases, namely a monomial-basis  $\langle e_i | = \langle \phi_i |$ , and a dlog-basis  $|h_j\rangle = |\varphi_j\rangle$ , we can decompose our integrals in terms of a monomial basis, which can be directly mapped onto eq. [\(4.140\)](#), without loosing the advantages of simpler expressions due to the dlog-basis algebra. In this case, the intersection matrix becomes

$$\mathbf{C} = \langle \phi_i | \varphi_j \rangle = \begin{pmatrix} \frac{1}{c-a-1} & \frac{x-1}{(1+a-c)x} \\ \frac{a-ax+bx}{(a-c)(1+a-c)x} & \frac{(x-1)(1-c+ax-bx)}{(a-c)(1+a-c)x^2} \end{pmatrix} \quad (4.149)$$

whose entries look slightly more involved than in the dlog case, but much simpler than in the monomial case. To reproduce eq. [\(4.140\)](#), we also need the intersections

$$\langle \phi_3 | \varphi_1 \rangle = \frac{a(x-1)(c+(2b-a+1)x) - b(1+b)x^2}{(a-c-1)(a-c)(1+a-c)x^2} \quad (4.150)$$

$$\langle \phi_3 | \varphi_2 \rangle = \frac{(x-1)(bx(a+c+(b-2a+1)x-1) + (c-ax-1)(c+x-ax))}{(a-c-1)(a-c)(1+a-c)x^3} \quad (4.151)$$

both of which are much simpler than in the monomial basis. As expected, using them in eq. [\(4.53\)](#) yields eq. [\(4.140\)](#).

### 4.4.3 Two-Loop Pentabox

In general, the prefactor  $K'$  appearing in eq. [\(2.30\)](#) can be factorized in a component proportional to the kinematic variables, and another which depends only on the dimensional parameter:

$$K' = \kappa(d) K''(d, v_{ij}) \quad (4.152)$$

with  $v_{ij} \equiv p_i \cdot p_j$ .

The factor  $\kappa(d)$  do not affect neither IBPs nor differential equations, and therefore we disregard it in the following.

From here on we refer to  $K''$  as  $K$  to ease our notation.

## Planar Diagram

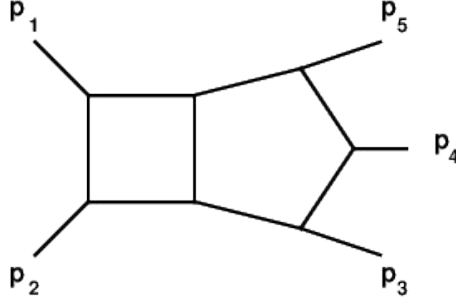


Figure 4.1: Massless planar pentabox.

Let us consider the massless five-point planar topology at two-loop [143,144] in Fig. 4.1 with the following list of denominators:

$$\begin{aligned} D_1 &= k_1^2, & D_2 &= (k_1 + p_1)^2, & D_3 &= (k_1 + p_1 + p_2)^2, & D_4 &= (k_1 - k_2)^2, \\ D_5 &= (k_2 + p_1 + p_2)^2, & D_6 &= (k_2 + p_1 + p_2 + p_3)^2, \\ D_7 &= (k_2 + p_1 + p_2 + p_3 + p_4)^2, & D_8 &= k_2^2. \end{aligned} \quad (4.153)$$

The ISP considered in the Loop-by-Loop procedure is:

$$z = D_9 = (k_2 + p_1)^2. \quad (4.154)$$

We find:

$$\begin{aligned} u &= z^\alpha (a + z)^\beta (b + ez + fz^2)^\alpha, \\ K &= v_{34}^{\frac{d-6}{2}} v_{45}^{\frac{d-6}{2}} v_{12}^{\frac{d-6}{2}} \left( (v_{15} - v_{23})^2 v_{12}^2 + 2((v_{15} - v_{23}) v_{23} v_{34} + (v_{15} (v_{23} - v_{15}) \right. \\ &\quad \left. + (v_{15} + v_{23}) v_{34}) v_{45}) v_{12} + (v_{23} v_{34} + (v_{15} - v_{34}) v_{45})^2 \right)^{\frac{5-d}{2}}, \end{aligned} \quad (4.155)$$

where:

$$\alpha = \frac{d}{2} - 3, \quad \beta = 2 - \frac{d}{2}, \quad a = 2v_{12}, \quad b = 4v_{12}v_{15}v_{23}, \quad (4.156)$$

$$e = -2(v_{12}v_{15} - v_{45}v_{15} + v_{12}v_{23} - v_{23}v_{34} + v_{34}v_{45}), \quad f = v_{12} - v_{34} - v_{45}, \quad (4.157)$$

Thus:

$$\omega = \left( \frac{\beta}{a+z} + \frac{\alpha(b+z(2e+3fz))}{z(b+z(e+fz))} \right) dz, \quad (4.158)$$

$$\nu = 3, \quad \mathcal{P} = \left\{ 0, -a, \frac{-\sqrt{e^2 - 4bf} - e}{2f}, \frac{\sqrt{e^2 - 4bf} - e}{2f}, \infty \right\}. \quad (4.159)$$

We observe that the combination  $e^2 - 4bf$  is proportional to the Gram determinant  $\Delta = |2p_i \cdot p_j|$  with  $1 \leq i, j \leq 4$ . Similar relations hold for the cases studied in the other multileg cases (see also [145,146]).

**Monomial Basis.** Let us consider the decomposition of  $I_{1,1,1,1,1,1,1,-3} = \langle \phi_4 | \mathcal{C} \rangle$  in terms of  $J_1 = I_{1,1,1,1,1,1,1,0} = \langle \phi_1 | \mathcal{C} \rangle$ ,  $J_2 = I_{1,1,1,1,1,1,1,-1} = \langle \phi_2 | \mathcal{C} \rangle$ , and  $J_3 = I_{1,1,1,1,1,1,1,-2} = \langle \phi_3 | \mathcal{C} \rangle$ . We can compute the  $\mathbf{C}$  matrix:

$$\mathbf{C}_{ij} = \langle \phi_i | \phi_j \rangle, \quad i, j = 1, 2, 3, \quad (4.160)$$

and the intersection numbers:

$$\langle \phi_4 | \phi_i \rangle, \quad i = 1, 2, 3 : \quad (4.161)$$

Then, eq. (4.53) yields:

$$I_{1,1,1,1,1,1,1,1;-3} = c_1 J_1 + c_2 J_2 + c_3 J_3, \quad (4.162)$$

with the coefficients:

$$\begin{aligned} c_1 &= -\frac{a(\alpha+1)b}{f(3\alpha+\beta+4)}, \\ c_2 &= -\frac{2a(\alpha+1)e+b(\alpha+\beta+2)}{f(3\alpha+\beta+4)}, \\ c_3 &= -\frac{3a(\alpha+1)f+e(2\alpha+\beta+3)}{f(3\alpha+\beta+4)}. \end{aligned} \quad (4.163)$$

In agreement with REDUZE.

**Differential Equations in Monomial Basis.** We define the variable  $x = v_{12}$  with respect to which we build the system of differential equations. In order to do it, one also needs

$$\begin{aligned} \sigma(x) &= \partial_x \log(u) \\ &= \frac{(z-2v_{23})((z-2v_{15})((d-6)z-4x) + 2(d-4)v_{34}z) + 2(d-4)v_{45}z(-2v_{15}+2v_{34}+z)}{2(2x+z)((z-2v_{23})(x(z-2v_{15})-v_{34}z) - v_{45}z(-2v_{15}+2v_{34}+z))} \end{aligned} \quad (4.164)$$

and  $\langle \Phi_i(x) | = \langle (\partial_x + \sigma(x))\phi_i |$ , which are:

$$\langle \Phi_1(x) | = \sigma dz, \quad (4.165)$$

$$\langle \Phi_2(x) | = z \sigma dz, \quad (4.166)$$

$$\langle \Phi_3(x) | = z^2 \sigma dz. \quad (4.167)$$

Then, according to the procedure described in Sec. 4.2.1, we can compute the analytic expression of  $\mathbf{A}$ .

For readability we present the result in a single phase space point:

$$v_{23} = \frac{1}{2}, \quad v_{34} = \frac{1}{3}, \quad v_{45} = \frac{1}{5}, \quad v_{15} = \frac{1}{7}, \quad (4.168)$$

The entries of  $\mathbf{A}$  read:

$$\begin{aligned} \mathbf{A}_{11} &= \frac{d-6}{x} + \frac{2(d-4)}{10x+3} - \frac{735(d-4)}{134(21x-4)} + \frac{22556d+375(2263-482d)x-96589}{67(5x(375x-38)+243)}, \\ \mathbf{A}_{12} &= \frac{4(x(45x(11830x+21893)-268886)-459)-d(x(45x(8890x+19219)-272918)+5589)}{4x(10x+3)(21x-4)(5x(375x-38)+243)}, \\ \mathbf{A}_{13} &= \frac{7(d-4)(15x-8)(615x-1103)}{2x(10x+3)(21x-4)(5x(375x-38)+243)}, \\ \mathbf{A}_{21} &= -\frac{15(d-4)x(615x-1103)}{(10x+3)(21x-4)(5x(375x-38)+243)}, \\ \mathbf{A}_{22} &= \frac{d-5}{x} - \frac{16(d-4)}{10x+3} - \frac{609(d-4)}{134(21x-4)} + \frac{2(d-4)(19875x-21104)}{67(5x(375x-38)+243)}, \\ \mathbf{A}_{23} &= -\frac{7(d-4)(25x(9x(125x-19)+376)-864)}{x(10x+3)(21x-4)(5x(375x-38)+243)}, \\ \mathbf{A}_{31} &= \frac{30(d-4)x(25x(9x(125x-19)+376)-864)}{(10x+3)(15x-8)(21x-4)(5x(375x-38)+243)}, \end{aligned} \quad (4.169)$$

$$\mathbf{A}_{32} = \frac{1}{1005} \left( -\frac{9648(d-4)}{10x+3} + \frac{1740(d-4)}{21x-4} + \frac{-5633500x + 9d(137875x - 9963) + 250128}{5x(375x - 38) + 243} - \frac{5360(3d-13)}{15x-8} \right),$$

$$\mathbf{A}_{33} = \frac{d-6}{2x} + \frac{15(d-2)}{16-30x} + \frac{14(d-4)}{10x+3} + \frac{672(d-4)}{67(21x-4)} + \frac{126d(257-875x) + 566625x - 135893}{67(5x(375x - 38) + 243)},$$

in agreement with REDUZE.

### Non-Planar Diagram

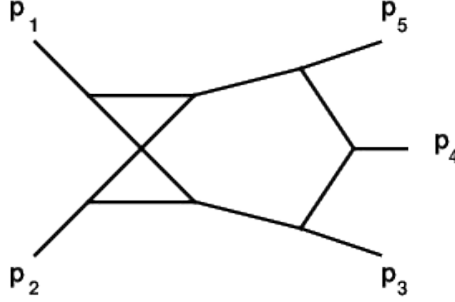


Figure 4.2: Massless non-planar pentabox.

We consider the massless non-planar five-point topology at two-loop [147], shown in Fig. 4.2. We denote the scalar products as:  $v_{ij} = p_i \cdot p_j$ . We consider the following list of denominators:

$$\begin{aligned} D_1 &= k_1^2, & D_2 &= (k_1 + p_1)^2, & D_3 &= (k_1 - k_2 - p_2)^2, & D_4 &= (k_1 - k_2)^2, \\ D_5 &= (k_2 + p_1 + p_2)^2, & D_6 &= (k_2 + p_1 + p_2 + p_3)^2, \\ D_7 &= (k_2 + p_1 + p_2 + p_3 + p_4)^2, & D_8 &= k_2^2. \end{aligned} \quad (4.170)$$

The ISP considered in the Loop-by-Loop approach is:

$$z = D_9 = (k_2 + p_1)^2. \quad (4.171)$$

Performing a maximal cut we find:

$$\begin{aligned} u &= (z(a+z)(b+ez+fz^2))^\alpha, \\ K &= v_{12}^{2-\frac{d}{2}} v_{34}^{\frac{d-6}{2}} v_{45}^{\frac{d-6}{2}} (v_{12}^2 (v_{15} - v_{23})^2 + (v_{23}v_{34} + (v_{15} - v_{34})v_{45})^2 + 2v_{12}((v_{15} - v_{23})v_{23}v_{34} \\ &\quad + (v_{15}(v_{23} - v_{15}) + (v_{15} + v_{23})v_{34})v_{45}))^{\frac{5-d}{2}}. \end{aligned} \quad (4.172)$$

where

$$\begin{aligned} \alpha &= \frac{d}{2} - 3, & a &= 2v_{12}, & b &= 4v_{12}v_{15}v_{23}, \\ e &= -2(v_{12}v_{15} - v_{45}v_{15} + v_{12}v_{23} - v_{23}v_{34} + v_{34}v_{45}), & f &= v_{12} - v_{34} - v_{45} \end{aligned} \quad (4.173)$$

Then:

$$\omega = \frac{\alpha(2z(ae+b) + ab + 3z^2(af+e) + 4fz^3)}{z(a+z)(b+z(e+fz))} dz, \quad (4.174)$$

and so:

$$\nu = 3, \quad \mathcal{P} = \left\{ 0, -a, \frac{-\sqrt{e^2 - 4bf} - e}{2f}, \frac{\sqrt{e^2 - 4bf} - e}{2f}, \infty \right\}. \quad (4.175)$$



**Monomial Basis.** The MIs can be chosen as:  $J_1 = I_{1,1,1,1,1,1,1,1,0} = \langle \phi_1 | \mathcal{C} \rangle$ ,  $J_2 = I_{1,1,1,1,1,1,1,1,-1} = \langle \phi_2 | \mathcal{C} \rangle$ , and  $J_3 = I_{1,1,1,1,1,1,1,1,-2} = \langle \phi_3 | \mathcal{C} \rangle$ .

Let us consider the decomposition of  $I_{1,1,1,1,1,1,1,1,-3} = \langle \phi_4 | \mathcal{C} \rangle$  in this basis. We can compute the  $\mathbf{C}$  matrix,

$$\mathbf{C}_{ij} = \langle \phi_i | \phi_j \rangle, \quad i, j = 1, 2, 3, \quad (4.176)$$

and the additional intersection numbers:

$$\langle \phi_4 | \phi_i \rangle, \quad i = 1, 2, 3, \quad (4.177)$$

and then, eq. (4.53) yields:

$$I_{1,1,1,1,1,1,1,1,-3} = c_1 J_1 + c_2 J_2 + c_3 J_3, \quad (4.178)$$

with:

$$c_1 = -\frac{ab}{4f}, \quad c_2 = -\frac{ae+b}{2f}, \quad c_3 = -\frac{3(af+e)}{4f} \quad (4.179)$$

in agreement with REDUZE.

**Differential Equations in Monomial Basis.** Let us define the variable  $x = v_{12}$  with respect to which we build the system of differential equations. Then we consider:

$$\begin{aligned} \sigma(x) &= \partial_x \log(u) \\ &= \frac{(d-6)((z-2v_{23})((4v_{12}+z)(z-2v_{15})-2v_{34}z)-2v_{45}z(-2v_{15}+2v_{34}+z))}{2(2v_{12}+z)((z-2v_{23})(v_{12}(z-2v_{15})-v_{34}z)-v_{45}z(-2v_{15}+2v_{34}+z))} \end{aligned} \quad (4.180)$$

and  $\{\langle \Phi_i(x) | \rangle\}_{i=1,2,3}$  are given by:

$$\langle \Phi_1(x) | = \sigma dz, \quad (4.181)$$

$$\langle \Phi_2(x) | = z \sigma dz, \quad (4.182)$$

$$\langle \Phi_3(x) | = z^2 \sigma dz. \quad (4.183)$$

Then, according to the procedure described in Sec. 4.2.1, we can compute the analytic expression of  $\mathbf{A}$ .

For readability we present the result in a single phase space point:

$$v_{23} = \frac{1}{2}, \quad v_{34} = \frac{1}{3}, \quad v_{45} = \frac{1}{5}, \quad v_{15} = \frac{1}{7}. \quad (4.184)$$

The entries of  $\mathbf{A}$  become:

$$\begin{aligned} \mathbf{A}_{11} &= \frac{d-6}{x} + \frac{2(d-4)}{10x+3} - \frac{735(d-4)}{134(21x-4)} + \frac{22556d + 375(2263 - 482d)x - 96589}{67(5x(375x-38) + 243)}, \\ \mathbf{A}_{12} &= \frac{42(x(15x(9630x+6623)-33682)+4167)-d(x(45x(26390x+20249)-340738)+40959)}{4x(10x+3)(21x-4)(5x(375x-38)+243)}, \\ \mathbf{A}_{13} &= \frac{7(2d-9)(15x-8)(615x-1103)}{2x(10x+3)(21x-4)(5x(375x-38)+243)}, \\ \mathbf{A}_{21} &= -\frac{15(d-4)x(615x-1103)}{(10x+3)(21x-4)(5x(375x-38)+243)}, \\ \mathbf{A}_{22} &= \frac{4914-861d}{536-2814x} + \frac{d-5}{x} + \frac{84-20d}{10x+3} + \frac{-68225d+375(65d-219)x+298917}{67(5x(375x-38)+243)}, \\ \mathbf{A}_{23} &= -\frac{7(2d-9)(25x(9x(125x-19)+376)-864)}{x(10x+3)(21x-4)(5x(375x-38)+243)}, \end{aligned} \quad (4.185)$$

$$\begin{aligned} \mathbf{A}_{31} &= \frac{30(d-4)x(25x(9x(125x-19)+376)-864)}{(10x+3)(15x-8)(21x-4)(5x(375x-38)+243)}, \\ \mathbf{A}_{32} &= \frac{450x(3x(45x(500x-227)+8107)-8504)}{67(5x(375x-38)+243)} \\ &\quad + \frac{-3d(5x(225x(x(2250x-1001)+763)-59368)+24192)+290304}{(10x+3)(15x-8)(21x-4)(5x(375x-38)+243)}, \\ \mathbf{A}_{33} &= \frac{45(d-4)}{16-30x} - \frac{d-4}{2x} + \frac{14(2d-9)}{10x+3} + \frac{672(2d-9)}{67(21x-4)} + \frac{d(58399-94875x)+489750x-265978}{67(5x(375x-38)+243)}. \end{aligned}$$

in agreement with REDUZE.

#### 4.4.4 Multileg and Massive Cases

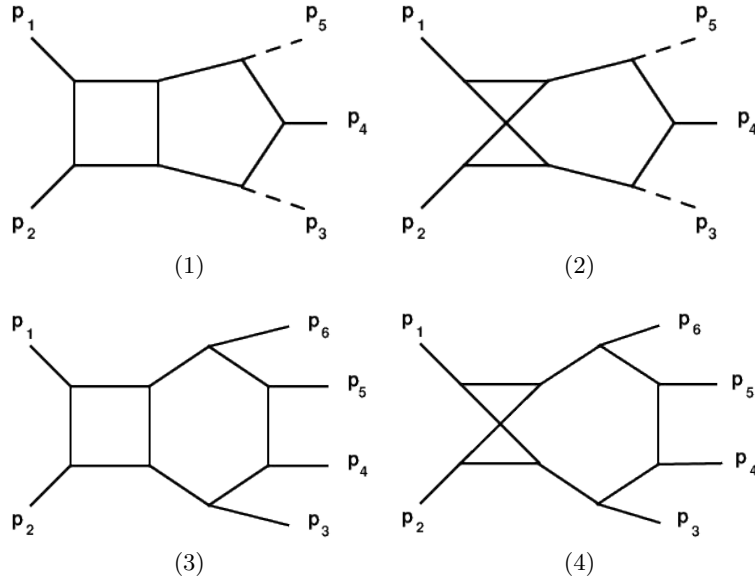


Figure 4.3: Planar and non-planar pentabox with two external masses (1,2), as well as planar and non-planar hexagon-box (3,4).

Let us now study how the polynomial  $u$  changes when we compute Feynman integrals such as those in Sec. 4.4.3, but with massive external legs, or with more massless external legs<sup>3</sup> as shown in Fig. 4.3.

- **Case (1), planar massive pentabox:** the external kinematic is defined by  $p_3^2 = p_5^2 = m^2$  and  $p_i^2 = 0$  for  $i = 1, 2, 4$ , with the denominators

$$\begin{aligned} D_1 &= k_1^2, & D_2 &= (k_1 + p_1)^2, & D_3 &= (k_1 + p_1 + p_2)^2, & D_4 &= (k_1 - k_2)^2, \\ D_5 &= (k_2 + p_1 + p_2)^2, & D_6 &= (k_2 + p_1 + p_2 + p_3)^2, \\ D_7 &= (k_2 + p_1 + p_2 + p_3 + p_4)^2, & D_8 &= k_2^2. \end{aligned} \tag{4.186}$$

<sup>3</sup>We assume the number of space-time dimensions  $d$  to not be smaller than the number of independent external momenta.

- **Case (2), non-planar massive pentabox:** the external kinematic is defined by  $p_3^2 = p_5^2 = m^2$  and  $p_i^2 = 0$  for  $i = 1, 2, 4$ , with the denominators

$$\begin{aligned} D_1 &= k_1^2, & D_2 &= (k_1 + p_1)^2, & D_3 &= (k_1 - k_2 - p_2)^2, & D_4 &= (k_1 - k_2)^2, \\ D_5 &= (k_2 + p_1 + p_2)^2, & D_6 &= (k_2 + p_1 + p_2 + p_3)^2, \\ D_7 &= (k_2 + p_1 + p_2 + p_3 + p_4)^2, & D_8 &= k_2^2. \end{aligned} \quad (4.187)$$

- **Case (3), planar massless hexagon-box:** the external kinematic is defined by  $p_i^2 = 0$  for  $i = 1, \dots, 5$ , with the denominators

$$\begin{aligned} D_1 &= k_1^2, & D_2 &= (k_1 + p_1)^2, & D_3 &= (k_1 + p_1 + p_2)^2, & D_4 &= (k_1 - k_2)^2, \\ D_5 &= (k_2 + p_1 + p_2)^2, & D_6 &= (k_2 + p_1 + p_2 + p_3)^2, \\ D_7 &= (k_2 + p_1 + p_2 + p_3 + p_4)^2, & D_8 &= k_2^2, \\ D_9 &= (k_2 + p_1 + p_2 + p_3 + p_4 + p_5)^2. \end{aligned} \quad (4.188)$$

- **Case (4), non-planar massless hexagon-box:** the external kinematic is defined by  $p_i^2 = 0$  for  $i = 1, \dots, 5$ , with the denominators

$$\begin{aligned} D_1 &= k_1^2, & D_2 &= (k_1 + p_1)^2, & D_3 &= (k_1 - p_1 - p_2)^2, & D_4 &= (k_1 - k_2)^2, \\ D_5 &= (k_2 + p_1 + p_2)^2, & D_6 &= (k_2 + p_1 + p_2 + p_3)^2, \\ D_7 &= (k_2 + p_1 + p_2 + p_3 + p_4)^2, & D_8 &= k_2^2, \\ D_9 &= (k_2 + p_1 + p_2 + p_3 + p_4 + p_5)^2. \end{aligned} \quad (4.189)$$

The only ISP appearing using the Loop-by-Loop procedure in these four cases is:

$$z = (k_2 + p_1)^2. \quad (4.190)$$

In all the 4 cases show in Fig. [4.3](#), the Loop-by-Loop Baikov polynomials on the maximal cut give the common expression,

$$u = z^{\alpha_i} (a_i + z)^{\beta_i} (b_i + e_i z + f_i z^2)^{\gamma_i}; \quad (4.191)$$

- **Case (1), planar massive pentabox:**

$$\begin{aligned} \alpha_1 &= \gamma_1 = \frac{d}{2} - 3, & \beta_1 &= 2 - \frac{d}{2}, & a_1 &= 2v_{12}, \\ b_1 &= 2v_{12} (m^2 (v_{15} - v_{23}) - v_{34} (m^2 + 2v_{23})) (m^2 (v_{45} - v_{23}) + v_{15} (m^2 + 2v_{45})), \\ e_1 &= 2v_{12} (m^2 (v_{15} - v_{23}) v_{34} + v_{45} (m^2 (v_{23} - v_{15}) + 2v_{34} (m^2 + v_{15} + v_{23}))) \\ &\quad - 2(v_{23}v_{34} + (v_{15} - v_{34})v_{45}) (m^2 v_{45} + v_{34} (m^2 + 2v_{45})), \\ f_1 &= v_{34}^2 (m^2 + 2v_{45}) + 2v_{45}v_{34} (m^2 - v_{12} + v_{45}) + m^2 v_{45}^2, \end{aligned}$$

- **Case (2), non-planar massive pentabox:**

$$\begin{aligned} \alpha_2 &= \beta_2 = \gamma_2 = \frac{d}{2} - 3, & a_2 &= 2v_{12}, \\ b_2 &= 2v_{12} (m^2 (v_{15} - v_{23}) - v_{34} (m^2 + 2v_{23})) (m^2 (v_{45} - v_{23}) + v_{15} (m^2 + 2v_{45})), \\ e_2 &= 2v_{12} (m^2 (v_{15} - v_{23}) v_{34} + v_{45} (m^2 (v_{23} - v_{15}) + 2v_{34} (m^2 + v_{15} + v_{23}))) \\ &\quad - 2(v_{23}v_{34} + (v_{15} - v_{34})v_{45}) (m^2 v_{45} + v_{34} (m^2 + 2v_{45})), \\ f_2 &= v_{34}^2 (m^2 + 2v_{45}) + 2v_{45}v_{34} (m^2 - v_{12} + v_{45}) + m^2 v_{45}^2. \end{aligned}$$

In the cases concerning 6 external legs, the number of independent kinematic variables grows a lot and the expressions for the constants become rather heavy.

We present them evaluated at the phase space point:

$$\begin{aligned} v_{12} &= 1, & v_{13} &= \frac{1}{2}, & v_{14} &= \frac{1}{3}, & v_{15} &= \frac{1}{5}, & v_{23} &= \frac{1}{7}, \\ v_{24} &= \frac{1}{11}, & v_{25} &= \frac{1}{13}, & v_{34} &= \frac{1}{17}, & v_{35} &= \frac{1}{19}. \end{aligned} \quad (4.192)$$

• **Case (3), planar massless hexagon-box:**

$$\begin{aligned} \alpha_3 &= \frac{d-6}{2}, & \beta_3 &= 2 - \frac{d}{2}, & \gamma_3 &= \frac{d-7}{2}, & a_3 &= 2, \\ b_3 &= \frac{619142135915328239231}{1450900103219383716900}, & e_3 &= -\frac{7218174020286869797}{2586274693795692900}, \\ f_3 &= -\frac{47636820419356249}{18440461274835600}. \end{aligned} \quad (4.193)$$

• **Case (4), non-planar massless hexagon-box:**

$$\begin{aligned} \alpha_4 &= \beta_4 = \frac{d}{2} - 3, & \gamma_4 &= \frac{d-7}{2}, & a_4 &= 2, \\ b_4 &= \frac{619142135915328239231}{1450900103219383716900}, & e_4 &= -\frac{7218174020286869797}{2586274693795692900}, \\ f_4 &= \frac{47636820419356249}{18440461274835600}. \end{aligned} \quad (4.194)$$

We define:

$$\omega_i = \left( \frac{\beta_i}{a_i + z} + \frac{\gamma_i (e_i + 2f_i z)}{b_i + z(e_i + f_i z)} + \frac{\alpha_i}{z} \right) dz. \quad (4.195)$$

So we get:

$$\nu = 3, \quad \mathcal{P} = \left\{ 0, -a_i, \frac{-\sqrt{e_i^2 - 4b_i f_i} - e_i}{2f_i}, \frac{\sqrt{e_i^2 - 4b_i f_i} - e_i}{2f_i}, \infty \right\}. \quad (4.196)$$

**Monomial Basis.** The MIs are chosen to be:  $J_1 = I_{1,1,1,1,1,1,1,0} = \langle \phi_1 | \mathcal{C} \rangle$ ,  $J_2 = I_{1,1,1,1,1,1,1,-1} = \langle \phi_2 | \mathcal{C} \rangle$  and  $J_3 = I_{1,1,1,1,1,1,1,-2} = \langle \phi_3 | \mathcal{C} \rangle$ .

Let us consider the decomposition of  $I_{1,1,1,1,1,1,1,-3} = \langle \phi_4 | \mathcal{C} \rangle$  in terms of this basis.

We compute the the  $\mathbf{C}$  matrix:

$$\mathbf{C}_{ij} = \langle \phi_i | \phi_j \rangle, \quad i, j = 1, 2, 3, \quad (4.197)$$

and the intersection numbers:

$$\langle \phi_4 | \phi_i \rangle, \quad i = 1, 2, 3, \quad (4.198)$$

and the eq. (4.53) gives:

$$I_{1,1,1,1,1,1,1,-3} = c_1 J_1 + c_2 J_2 + c_3 J_3, \quad (4.199)$$

with:

$$\begin{aligned} c_1 &= -\frac{a_i (\alpha_i + 1) b_i}{f_i (\alpha_i + \beta_i + 2\gamma_i + 4)}, \\ c_2 &= -\frac{a_i e_i (\alpha_i + \gamma_i + 2) + b_i (\alpha_i + \beta_i + 2)}{f_i (\alpha_i + \beta_i + 2\gamma_i + 4)}, \\ c_3 &= -\frac{a_i f_i (\alpha_i + 2\gamma_i + 3) + e_i (\alpha_i + \beta_i + \gamma_i + 3)}{f_i (\alpha_i + \beta_i + 2\gamma_i + 4)}, \end{aligned} \quad (4.200)$$

in agreement with REDUZE, for all four cases.

### Arbitrary Number of External Legs Case

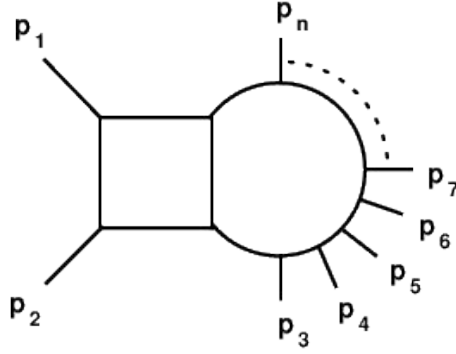


Figure 4.4: Multileg generalization of the topologies portrayed in Fig. 4.3.

The direct generalization of the cases discussed above is portrayed in Fig. 4.4.

Here, choosing the following list of denominators:

$$\begin{aligned}
 D_1 &= k_1^2, & D_2 &= (k_1 + p_1)^2, & D_3 &= (k_1 + p_1 + p_2)^2, & D_4 &= (k_1 - k_2)^2, \\
 D_5 &= (k_2 + p_1 + p_2)^2, & D_{5+j} &= \left( k_2 + p_1 + p_2 + \sum_{r=1}^j p_{2+r} \right)^2
 \end{aligned}
 \tag{4.201}$$

for a diagram with a number of external legs  $E$  equal to  $E = 4 + j$  with  $j > 1$ , and choosing as ISP

$$z = D_{8+j} = (k_2 + p_1)^2. \tag{4.202}$$

the Loop-by-Loop Baikov polynomials on the maximal cut have the same structure as the previous 5 and 6 point cases, where at least one of  $p_1$  and  $p_2$  is massless:

$$u = z^{\alpha_i} (a_i + z)^{\beta_i} (b_i + e_i z + f_i z^2)^{\gamma_i}; \tag{4.203}$$

Therefore the reduction derived in eq. (4.199) remains valid for any number of external legs. This result has been checked numerically with REDUZE up to 8 external legs.

### 4.4.5 Arbitrary Loop Examples

#### Planar Rocket Diagram for $H+j$ : $(3+2n)$ -Loop Case

In this Section we consider certain higher-loop topologies that contribute to the Higgs+jet production. As done in Sec. 4.4.3, we define  $K$  as described in and around eq. (4.152).

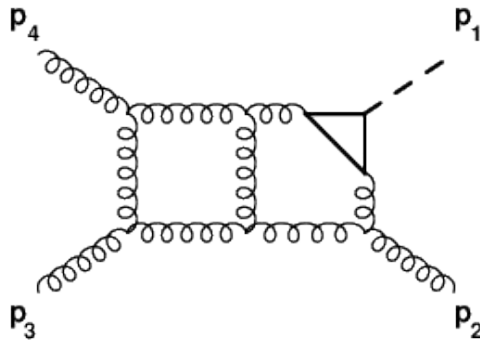


Figure 4.5: Planar three-loop diagram contributing to  $H+jet$  production.

Let us consider a specific planar integral sector for Higgs+jet production from gluon fusion at three loops, depicted in Fig. 4.5. The kinematics is such that:  $p_1^2 = m_H^2$ ,  $p_i^2 = 0$  with  $i = 2, 3$ ,  $s = (p_1 + p_2)^2$ ,  $t = (p_2 + p_3)^2$  and  $(p_1 + p_2 + p_3)^2 = 0$ .

The denominators are chosen as:

$$\begin{aligned} D_1 &= k_1^2 - m_t^2, & D_2 &= (k_1 - p_1)^2 - m_t^2, & D_3 &= (k_1 - k_2)^2 - m_t^2, \\ D_4 &= (k_2 - p_1)^2, & D_5 &= (k_2 - p_1 - p_2)^2, & D_6 &= k_2^2, & D_7 &= (k_2 - k_3)^2, \\ D_8 &= (k_3 - p_1 - p_2)^2, & D_9 &= (k_3 - p_1 - p_2 - p_3)^2, & D_{10} &= k_3^2, \end{aligned} \quad (4.204)$$

while the ISP is:

$$z = D_{11} = (k_3 + p_1)^2. \quad (4.205)$$

The Loop-by-Loop Baikov representation on the maximal cut, gives:

$$u = (z - 2m_H^2)^{\frac{d}{2}-3} (m_H^2 + s - z)^{2-\frac{d}{2}} (-2m_H^2 + t + z)^{d-5}, \quad (4.206)$$

$$K = \frac{s^{d-6} t^{2-\frac{d}{2}} m_t^{d-4} (-m_H^2 + s + t)^{2-\frac{d}{2}}}{m_H^2}. \quad (4.207)$$

On the other hand let us consider the five-loop topology in Fig 4.6

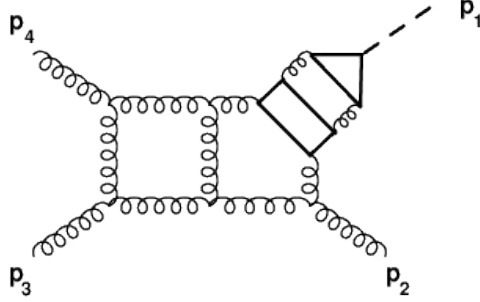


Figure 4.6: Planar five-loop diagram contributing to  $H+j$  production.

Given the set of denominators:

$$\begin{aligned} D_1 &= k_1^2 - m_t^2, & D_2 &= (k_1 - p_1)^2 - m_t^2, & D_3 &= (k_1 - k_2)^2 - m_t^2, \\ D_4 &= (k_2 - p_1)^2, & D_5 &= (k_2 - k_3)^2 - m_t^2, & D_6 &= k_2^2, \\ D_7 &= (k_3 - p_1)^2 - m_t^2, & D_8 &= (k_3 - k_4)^2 - m_t^2, & D_9 &= k_3^2 - m_t^2, \\ D_{10} &= (k_4 - p_1)^2, & D_{11} &= (k_4 - p_1 - p_2)^2, & D_{12} &= k_4^2, & D_{13} &= (k_4 - k_5)^2, \\ D_{14} &= (k_5 - p_1 - p_2)^2, & D_{15} &= (k_5 - p_1 - p_2 - p_3)^2, & D_{16} &= k_5^2. \end{aligned} \quad (4.208)$$

and choosing the ISP as:

$$z = D_{17} = (k_5 + p_1)^2, \quad (4.209)$$

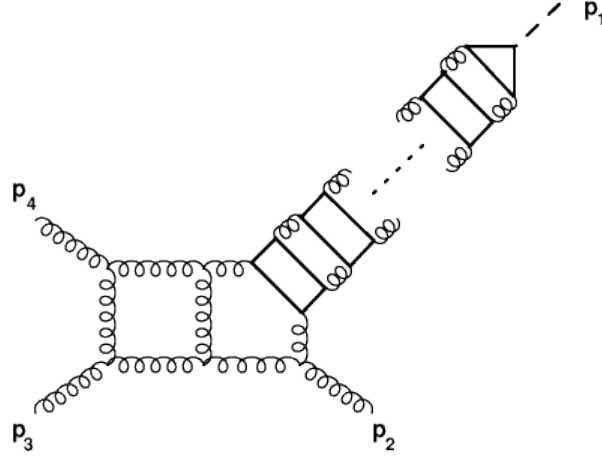
the Loop-by-Loop Baikov representation on the maximal cut gives:

$$u = (z - 2m_H^2)^{\frac{d}{2}-3} (m_H^2 + s - z)^{2-\frac{d}{2}} (-2m_H^2 + t + z)^{d-5}, \quad (4.210)$$

$$K = s^{d-6} t^{2-\frac{d}{2}} m_H^{d-9} m_t^{3(d-4)} (4m_t^2 - m_H^2)^{\frac{3-d}{2}} (-m_H^2 + s + t)^{2-\frac{d}{2}}. \quad (4.211)$$

We notice that  $u$  is exactly the same as eq. (4.206), while  $K$  slightly changes from eq. (4.207).

Iterating the Loop-by-Loop procedure to topologies with higher number of loops, we observe that the structure remains the same; thus, we can generalize that formula to the  $(3+2n)$ -loop case ( $n \geq 0$ ) shown in Fig. 4.7

Figure 4.7: Planar box-rocket diagram contributing to  $H+j$  production.

In fact choosing the ISP as:

$$z = D_{11+6n} = (k_{3+2n} + p_1)^2, \quad (4.212)$$

the Loop-by-Loop Baikov representation on the maximal cut gives:

$$u = (z - 2m_H^2)^{\frac{d}{2}-3} (m_H^2 + s - z)^{2-\frac{d}{2}} (-2m_H^2 + t + z)^{d-5}, \quad (4.213)$$

$$K = s^{d-6} t^{2-\frac{d}{2}} m_H^{(d-7)n-2} m_t^{(d-4)(2n+1)} (4m_t^2 - m_H^2)^{-\frac{1}{2}(d-3)n} (-m_H^2 + s + t)^{2-\frac{d}{2}}. \quad (4.214)$$

And so:

$$\omega = \frac{1}{2} \left( \frac{d-4}{m_H^2 + s - z} + \frac{2(d-5)}{-2m_H^2 + t + z} + \frac{d-6}{z - 2m_H^2} \right) dz, \quad (4.215)$$

$$\nu = 2, \quad \mathcal{P} = \{2m_H^2, 2m_H^2 - t, m_H^2 + s, \infty\}, \quad (4.216)$$

which are valid for all the  $(3+2n)$ -loop diagrams.

**Monomial Basis.** Let us consider the decomposition of  $I_{1,1,\dots,1;-3} = \langle \phi_4 | \mathcal{C} \rangle$  in terms of the MIs:  $J_1 = I_{1,1,\dots,1;0} = \langle \phi_1 | \mathcal{C} \rangle$  and  $J_2 = I_{1,1,\dots,1;-1} = \langle \phi_2 | \mathcal{C} \rangle$ . We compute the  $\mathbf{C}$  matrix:

$$\mathbf{C}_{ij} = \langle \phi_i | \phi_j \rangle, \quad i, j = 1, 2, \quad (4.217)$$

and the intersection numbers:

$$\langle \phi_4 | \phi_i \rangle, \quad i = 1, 2, \quad (4.218)$$

Then, we obtain the final decomposition by means of eq. (4.53):

$$I_{1,1,\dots,1;-3} = c_1 J_1 + c_2 J_2, \quad (4.219)$$

with:

$$\begin{aligned} c_1 = & - \frac{m_H^2 (9d^2 s^2 - d^2 st - 66ds^2 - 14dst - 2dt^2 + 120s^2 + 72st + 16t^2)}{2(d-3)(d-2)} \\ & - \frac{m_H^4 (36d^2 s + 5d^2 t - 168ds - 42dt + 96s - 8t)}{4(d-3)(d-2)} \\ & - \frac{(5d^2 - 10d + 24) m_H^6}{2(d-3)(d-2)} + \frac{(d-4)st(3ds - 10s - 4t)}{4(d-3)(d-2)}, \end{aligned} \quad (4.220)$$

$$c_2 = \frac{m_H^2 (9d^2 s - d^2 t - 42ds + 2dt + 24s - 16t)}{2(d-3)(d-2)} + \frac{3(7d^2 - 30d + 40)m_H^4}{4(d-3)(d-2)} \quad (4.221)$$

$$+ \frac{9d^2 s^2 + 2d^2 st - 66ds^2 - 28dst + 120s^2 + 80st + 8t^2}{4(d-3)(d-2)},$$

in (numerical) agreement with REDUZE in the *three* loop case.

**Differential Equation in Monomial Basis.** We build the system of differential equations with respect to the variable  $s$ .

We consider:

$$\sigma(s) = \partial_s \log(u) = -\frac{d-4}{2(m_H^2 + s - z)}. \quad (4.222)$$

Then,  $\{\langle \Phi_i | \}$  are given by:

$$\langle \Phi_1 | = \sigma dz, \quad (4.223)$$

$$\langle \Phi_2 | = \sigma z dz. \quad (4.224)$$

Following the discussion presented in Sec. (4.2.1) we determine the  $\mathbf{A}$  matrix; the entries read:

$$\mathbf{A}_{11} = \frac{(d-4)(2s+t)}{t(-m_H^2 + s + t)} + \frac{2(d-4)s}{t(m_H^2 - s)} + \frac{d-6}{s}, \quad (4.225)$$

$$\mathbf{A}_{12} = \frac{d-4}{(s-m_H^2)(-m_H^2 + s + t)}, \quad (4.226)$$

$$\mathbf{A}_{21} = \frac{(d-4)(st - m_H^2(2m_H^2 + 6s + t))}{2(s-m_H^2)(-m_H^2 + s + t)}, \quad (4.227)$$

$$\mathbf{A}_{22} = -\frac{3(d-4)}{2(-m_H^2 + s + t)} + \frac{2(d-4)s}{(s-m_H^2)(-m_H^2 + s + t)} + \frac{d-6}{s}, \quad (4.228)$$

in (numerical) agreement with REDUZE in the *three* loop case.

### Non-Planar Rocket Diagram for $H+j$ : $(3+2n)$ -Loop Case

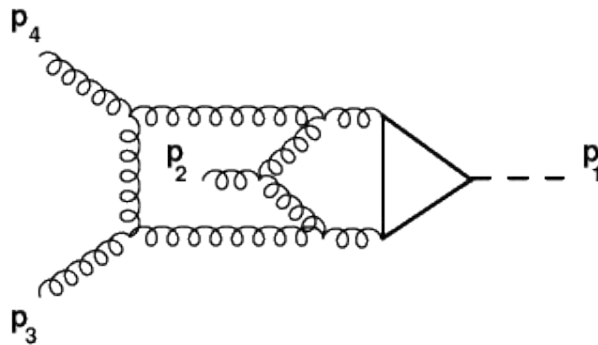


Figure 4.8: Non-planar three-loop diagram contributing to the  $H+j$  production.

Let us consider the non-planar topology for the  $H+j$  production at *three* loop portrayed in Fig. (4.8). The kinematics is such that:  $p_1^2 = m_H^2$ ,  $p_i^2 = 0$  with  $i = 2, 3$ ,  $s = (p_1 + p_2)^2$ ,  $t = (p_2 + p_3)^2$  and  $(p_1 + p_2 + p_3)^2 = 0$ .

The denominators are given by:

$$D_1 = k_1^2 - m_t^2, \quad D_2 = (k_1 - p_1)^2 - m_t^2, \quad D_3 = (k_1 - k_2)^2 - m_t^2, \quad (4.229)$$



$$D_4 = (k_2 - p_1)^2 \quad D_5 = (k_2 - k_3 + p_2)^2, \quad D_6 = k_2^2, \quad D_7 = (k_2 - k_3)^2, \quad (4.230)$$

$$D_8 = (k_3 - p_1 - p_2)^2, \quad D_9 = (k_3 - p_1 - p_2 - p_3)^2, \quad D_{10} = k_3^2, \quad (4.231)$$

while the ISP is:

$$z = D_{11} = (k_3 + p_1)^2. \quad (4.232)$$

Using the Loop-by-Loop Baikov representation, on the maximal cut we obtain:

$$u = (z - 2m_H^2)^{\frac{d}{2}-3} (m_H^2 + s - z)^{\frac{d}{2}-3} (-2m_H^2 + t + z)^{d-5}, \quad (4.233)$$

$$K = \frac{t^{2-\frac{d}{2}} m_t^{d-4} (-m_H^2 + s + t)^{2-\frac{d}{2}}}{s m_H^2}. \quad (4.234)$$

As done for the planar diagram, we can infer the general structure for the corresponding  $3 + 2n$ -loop integral ( $n \geq 0$ ) shown in Fig. 4.9:

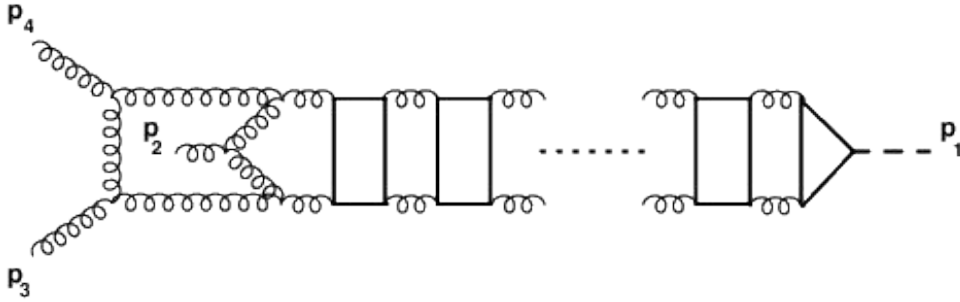


Figure 4.9: Non-planar box-rocket diagram contributing to  $H+j$  production.

In fact choosing the ISP as:

$$z = D_{11+6n} = (k_{3+2n} + p_1)^2, \quad (4.235)$$

after the maximal cut, we find:

$$u = (z - 2m_H^2)^{\frac{d}{2}-3} (m_H^2 + s - z)^{\frac{d}{2}-3} (-2m_H^2 + t + z)^{d-5}, \quad (4.236)$$

$$K = \frac{t^{2-\frac{d}{2}} m_H^{(d-7)n-2} m_t^{(d-4)(2n+1)} (4m_t^2 - m_H^2)^{-\frac{1}{2}(d-3)n} (-m_H^2 + s + t)^{2-\frac{d}{2}}}{s}, \quad (4.237)$$

thus:

$$\omega = \frac{1}{2} \left( \frac{6-d}{m_H^2 + s - z} + \frac{2(d-5)}{-2m_H^2 + t + z} + \frac{d-6}{z - 2m_H^2} \right) dz, \quad (4.238)$$

$$\nu = 2, \quad \mathcal{P} = \{2m_H^2, -t+2m_H^2, (m_H^2+s), \infty\}, \quad (4.239)$$

which are valid for all the  $(3+2n)$ -loop diagrams.

**Monomial Basis.** Let us consider the decomposition of  $I_{1,1,\dots,1,-3} = \langle \phi_4 | \mathcal{C} \rangle$  in terms of  $J_1 = I_{1,1,\dots,1,0} = \langle \phi_1 | \mathcal{C} \rangle$  and  $J_2 = I_{1,1,\dots,1,-1} = \langle \phi_2 | \mathcal{C} \rangle$ .

We can compute the  $\mathbf{C}$  matrix:

$$\mathbf{C}_{ij} = \langle \phi_i | \phi_j \rangle, \quad i, j = 1, 2, \quad (4.240)$$

and the additional intersection numbers:

$$\langle \phi_4 | \phi_i \rangle, \quad i = 1, 2, \quad (4.241)$$

and finally eq. (4.53) gives:

$$I_{1,1,\dots,1;-3} = c_1 J_1 + c_2 J_2, \quad (4.242)$$

with:

$$\begin{aligned} c_1 = & -\frac{m_H^2 (9ds^2 - 17dst + 3dt^2 - 30s^2 + 62st - 9t^2)}{4(2d-7)} \\ & -\frac{m_H^4 (108ds - 59dt - 384s + 202t)}{8(2d-7)} \\ & -\frac{(65d-226)m_H^6}{4(2d-7)} + \frac{st(3ds - 2dt - 10s + 6t)}{8(2d-7)}, \end{aligned} \quad (4.243)$$

$$\begin{aligned} c_2 = & \frac{m_H^2 (27ds - 20dt - 96s + 69t)}{4(2d-7)} + \frac{3(43d-150)m_H^4}{8(2d-7)} \\ & + \frac{9ds^2 - 8dst + 4dt^2 - 30s^2 + 30st - 12t^2}{8(2d-7)}, \end{aligned} \quad (4.244)$$

in (numerical) agreement with REDUZE in the *three* loop case.

**Differential Equations in Monomial Basis.** We build the system of differential equation with respect to the variable  $s$ .

We consider:

$$\sigma(s) = \partial_s \log(u) = \frac{d-6}{2(m_H^2 + s - z)}, \quad (4.245)$$

which gives  $\{\langle \Phi_i | \}_{i=1,2}$  :

$$\langle \Phi_1 | = \sigma dz, \quad (4.246)$$

$$\langle \Phi_2 | = \sigma z dz. \quad (4.247)$$

Then, following the discussion in Sec. 4.2.1, we build the  $\mathbf{A}$  matrix, with:

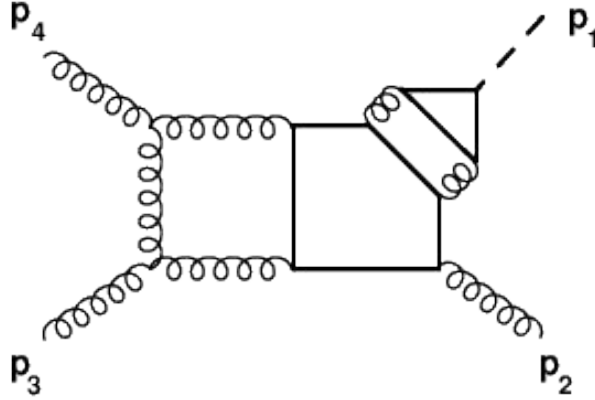
$$\mathbf{A}_{11} = \frac{m_H^2 ((21-4d)s + t) + s((d-6)t - 2s) - m_H^4}{s(s-m_H^2)(-m_H^2 + s + t)}, \quad (4.248)$$

$$\mathbf{A}_{12} = \frac{2d-9}{(s-m_H^2)(-m_H^2 + s + t)}, \quad (4.249)$$

$$\mathbf{A}_{21} = \frac{m_H^2 ((3d-16)t - 6(d-4)s) + (48-10d)m_H^4 + (d-4)st}{2(s-m_H^2)(-m_H^2 + s + t)}, \quad (4.250)$$

$$\mathbf{A}_{22} = \frac{m_H^2 ((5d-18)s + 2t) + s((3d-16)s - 2t) - 2m_H^4}{2s(s-m_H^2)(-m_H^2 + s + t)}. \quad (4.251)$$

in (numerical) agreement with REDUZE in the *three* loop case.

Planar Rocket Diagram for  $H+j$ :  $(2+2n)$ -Loop CaseFigure 4.10: Planar four-loop diagram contributing to  $H+j$  production.

Let us consider the *four* loop planar topology in Fig. 4.10 which contributes to the  $H+j$  production. The kinematics is such that:  $p_1^2 = m_H^2$ ,  $p_i^2 = 0$  with  $i = 2, 3$ ,  $s = (p_1 + p_2)^2$ ,  $t = (p_2 + p_3)^2$  and  $(p_1 + p_2 + p_3)^2 = 0$ .

The denominators are:

$$\begin{aligned} D_1 &= k_1^2 - m_t^2, & D_2 &= (k_1 - p_1)^2 - m_t^2, & D_3 &= (k_1 - k_2)^2 - m_t^2, \\ D_4 &= (k_2 - p_1)^2, & D_5 &= (k_2 - k_3)^2 - m_t^2, & D_6 &= k_2^2, \\ D_7 &= (k_3 - p_1)^2 - m_t^2, & D_8 &= (k_3 - p_1 - p_2)^2 - m_t^2, & D_9 &= (k_3 - k_4)^2 - m_t^2, \\ D_{10} &= k_3^2 - m_t^2, & D_{11} &= (k_4 - p_1 - p_2)^2, & D_{12} &= (k_4 - p_1 - p_2 - p_3)^2, & D_{13} &= k_4^2. \end{aligned} \quad (4.252)$$

While the ISP is:

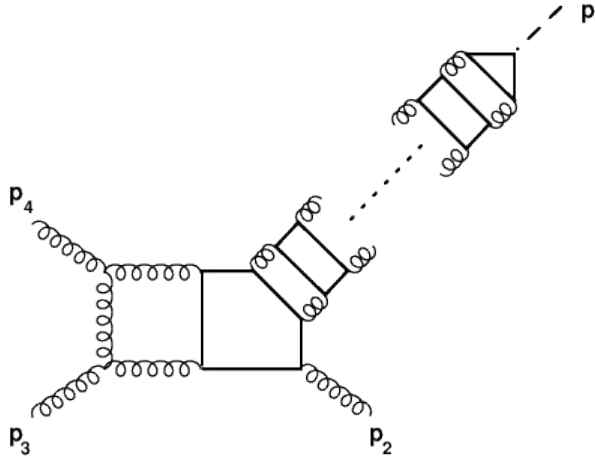
$$z = D_{14} = (k_4 + p_1)^2. \quad (4.253)$$

The Loop-by-Loop Baikov representation, on the maximal cut gives: with

$$u = \frac{(m_H^2 + s - z)^{2 - \frac{d}{2}} (-2m_H^2 + t + z)^{d-5} (2sm_H^2 - 4m_H^2 m_t^2 - 4sm_t^2 + z(4m_t^2 - s))^{\frac{d-5}{2}}}{\sqrt{z - 2m_H^2}}, \quad (4.254)$$

$$K = s^{\frac{d-7}{2}} t^{2 - \frac{d}{2}} m_H^{(d-7)} m_t^{2(d-4)} (4m_t^2 - m_H^2)^{-\frac{1}{2}(d-3)} (-m_H^2 + s + t)^{2 - \frac{d}{2}}. \quad (4.255)$$

We can generalize such a construction in order to describe the  $(2+2n)$ -loop diagram ( $n \geq 0$ ), shown in Fig. 4.11:

Figure 4.11: Planar All-loop diagram contributing to  $H+j$  production.

In fact choosing as ISP:

$$D_{8+6n} = (k_{2+2n} + p_1)^2, \quad (4.256)$$

we obtain:

$$u = \frac{(m_H^2 + s - z)^{2-\frac{d}{2}} (-2m_H^2 + t + z)^{d-5} (2sm_H^2 - 4m_H^2 m_t^2 - 4sm_t^2 + z(4m_t^2 - s))^{\frac{d-5}{2}}}{\sqrt{z - 2m_H^2}}, \quad (4.257)$$

$$K = s^{\frac{d-7}{2}} t^{2-\frac{d}{2}} m_H^{(d-7)n} m_t^{2(d-4)n} (4m_t^2 - m_H^2)^{-\frac{1}{2}(d-3)n} (-m_H^2 + s + t)^{2-\frac{d}{2}}, \quad (4.258)$$

from which we can evaluate:

$$\begin{aligned} \omega &= \frac{1}{2} \left( \frac{(d-5)(s-4m_t^2)}{m_H^2(4m_t^2-2s) + 4m_t^2(s-z) + sz} + \frac{d-4}{m_H^2 + s - z} + \frac{2(d-5)}{-2m_H^2 + t + z} + \frac{1}{2m_H^2 - z} \right) dz, \\ \nu &= 3, \quad \mathcal{P} = \{2m_H^2, m_H^2 + s, 2m_H^2 - t, -\frac{2(-sm_H^2 + 2m_H^2 m_t^2 + 2sm_t^2)}{s - 4m_t^2}, \infty\}. \end{aligned} \quad (4.259)$$

which are valid for all the  $(2+2n)$ -loop diagrams.

**Monomial Basis.** Let us consider the reduction of  $I_{1,1,\dots,1;-3} = \langle \phi_4 | \mathcal{C} \rangle$  in terms of:  $J_1 = I_{1,1,\dots,1;0} = \langle \phi_1 | \mathcal{C} \rangle$  and  $J_2 = I_{1,1,\dots,1;-1} = \langle \phi_2 | \mathcal{C} \rangle$  and  $J_3 = I_{1,1,\dots,1;-2} = \langle \phi_3 | \mathcal{C} \rangle$ .

We can compute the  $\mathbf{C}$  matrix:

$$\mathbf{C} = \langle \phi_i | \phi_j \rangle, \quad i = 1, 2, 3, \quad (4.260)$$

and the intersection numbers:

$$\langle \phi_4 | \phi_i \rangle, \quad i = 1, 2, 3, \quad (4.261)$$

thus, eq. (4.53) leads to:

$$I_{1,1,\dots,1;-3} = c_1 J_1 + c_2 J_2 + c_3 J_3, \quad (4.262)$$

with:

$$c_1 = \left( sm_H^2 (m_H^2((6d-20)s + (d-10)t) + 2(d+2)m_H^4 + (2-d)st) + 2m_t^2 (m_H^2 + s) (m_H^2((14-4d)s + 7t) + (2-4d)m_H^4 + st) \right) / \left( (d-2)(s-4m_t^2) \right), \quad (4.263)$$

$$c_2 = \left( 4m_t^2 (m_H^2(6(2d-5)s - 11t) + (10d-11)m_H^4 + s((2d-7)s - 5t)) + s(m_H^2((40-12d)s - (d-18)t) + (8-12d)m_H^4 + (d-2)st) \right) / \left( 2(d-2)(s-4m_t^2) \right), \quad (4.264)$$

$$c_3 = \left( 4m_t^2 ((13-8d)m_H^2 + (11-4d)s + 4t) + s((9d-14)m_H^2 + (3d-10)s - 4t) \right) / \left( 2(d-2)(s-4m_t^2) \right). \quad (4.265)$$

in agreement with REDUZE in the *two* loop case.

**Differential Equations in Monomial Basis.** We derive:

$$\sigma(s) = -\frac{(z - 2m_H^2) \left( -(d-5)m_H^2 + (d-5)z + s \right) + 4m_t^2 (m_H^2 + s - z)}{2(m_H^2 + s - z) (4m_t^2 (m_H^2 + s - z) + s(z - 2m_H^2))}. \quad (4.266)$$

The  $\{\langle \Phi_i | \}_{i=1,2,3}$  are given by:

$$\langle \Phi_1 | = \sigma dz, \quad (4.267)$$

$$\langle \Phi_2 | = \sigma z dz, \quad (4.268)$$

$$\langle \Phi_3 | = \sigma z^2 dz. \quad (4.269)$$

Then, the  $\mathbf{A}$  matrix can be computed following Sec. (4.2.1); the entries are presented evaluated at the phase space point:

$$m_t^2 = 1, \quad m_H^2 = 3, \quad t = 5. \quad (4.270)$$

We find:

$$\mathbf{A}_{11} = \frac{d(13s^2 + 7s - 120) - 2(s^3 + 19s^2 + 10s - 186)}{s(s^3 - 9s^2 + 2s + 48)}, \quad (4.271)$$

$$\mathbf{A}_{12} = \frac{d(-2s^2 - 15s + 72) + 8s^2 + 50s - 244}{(s-8)(s-3)s(s+2)}, \quad (4.272)$$

$$\mathbf{A}_{13} = \frac{2(d-3)(s-4)}{(s-8)(s-3)s(s+2)}, \quad (4.273)$$

$$\mathbf{A}_{21} = \frac{2(3d(5s^2 - 15s - 72) - 59s^2 + 168s + 810)}{(s-8)(s-3)s(s+2)}, \quad (4.274)$$

$$\mathbf{A}_{22} = \frac{d(-10s^2 + 28s + 240) - 2s^3 + 51s^2 - 84s - 900}{s(s^3 - 9s^2 + 2s + 48)}, \quad (4.275)$$

$$\mathbf{A}_{23} = \frac{(d-3)(s^2 - 4s - 24)}{(s-8)(s-3)s(s+2)}, \quad (4.276)$$

$$\mathbf{A}_{31} = \frac{3d(5s^4 - 35s^3 - 132s^2 + 648s + 1728) - 2(28s^4 - 193s^3 - 753s^2 + 3636s + 9720)}{(s-8)(s-4)(s-3)s(s+2)}, \quad (4.277)$$

$$\mathbf{A}_{32} = \frac{d(-23s^4 + 173s^3 + 408s^2 - 2088s - 5184) + 2(41s^4 - 307s^3 - 712s^2 + 3588s + 8784)}{2(s-8)(s-4)(s-3)s(s+2)}, \quad (4.278)$$

$$\mathbf{A}_{33} = \frac{d(3s^4 - 21s^3 - 76s^2 + 376s + 384) - 2(7s^4 - 59s^3 - 70s^2 + 740s + 192)}{2(s-8)(s-4)(s-3)s(s+2)}. \quad (4.279)$$

in agreement with REDUZE in the *two* loop case.

#### Non-Planar Rocket Diagram for $H+j$ : $(2+2n)$ -Loop Case

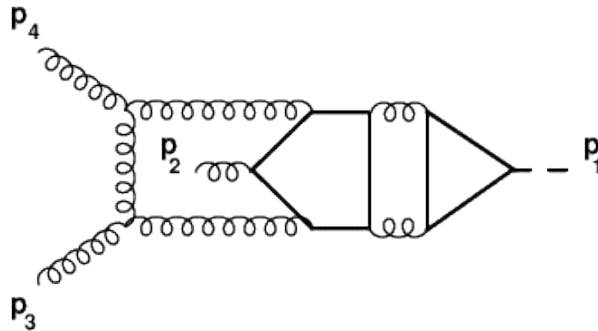


Figure 4.12: Non-planar four loop contribution to  $H+j$  production.

Let us consider the non-planar *four* loop contribution to  $H+j$  production in Fig. 4.12. The kinematics is such that:  $p_1^2 = m_H^2$ ,  $p_i^2 = 0$  with  $i = 2, 3$ ,  $s = (p_1 + p_2)^2$ ,  $t = (p_2 + p_3)^2$  and  $(p_1 + p_2 + p_3)^2 = 0$ .

In this case the denominators are:

$$D_1 = k_1^2 - m_t^2, \quad D_2 = (k_1 - p_1)^2 - m_t^2, \quad D_3 = (k_1 - k_2)^2 - m_t^2,$$

$$\begin{aligned}
D_4 &= (k_2 - p_1)^2, & D_5 &= (k_2 - k_3)^2 - m_t^2, & D_6 &= k_2^2, \\
D_7 &= (k_3 - p_1)^2 - m_t^2, & D_8 &= (k_3 - k_4 + p_2)^2 - m_t^2, & D_9 &= (k_3 - k_4)^2 - m_t^2, \\
D_{10} &= k_3^2 - m_t^2, & D_{11} &= (k_4 - p_1 - p_2)^2, & D_{12} &= (k_4 - p_1 - p_2 - p_3)^2, & D_{13} &= k_4^2.
\end{aligned} \tag{4.280}$$

We choose the ISP as:

$$z = D_{14} = (k_4 + p_1)^2, \tag{4.281}$$

The Loop-by-Loop Baikov representation, after the maximal cut gives:

$$u = \frac{(-2m_H^2 + t + z)^{d-5} ((2m_H^2 - z)(m_H^2 + s - z) - 4sm_t^2)^{\frac{d-5}{2}}}{\sqrt{z - 2m_H^2} \sqrt{m_H^2 + s - z}}, \tag{4.282}$$

$$K = \frac{t^{2-\frac{d}{2}} m_H^{d-7} m_t^{2(d-4)} (4m_t^2 - m_H^2)^{\frac{3-d}{2}} (-m_H^2 + s + t)^{2-\frac{d}{2}}}{s}. \tag{4.283}$$

As stated above, we can generalize such Baikov polynomial in order to describe the  $(2+2n)$ -loop diagram ( $n \geq 0$ ) shown in Fig. 4.13.

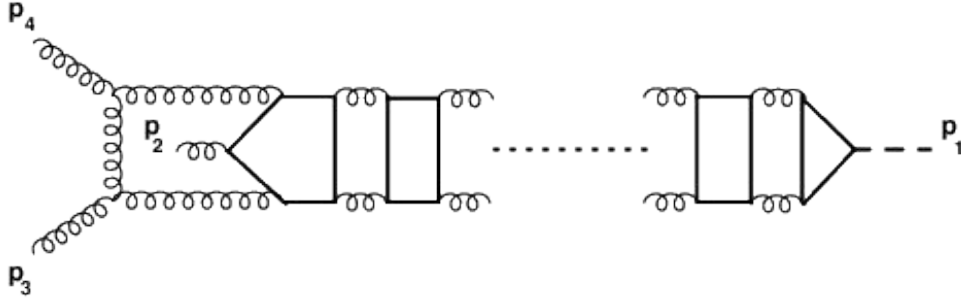


Figure 4.13: Non-planar  $(2+2n)$ -loop contribution to  $H+j$  production.

In fact choosing the ISP as:

$$D_{8+6n} = (k_{2+2n} + p_1)^2, \tag{4.284}$$

we obtain:

$$u = \frac{(-2m_H^2 + t + z)^{d-5} ((2m_H^2 - z)(m_H^2 + s - z) - 4sm_t^2)^{\frac{d-5}{2}}}{\sqrt{z - 2m_H^2} \sqrt{m_H^2 + s - z}}, \tag{4.285}$$

$$K = \frac{t^{2-\frac{d}{2}} m_H^{(d-7)n} m_t^{2(d-4)n} (4m_t^2 - m_H^2)^{-\frac{1}{2}(d-3)n} (-m_H^2 + s + t)^{2-\frac{d}{2}}}{s}, \tag{4.286}$$

from which we evaluate:

$$\omega = \frac{1}{2} \left( \frac{(d-5)(3m_H^2 + s - 2z)}{(z - 2m_H^2)(m_H^2 + s - z) + 4sm_t^2} + \frac{2(d-5)}{-2m_H^2 + t + z} + \frac{1}{m_H^2 + s - z} + \frac{1}{2m_H^2 - z} \right) dz, \tag{4.287}$$

$$\nu = 4, \quad \mathcal{P} = \{2m_H^2, m_H^2 + s, 2m_H^2 - t, \rho_1, \rho_2, \infty\}. \tag{4.288}$$

which are valid for all the  $(2+2n)$ -loop diagrams.

**Monomial Basis.** Let us consider the reduction of  $I_{1,1,\dots,1;-4} = \langle \phi_5 | \mathcal{C} \rangle$  in terms of:  $J_1 = I_{1,1,\dots,1;0} = \langle \phi_1 | \mathcal{C} \rangle$ ,  $J_2 = I_{1,1,\dots,1;-1} = \langle \phi_2 | \mathcal{C} \rangle$ ,  $J_3 = I_{1,1,\dots,1;-2} = \langle \phi_3 | \mathcal{C} \rangle$  and  $J_4 = I_{1,1,\dots,1;-3} = \langle \phi_4 | \mathcal{C} \rangle$ .

We compute the  $\mathbf{C}$  matrix:

$$\mathbf{C} = \langle \phi_i | \phi_j \rangle, \quad 1 \leq i, j \leq 4, \quad (4.289)$$

and the intersection numbers:

$$\langle \phi_5 | \phi_i \rangle, \quad 1 \leq i \leq 4, \quad (4.290)$$

then eq. (4.53) gives:

$$I_{1,1,\dots,1;-4} = c_1 J_1 + c_2 J_2 + c_3 J_3 + c_4 J_4, \quad (4.291)$$

with:

$$c_1 = \frac{m_H^2 (m_H^2 + s) (m_H^2 ((20 - 6d)s + 3(d - 2)t) + (28 - 10d)m_H^4 + (d - 2)st)}{2(d - 3)} + \frac{-2s m_t^2 (m_H^2 ((14 - 4d)s + 3t) + (10 - 4d)m_H^4 + st)}{2(d - 3)}, \quad (4.292)$$

$$c_2 = \frac{m_H^4 (4(15d - 46)s - 13(d - 2)t) + 2s m_H^2 ((6d - 20)s - 5(d - 2)t)}{4(d - 3)} + \frac{4s m_t^2 ((17 - 6d)m_H^2 + (7 - 2d)s + 2t) + 8(7d - 20)m_H^6 + (2 - d)s^2 t}{4(d - 3)}, \quad (4.293)$$

$$c_3 = \frac{m_H^2 (4(28 - 9d)s + 9(d - 2)t) + (166 - 57d)m_H^4 + s(8(d - 3)m_t^2)}{4(d - 3)} + \frac{(10 - 3d)s + 3(d - 2)t}{4(d - 3)}, \quad (4.294)$$

$$c_4 = \frac{(25d - 74)m_H^2 + (7d - 22)s - 2(d - 2)t}{4(d - 3)}. \quad (4.295)$$

in agreement with REDUZE in the *two* loop case.

**Differential Equations in Monomial Basis.** In the *two* loop case ( $n = 0$ ) we derive:

$$\sigma(s) = \frac{4m_t^2 ((d - 5)m_H^2 + (d - 6)s - (d - 5)z) + (d - 6)(z - 2m_H^2)(m_H^2 + s - z)}{2(m_H^2 + s - z)((z - 2m_H^2)(m_H^2 + s - z) + 4sm_t^2)}. \quad (4.296)$$

The  $\{\langle \Phi_i | \rangle\}_{i=1,2,3,4}$  are given by:

$$\langle \Phi_1 | = \sigma dz, \quad (4.297)$$

$$\langle \Phi_2 | = \sigma z dz, \quad (4.298)$$

$$\langle \Phi_3 | = \sigma z^2 dz, \quad (4.299)$$

$$\langle \Phi_4 | = \sigma z^3 dz. \quad (4.300)$$

Then, the  $\mathbf{A}$  matrix can be computed following Sec. (4.2.1); the entries are presented evaluated at the phase space point:

$$m_t^2 = 1, \quad m_H^2 = 3, \quad t = 5. \quad (4.301)$$

We find:

$$\mathbf{A}_{11} = \frac{-2s^5 + 13s^4 + 92s^3 - 3751s^2 - 19284s + d(-11s^4 - 43s^3 + 1063s^2 + 5235s + 4860)}{(s - 3)s(s + 2)(s + 10)(s^2 + 10s + 9)} + \frac{-18144}{(s - 3)s(s + 2)(s + 10)(s^2 + 10s + 9)},$$

$$\begin{aligned}
\mathbf{A}_{12} &= \frac{3(-3s^4 + 2s^3 + 851s^2 + 4976s + 5058) + d(2s^4 - 8s^3 - 703s^2 - 4002s - 4077)}{(s-3)s(s+2)(s+10)(s^2+10s+9)}, \\
\mathbf{A}_{13} &= \frac{d(3s^3 + 113s^2 + 899s + 1041) - 2(5s^3 + 200s^2 + 1617s + 1872)}{(s-3)s(s+2)(s+10)(s^2+10s+9)}, \\
\mathbf{A}_{14} &= -\frac{2(2d-7)(s^2+16s+21)}{(s-3)s(s+2)(s+10)(s^2+10s+9)}, \\
\mathbf{A}_{21} &= \frac{30d(s^3 + 19s^2 + 69s + 63) - 2(53s^3 + 1079s^2 + 3972s + 3618)}{(s-3)s(s+1)(s+2)(s+10)}, \\
\mathbf{A}_{22} &= \frac{-2s^4 + 106s^3 + 1560s^2 + 6126s - d(34s^3 + 423s^2 + 1628s + 1623) + 6066}{(s-3)s(s+1)(s+2)(s+10)}, \\
\mathbf{A}_{23} &= \frac{d(5s^3 + 80s^2 + 378s + 429) - 2(9s^3 + 143s^2 + 677s + 768)}{(s-3)s(s+1)(s+2)(s+10)}, \\
\mathbf{A}_{24} &= -\frac{2(2d-7)(s^2+7s+9)}{(s-3)s(s+1)(s+2)(s+10)}, \\
\mathbf{A}_{31} &= \frac{30d(s^4 + 19s^3 + 120s^2 + 297s + 243) - 4(28s^4 + 535s^3 + 3426s^2 + 8514s + 6939)}{(s-3)s(s+1)(s+2)(s+10)}, \\
\mathbf{A}_{32} &= \frac{2(41s^4 + 813s^3 + 5128s^2 + 13425s + 11853) - d(23s^4 + 449s^3 + 2790s^2)}{(s-3)s(s+1)(s+2)(s+10)} \\
&\quad + \frac{7281s + 6453}{(s-3)s(s+1)(s+2)(s+10)}, \\
\mathbf{A}_{33} &= -\frac{12s^4 + 271s^3 + 2061s^2 + 6278s - d(3s^4 + 72s^3 + 577s^2 + 1783s + 1779) + 6276}{(s-3)s(s+1)(s+2)(s+10)}, \\
\mathbf{A}_{34} &= -\frac{(2d-7)(s^3 + 17s^2 + 70s + 78)}{(s-3)s(s+1)(s+2)(s+10)}, \\
\mathbf{A}_{41} &= \frac{(s+9)(15d(s^4 + 20s^3 + 121s^2 + 288s + 234) - 2(28s^4 + 569s^3 + 3457s^2)}{(s-3)s(s+1)(s+2)(s+10)} \\
&\quad + \frac{8214s + 6642)}{(s-3)s(s+1)(s+2)(s+10)}, \\
\mathbf{A}_{42} &= \frac{82s^5 + 2362s^4 + 25034s^3 + 119834s^2 + 263028s - d(23s^5 + 649s^4 + 6803s^3)}{2(s-3)s(s+1)(s+2)(s+10)} \\
&\quad + \frac{32613s^2 + 71874s + 57726) + 210492}{2(s-3)s(s+1)(s+2)(s+10)}, \\
\mathbf{A}_{43} &= \frac{d(3s^5 + 90s^4 + 1135s^3 + 7030s^2 + 18528s + 16578) - 2(5s^5 + 162s^4 + 2081s^3)}{2(s-3)s(s+1)(s+2)(s+10)} \\
&\quad + \frac{12586s^2 + 32838s + 29376)}{2(s-3)s(s+1)(s+2)(s+10)}, \\
\mathbf{A}_{44} &= \frac{2(s^4 + 62s^3 + 773s^2 + 2746s + 2706) - d(s^4 + 40s^3 + 441s^2 + 1530s + 1512)}{2(s-3)s(s+1)(s+2)(s+10)}.
\end{aligned}$$

in agreement with REDUZE in the *two* loop case.

## 4.5 Multivariate intersection number

In this Section we discuss the details of the recursive algorithm employed for the evaluation of intersection numbers of multivariate differential forms introduced in [81]; the algorithm was successfully applied in the context of Feynman integrals as well as hypergeometric functions



in [2,3]. The recursive algorithm expresses the  $n$ -variable intersection number in terms of  $(n-1)$ -variable intersection numbers and so on, where the last term of this sequence is the univariate intersection number discussed in refs. [1,68].

In particular, we consider integrals with  $n$  integration variables  $\{z_{i_1}, \dots, z_{i_n}\}$ , which can be seen as iterative integrals, with a nested structure that follows from the chosen ordering  $\{i_1, \dots, i_k\}$  of the integers  $\{1, \dots, n\}$ . In order to compute multivariate intersection number for  $n$ -differential forms, we need to calculate the dimension of the cohomology groups for all  $k$ -differential forms, from  $k=1$  to  $k=n$ . They can be obtained, for instance, by counting the number  $\nu_{\mathbf{k}}$  of solutions to the equation system given by eq. (4.40),

$$\hat{\omega}_j \equiv \partial_{z_j} \log u(\mathbf{z}) = 0, \quad j = i_1, \dots, i_k, \quad (4.302)$$

where  $\mathbf{k} = \{i_1, \dots, i_k\}$  is a subset of  $\{1, \dots, n\}$  with  $k$  distinct elements. In this way, one obtains a list of dimensions  $\nu_{\mathbf{1}}, \nu_{\mathbf{2}}, \dots, \nu_{\mathbf{n}}$ , respectively corresponding to the iterative integration in  $\{z_{i_1}\}$ , in  $\{z_{i_1}, z_{i_2}\}$ ,  $\dots$ , in  $\{z_{i_1}, \dots, z_{i_n}\}$  variables, and where we used the vector notation,

$$\mathbf{1} = \{i_1\}, \quad \mathbf{2} = \{i_1, i_2\}, \quad \dots, \quad \mathbf{n} = \{i_1, i_2, \dots, i_n\}, \quad (4.303)$$

to indicate the integration variables.

It is interesting to observe that, while  $\nu_{\mathbf{n}}$  is trivially independent of the ordering of the integration variables, the dimensions of the subspaces  $\nu_{\mathbf{k}}$  may indeed depend on which specific subsets  $\mathbf{k}$  of  $\{1, 2, \dots, n\}$  are chosen and in which order. As a working principle, we choose the ordering that minimizes the sizes of  $\nu_{\mathbf{k}}$  for all  $k$ -forms ( $k=1, \dots, n$ ).

Before delving into the  $n$ -variable intersection number, we start with the example of 2-variable intersection numbers, written recursively in terms of univariate intersection numbers; an approach which will later be generalized to the  $n$ -variate case.

#### 4.5.1 2-variable intersection number

We start by considering an integral with two integration variables  $\{z_1, z_2\}$ , written as follows,

$$I = \int_{\mathcal{C}_R^{(2)}} \varphi_L^{(2)}(z_1, z_2) u(z_1, z_2) = \langle \varphi_L^{(2)} | \mathcal{C}_R^{(2)} \rangle, \quad (4.304)$$

where  $\mathbf{2} = \{1, 2\}$ ,  $\varphi_L^{(2)}$  is a differential 2-form in variables  $z_1$  and  $z_2$ , while  $\mathcal{C}_R^{(2)}$  is a two-dimensional integration domain embedded in some ambient space  $X$  with complex dimension 2. We assume that  $X$  admits a fibration into one-dimensional spaces  $X_2 \ni z_2$  and  $X_1 \ni z_1$ <sup>4</sup>, and correspondingly  $\varphi_L^{(2)}, \mathcal{C}_R^{(2)}$  can be decomposed in a similar manner. Similarly, we can consider a dual integral, given by

$$\tilde{I} = \int_{\mathcal{C}_L^{(2)}} \varphi_R^{(2)}(z_1, z_2) u^{-1}(z_1, z_2) = [\mathcal{C}_L^{(2)} | \varphi_R^{(2)}], \quad (4.305)$$

with all the variables defined analogously to the ones above.

As before, we have

$$\omega = d \log u(\mathbf{z}) = \sum_{i=1}^2 \hat{\omega}_i dz_i \quad (4.306)$$

and employing eq. (4.40), we can count the number of MIs in the  $X_1$  space, which we label as  $\nu_{\mathbf{1}}$  with  $\mathbf{1} = \{1\}$ . Then the goal is to determine the 2-variable intersection number  $\langle \varphi_L^{(2)} | \varphi_R^{(2)} \rangle$  in terms of the univariate intersection numbers on the  $X_1$  space, which are calculable with the univariate methods discussed in [1,68] and assumed to be already computed.

<sup>4</sup>This does not necessarily mean that  $X = X_2 \times X_1$ , since  $X_1 = X_1(z_2)$  can depend on  $z_2$  (but  $X_2$  does not depend on  $z_1$ ).

We start by decomposing the differential forms as

$$\langle \varphi_L^{(2)} | = \sum_{i=1}^{\nu_1} \langle e_i^{(1)} | \wedge \langle \varphi_{L,i}^{(2)} | , \quad (4.307)$$

$$| \varphi_R^{(2)} \rangle = \sum_{i=1}^{\nu_1} | h_i^{(1)} \rangle \wedge | \varphi_{R,i}^{(2)} \rangle , \quad (4.308)$$

into an arbitrary basis forms  $\langle e_i^{(1)} |$  and their duals  $| h_i^{(1)} \rangle$  on  $X_1$ . In the above expressions  $\langle \varphi_{L,i}^{(2)} |$  and  $| \varphi_{R,j}^{(2)} \rangle$  are one-forms in the variables  $z_2$ , and they are treated as coefficients of the basis expansion. They can be obtained by a projection similar to eq. (4.53), using only univariate intersection, namely (sum over repeated indices is understood)

$$\langle \varphi_{L,i}^{(2)} | = \langle \varphi_L^{(2)} | h_j^{(1)} \rangle (\mathbf{C}_{(1)}^{-1})_{ji} , \quad (4.309)$$

$$| \varphi_{R,i}^{(2)} \rangle = (\mathbf{C}_{(1)}^{-1})_{ij} \langle e_j^{(1)} | \varphi_R^{(2)} \rangle , \quad (4.310)$$

with the metric matrix, which is also a univariate intersection matrix

$$(\mathbf{C}_{(1)})_{ij} \equiv \langle e_i^{(1)} | h_j^{(1)} \rangle . \quad (4.311)$$

From refs. [1,68] we know that the univariate intersection number is given as

$$\langle e_i^{(1)} | h_j^{(1)} \rangle = \sum_{p \in \mathcal{P}_{\omega_1}} \text{Res}_{z_1=p} \left[ \psi_i^{(p)} h_j^{(1)} \right] , \quad (4.312)$$

where  $\psi_i^{(p)}$  is the local solution of the differential equation

$$\nabla_{\omega_1} \psi_i^{(p)} = e_i^{(1)} , \quad (4.313)$$

around every pole  $p$  of  $\omega_1$ , denoted by the set  $\mathcal{P}_{\omega_1}$ . Here the connection  $\omega_1$  is just the  $dz_1$  component of  $\omega$ , and  $\nabla_{\omega_1} = (d + \omega_1 \wedge)$ . In [81] it was shown that putting these ingredients together one can write the 2-variable intersection number as

$$\langle \varphi_L^{(2)} | \varphi_R^{(2)} \rangle = \sum_{i,j=1}^{\nu_1} \sum_{q \in \mathcal{P}_{\Omega^{(2)}}} \text{Res}_{z_2=q} \left[ \psi_i^{(q)} (\mathbf{C}_{(1)})_{ij} \varphi_{R,j}^{(2)} \right] , \quad (4.314)$$

where  $\psi_i^{(q)}$  is the local solution of the differential equation

$$\nabla_{\Omega^{(2)}} \psi_i^{(q)} = d\psi_i^{(q)} + \psi_j^{(q)} \wedge \Omega_{ji}^{(2)} = \varphi_{L,i}^{(2)} \quad (4.315)$$

around each point  $q$  from the set of poles of  $\Omega^{(2)}$  denoted by  $\mathcal{P}_{\Omega^{(2)}}$ . In eq. (4.314), the 2-variable intersection number  $\langle \varphi_L^{(2)} | \varphi_R^{(2)} \rangle$  has been expressed in terms of the known univariate intersection numbers and a new connection matrix  $\Omega^{(2)}$ . To determine  $\Omega^{(2)}$ , we will follow the same trick as adopted in the case of single variable, namely starting from the integral and defining the equivalence class of the single valued differential form. We want to find an analogue of the fact that

$$0 = \int_{\mathcal{C}_R} d(\xi_L u) = \int_{\mathcal{C}_R} (d\xi_L + d \log u \wedge \xi_L) u \equiv \int_{\mathcal{C}_R} \nabla_{\omega} \xi_L u , \quad (4.316)$$

with  $du = \omega u$ , but for two-fold integrals.

Let us consider the original integral  $I$  from eq. (4.304) and apply the decomposition we used in eq. (4.307):

$$\begin{aligned} \int_{\mathcal{C}_R^{(2)}} \varphi_L^{(2)}(z_1, z_2) u(z_1, z_2) &= \sum_{i=1}^{\nu_1} \int_{\mathcal{C}_R^{(2)}} \varphi_{L,i}^{(2)}(z_2) \int_{\mathcal{C}_R^{(1)}} e_i^{(1)}(z_1, z_2) u(z_1, z_2) \\ &= \sum_{i=1}^{\nu_1} \int_{\mathcal{C}_R^{(2)}} \varphi_{L,i}^{(2)}(z_2) u_i(z_2), \end{aligned} \quad (4.317)$$

where we defined

$$u_i(z_2) = \int_{\mathcal{C}_R^{(1)}} e_i^{(1)}(z_1, z_2) u(z_1, z_2). \quad (4.318)$$

Now, there could exist many forms  $\varphi_{L,i}^{(2)}$  that integrate to give the same result. Let us consider a total derivative of  $u_i$  times any function (0-form)  $\xi_i(z_2)$  with poles correctly regulated,

$$0 = \int_{\mathcal{C}_R^{(1)}} d_{z_2}(\xi_i(z_2) u_i(z_2)) = \int_{\mathcal{C}_R^{(1)}} (d_{z_2} \xi_i(z_2) u_i(z_2) + \xi_i(z_2) d_{z_2} u_i(z_2)), \quad (4.319)$$

where  $d_{z_2}$  denotes the differential acting only on  $z_2$ , i.e.  $d_{z_2} = dz_2 \partial_{z_2}$ . Let us notice that  $u_i(z_2)$  satisfies the following differential equation in  $z_2$  following Sec. 4.2.1:

$$d_{z_2} u_i(z_2) = \Omega_{ij}^{(2)} u_j(z_2), \quad (4.320)$$

where  $\Omega^{(2)}$  is a  $\nu_1 \times \nu_1$  matrix. Inserting this into eq. (4.319), we obtain:

$$\begin{aligned} 0 &= \int_{\mathcal{C}_R^{(2)}} \left( d_{z_2} \xi_i(z_2) u_i(z_2) + \xi_i(z_2) (\Omega^{(2)})_{ij} u_j(z_2) \right) \\ &= \int_{\mathcal{C}_R^{(2)}} \left( d_{z_2} \xi \mathbb{I} + \xi \Omega^{(2)} \right) \cdot \mathbf{u} \\ &= \int_{\mathcal{C}_R^{(2)}} (\nabla_{\Omega^{(2)}} \xi) \cdot \mathbf{u}, \end{aligned} \quad (4.321)$$

where the final equation defines our new connection  $\nabla_{\Omega^{(2)}}$ .

The  $\Omega^{(2)}$  can be obtained directly from computing the  $z_2$ -differential of  $u_i(z_2)$ ,

$$\begin{aligned} d_{z_2} u_i(z_2) &= d_{z_2} \int_{\mathcal{C}_R^{(1)}} e_i^{(1)}(z_1, z_2) u(z_1, z_2) \\ &= \int_{\mathcal{C}_R^{(1)}} \left( d_{z_2} e_i^{(1)}(z_1, z_2) + d_{z_2} \log u(z_1, z_2) \wedge e_i^{(1)}(z_1, z_2) \right) u(z_1, z_2) \\ &= \int_{\mathcal{C}_R^{(1)}} (d_{z_2} + \omega_2 \wedge) e_i^{(1)}(z_1, z_2) u(z_1, z_2) \\ &= \langle (d_{z_2} + \omega_2 \wedge) e_i^{(1)} | \mathcal{C}_R^{(1)} \rangle. \end{aligned} \quad (4.322)$$

The final line can be further simplified by using the master decomposition formula in eq. (4.53) in the  $z_1$ -variable, such that

$$\langle (d_{z_2} + \omega_2 \wedge) e_i^{(1)} | \rangle = \langle (d_{z_2} + \omega_2 \wedge) e_i^{(1)} | h_k^{(1)} \rangle (\mathbf{C}_{(1)}^{-1})_{kj} \langle e_j^{(1)} | \rangle. \quad (4.323)$$

Using eq. (4.320), we can identify  $\Omega^{(2)}$  through

$$\Omega_{ij}^{(2)} = \langle (d_{z_2} + \omega_2 \wedge) e_i^{(1)} | h_k^{(1)} \rangle (\mathbf{C}_{(1)}^{-1})_{kj}. \quad (4.324)$$

### A dual formula

Let us discuss an alternative recursive formula for intersection numbers, which uses the dual connection matrix  $\tilde{\Omega}^{(2)}$  instead of  $\Omega^{(2)}$ . This amounts to repeating the same steps, but now using the decomposition of the differential forms as described in eq. (4.307). Following [81] the 2-variable intersection number can be written as

$$\langle \varphi_L^{(2)} | \varphi_R^{(2)} \rangle = - \sum_{i,j=1}^{\nu_1} \sum_{q \in \mathcal{P}_{\tilde{\Omega}^{(2)}}} \text{Res}_{z_2=q} \left[ \varphi_{L,i}^{(2)}(\mathbf{C}(1))_{ij} \psi_j^{(q)} \right], \quad (4.325)$$

where  $\psi_j^{(q)}$  is the solution of

$$\nabla_{\Omega^{\vee(2)}} \psi_j^{(q)} = d\psi_j^{(q)} - \Omega_{ji}^{\vee(2)} \wedge \psi_i^{(q)} = \varphi_{R,j}^{(2)}. \quad (4.326)$$

In the above equation, the 2-variable intersection number  $\langle \varphi_L^{(2)} | \varphi_R^{(2)} \rangle$  has been expressed in terms of the known univariate intersection numbers and a new connection  $\Omega^{\vee(2)}$ . To determine  $\Omega^{\vee(2)}$  one follows steps similar to those described above.

Let us consider the dual integral with two variables as follows:

$$\begin{aligned} \int_{\mathcal{C}_L^{(2)}} \varphi_R^{(2)}(z_1, z_2) u^{-1}(z_1, z_2) &= \sum_{i=1}^{\nu_1} \int_{\mathcal{C}_L^{(2)}} \varphi_{R,i}^{(2)}(z_2) \int_{\mathcal{C}_L^{(1)}} h_i^{(1)}(z_1, z_2) u^{-1}(z_1, z_2) \\ &= \sum_{i=1}^{\nu_1} \int_{\mathcal{C}_L^{(2)}} \varphi_{R,i}^{(2)}(z_2) u_i^{\vee}(z_2), \end{aligned} \quad (4.327)$$

where we use the decomposition of  $\varphi_R^{(2)}$  from eq. (4.307) in the first step and defined

$$u_i^{\vee}(z_2) = \int_{\mathcal{C}_L^{(1)}} h_i^{(1)}(z_1, z_2) u^{-1}(z_1, z_2). \quad (4.328)$$

We then consider a total derivative of  $u_i^{\vee}$  times a function  $\xi_i(z_2)$

$$0 = \int_{\mathcal{C}_L^{(2)}} d_{z_2}(\xi_i(z_2) u_i^{\vee}(z_2)) = \int_{\mathcal{C}_L^{(2)}} (d_{z_2} \xi_i(z_2) u_i^{\vee}(z_2) + \xi_i(z_2) d_{z_2} u_i^{\vee}(z_2)). \quad (4.329)$$

Using the results from Sec. 4.2.1, the vector  $u_i^{\vee}(z_2)$  satisfies the following differential equation in  $z_2$ :

$$d_{z_2} u_i^{\vee}(z_2) = -u_j^{\vee}(z_2) \Omega_{ji}^{\vee(2)}, \quad (4.330)$$

where  $\Omega^{\vee(2)}$  is a  $\nu_1 \times \nu_1$  matrix. Inserting this into eq. (4.329), we obtain:

$$\begin{aligned} 0 &= \int_{\mathcal{C}_L^{(2)}} \left( d_{z_2} \xi_i(z_2) u_i^{\vee}(z_2) - \xi_i(z_2) u_j^{\vee}(z_2) \Omega_{ji}^{\vee(2)} \right) \\ &= \int_{\mathcal{C}_L^{(2)}} \mathbf{u}^{\vee} \cdot \left( d_{z_2} \boldsymbol{\xi} \mathbb{I} - \Omega^{\vee(2)} \boldsymbol{\xi} \right) \\ &= \int_{\mathcal{C}_L^{(2)}} \mathbf{u}^{\vee} \cdot \left( \nabla_{-\Omega^{\vee(2)}} \boldsymbol{\xi} \right), \end{aligned} \quad (4.331)$$

Finally, the matrix  $\Omega^{\vee(2)}$  can be obtained directly by computing the  $z_2$ -differential of  $u_i^{\vee}(z_2)$ , which shows that its components are given by

$$\Omega_{ij}^{\vee(2)} = -(\mathbf{C}_{(1)}^{-1})_{ik} \langle e_k^{(1)} | (d_{z_2} - \omega_2 \wedge) h_j^{(1)} \rangle. \quad (4.332)$$

### 4.5.2 $n$ -variable intersection number

Following the above discussion, we can generalize the 2-variable intersection number to the  $n$ -variable case, where we start by considering an integral with  $n$  integration variables  $(z_1, z_2, \dots, z_n)$ , written as

$$I(z_1, z_2, \dots, z_n) = \int_{\mathcal{C}_R^{(\mathbf{n})}} \varphi_L^{(\mathbf{n})}(z_1, z_2, \dots, z_n) u(z_1, z_2, \dots, z_n) = \langle \varphi_L^{(\mathbf{n})} | \mathcal{C}_R^{(\mathbf{n})} \rangle \quad (4.333)$$

with the notation  $\mathbf{n} = \{1, \dots, n\}$ . The  $\varphi_L^{(\mathbf{n})}$  is an  $n$ -variable differential form on some space  $X$ . Similarly, one can define a dual form  $\varphi_R^{(\mathbf{n})}$ . We assume that the  $n$ -complex-dimensional space with coordinates  $(z_1, \dots, z_n)$  admits a fibration into a  $(n-1)$ -dimensional subspace parametrized by  $(z_1, \dots, z_{n-1})$ , denoted by  $\mathbf{n}-\mathbf{1}$ , which we call the *inner* space, and a one-dimensional subspace with  $z_n$ , which we refer to as the *outer* space. We have

$$\omega = d \log u(\mathbf{z}) = \sum_{i=1}^n \hat{\omega}_i dz_i \quad (4.334)$$

and employing eq. (4.40), we can count the number of MIs on the *inner space*, which we define as  $\nu_{\mathbf{n}-\mathbf{1}}$ . The aim is to express the  $n$ -variables intersection number  $\langle \varphi_L^{(\mathbf{n})} | \varphi_R^{(\mathbf{n})} \rangle$  in terms of intersection numbers in  $(n-1)$ -variables on the inner space, which are assumed to be known at this stage, following the recursive nature of the algorithm. The choice of the variables (and their ordering) parametrizing the inner and outer spaces is arbitrary: as before, we use the generic notation  $\mathbf{k} \equiv \{i_1, i_2, \dots, i_k\}$  to denote the variables taking part in a specific computation.

Thus, the original  $\mathbf{n}$ -forms can be decomposed according to

$$\langle \varphi_L^{(\mathbf{n})} | = \sum_{i=1}^{\nu_{\mathbf{n}-\mathbf{1}}} \langle e_i^{(\mathbf{n}-\mathbf{1})} | \wedge \langle \varphi_{L,i}^{(n)} | , \quad (4.335)$$

$$| \varphi_R^{(\mathbf{n})} \rangle = \sum_{i=1}^{\nu_{\mathbf{n}-\mathbf{1}}} | h_i^{(\mathbf{n}-\mathbf{1})} \rangle \wedge | \varphi_{R,i}^{(n)} \rangle , \quad (4.336)$$

where  $\nu_{\mathbf{n}-\mathbf{1}}$  is the number of master integrals on the inner space with arbitrary bases  $\langle e_i^{(\mathbf{n}-\mathbf{1})} |$ ,  $| h_i^{(\mathbf{n}-\mathbf{1})} \rangle$ . In the above expressions  $\langle \varphi_{L,i}^{(n)} |$  and  $| \varphi_{R,i}^{(n)} \rangle$  are one-forms in the variable  $z_n$ , and they are treated as coefficients of the basis expansion. They can be obtained by a projection similar to eq. (4.53), giving

$$\langle \varphi_{L,i}^{(n)} | = \langle \varphi_L^{(\mathbf{n})} | h_j^{(\mathbf{n}-\mathbf{1})} \rangle (\mathbf{C}_{(\mathbf{n}-\mathbf{1})}^{-1})_{ji} , \quad (4.337)$$

$$| \varphi_{R,i}^{(n)} \rangle = (\mathbf{C}_{(\mathbf{n}-\mathbf{1})}^{-1})_{ij} \langle e_j^{(\mathbf{n}-\mathbf{1})} | \varphi_R^{(\mathbf{n})} \rangle , \quad (4.338)$$

with

$$(\mathbf{C}_{(\mathbf{n}-\mathbf{1})})_{ij} = \langle e_i^{(\mathbf{n}-\mathbf{1})} | h_j^{(\mathbf{n}-\mathbf{1})} \rangle . \quad (4.339)$$

We stress again that the  $(n-1)$ -variable intersection numbers are assumed to be known at this stage. The recursive formula for the intersection number reads [81]:

$$\langle \varphi_L^{(\mathbf{n})} | \varphi_R^{(\mathbf{n})} \rangle = \sum_{p \in \mathcal{P}_n} \text{Res}_{z_n=p} \left( \psi_i^{(n)} (\mathbf{C}_{(\mathbf{n}-\mathbf{1})})_{ij} \varphi_{R,j}^{(n)} \right) , \quad (4.340)$$

where the functions  $\psi_i^{(n)}$  are the solution of the system of differential equations

$$\partial_{z_n} \psi_i^{(n)} + \psi_j^{(n)} \hat{\Omega}_{ji}^{(n)} = \hat{\varphi}_{L,i}^{(n)} , \quad (4.341)$$

and  $\hat{\varphi}_{L,i}$  are obtained through eq. (4.337). Here,  $\hat{\Omega}^{(n)}$  is a  $\nu_{\mathbf{n}-1} \times \nu_{\mathbf{n}-1}$  matrix, whose entries are given by

$$\hat{\Omega}_{ji}^{(n)} = \langle (\partial_{z_n} + \hat{\omega}_n) e_j^{(\mathbf{n}-1)} | h_k^{(\mathbf{n}-1)} \rangle (\mathbf{C}_{(\mathbf{n}-1)}^{-1})_{ki} \quad (4.342)$$

and finally  $\mathcal{P}_n$  is the set of poles of  $\hat{\Omega}^{(n)}$  defined as the union of the poles of its entries (including a possible pole at infinity). We observe that the solution of eq. (4.341) around  $z_n=p$  can be formally written in terms of a path-ordered matrix exponential

$$\vec{\psi}^{(n)}(z_n) = \left( \mathcal{P} e^{-\int_p^{z_n} \Omega^{(n)\top}(w)} \right) \left( \int_p^{z_n} \mathcal{P} e^{\int_p^y \Omega^{(n)\top}(w)} \vec{\varphi}_L^{(n)}(y) \right) \quad (4.343)$$

for a vector  $\vec{\psi}^{(n)}$  with entries  $\psi_i^{(n)}$ . Nevertheless for its use in eq. (4.340), it is sufficient to know only a few leading orders of  $\vec{\psi}^{(n)}$  around each  $p \in \mathcal{P}_n$ . Therefore, it is easier to find the solution of the system eq. (4.341) by a *holomorphic* Laurent series expansion, using an ansatz for each component  $\psi_i^{(n)}$ , see [1, 68]. Such a solution exists if the matrix  $\text{Res}_{z_n=p} \Omega^{(n)}$  does not have any non-negative integer eigenvalues, which we assume from now on (when this is not the case one can employ a regularization discussed in Sec. 4.6.1). Moreover, the number of critical points of the determinant of the  $\Omega^{(n)}$  provides the dimension of that cohomology group, i.e. the number of the corresponding MIs, see also [129].

The recursion terminates when  $n=1$ , in which case the inner space is trivial:  $\nu_0 = \langle e_1^{(0)} | = |h_1^{(0)}\rangle = 1$ , and we impose the initial conditions

$$\hat{\Omega}_{11}^{(1)} = \hat{\omega}_1, \quad \mathbf{C}_0 = 1, \quad \varphi_{L,1}^{(1)} = \varphi_L^{(1)}, \quad \varphi_{R,1}^{(1)} = \varphi_R^{(1)}. \quad (4.344)$$

In this case eq. (4.340) reduces to a computation of an univariate intersection number [72, 142] previously studied in refs. [1, 68].

Let us notice also that combining eqs. (4.340) and (4.338) gives

$$\langle \varphi_L^{(\mathbf{n})} | \varphi_R^{(\mathbf{n})} \rangle = \sum_{p \in \mathcal{P}_n} \text{Res}_{z_n=p} \left( \psi_i^{(\mathbf{n})} \langle e_i^{(\mathbf{n}-1)} | \varphi_R^{(\mathbf{n})} \rangle \right), \quad (4.345)$$

which is suitable for practical calculation purposes. Using the above identity recursively, the intersection number can be expressed as

$$\langle \varphi_L^{(\mathbf{n})} | \varphi_R^{(\mathbf{n})} \rangle = \sum_{p_n \in \mathcal{P}_n} \cdots \sum_{p_1 \in \mathcal{P}_1} \text{Res}_{z_n=p_n} \cdots \text{Res}_{z_1=p_1} \left( \psi_{i_{\mathbf{n}-1}}^{(\mathbf{n})} \psi_{i_{\mathbf{n}-1} i_{\mathbf{n}-2}}^{(\mathbf{n}-1)} \cdots \psi_{i_2 i_1}^{(2)} \psi_{i_1}^{(1)} \varphi_R^{(\mathbf{n})} \right), \quad (4.346)$$

where the ranges of the summations are  $i_{\mathbf{m}} = 1, \dots, \nu_{\mathbf{m}}$  and where the  $\psi_{i_{\mathbf{m}} i_{\mathbf{m}-1}}^{(m)}$  are the solutions of

$$\partial_{z_m} \psi_{i_{\mathbf{m}} i_{\mathbf{m}-1}}^{(m)} + \psi_{i_{\mathbf{m}} j_{\mathbf{m}-1}}^{(m)} \hat{\Omega}_{j_{\mathbf{m}-1} i_{\mathbf{m}-1}}^{(m)} = \hat{e}_{i_{\mathbf{m}} i_{\mathbf{m}-1}}^{(m)} \quad (4.347)$$

for all  $i_{\mathbf{m}}$  with  $\langle e_{i_{\mathbf{m}} i_{\mathbf{m}-1}}^{(m)} | = \hat{e}_{i_{\mathbf{m}} i_{\mathbf{m}-1}}^{(m)} dz_m$  coming from the projection

$$\langle e_{i_{\mathbf{m}}}^{(\mathbf{m})} | = \langle e_{i_{\mathbf{m}-1}}^{(\mathbf{m}-1)} | \wedge \langle e_{i_{\mathbf{m}} i_{\mathbf{m}-1}}^{(m)} |, \quad (4.348)$$

which may be computed initially, since the bases of all inner spaces are arbitrarily chosen. The matrices  $\hat{\Omega}^{(m)}$  needed in eq. (4.347) are computed analogously to eq. (4.342). Notice that all  $\psi^{(m)}$  entering eq. (4.346) need to be computed only *once* for a given family of integrals.

### 4.5.3 An explicit example in two variables

Let us consider intersection numbers based on the following function:

$$u(\mathbf{z}) = (z_1 z_2 (1 - z_1 - z_2))^\gamma, \quad (4.349)$$

which gives

$$\hat{\omega}_1 = \gamma \left( \frac{1}{z_1} - \frac{1}{1 - z_1 - z_2} \right), \quad \hat{\omega}_2 = \gamma \left( \frac{1}{z_2} - \frac{1}{1 - z_1 - z_2} \right). \quad (4.350)$$

We will focus on the steps required for the computation of the intersection number given by

$$\langle \varphi_L^{(2)} | \varphi_R^{(2)} \rangle \quad \text{with} \quad \hat{\varphi}_L^{(2)} = \hat{\varphi}_R^{(2)} = 1. \quad (4.351)$$

These forms only have poles at infinities.

Letting  $\mathbf{1} = \{1\}$  define the inner space, we find

$$\nu_{\mathbf{1}} = 1, \quad (4.352)$$

corresponding to the fact that  $\hat{\omega}_1 = 0$  has one solution. We choose the inner basis for the left and right forms, denoted by  $\langle e^{(1)} |$  and  $|h^{(1)}\rangle$  respectively, as

$$\hat{e}^{(1)} = \hat{h}^{(1)} = z_1. \quad (4.353)$$

Given two arbitrary forms  $\langle \varphi_L^{(2)} |$  and  $|\varphi_R^{(2)}\rangle$  the following decompositions hold:

$$\begin{aligned} \langle \varphi_L^{(2)} | &= \langle e^{(1)} | \wedge \langle \varphi_L^{(2)} |, \\ |\varphi_R^{(2)}\rangle &= |h^{(1)}\rangle \wedge |\varphi_R^{(2)}\rangle, \end{aligned} \quad (4.354)$$

where  $\langle \varphi_L^{(2)} |$  and  $|\varphi_R^{(2)}\rangle$ , regarded as one forms in the variable  $z_2$ , have to be determined. We have from eqs. (4.309) and (4.310):

$$\langle \varphi_L^{(2)} | = \langle \varphi_L^{(2)} | h^{(1)} \rangle \mathbf{C}_{(\mathbf{1})}^{-1}, \quad (4.355)$$

$$|\varphi_R^{(2)}\rangle = \mathbf{C}_{(\mathbf{1})}^{-1} \langle e^{(1)} | \varphi_R^{(2)} \rangle, \quad (4.356)$$

with

$$\mathbf{C}_{(\mathbf{1})} = \langle e^{(1)} | h^{(1)} \rangle. \quad (4.357)$$

In the recursive approach we assume the one-variable intersection numbers w.r.t.  $z_1$ , to be computed in the previous step. They are given by:

$$\mathbf{C}_{(\mathbf{1})} = \langle z_1 | z_1 \rangle = \frac{\gamma(z_2 - 1)^4}{8(2\gamma - 1)(2\gamma + 1)}, \quad (4.358)$$

$$\hat{\varphi}_L^{(2)} = \langle 1 | z_1 \rangle \mathbf{C}_{(\mathbf{1})}^{-1} = \frac{-2}{z_2 - 1}, \quad (4.359)$$

$$\hat{\varphi}_R^{(2)} = \mathbf{C}_{(\mathbf{1})}^{-1} \langle z_1 | 1 \rangle = \frac{-2}{z_2 - 1}, \quad (4.360)$$

while the new  $1 \times 1$  connection matrix  $\hat{\Omega}^{(2)}$  is given by:

$$\hat{\Omega}^{(2)} = \langle (\partial_{z_2} + \hat{\omega}_2) z_1 | z_1 \rangle \mathbf{C}_{(\mathbf{1})}^{-1} = \frac{(3\gamma + 2)z_2 - \gamma}{(z_2 - 1)z_2}, \quad (4.361)$$

and we see that the poles of  $\hat{\Omega}^{(2)}$  are located at

$$\mathcal{P}_2 = \{0, 1, \infty\}. \quad (4.362)$$

Next, we consider the differential equation:

$$\left(\partial_{z_2} + \hat{\Omega}^{(2)}\right) \psi^{(2)} = \hat{\varphi}_L^{(2)}. \quad (4.363)$$

The full analytic solution of (4.363) is not required, but rather a *power series* around each  $p \in \mathcal{P}_2$  is sufficient. Denoting by  $y$  the local coordinate around the pole, the solutions of (4.363) to leading orders in  $y$  read:

- **Solution around  $p = 0$  ( $y = z_2$ ):**

$$\psi_0^{(2)}(y) = \frac{2y}{\gamma + 1} + \mathcal{O}(y^2); \quad (4.364)$$

- **Solution around  $p = 1$  ( $y = z_2 - 1$ ):**

$$\psi_1^{(2)}(y) = -\frac{1}{\gamma + 1} + \mathcal{O}(y^1); \quad (4.365)$$

- **Solution around  $p = \infty$  ( $y = 1/z_2$ ):**

$$\psi_\infty^{(2)}(y) = c_{0,\infty} + c_{1,\infty} y + c_{2,\infty} y^2 + c_{3,\infty} y^3 + c_{4,\infty} y^4 + \mathcal{O}(y^5) \quad (4.366)$$

with

$$\begin{aligned} c_{0,\infty} &= \frac{-2}{3\gamma + 2}, & c_{1,\infty} &= \frac{-2\gamma}{(3\gamma + 1)(3\gamma + 2)}, \\ c_{2,\infty} &= \frac{-2(\gamma - 1)}{3(3\gamma + 1)(3\gamma + 2)}, & c_{3,\infty} &= \frac{-2(\gamma - 2)(\gamma - 1)}{3(3\gamma - 1)(3\gamma + 1)(3\gamma + 2)}, \\ c_{4,\infty} &= \frac{-2(\gamma - 3)(\gamma - 2)(\gamma - 1)}{3(3\gamma - 2)(3\gamma - 1)(3\gamma + 1)(3\gamma + 2)}. \end{aligned} \quad (4.367)$$

Finally we may evaluate the bi-variate intersection number as a sum of univariate residues, as given by eq. (4.314):

$$\langle \varphi_L^{(2)} | \varphi_R^{(2)} \rangle = \sum_{p \in \mathcal{P}_2} \text{Res}_{z_2=p} \left( \psi^{(2)} \mathbf{C}_{(1)} \varphi_R^{(2)} \right) \quad (4.368)$$

giving the final result for the intersection number:

$$\langle 1 | 1 \rangle = \frac{\gamma^2}{3(3\gamma - 2)(3\gamma - 1)(3\gamma + 1)(3\gamma + 2)}. \quad (4.369)$$

We notice that, in the case at hand, only the residue at  $p = \infty$  gives a *non-zero* contribution to the intersection number.

#### 4.5.4 Intersection numbers of logarithmic forms

Intersection numbers for multivariate logarithmic forms were first considered in [142]. Alternative formulas for more direct calculations were later presented in [75, 81]. In particular, if  $\varphi_L$  and  $\varphi_R$  are both dlog, we have

$$\langle \varphi_L | \varphi_R \rangle = (-1)^n \sum_{(z_1^*, \dots, z_n^*)} \det^{-1} \begin{bmatrix} \partial_{z_1} \hat{\omega}_1 & \dots & \partial_{z_n} \hat{\omega}_1 \\ \vdots & \ddots & \vdots \\ \partial_{z_1} \hat{\omega}_n & \dots & \partial_{z_n} \hat{\omega}_n \end{bmatrix} \hat{\varphi}_L \hat{\varphi}_R \Big|_{(z_1, \dots, z_n) = (z_1^*, \dots, z_n^*)} \quad (4.370)$$



where the sum goes over all the  $\nu$  *critical points* given by the solutions of the system of equations

$$\hat{\omega}_i = 0, \quad i = 1, \dots, n, \quad (4.371)$$

as in eq. (4.40). When at least one of the forms is non-logarithmic, the formula (4.370) is only valid asymptotically in the limit  $\gamma \rightarrow \infty$ . In those cases one can still calculate intersection numbers as a series expansion in  $1/\gamma$ , which was successfully applied to the computation of differential equations for certain Feynman integrals in [127].

The recursive algorithm for the computation of the multivariate intersection numbers presented in Sec. 4.5 is applicable for any rational form. However, at each step of the recursive algorithm, the coefficients  $\hat{\varphi}_{L,R}^{(n)}$  in eqs. (4.335), (4.336) are defined modulo the equivalence relations

$$\hat{\varphi}_{L,i}^{(n)} \sim \hat{\varphi}'_{L,i}{}^{(n)} = \hat{\varphi}_{L,i}^{(n)} + \left( \partial_{z_n} \xi_{L,i} + \xi_{L,j} \hat{\Omega}_{ji}^{(n)} \right), \quad (4.372)$$

$$\hat{\varphi}_{R,i}^{(n)} \sim \hat{\varphi}'_{R,i}{}^{(n)} = \hat{\varphi}_{R,i}^{(n)} + \left( \partial_{z_n} \xi_{R,i} - \hat{\Omega}_{ij}^{\vee(n)} \xi_{R,j} \right). \quad (4.373)$$

Thus, under the assumption that the connection matrices  $\Omega^{(n)}$  and  $\tilde{\Omega}^{(n)}$  contain only simple poles, it's possible to replace the coefficients  $\hat{\varphi}_{L,R}^{(n)}$  containing higher-degree poles, with a suitably chosen  $\hat{\varphi}'_{L,R}{}^{(n)}$  belonging to the same equivalence class, but containing simple poles only. One may exploit this fact to compute intersection numbers in one variable as a univariate global residue, without introducing any algebraic extensions as observed in [129].

## 4.6 Feynman integrals decomposition

As proposed in refs. [1, 3, 68, 127, 129], the use of multivariate intersection numbers yields a direct decomposition of a given Feynman integral  $I$  in terms of an a priori chosen set of MIs  $J_i$ , with  $i = 1, \dots, \nu$ .

The decomposition given by eq. (4.45) is on the form

$$I = \sum_{i=1}^{\nu} c_i J_i, \quad (4.374)$$

where the determination of the coefficients  $c_i$  is the goal of this Section. We identify *three* possible strategies which can be adopted in order to achieve this task. They all employ the master projection formula from eq. (4.53), which is applied to differential forms constructed differently in the three cases. We name them the *straight decomposition*, the *bottom-up decomposition*, and the *top-down decomposition*.

All the approaches have the first step in common: *finding the number* of MIs which appear in the decomposition and *choosing* them accordingly.

We introduce the following definitions:

- $\Sigma$  denotes the set of integers used to label the full set of denominators;
- $\sigma$  denotes a set of integers that label a subset of denominators,  $\sigma \subseteq \Sigma$ ;
- *sector* is the set of integrals for which only the subset of propagators specified by  $\sigma$  appear in the denominator (thus, a sector is unambiguously identified by  $\sigma$ ).

There is a *one-to-one* correspondence between sectors and (generalized unitarity) cuts. On the level of the function  $u$ , this correspondence is manifested by setting all  $z_j$ 's belonging to  $\sigma$  to zero in the original  $u(\mathbf{z})$ ,

$$u_\sigma = u(\mathbf{z})|_{z_j \in \sigma \rightarrow 0}, \quad (4.375)$$

where we work in Baikov representation. Given  $u_\sigma$ , the number of MIs in the corresponding sector,  $\nu_\sigma$ , can be determined through the criteria given in Sec. 4.1.4. The total number of MIs (without taking into account any symmetry relations) is then given by

$$\nu = \sum_{\sigma} \nu_{\sigma}, \quad (4.376)$$

where the sum is over all sectors. Finally we can choose the forms  $\langle e_i |$  associated to the (arbitrarily chosen) MIs  $J_i$ , through the identification

$$J_i = \langle e_i | \mathcal{C} \rangle. \quad (4.377)$$

#### 4.6.1 Straight decomposition

We consider the following decomposition

$$I = \int_{\mathcal{C}} u \varphi = \langle \varphi | \mathcal{C} \rangle = \sum_{i=1}^{\nu} c_i \langle e_i | \mathcal{C} \rangle = \sum_{i=1}^{\nu} c_i \int_{\mathcal{C}} u e_i = \sum_{i=1}^{\nu} c_i J_i \quad (4.378)$$

with

$$c_i = \sum_{j=1}^{\nu} \langle \varphi | h_j \rangle (\mathbf{C}^{-1})_{ji}, \quad \mathbf{C}_{ij} = \langle e_i | h_j \rangle. \quad (4.379)$$

Here  $\hat{\varphi}$  and  $\hat{e}_i$  correspond simply to the integrands of the integral  $I$  to decompose and of the chosen master integrals,  $J_i$ , respectively. In order to evaluate the intersection numbers, all the poles present in the differential forms must be regulated in  $u$ . If this assumption is violated, we can introduce a *regulated*  $u$ , denoted by  $u_\rho$ , which contains a monomial  $z_k^{\rho_k}$  for each (non-regulated) pole present in the differential forms, that is

$$u_\rho(\mathbf{z}) = \left( \prod_{k \in \Sigma} z_k^{\rho_k} \right) u(\mathbf{z}) \quad (4.380)$$

and correspondingly

$$\omega_\rho(\mathbf{z}) = d \log u_\rho(\mathbf{z}) = d \log u(\mathbf{z}) + \sum_{k \in \Sigma} \rho_k \frac{dz_k}{z_k} = \omega(\mathbf{z}) + \sum_{k \in \Sigma} \rho_k \frac{dz_k}{z_k}, \quad (4.381)$$

where we emphasized the action of regulators. By analogy, we also introduce a regularized version of  $\hat{\Omega}^{(n)}$ , whenever  $\text{Res}_{z_n=p} \hat{\Omega}^{(n)}$  has any non-negative integer eigenvalue. The regularized  $\hat{\Omega}^{(n)}$  reads:

$$\hat{\Omega}_\Lambda^{(n)} = \hat{\Omega}^{(n)} + \frac{\Lambda}{z_n - p} \mathbb{I}. \quad (4.382)$$

Thus, we obtain a new system of differential equations, analogous to eq. (4.341), which is, in this case, controlled by  $\hat{\Omega}_\Lambda^{(n)}$ . We assume that the solution of the latter around a pole  $p$ , denoted by  $\psi_{\Lambda,p}^{(n)}$ , reproduces in the limit  $\Lambda \rightarrow 0$ , a solution for the original system (around the pole  $p$ ).

The intersection numbers are computed through  $\omega_\rho$ , and lead to a set of coefficients, denoted by  $c_{\rho,i}$ , which depend on the set of regulators, collectively indicated by  $\rho$ . The coefficients  $c_i$ , which appear in the original decomposition eq. (4.378), are recovered in the limit  $\rho \rightarrow 0$ <sup>5</sup>

$$c_i = \lim_{\rho \rightarrow 0} c_{\rho,i} = \lim_{\rho \rightarrow 0} \sum_{j=1}^{\nu} \langle \varphi | h_j \rangle_\rho (\mathbf{C}_\rho^{-1})_{ji}, \quad (\mathbf{C}_\rho)_{ij} = \langle e_i | h_j \rangle_\rho. \quad (4.383)$$

<sup>5</sup>Strictly speaking, we take it as an assumption that the limit  $\rho \rightarrow 0$  is smooth, which turns out to be true in all practical examples we studied.

This approach requires the evaluation of intersection numbers, for which all the integration variables are present simultaneously.

For ease of notation, whenever the regulated  $u$  is introduced, in the following we will omit the subscript  $\rho$  from the individual intersection numbers  $\langle \varphi | h_j \rangle_\rho$  and  $\langle e_i | h_j \rangle_\rho$ .

### 4.6.2 Bottom-up decomposition

In this approach, proposed in [2], the decomposition is applied to the *spanning set of cuts*, defined as the minimal set of cuts such that each MIs appears at least once [2,148] (a cut behave like a *pass-high* filter, therefore MIs with a number of internal lines smaller than the number of cut variables do not contribute to the decomposition on the cut). We denote a given *spanning cut* (i.e. an element in the spanning set of cuts) by  $\tau$ ; moreover  $\mathcal{S}_\tau$  is the set of sectors which survive on that spanning cut

$$\mathcal{S}_\tau = \{ \sigma \mid \sigma \supseteq \tau \}. \quad (4.384)$$

Finally, the number of MIs which survive on the spanning cut  $\tau$ , denoted by  $\nu_{\mathcal{S}_\tau}$  is

$$\nu_{\mathcal{S}_\tau} = \sum_{\sigma \in \mathcal{S}_\tau} \nu_\sigma. \quad (4.385)$$

On the spanning cut  $\tau$ , we define

$$u_\tau = u(\mathbf{z})|_{z_j \in \tau \rightarrow 0} \quad (4.386)$$

and we consider the following decomposition

$$\begin{aligned} I_\tau &= \int_{\mathcal{C}_\tau} u_\tau \varphi_\tau = \langle \varphi_\tau | \mathcal{C}_\tau \rangle = \sum_{i=1}^{\nu_{\mathcal{S}_\tau}} c_i \langle e_{i,\tau} | \mathcal{C}_\tau \rangle \\ &= \sum_{i=1}^{\nu_{\mathcal{S}_\tau}} c_i \int_{\mathcal{C}_\tau} u_\tau e_{i,\tau} = \sum_{i=1}^{\nu_{\mathcal{S}_\tau}} c_i J_{i,\tau} \end{aligned} \quad (4.387)$$

with

$$c_i = \sum_{j=1}^{\nu_{\mathcal{S}_\tau}} \langle \varphi_\tau | h_{j,\tau} \rangle (\mathbf{C}^{-1})_{ji}, \quad \mathbf{C}_{ij} = \langle e_{i,\tau} | h_{j,\tau} \rangle. \quad (4.388)$$

As expected,  $\hat{\varphi}_\tau$  and  $\hat{e}_{i,\tau}$  are inferred from the cut-integrals. As in any unitarity-based approach [84,86,149], the coefficients  $c_i$  determined from a cut decomposition are identical to those appearing in the original decomposition - the coefficients are invariant under cuts. Therefore, the complete decomposition for the (uncut) integral  $I$  can be obtained by combining the coefficients determined from the individual spanning cuts.

As described in Subsec. 4.6.1, all the poles present in the differential forms must be regulated in  $u_\tau$ . If this is not the case, we can introduce the *regularized*  $u_\tau$ , denoted by  $u_{\rho,\tau}$

$$u_{\rho,\tau} = \left( \prod_{k \in \Sigma \setminus \tau} z_k^{\rho_k} \right) u_\tau, \quad (4.389)$$

which leads to

$$\omega_{\rho,\tau} = d \log u_{\rho,\tau} = d \log u(\mathbf{z}) + \sum_{k \in \Sigma \setminus \tau} \rho_k \frac{dz_k}{z_k} = \omega(\mathbf{z}) + \sum_{k \in \Sigma \setminus \tau} \rho_k \frac{dz_k}{z_k}, \quad (4.390)$$

used in the evaluation of the intersection number. We also use a regularized version of  $\hat{\Omega}^{(n)}$ , whenever  $\text{Res}_{z_n=p} \hat{\Omega}^{(n)}$  has any non-negative integer eigenvalue, as explained above. Now, the

coefficients of the decomposition,  $c_{\rho,i}$  depend on the set of regulators  $\rho$ . The coefficients of the original decomposition (4.387) are recovered in the  $\rho \rightarrow 0$  limit:

$$c_i = \lim_{\rho \rightarrow 0} c_{\rho,i} = \lim_{\rho \rightarrow 0} \sum_{j=1}^{\nu_{S_\tau}} \langle \varphi_\tau | h_{j,\tau} \rangle_\rho (\mathbf{C}_\rho^{-1})_{ji}, \quad (\mathbf{C}_\rho)_{ij} = \langle e_{i,\tau} | h_{j,\tau} \rangle_\rho. \quad (4.391)$$

This procedure requires the evaluation of the intersection numbers only for the uncut variables, therefore it can be significantly less demanding than the previous case.

As before, whenever the regulated  $u$  is introduced, we will omit the subscript  $\rho$  from the individual intersection numbers.

### 4.6.3 Top-down decomposition

As proposed in [3], this approach combines the advantages of the decomposition by intersection numbers with the top-down subtraction algorithm traditionally used in methods of *integrand decomposition* [16,35,37,150]. In particular, as for the integrand decomposition, one can determine the coefficients of the MIs systematically, beginning from the ones with the highest number of internal lines (the top sector) and moving downward, ending with the sector with a minimal number of lines equal to the number of the loops (built from product of tadpoles). At any step, the determination of the coefficients of a given MI, say  $J_i$ , is obtained on the corresponding cut, after *subtracting off* the known contributions coming from higher sectors, as the latter are written as a linear combination of the MIs with a higher number of internal lines (whose graph contain the one corresponding to  $J_i$  as subdiagram), coming from the earlier steps of the decomposition. In particular, let us reconsider the complete decomposition,

$$I = \int_{\mathcal{C}} u \varphi = \langle \varphi | \mathcal{C} \rangle = \sum_{i=1}^{\nu} c_i \langle e_i | \mathcal{C} \rangle = \sum_{i=1}^{\nu} c_i \int_{\mathcal{C}} u e_i = \sum_{i=1}^{\nu} c_i J_i, \quad (4.392)$$

and assume that, within the top-down approach, after *at most*  $n$ -steps, the coefficients  $c_i$ , with  $i = 1, \dots, n$  have been determined, and can be considered as known. We can write,

$$I - \sum_{i=1}^n c_i J_i = \sum_{i=n+1}^{\nu} c_i J_i, \quad (4.393)$$

which, in terms of pairings, reads,

$$\langle \phi_n | \mathcal{C} \rangle = \sum_{i=1}^n c_i \langle e_i | \mathcal{C} \rangle, \quad (4.394)$$

where  $\langle \phi_n |$ , defined as,

$$\langle \phi_n | \equiv \langle \varphi | - \sum_{i=1}^n c_i \langle e_i | \quad (4.395)$$

is a *known* differential form.

By applying a properly chosen maximal cut, identified by  $\tau$ , we can then determine the coefficients  $c_i$  of a number  $\nu_\tau$  MIs  $J_i$ , whose graph contains exactly those lines that are cut. In fact, on the maximal cut  $\tau$ , we can define

$$u_\tau = u(\mathbf{z})|_{z_{j \in \tau} \rightarrow 0} \quad (4.396)$$

and

$$\omega_\tau = d \log u_\tau \quad (4.397)$$

and the decomposition simplifies and becomes,

$$\begin{aligned} I_\tau &= \int_{\mathcal{C}_\tau} u_\tau \phi_{n,\tau} = \langle \phi_{n,\tau} | \mathcal{C}_\tau \rangle = \sum_{i=n+1}^{n+\nu_\tau} c_i \langle e_{i,\tau} | \mathcal{C}_\tau \rangle \\ &= \sum_{i=n+1}^{n+\nu_\tau} c_i \int_{\mathcal{C}_\tau} u_\tau e_{i,\tau} = \sum_{i=n+1}^{n+\nu_\tau} c_i J_{i,\tau} \end{aligned} \quad (4.398)$$

with

$$c_{n+i} = \sum_{j=1}^{\nu_\tau} \langle \phi_{n,\tau} | h_{n+j,\tau} \rangle (\mathbf{C}^{-1})_{ji}, \quad \mathbf{C}_{ij} = \langle e_{n+i,\tau} | h_{n+j,\tau} \rangle. \quad (4.399)$$

Two important observations are in order. First, we notice that the subtraction in eq. (4.393), is similar in spirit to the subtraction performed in an integrand decomposition, although the known coefficients depend also on  $d$ , and not only on the kinematical variables. Second, after the subtraction of the known terms, the differential form  $\phi_{n,\tau}$  may contain *spurious poles*, which are not regulated by  $u_\tau$ . These poles can be eliminated by redefining  $\phi_{n,\tau}$ ,

$$\phi_{n,\tau} \rightarrow \phi'_{n,\tau} = \phi_{n,\tau} + \nabla_{\omega_\tau} \xi_{L,\tau}, \quad (4.400)$$

using a suitable  $\xi_{L,\tau}$ , which can be systematically built. Thus, in this approach, the regulators are not introduced. At this point the determination of the coefficients via intersection numbers can proceed iteratively, *top-down*, until all sectors have had their  $c_i$  coefficients determined.

## 4.7 Multivariate examples

In this Section we illustrate the previously-discussed decomposition algorithms on a few examples.

### 4.7.1 The one-loop massless box

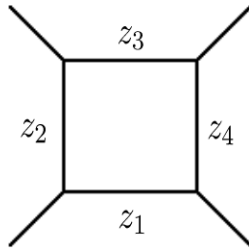


Figure 4.14: Massless Box

As the first example we will discuss the one-loop massless box. This diagram was discussed in the context of intersection theory already in ref. [2], but we will here add further details, and go through the reduction with each of the three methods presented in Sec. 4.6.

The kinematics is such that

$$\begin{aligned} D_1 &= k^2, & D_2 &= (k + p_1)^2, \\ D_3 &= (k + p_1 + p_2)^2, & D_4 &= (k + p_1 + p_2 + p_3)^2, \end{aligned} \quad (4.401)$$

with  $p_i^2 = 0$ ,  $(p_1 + p_2)^2 = s$ ,  $(p_2 + p_3)^2 = t$ ,  $(p_1 + p_3)^2 = -s - t$ .

Performing the Baikov parametrization yields

$$u = \mathcal{B}^{(d-5)/2} \quad (4.402)$$

with

$$\begin{aligned} \mathcal{B} = & 2st(s(z_2 + z_4) + t(z_1 + z_3) - z_1z_2 - z_2z_3 - z_3z_4 - z_4z_1 + 2z_1z_3 + 2z_2z_4) \\ & - s^2t^2 - t^2(z_1 - z_3)^2 - s^2(z_2 - z_4)^2 \end{aligned} \quad (4.403)$$

and performing the sector-by-sector analysis described in the beginning of Sec. 4.6 yields  $\nu_\sigma = 1$  for the sectors

$$\sigma \in \{\{1, 2, 3, 4\}, \{1, 3\}, \{2, 4\}\} \quad (4.404)$$

and  $\nu_\sigma = 0$  for the remaining sectors, corresponding to the well-known set of master integrals: the box and the  $s$ - and the  $t$ -channel bubble:

$$J_1 = \begin{array}{c} \diagup \quad \diagdown \\ \square \\ \diagdown \quad \diagup \end{array}, \quad J_2 = \begin{array}{c} \diagdown \quad \diagup \\ \circ \\ \diagup \quad \diagdown \end{array}, \quad J_3 = \begin{array}{c} \diagup \quad \diagdown \\ \circ \\ \diagdown \quad \diagup \end{array}. \quad (4.405)$$

The corresponding differential forms read

$$\hat{e}_1 = \frac{1}{z_1z_2z_3z_4}, \quad \hat{e}_2 = \frac{1}{z_1z_3}, \quad \hat{e}_3 = \frac{1}{z_2z_4}. \quad (4.406)$$

In the following we will decompose the example

$$\begin{array}{c} \diagup \quad \diagdown \\ \square \\ \diagdown \quad \diagup \end{array} \text{ with three dots on the left edge} = \int u \frac{d^4 \mathbf{z}}{z_1^3 z_2^2 z_3 z_4}, \quad (4.407)$$

which can be expressed in terms of the chosen master integrals as

$$\begin{array}{c} \diagup \quad \diagdown \\ \square \\ \diagdown \quad \diagup \end{array} \text{ with three dots on the left edge} = c_1 \begin{array}{c} \diagup \quad \diagdown \\ \square \\ \diagdown \quad \diagup \end{array} + c_2 \begin{array}{c} \diagdown \quad \diagup \\ \circ \\ \diagup \quad \diagdown \end{array} + c_3 \begin{array}{c} \diagup \quad \diagdown \\ \circ \\ \diagdown \quad \diagup \end{array}. \quad (4.408)$$

We will determine these coefficients with the three methods presented in Sec. 4.6.

### Straight decomposition

As prescribed in Sec. 4.6.1 we may construct the regulated  $u$  as

$$u_\rho = u \times z_1^\rho z_2^\rho z_3^\rho z_4^\rho, \quad (4.409)$$

where in this case we pick the regulators to be all equal. From this definition we may construct the corresponding  $\omega$  as

$$\omega_\rho = \sum_{i=1}^4 \hat{\omega}_i dz_i \quad \text{with} \quad \hat{\omega}_i = \partial_{z_i} \log u_\rho. \quad (4.410)$$

Choosing the variable ordering to be, from the innermost to the outermost,  $z_4, z_3, z_2, z_1$ , we can compute the dimensions of the twisted cohomology groups corresponding to the individual layers of the fibration. The result is

$$\nu_{\{4321\}} = 3, \quad \nu_{\{432\}} = 4, \quad \nu_{\{43\}} = 3, \quad \nu_{\{4\}} = 2. \quad (4.411)$$

Corresponding to the order of variables given above, we pick the basis for each level to be

$$\begin{aligned} \hat{e}^{(4321)} = \hat{e} &= \left\{ \frac{1}{z_1 z_2 z_3 z_4}, \frac{1}{z_1 z_3}, \frac{1}{z_2 z_4} \right\}, & \hat{e}^{(432)} &= \left\{ \frac{1}{z_2}, \frac{1}{z_3}, \frac{1}{z_2 z_3}, \frac{1}{z_2 z_3 z_4} \right\}, \\ \hat{e}^{(43)} &= \left\{ \frac{1}{z_4}, \frac{1}{z_3}, \frac{1}{z_3 z_4} \right\}, & \hat{e}^{(4)} &= \left\{ \frac{1}{z_4}, 1 \right\}. \end{aligned} \quad (4.412)$$

We choose the dual bases to be  $\hat{h}_i = \hat{e}_i$ . In the following, we will decompose

$$\hat{\varphi} = \frac{1}{z_1^3 z_2^2 z_3 z_4}. \quad (4.413)$$

The required intersection numbers are

$$\mathbf{C}_{ij} = \langle e_i | h_j \rangle, \quad 1 \leq i, j \leq 3, \quad (4.414)$$

and

$$\langle \varphi | h_k \rangle, \quad 1 \leq k \leq 3. \quad (4.415)$$

The individual intersection numbers, up to the leading order in  $\rho$ , are presented in App. [B](#). Combining the intersection numbers as dictated by eq. [\(4.383\)](#), we obtain, after taking the limit  $\rho \rightarrow 0$ , the coefficients

$$\begin{aligned} c_1 &= \frac{-(d-7)(d-6)(d-5)}{2s^2 t}, & c_2 &= \frac{2(d-7)(d-5)(d-3)}{s^4 t}, \\ c_3 &= \frac{2(d-7)(d-5)(d-3)(2s + (d-8)t)}{(d-8)s^2 t^4}. \end{aligned} \quad (4.416)$$

These results are in agreement with the values obtained with FIRE [\[151\]](#).

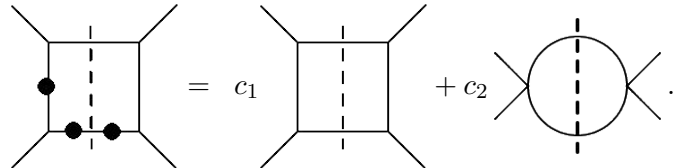
### Bottom-up decomposition

The first step of a bottom-up decomposition is to identify a spanning set of cuts  $\tau$ . That set is easily seen to be the cuts corresponding the two bubbles

$$\tau \in \{\{1, 3\}, \{2, 4\}\}. \quad (4.417)$$

• **Cut**  $\tau = \{1, 3\}$ . Let us first consider the  $\tau = \{1, 3\}$  cut.

On this cut, the decomposition reads:



$$= c_1 \left[ \text{square with dashed cut} \right] + c_2 \left[ \text{circle with dashed cut} \right]. \quad (4.418)$$

We have

$$u_{\rho, \tau} = z_2^\rho z_4^\rho \mathcal{B}_\tau^{(d-5)/2}, \quad (4.419)$$

where

$$\mathcal{B}_\tau = \left( st^2 + s(z_2 - z_4)^2 - 2t(s(z_2 + z_4) + 2z_2 z_4) \right), \quad (4.420)$$

and  $\omega_{\rho, \tau} = \hat{\omega}_2 dz_2 + \hat{\omega}_4 dz_4$  with

$$\hat{\omega}_2 = \partial_{z_2} \log u_{\rho, \tau}, \quad \hat{\omega}_4 = \partial_{z_4} \log u_{\rho, \tau}. \quad (4.421)$$

The variable ordering, from the innermost to the outermost, is chosen as  $z_2, z_4$ . The dimensions of the cohomology groups read:

$$\nu_{\{24\}} = 2, \quad \nu_{\{2\}} = 2. \quad (4.422)$$

The basis elements, on the cut, are:

$$\hat{e}_\tau^{(24)} = \hat{e}_\tau = \left\{ \frac{1}{z_2 z_4}, 1 \right\}, \quad \hat{e}_\tau^{(2)} = \left\{ 1, \frac{1}{z_2} \right\}. \quad (4.423)$$

The dual basis elements are chosen as  $\hat{h}_{i,\tau} = \hat{e}_{i,\tau}$ .

We will show the decomposition, on the cut, of:

$$\hat{\varphi}_\tau = \frac{\frac{1}{2} \partial_{z_1}^2 u}{u z_2^2 z_4} \Big|_{z_1, z_3=0} = \frac{(d-5)t^2((d-6)s(z_2+z_4-t)^2 - 4(s+t)z_2 z_4)}{2s z_2^2 z_4 \mathcal{B}_\tau^2}. \quad (4.424)$$

This requires the intersection numbers

$$\mathbf{C}_{ij} = \langle e_{i,\tau} | h_{j,\tau} \rangle, \quad 1 \leq i, j \leq 2, \quad (4.425)$$

and

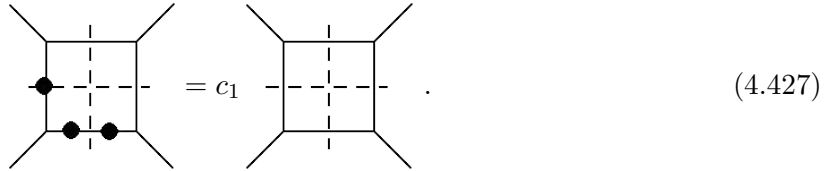
$$\langle \varphi_\tau | h_{k,\tau} \rangle, \quad 1 \leq k \leq 2. \quad (4.426)$$

Expressions for the individual intersection numbers are presented in Appendix [B](#). Combining them as prescribed by eq. [\(4.391\)](#), and considering the limit  $\rho \rightarrow 0$ , we obtain the coefficients  $c_1$  and  $c_2$  in agreement with eq. [\(4.416\)](#).

• **Cut**  $\tau = \{2, 4\}$ . Performing instead the decomposition on the second of the spanning cuts,  $\tau = \{2, 4\}$  will allow us to reconstruct  $c_1$  and  $c_3$  in eq. [\(4.416\)](#), which means that in total all of the master integral coefficients  $c_i$  have been extracted.

### Top-down decomposition

The first step in the top-down decomposition is the extraction of the box-coefficient.

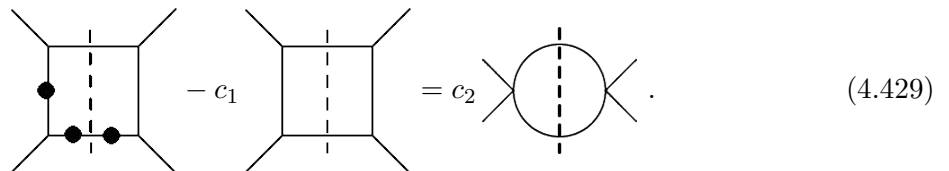


The coefficient  $c_1$  can be computed as  $\varphi/e_1$  on the maximal cut:

$$c_1 = \frac{\frac{1}{2} \partial_{z_1}^2 \partial_{z_2} u}{u} \Big|_{z_i \rightarrow 0} = \frac{-(d-7)(d-6)(d-5)}{2s^2 t}, \quad (4.428)$$

in agreement with eqs. [\(4.416\)](#).

We then consider the  $s$ -channel bubble corresponding to the cut  $\tau = \{1, 3\}$ .



Here we have

$$u_\tau = \mathcal{B}_\tau^{(d-5)/2} \quad \text{with} \quad \mathcal{B}_\tau = \left( st^2 + s(z_2 - z_4)^2 - 2t(s(z_2 + z_4) + 2z_2 z_4) \right), \quad (4.430)$$



and

$$\hat{\varphi} = \frac{\frac{1}{2} \frac{\partial_{z_1}^2 u}{z_2^2 z_4}}{u} \Big|_{z_1, z_3=0} = \frac{(d-5)t^2((d-6)s(z_2+z_4-t)^2 - 4(s+t)z_2z_4)}{2sz_2^2z_4\mathcal{B}_\tau^2}. \quad (4.431)$$

We also get

$$\omega = \frac{-(d-5)\left(\left(t(z_4-z_2)+s(t+2z_4)\right) dz_2 + \left(s(t+2z_2)+t(z_2-z_4)\right) dz_4\right)}{\mathcal{B}_\tau} \quad (4.432)$$

from which we can extract  $\nu_\tau = 1$  corresponding to the  $s$ -channel bubble.

We know that

$$\begin{array}{c} \text{Diagram 1} \\ \text{Diagram 2} \end{array} - c_1 \begin{array}{c} \text{Diagram 3} \\ \text{Diagram 4} \end{array} = \int u_\tau \underbrace{\left(\hat{\varphi} - \frac{c_1}{z_2z_4}\right)}_{\equiv \hat{\phi}} dz_2 \wedge dz_4 \quad (4.433)$$

has to be reducible to the  $s$ -channel bubble. This property is not apparent as  $\hat{\phi}$  contains poles in  $z_2$  and  $z_4$  that distinguishes the box and the bubble sectors. However, we know that  $\phi$  is in the same equivalence class as a  $\phi'$  without these poles. Writing

$$\phi \sim \phi' = \phi - \nabla_\omega \xi \quad (4.434)$$

we may make the following ansatz for  $\xi$ ,

$$\xi = \frac{\sum_{i=-1, j=-1}^{2,2} \kappa_{1,i,j} z_2^i z_4^j dz_4 + \sum_{i=-2, j=0}^{2,2} \kappa_{2,i,j} z_2^i z_4^j dz_2}{\mathcal{B}_\tau}. \quad (4.435)$$

Fitting the free coefficients  $\kappa$  with the requirement that all poles of  $\phi'$  in  $z_2$  or  $z_4$  vanish, gives a solution

$$\begin{array}{ll} \kappa_{1,-1,-1} = \frac{-(d-6)(d-5)t^2}{2s}, & \kappa_{1,-1,0} = \frac{(d-6)(d-5)t}{2s}, \\ \kappa_{1,-1,1} = 0, & \kappa_{1,-1,2} = 0, \\ \kappa_{1,0,-1} = \frac{(3d^2-36d+107)t}{2s}, & \kappa_{1,1,-1} = \frac{-(d-7)(3d-17)}{2s}, \\ \kappa_{1,2,-1} = \frac{(d-7)(d-6)}{2st}, & \kappa_{2,-2,0} = \frac{-(d-5)t^2}{2s}, \\ \kappa_{2,-2,1} = \frac{(d-5)t}{2s}, & \kappa_{2,-2,2} = 0, \\ \kappa_{2,-1,0} = \frac{t(71s-24ds+2d^2s+35t-12dt+d^2t)}{s^2}, & \kappa_{2,-1,1} = \frac{-(d-7)(3d-17)}{2s}, \\ \kappa_{2,-1,2} = \frac{(d-7)(d-6)}{2st}, & \kappa_{\text{remain.}} = 0. \end{array} \quad (4.436)$$

The corresponding  $\phi$  is of the form

$$\hat{\phi} = \frac{\mathcal{P}(z_2, z_4)}{\mathcal{B}_\tau^2}, \quad (4.437)$$

where  $\mathcal{P}$  is a polynomial, so we see explicitly that the  $z_2$  and  $z_4$  poles are gone, and that no poles are present in  $\phi$  that are not poles of  $\omega$ . With this we may perform the bi-variate intersections, and we get

$$c_2 = \frac{\langle \phi | 1 \rangle}{\langle 1 | 1 \rangle} = \frac{2(d-7)(d-5)(d-3)}{s^4 t} \quad (4.438)$$

in agreement with eqs. (4.416). The expressions for the two intersection numbers are listed in App. B, and please note that they are much simpler than for the other two approaches due to the absence of the regulator.

For the  $t$ -channel cut one may proceed likewise, and extract the coefficient of the  $t$ -channel bubble, again in agreement with eqs. (4.416).

Let us note that one could use the subtraction

$$\hat{\phi} = \hat{\varphi} - \frac{\kappa_1}{z_2 z_4} , \quad (4.439)$$

in eq. (4.433), where  $\kappa_1$  is a free coefficient. Then, the fitting of the unknown coefficients of eq. (4.435) generates a system whose solution does require the value  $\kappa_1 = c_1$ . In other words,  $\kappa_1$ , which in this case corresponds to the coefficient of a master integral in the higher sector (the box function) may be fixed together with the remaining  $\kappa$ -parameters<sup>6</sup>.

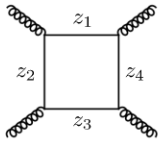
## 4.8 Further Examples

In the following, we present the key information useful to perform the reduction by means of intersection theory, in a set of cases all corresponding to physically relevant Feynman integrals. In particular, for each case, we provide a table containing: the definition of the integral family; the spanning cuts ( $\tau$ ); the dimensions of the vector spaces at each step of the recursive algorithm ( $\nu$ ) and the corresponding bases ( $e$ ), for the evaluation of multivariate intersection numbers; a pictorial decomposition of a generic integral, whose coefficients can be determined by means of our master decomposition formula eq. (4.53). In all these cases, the reduction and/or the differential equations were computed successfully, in agreement with the results of public IBP codes [61, 62, 64, 151].

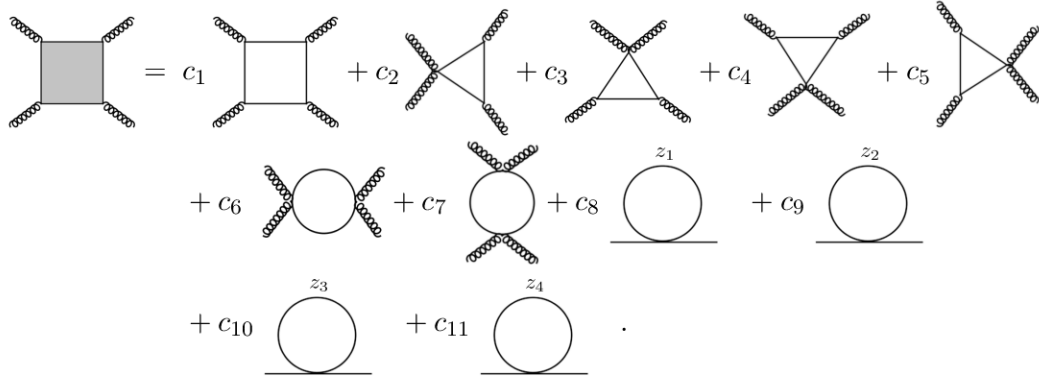
---

<sup>6</sup>In principle such a procedure generalises beyond this example, to cases where more masters are present in the higher sectors.

Box with four different masses

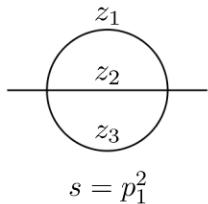
Integral family	Denominators
 $s = (p_1 + p_2)^2, \quad t = (p_2 + p_3)^2$	$z_1 = k^2 - m_1^2$ $z_2 = (k + p_1)^2 - m_2^2$ $z_3 = (k + p_1 + p_2)^2 - m_3^2$ $z_4 = (k + p_1 + p_2 + p_3)^2 - m_4^2$

$\tau$	$\nu$	$e$
$z_4 = 0$	$\nu_{\{3\}} = 2$ $\nu_{\{32\}} = 3$ $\nu_{\{321\}} = 6$	$e^{(3)} = \left\{ 1, \frac{1}{z_3} \right\}$ $e^{(32)} = \left\{ \frac{1}{z_2}, \frac{1}{z_3}, \frac{1}{z_2 z_3} \right\}$ $e^{(321)} = \left\{ 1, \frac{1}{z_2}, \frac{1}{z_1 z_2}, \frac{1}{z_1 z_3}, \frac{1}{z_2 z_3}, \frac{1}{z_1 z_2 z_3} \right\}$
$z_3 = 0$	$\nu_{\{4\}} = 2$ $\nu_{\{41\}} = 3$ $\nu_{\{412\}} = 6$	$e^{(4)} = \left\{ 1, \frac{1}{z_4} \right\}$ $e^{(41)} = \left\{ \frac{1}{z_1}, \frac{1}{z_4}, \frac{1}{z_1 z_4} \right\}$ $e^{(412)} = \left\{ 1, \frac{1}{z_1}, \frac{1}{z_1 z_2}, \frac{1}{z_1 z_4}, \frac{1}{z_2 z_4}, \frac{1}{z_1 z_2 z_4} \right\}$
$z_2 = 0$	$\nu_{\{4\}} = 2$ $\nu_{\{43\}} = 3$ $\nu_{\{431\}} = 6$	$e^{(4)} = \left\{ 1, \frac{1}{z_4} \right\}$ $e^{(43)} = \left\{ \frac{1}{z_3}, \frac{1}{z_4}, \frac{1}{z_3 z_4} \right\}$ $e^{(431)} = \left\{ 1, \frac{1}{z_4}, \frac{1}{z_1 z_3}, \frac{1}{z_1 z_4}, \frac{1}{z_3 z_4}, \frac{1}{z_1 z_3 z_4} \right\}$
$z_1 = 0$	$\nu_{\{4\}} = 2$ $\nu_{\{43\}} = 3$ $\nu_{\{432\}} = 6$	$e^{(4)} = \left\{ 1, \frac{1}{z_4} \right\}$ $e^{(43)} = \left\{ \frac{1}{z_3}, \frac{1}{z_4}, \frac{1}{z_3 z_4} \right\}$ $e^{(432)} = \left\{ 1, \frac{1}{z_3}, \frac{1}{z_2 z_3}, \frac{1}{z_2 z_4}, \frac{1}{z_3 z_4}, \frac{1}{z_2 z_3 z_4} \right\}$



$$\begin{aligned}
 &= c_1 \text{ (triangle)} + c_2 \text{ (triangle)} + c_3 \text{ (triangle)} + c_4 \text{ (triangle)} + c_5 \text{ (triangle)} \\
 &+ c_6 \text{ (bubble } z_1) + c_7 \text{ (bubble } z_2) + c_8 \text{ (bubble } z_1) + c_9 \text{ (bubble } z_2) \\
 &+ c_{10} \text{ (bubble } z_3) + c_{11} \text{ (bubble } z_4) .
 \end{aligned}
 \tag{4.440}$$

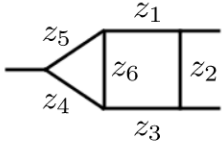
Sunrise with different masses

Integral family	Denominators
	$z_1 = k_1^2 - m_1^2$ $z_2 = (k_1 - k_2)^2 - m_2^2$ $z_3 = (k_2 - p_1)^2 - m_3^2$ $z_4 = k_2^2 - m_1^2$ $z_5 = (k_1 - p_1)^2 - m_3^2$

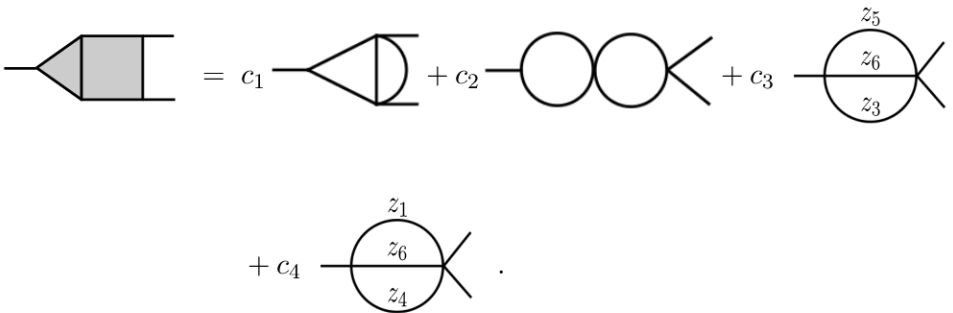
$\tau$	$\nu$	$e$
$z_1 = 0$ $z_2 = 0$	$\nu_{\{5\}} = 1$ $\nu_{\{53\}} = 2$ $\nu_{\{534\}} = 5$	$e^{(5)} = \{1\}$ $e^{(53)} = \left\{1, \frac{1}{z_3}\right\}$ $e^{(534)} = \left\{1, \frac{1}{z_3}, \frac{z_4}{z_3}, \frac{z_5}{z_3}, \frac{z_4^2}{z_3}\right\}$
$z_1 = 0$ $z_3 = 0$	$\nu_{\{5\}} = 1$ $\nu_{\{52\}} = 2$ $\nu_{\{524\}} = 5$	$e^{(5)} = \{1\}$ $e^{(52)} = \left\{1, \frac{1}{z_2}\right\}$ $e^{(524)} = \left\{1, \frac{1}{z_2}, \frac{z_4}{z_2}, \frac{z_5}{z_2}, \frac{z_4^2}{z_2}\right\}$
$z_2 = 0$ $z_3 = 0$	$\nu_{\{5\}} = 1$ $\nu_{\{51\}} = 2$ $\nu_{\{514\}} = 5$	$e^{(5)} = \{1\}$ $e^{(51)} = \left\{1, \frac{1}{z_1}\right\}$ $e^{(514)} = \left\{1, \frac{1}{z_1}, \frac{z_4}{z_1}, \frac{z_5}{z_1}, \frac{z_4^2}{z_1}\right\}$

$$\begin{aligned}
 & \text{Sunrise diagram} = c_1 \text{Sunrise}(z_4^2) + c_2 \text{Sunrise}(z_5) + \\
 & c_3 \text{Sunrise}(z_4) + c_4 \text{Sunrise}(\text{other}) + \\
 & c_5 \text{Bubble}(z_1, z_2) + c_6 \text{Bubble}(z_1, z_3) + c_7 \text{Bubble}(z_1, z_3) . \tag{4.441}
 \end{aligned}$$

Massless planar box-triangle

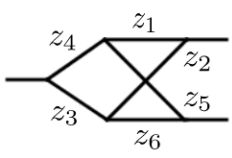
Integral family	Denominator
 <p><math>s = (p_1 + p_2)^2</math></p>	$z_1 = k_1^2 \quad z_2 = (k_1 + p_1)^2$ $z_3 = (k_1 + p_1 + p_2)^2$ $z_4 = (k_2 + p_1 + p_2)^2$ $z_5 = k_2^2 \quad z_6 = (k_1 - k_2)^2$ $z_7 = (k_2 + p_1)^2$

$\tau$	$\nu$	$e$
$z_2 = 0$ $z_4 = 0$ $z_5 = 0$ $z_6 = 0$	$\nu_{\{7\}} = 1$ $\nu_{\{73\}} = 2$ $\nu_{\{731\}} = 1$	$e^{(7)} = \{1\}$ $e^{(73)} = \left\{1, \frac{1}{z_3}\right\}$ $e^{(731)} = \{1\}$
$z_1 = 0$ $z_3 = 0$ $z_4 = 0$ $z_5 = 0$	$\nu_{\{7\}} = 1$ $\nu_{\{76\}} = 1$ $\nu_{\{762\}} = 1$	$e^{(7)} = \{1\}$ $e^{(76)} = \left\{\frac{1}{z_6}\right\}$ $e^{(762)} = \{1\}$
$z_3 = 0$ $z_5 = 0$ $z_6 = 0$	$\nu_{(7)} = 1$ $\nu_{\{74\}} = 1$ $\nu_{\{742\}} = 1$ $\nu_{\{7421\}} = 1$	$e^{(7)} = \{1\}$ $e^{(74)} = \left\{\frac{1}{z_4}\right\}$ $e^{(742)} = \left\{\frac{1}{z_2 z_4}\right\}$ $e^{(7421)} = \{1\}$
$z_1 = 0$ $z_4 = 0$ $z_6 = 0$	$\nu_{\{7\}} = 1$ $\nu_{\{75\}} = 1$ $\nu_{\{752\}} = 1$ $\nu_{\{7523\}} = 1$	$e^{(7)} = \{1\}$ $e^{(75)} = \left\{\frac{1}{z_5}\right\}$ $e^{(752)} = \left\{\frac{1}{z_2 z_5}\right\}$ $e^{(7523)} = \{1\}$

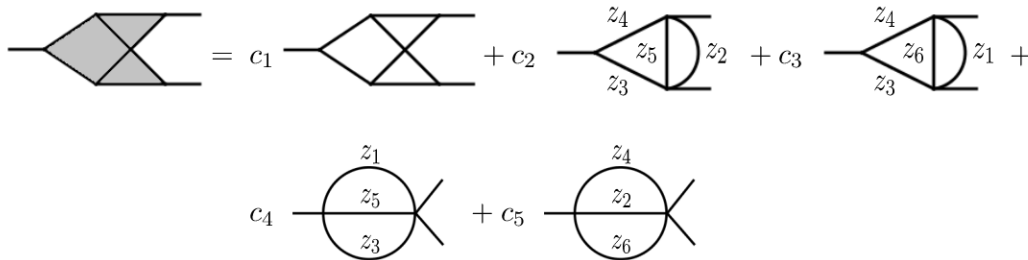


$$\begin{aligned}
 &= c_1 \text{ (triangle with vertical line)} + c_2 \text{ (two circles)} + c_3 \text{ (circle with horizontal line)} \\
 &+ c_4 \text{ (circle with vertical line)} .
 \end{aligned}
 \tag{4.442}$$

Massless non-planar triangle-box

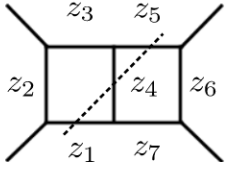
Integral family	Denominators
 <p><math>s = (p_1 + p_2)^2</math></p>	$z_1 = k_1^2 \quad z_2 = (k_1 + p_1)^2$ $z_3 = (k_2 + p_1 + p_2)^2$ $z_4 = k_2^2 \quad z_5 = (k_1 - k_2)^2$ $z_6 = (k_1 - k_2 - p_2)^2$ $z_7 = (k_2 + p_1)^2$

$\tau$	$\nu$	$e$
$z_2 = 0$ $z_3 = 0$ $z_4 = 0$ $z_5 = 0$	$\nu_{\{1\}} = 2$ $\nu_{\{16\}} = 2$ $\nu_{\{167\}} = 2$	$e^{(1)} = \left\{ 1, \frac{1}{z_1} \right\}$ $e^{(16)} = \left\{ \frac{1}{z_6}, \frac{1}{z_1 z_6} \right\}$ $e^{(167)} = \left\{ 1, \frac{1}{z_1 z_6} \right\}$
$z_1 = 0$ $z_3 = 0$ $z_4 = 0$ $z_6 = 0$	$\nu_{\{2\}} = 2$ $\nu_{\{25\}} = 2$ $\nu_{\{257\}} = 2$	$e^{(2)} = \left\{ 1, \frac{1}{z_2} \right\}$ $e^{(25)} = \left\{ \frac{1}{z_5}, \frac{1}{z_2 z_5} \right\}$ $e^{(257)} = \left\{ 1, \frac{1}{z_2 z_5} \right\}$
$z_1 = 0$ $z_3 = 0$ $z_5 = 0$	$\nu_{\{2\}} = 2$ $\nu_{\{24\}} = 2$ $\nu_{\{246\}} = 3$ $\nu_{\{2467\}} = 2$	$e^{(2)} = \left\{ 1, \frac{1}{z_2} \right\}$ $e^{(24)} = \left\{ \frac{1}{z_4}, \frac{1}{z_2 z_4} \right\}$ $e^{(246)} = \left\{ \frac{1}{z_6}, \frac{1}{z_4 z_6}, \frac{1}{z_2 z_4 z_6} \right\}$ $e^{(2467)} = \left\{ 1, \frac{1}{z_2 z_4 z_6} \right\}$
$z_2 = 0$ $z_4 = 0$ $z_6 = 0$	$\nu_{\{1\}} = 2$ $\nu_{\{15\}} = 2$ $\nu_{\{153\}} = 3$ $\nu_{\{1537\}} = 2$	$e^{(1)} = \left\{ 1, \frac{1}{z_1} \right\}$ $e^{(15)} = \left\{ \frac{1}{z_5}, \frac{1}{z_1 z_5} \right\}$ $e^{(153)} = \left\{ \frac{1}{z_3}, \frac{1}{z_3 z_5}, \frac{1}{z_1 z_3 z_5} \right\}$ $e^{(1537)} = \left\{ 1, \frac{1}{z_1 z_3 z_5} \right\}$

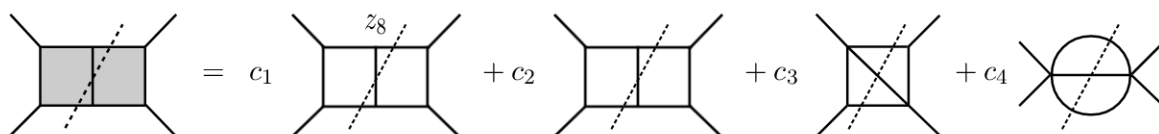


$$= c_1 \dots + c_2 \dots + c_3 \dots + c_4 \dots + c_5 \dots \tag{4.443}$$

### Massless double-box on a triple cut

Integral family	Denominators
 <p><math>s = (p_1 + p_2)^2 \quad t = (p_2 + p_3)^2</math></p>	$z_1 = k_1^2 \quad z_2 = (k_1 - p_1)^2$ $z_3 = (k_1 - p_1 - p_2)^2$ $z_4 = (k_1 - k_2)^2$ $z_5 = (k_2 - p_1 - p_2)^2$ $z_6 = (k_2 - p_1 - p_2 - p_3)^2$ $z_7 = k_2^2 \quad z_8 = (k_2 - p_1)^2$ $z_9 = (k_1 - p_1 - p_2 - p_3)^2$

$\tau$	$\nu$	$e$
$z_1 = 0$ $z_4 = 0$ $z_5 = 0$	$\nu_{\{8\}} = 1$ $\nu_{\{87\}} = 2$ $\nu_{\{876\}} = 2$ $\nu_{\{8762\}} = 4$ $\nu_{\{87629\}} = 5$ $\nu_{\{876293\}} = 4$	$e^{(8)} = \{1\}$ $e^{(87)} = \left\{1, \frac{1}{z_7}\right\}$ $e^{(876)} = \left\{\frac{1}{z_6}, \frac{1}{z_7}\right\}$ $e^{(8762)} = \left\{\frac{1}{z_2}, \frac{1}{z_6}, \frac{1}{z_7}, \frac{1}{z_2 z_6}\right\}$ $e^{(87629)} = \left\{1, \frac{1}{z_2}, \frac{1}{z_6}, \frac{1}{z_7}, \frac{1}{z_2 z_6}\right\}$ $e^{(876293)} = \left\{1, \frac{1}{z_2 z_6}, \frac{1}{z_2 z_3 z_6 z_7}, \frac{z_8}{z_2 z_3 z_6 z_7}\right\}$



(4.444)





## Chapter 5

# Conclusions

The ever growing precision of the measurement performed at modern colliders, entails an enhancement in our knowledge of the theoretical predictions of the observables studied in said facilities.

In this thesis we considered the problem of the accurate evaluation of multiloop amplitudes, fundamental for the search of BSM effects at present colliders. In particular, we presented the first fully analytic evaluation of the 4 leptons scattering amplitude, with 2 different type of leptons involved, one of which is considered massless, up to the second order corrections in the electromagnetic coupling constant. This result was obtained by means of state of the art techniques embedded in a general framework for multi-loop computation which has been implemented in an in house code.

Moreover we have investigated novel techniques based on algebraic topology aiming at better understanding the mathematical structure characterizing Feynman integrals and paving the way to a new method for their reduction to a minimal basis, which is a key step in the analytical evaluation of multi-loop scattering amplitudes.

In the first part of this work, we have explored the capabilities of modern techniques for multi-loop amplitude computation.

By means of a generalization of integrand decomposition at multi-loop level, the *adaptive integrand decomposition*, which exploits a parametric representation of Feynman integrals where the loop momenta are split between the directions parallel to the momenta of the external particles and their transverse ones, together with *algebraic geometry* techniques, allow us to write our scattering amplitudes in terms of scalar integrals. It is then possible to derive a system of identities among them by means of *integration by parts*, which are based on the vanishing of the total derivative of Feynman integrals in dimensional regularization, which upon solution greatly simplifies the structure of our scattering amplitude writing it in terms of a basis of independent integrals. Lastly, by choosing accordingly such basis, it is possible to exploit the advantages given by *canonical* integrals, integrals that satisfy a system of differential equations in which the dimensional parameter  $\epsilon = (d - 4)/2$  is factorized from the kinematical dependence, and the latter can be cast in forms of  $d \log$ . One could even derive a similarity transformation for the differential equation system via *Magnus exponential* in order to bring a system at most linear in epsilon in to canonical forms, when the said Magnus exponential converges. In this way, the evaluation of the MI trivializes into iterated integrals of the type of *generalized polylogarithm*. In this thesis we apply the framework outlined above in the evaluation of the NNLO scattering amplitude for the  $\mu^\pm e^- \rightarrow \mu^\pm e^-$  process, which is relevant for the recently proposed MUonE experiment at CERN. This computation aims to give crucial contribution in clarifying the existing tension between the theoretical expectation values and the measured one of the muon anomalous dipole moment, and it represents a result that stands at the cutting edge of analytical multi-loop scattering amplitudes computation.

In the second part of this thesis, we have presented the application of *twisted intersection theory* to Feynman integrals, exploring the new instruments provided by this branch of mathematics in order to obtain novel method for scattering amplitudes computation.

By reinterpreting Feynman integrals as a pairing between elements of twisted cohomology (which represents the integrand) and twisted homology (which characterizes the integration domain), we studied the geometric nature of MI, relating the number of independent integrals to the Euler characteristic and their number of critical points using Morse / Picard-Lefschetz theory. Furthermore, we discuss an alternative way to compute the reduction of a Feynman integral on its basis by means of the *master decomposition formula* (4.53) which takes advantage of a pairing between integrals (linking forms and dual forms in our case) called *twisted intersection number*. This object, which boils down to the application of Stokes theorem for forms together with Cauchy residue theorem, acts as a scalar product in the vector space of Feynman integrals, allowing us to define an operation which extracts directly the coefficient of the reduction in the chosen basis. This produces a novel, completely independent method for scattering amplitudes computation, bypassing the standard system solving procedure required by IBPs which is quite demanding in high-loop high-multiplicity cases.

We discuss in depth this new technique, providing multiple interesting choice of basis such as the  $d \log$  and the orthonormal basis in which the reduction greatly simplifies, other than showing how this method also allows one to derive the differential equations and dimensional recurrence relations.

We worked out several explicit examples in the case of univariate intersection numbers, applying the twisted intersection theory to special functions as well as several Feynman integrals in parametric representation. For these cases, we exploited generalized unitarity together with Baikov representation, both standard and loop by loop, in order to extract IBPs on the maximal cut, when Feynman integrals on the cut could be represented as a univariate integrals. This provides clear evidence of the validity of the framework, fueling the extension of this technique to more general cases for the reduction of integrals out of the cut.

To achieve this, we applied iteratively the intersection number presented in the univariate case, highlighting an algorithm for the computation of the multivariate intersection number which has been implemented in an in-house code. Exploiting the versatility of generalized unitarity, we then used it together with twisted intersection theory, proposing several methods to perform the reduction to a minimal basis: the straight decomposition, *top-down*, and *bottom-up*. Lastly, we showed examples for the application of the three aforementioned algorithms, together with a summary of the cases in which the method was applied.

To conclude, in this work we faced the computation of a scattering amplitude as a whole, from the generation of the required Feynman integrals that constitute it up to its renormalization and numerical evaluation. Our results and the machinery used in such a calculation will be useful both in order to obtain the observables directly related to the process investigated and for computation of amplitudes that display a similar structure to it.

Besides, we have developed techniques for the simplification of scattering amplitudes, expressing them in terms of a minimal basis of integrals. This new approach provides many thrilling topics which require further investigation, such as the research and definition of an orthonormal basis in the multivariate case, the study of quadratic identities for Feynman integrals allowed by twisted intersection theory, as well as novel algorithm for the evaluation of twisted intersection numbers and the study of relative cohomology applied to Feynman integrals.





# Acknowledgements

Lungo il mio percorso, ho avuto la fortuna ed il piacere di essere accompagnato da molte persone che mi hanno sostenuto, permettendomi di arrivare al coronamento di uno dei miei sogni: aver fatto il dottorato.

Desidero ringraziare per prima, e con tutto il mio cuore, Laura. Non c'è persona che mi conosca più nel profondo di lei, né persona che mi abbia saputo star vicino e sostenere con tale cura. Incontrarla per me è stata una grande fortuna, e ringrazio ogni giorno per averla al mio fianco.

Desidero poi ringraziare il mio supervisor, Pierpaolo. Verso di lui provo la più profonda ammirazione e stima. Mi ha guidato ed accompagnato in questi anni di dottorato con decisione e sapienza, costruendo una strada su misura per me, che mi ha portato ad avere grandi opportunità. Sono felice di aver vissuto quest'esperienza con lui, che ha creato un ambiente di lavoro in cui tutti eravamo molto stimolati a fare il nostro meglio nonché spinti a vedere nei colleghi di lavoro dei compagni di squadra, con cui farsi forza per raggiungere l'agognato traguardo e condividere la propria quotidianità.

Ci tengo particolarmente a ringraziare Hjalte, Federico e Manoj, i miei primi "colleghi", con cui ho condiviso gioie, dolori, fatiche e riposo.

A loro poi si aggiunge la schiera di innumerevoli collaboratori con cui ho avuto il piacere di entrare in contatto, vecchi e nuovi, come Henrick, Seva, William, Jonathan, Amedeo, Uli, Stefano Laporta, Rey D. Sameshima, Giovanni Ossola, Tiziano Peraro, Ettore Remiddi e molti altri. Tutte persone stupende che hanno illuminato la mia strada in questi anni di dottorato.

Desidero poi ringraziare gli amici, Alessio, Emanuele e Davide per esser sempre stati al mio fianco, essenziale valvola di sfogo e di svago.

Desidero ringraziare in particolar modo Manuel, un amico caro a cui devo molto. Fedele, che c'è quando ne hai bisogno e con cui si può star solo che bene.

Desidero ringraziare anche gli altri miei amici dell'università, che mi sono rimasti a fianco in questi anni, Davide e Nicola, come anche ai molti amici che ho conosciuto all'interno del mio dottorato. Penso a Dario, Giovanni, Jay, Sarah, Alfredo... la lista diverrebbe troppo lunga se la completassi. Con gioia ho condiviso con loro le mie giornate all'interno di quel caro stanzone in via Marzolo.

Arrivando infine alla cerchia più stretta dei miei parenti, desidero ringraziare i miei cugini, praticamente fratelli, Davide, Simone, Paolo, Francesca, Marco, e mio fratello Fabio, per i bei momenti che ho condiviso con loro.

Ringrazio anche i miei genitori, senza di loro non sarei qui e non avrei potuto vivere le esperienze che ora mi sono tanto care.

Infine, un pensiero speciale va a mia nonna Maria e mia zia Lilli, che ci hanno lasciati qualche anno fa. Le porto sempre nel cuore dovunque vada.



# Appendices





# Appendix A

## Infrared Structure

The IR poles appearing in the two-loop corrections after UV renormalization can independently be obtained starting from the tree-level and the one-loop amplitudes, by following the same procedure employed to study the infrared structure of QCD amplitudes [152, 153].

In effect, the analytic expression of the two-loop amplitude  $\mathcal{M}^{(2)}$  for the process  $f^- f^+ \rightarrow F^- F^+$  is obtained both in the non-physical region  $s < 0, t < 0$  as well as directly in the production region.

The structure of the IR poles is governed by an anomalous dimension  $\Gamma$  that has the following structure,

$$\begin{aligned} \Gamma = & \gamma_{\text{cusp}}(\alpha) \ln\left(-\frac{s}{\mu^2}\right) + 2\gamma_{\text{cusp}}(\alpha) \ln\left(\frac{t-M^2}{u-M^2}\right) \\ & + \gamma_{\text{cusp,M}}(\alpha, s) + 2\gamma_h(\alpha) + 2\gamma_\psi(\alpha) , \end{aligned} \quad (\text{A.1})$$

where the  $\gamma_i$  ( $i \in \{\text{cusp}; \text{cusp,M}; h; \psi\}$ ) coefficients up to  $\mathcal{O}(\alpha^2)$  are extracted in analogy to the QCD case [152, 154]. In the physical region, the imaginary part of the anomalous dimension in Eq. (A.1) is computed by adding an infinitesimal positive imaginary part to  $s$ . Interested readers may find the expression of the quantities appearing in Eq. (A.1) in the Supplemental Material.

One can then introduce the IR renormalization factor  $Z_{\text{IR}}$ ,

$$\begin{aligned} Z = & 1 + \frac{\alpha}{4\pi} Z_1 + \left(\frac{\alpha}{4\pi}\right)^2 Z_2 + \dots \ln Z_{\text{IR}} & = \frac{\alpha}{4\pi} \left( \frac{\Gamma'_0}{4\epsilon^2} + \frac{\Gamma_0}{2\epsilon} \right) \\ & + \left(\frac{\alpha}{4\pi}\right)^2 \left( -\frac{3\beta_0\Gamma'_0}{16\epsilon^3} \right. \\ & \left. + \frac{\Gamma'_1 - 4\beta_0\Gamma_0}{16\epsilon^2} + \frac{\Gamma_1}{4\epsilon} \right) \\ & + \mathcal{O}(\alpha^3) , \end{aligned} \quad (\text{A.2})$$

where  $\Gamma_i, \Gamma'_i$  and  $\beta_i$  are the coefficients of the expansion of  $\Gamma$ , its derivative w.r.t.  $\ln \mu$ , and the QED beta function, respectively. The IR poles of the  $n^{\text{th}}$ -order term  $\mathcal{M}^{(n)}$  can be calculated using  $Z_{\text{IR}}$  and the lower order contributions,  $\mathcal{M}^{(0)}, \dots, \mathcal{M}^{(n-1)}$ . In particular, the IR pole structures at one and two loops are found to be,

$$\mathcal{M}^{(1)} \Big|_{\text{poles}} = \frac{1}{2} Z_1^{\text{IR}} \mathcal{M}^{(0)} \Big|_{\text{poles}} , \quad (\text{A.3a})$$

$$\begin{aligned} \mathcal{M}^{(2)} \Big|_{\text{poles}} = & \frac{1}{8} \left[ \left( Z_2^{\text{IR}} - (Z_1^{\text{IR}})^2 \right) \mathcal{M}^{(0)} \right. \\ & \left. + 2 Z_1^{\text{IR}} \mathcal{M}^{(1)} \right] \Big|_{\text{poles}} . \end{aligned} \quad (\text{A.3b})$$

All functions  $\mathcal{M}^{(n)}$  in the r.h.s. of Eqs. (A.3) must be evaluated in  $d = 4 - 2\epsilon$  space-time dimensions. The factors  $Z_i^{\text{IR}}$  are the coefficients of the series expansion of  $Z_{\text{IR}}$  in powers of  $\alpha/(4\pi)$ . The agreement of the IR poles structure obtained by direct calculation of the two-loop diagrams, in Eqs. (3.52), with the ones reconstructed starting from the tree-level and one-loop amplitudes, in Eqs. (A.3), constitutes a non trivial test of the complete two-loop calculation.

## Appendix B

# Intersection numbers for the multivariate example

In this appendix we provide the explicit form of intersection numbers needed for the Feynman integral decompositions performed in Sec. [4.7](#). Since we work in analytic regularization with a parameter  $\rho$  that is taken to zero at the end of the computation, it suffices to know only the leading  $\rho$ -orders of intersection numbers. While our algorithm computes them exactly in  $\rho$ , in order to save space in this appendix we list only the *leading* term for each intersection number *individually*. One can check that the orders given here are sufficient for reconstructing the coefficients  $c_i$  to order  $\mathcal{O}(\rho^0)$  and that their limit as  $\rho \rightarrow 0$  is in fact smooth.

### The one-loop massless box

#### Straight decomposition

Here we provide the intersection numbers, up to the leading order in  $\rho$  required for the decomposition presented in Subsec. [4.7.1](#):

$$\mathbf{C}_{ij} = \langle e_i | h_j \rangle, \quad 1 \leq i, j \leq 3 \quad (\text{B.1})$$

with

$$\langle e_1 | h_1 \rangle = \frac{1}{\rho^4} + \mathcal{O}(\rho^{-3}), \quad (\text{B.2})$$

$$\langle e_1 | h_2 \rangle = -\frac{st}{(d-7)(d-6)\rho^2} + \mathcal{O}(\rho^{-1}), \quad (\text{B.3})$$

$$\langle e_1 | h_3 \rangle = \langle e_1 | h_2 \rangle, \quad (\text{B.4})$$

$$\langle e_2 | h_1 \rangle = -\frac{st}{(d-4)(d-3)\rho^2} + \mathcal{O}(\rho^{-1}), \quad (\text{B.5})$$

$$\langle e_2 | h_2 \rangle = -\frac{s^2 t (s+t)}{4(d-7)(d-3)\rho^2} + \mathcal{O}(\rho^{-1}), \quad (\text{B.6})$$

$$\langle e_2 | h_3 \rangle = -\frac{st((d-4)^2 s^2 + ((d-10)d+28)st + (d-6)^2 t^2)}{(d-7)(d-6)^2(d-4)^2(d-3)} + \mathcal{O}(\rho), \quad (\text{B.7})$$

$$\langle e_3 | h_1 \rangle = \langle e_2 | h_1 \rangle, \quad (\text{B.8})$$

$$\langle e_3 | h_2 \rangle = -\frac{st((d-6)^2 s^2 + ((d-10)d+28)st + (d-4)^2 t^2)}{(d-7)(d-6)^2(d-4)^2(d-3)} + \mathcal{O}(\rho), \quad (\text{B.9})$$

$$\langle e_3 | h_3 \rangle = -\frac{st^2(s+t)}{4(d-7)(d-3)\rho^2} + \mathcal{O}(\rho^{-1}), \quad (\text{B.10})$$

and

$$\langle \varphi | h_k \rangle, \quad 1 \leq k \leq 3 \quad (\text{B.11})$$

with

$$\langle \varphi | h_1 \rangle = \frac{(7-d)(d-6)(d-5)}{2\rho^4 s^2 t} + \mathcal{O}(\rho^{-3}), \quad (\text{B.12})$$

$$\langle \varphi | h_2 \rangle = \frac{(5-d)t}{2\rho^2 s^2} + \mathcal{O}(\rho^{-1}), \quad (\text{B.13})$$

$$\langle \varphi | h_3 \rangle = -\frac{(d-5)((d-6)t+2s)}{2(d-8)\rho^2 t^2} + \mathcal{O}(\rho^{-1}). \quad (\text{B.14})$$

### Bottom-up decomposition

Here we provide the intersection numbers required for the decomposition presented in Subsec. [4.7.1](#), on the  $\tau = \{1, 3\}$  cut:

$$\mathbf{C}_{ij} = \langle e_{i,\tau} | h_{j,\tau} \rangle, \quad 1 \leq i, j \leq 2 \quad (\text{B.15})$$

with

$$\langle e_{1,\tau} | h_{1,\tau} \rangle = \frac{d-5}{\rho^2(d-5+2\rho)}, \quad (\text{B.16})$$

$$\langle e_{1,\tau} | h_{2,\tau} \rangle = \frac{-(d-5)st}{(d-7+2\rho)(d-6+2\rho)(d-5+2\rho)}, \quad (\text{B.17})$$

$$\langle e_{2,\tau} | h_{1,\tau} \rangle = \frac{-(d-5)st}{(d-5+2\rho)(d-4+2\rho)(d-3+2\rho)}, \quad (\text{B.18})$$

$$\langle e_{2,\tau} | h_{2,\tau} \rangle = \frac{(d-5)s^2 t(4\rho^2 t - (d-6+4\rho)(d-4+4\rho)(s+t))}{4(d-7+2\rho)(d-6+2\rho)(d-5+2\rho)(d-4+2\rho)(d-3+2\rho)}, \quad (\text{B.19})$$

and

$$\langle \varphi_\tau | h_{k,\tau} \rangle, \quad 1 \leq k \leq 2 \quad (\text{B.20})$$

with

$$\langle \varphi_\tau | h_{1,\tau} \rangle = \frac{(d-5)(d-7+2\rho)((d-6+4\rho)s+2\rho t)}{2(\rho-1)\rho^2 s^3 t}, \quad (\text{B.21})$$

$$\langle \varphi_\tau | h_{2,\tau} \rangle = \frac{(d-5)t}{2(\rho-1)s^2}. \quad (\text{B.22})$$

### Top-down decomposition

For consistency with the straight decomposition and the bottom-up decomposition, we also provide here the intersection numbers needed for the top-down decomposition of Subsec. [4.7.1](#) on the  $\tau = \{1, 3\}$  cut. They are

$$\langle \phi | 1 \rangle = \frac{-(d-5)(s+t)}{2s^2}, \quad \langle 1 | 1 \rangle = \frac{-s^2 t(s+t)}{4(d-7)(d-3)}. \quad (\text{B.23})$$

# Bibliography

- [1] H. Frellesvig, F. Gasparotto, S. Laporta, M. K. Mandal, P. Mastrolia, L. Mattiazzi, and S. Mizera, *Decomposition of Feynman Integrals on the Maximal Cut by Intersection Numbers*, *JHEP* **05** (2019) 153, [[arXiv:1901.11510](#)].
- [2] H. Frellesvig, F. Gasparotto, M. K. Mandal, P. Mastrolia, L. Mattiazzi, and S. Mizera, *Vector Space of Feynman Integrals and Multivariate Intersection Numbers*, *Phys. Rev. Lett.* **123** (2019), no. 20 201602, [[arXiv:1907.02000](#)].
- [3] H. Frellesvig, F. Gasparotto, S. Laporta, M. K. Mandal, P. Mastrolia, L. Mattiazzi, and S. Mizera, *Decomposition of Feynman Integrals by Multivariate Intersection Numbers*, *JHEP* **03** (2021) 027, [[arXiv:2008.04823](#)].
- [4] R. Bonciani et al., *Two-Loop Four-Fermion Scattering Amplitude in QED*, *Phys. Rev. Lett.* **128** (2022), no. 2 022002, [[arXiv:2106.13179](#)].
- [5] H. A. Frellesvig and L. Mattiazzi, *On the Application of Intersection Theory to Feynman Integrals: the univariate case*, *PoS MA2019* (2022) 017, [[arXiv:2102.01576](#)].
- [6] D. D. Canko, F. Gasparotto, L. Mattiazzi, C. G. Papadopoulos, and N. Syrrakos,  *$N^3LO$  calculations for  $2 \rightarrow 2$  processes using simplified differential equations*, *SciPost Phys. Proc.* **7** (2022) 028, [[arXiv:2110.08110](#)].
- [7] M. K. Mandal, L. Mattiazzi, J. Ronca, and W. J. Bobadilla Torres, *Analytic Evaluation of the NNLO virtual corrections to Muon–Electron scattering*, *PoS* (2022).
- [8] G. Abbiendi et al., *Mini-Proceedings of the STRONG2020 Virtual Workshop on “Space-like and Time-like determination of the Hadronic Leading Order contribution to the Muon  $g - 2$ ”*, in *STRONG2020 Virtual Workshop “Space-like and Time-like determination of the Hadronic Leading Order contribution to the Muon  $g - 2$ ”*, 1, 2022. [[arXiv:2201.12102](#)].
- [9] CMS Collaboration, S. Chatrchyan et al., *Observation of a New Boson at a Mass of 125 GeV with the CMS Experiment at the LHC*, *Phys. Lett. B* **716** (2012) 30–61, [[arXiv:1207.7235](#)].
- [10] Tech. Rep. ATLAS-CONF-2012-135, CERN, Geneva, Sep, 2012.
- [11] G. Colangelo et al., *Prospects for precise predictions of  $a_\mu$  in the Standard Model*, [[arXiv:2203.15810](#)].
- [12] Muon  $g-2$  Collaboration, B. Abi et al., *Measurement of the Positive Muon Anomalous Magnetic Moment to 0.46 ppm*, *Phys. Rev. Lett.* **126** (2021), no. 14 141801, [[arXiv:2104.03281](#)].
- [13] C. M. Carloni Calame, M. Passera, L. Trentadue, and G. Venanzoni, *A new approach to evaluate the leading hadronic corrections to the muon  $g-2$* , *Phys. Lett. B* **746** (2015) 325–329, [[arXiv:1504.02228](#)].

- [14] P. Banerjee et al., *Theory for muon-electron scattering @ 10 ppm: A report of the MUonE theory initiative*, *Eur. Phys. J. C* **80** (2020), no. 6 591, [arXiv:2004.13663](#).
- [15] G. Passarino and M. J. G. Veltman, *One Loop Corrections for  $e^+ e^-$  Annihilation Into  $\mu^+ \mu^-$  in the Weinberg Model*, *Nucl. Phys.* **B160** (1979) 151.
- [16] G. Ossola, C. G. Papadopoulos, and R. Pittau, *Reducing full one-loop amplitudes to scalar integrals at the integrand level*, *Nucl. Phys. B* **763** (2007) 147–169, [hep-ph/0609007](#).
- [17] G. Ossola, C. G. Papadopoulos, and R. Pittau, *Numerical evaluation of six-photon amplitudes*, *JHEP* **0707** (2007) 085, [arXiv:0704.1271](#).
- [18] R. Ellis, W. T. Giele, Z. Kunszt, and K. Melnikov, *Masses, fermions and generalized  $D$ -dimensional unitarity*, *Nucl. Phys. B* **822** (2009) 270–282, [arXiv:0806.3467](#).
- [19] R. Ellis, K. Melnikov, and G. Zanderighi, *Generalized unitarity at work: first NLO QCD results for hadronic  $W^+$  3jet production*, *JHEP* **0904** (2009) 077, [arXiv:0901.4101](#).
- [20] G. Ossola, C. G. Papadopoulos, and R. Pittau, *On the Rational Terms of the one-loop amplitudes*, *JHEP* **0805** (2008) 004, [arXiv:0802.1876](#).
- [21] P. Mastrolia, G. Ossola, C. G. Papadopoulos, and R. Pittau, *Optimizing the Reduction of One-Loop Amplitudes*, *JHEP* **06** (2008) 030, [arXiv:0803.3964](#).
- [22] G. Ossola, C. G. Papadopoulos, and R. Pittau, *CutTools: A Program implementing the OPP reduction method to compute one-loop amplitudes*, *JHEP* **03** (2008) 042, [arXiv:0711.3596](#).
- [23] P. Mastrolia, G. Ossola, T. Reiter, and F. Tramontano, *Scattering AMplitudes from Unitarity-based Reduction Algorithm at the Integrand-level*, *JHEP* **08** (2010) 080, [arXiv:1006.0710](#).
- [24] T. Peraro, *Ninja: Automated Integrand Reduction via Laurent Expansion for One-Loop Amplitudes*, *Comput. Phys. Commun.* **185** (2014) 2771–2797, [arXiv:1403.1229](#).
- [25] T. Hahn and M. Perez-Victoria, *Automatized one loop calculations in four-dimensions and  $D$ -dimensions*, *Comput.Phys.Commun.* **118** (1999) 153–165, [hep-ph/9807565](#).
- [26] A. van Hameren, C. Papadopoulos, and R. Pittau, *Automated one-loop calculations: A Proof of concept*, *JHEP* **0909** (2009) 106, [arXiv:0903.4665](#).
- [27] G. Bevilacqua, M. Czakon, C. Papadopoulos, R. Pittau, and M. Worek, *Assault on the NLO Wishlist:  $pp \rightarrow t$  anti- $t$   $b$  anti- $b$* , *JHEP* **0909** (2009) 109, [arXiv:0907.4723](#).
- [28] C. Berger, Z. Bern, L. Dixon, F. Febres Cordero, D. Forde, et al., *An Automated Implementation of On-Shell Methods for One-Loop Amplitudes*, *Phys.Rev.* **D78** (2008) 036003, [arXiv:0803.4180](#).
- [29] V. Hirschi, R. Frederix, S. Frixione, M. V. Garzelli, F. Maltoni, et al., *Automation of one-loop QCD corrections*, *JHEP* **1105** (2011) 044, [arXiv:1103.0621](#).
- [30] G. Cullen, N. Greiner, G. Heinrich, G. Luisoni, P. Mastrolia, G. Ossola, T. Reiter, and F. Tramontano, *Automated One-Loop Calculations with GoSam*, *Eur. Phys. J. C* **72** (2012) 1889, [arXiv:1111.2034](#).
- [31] F. Cascioli, P. Maierhofer, and S. Pozzorini, *Scattering Amplitudes with Open Loops*, *Phys. Rev. Lett.* **108** (2012) 111601, [arXiv:1111.5206](#).

- [32] S. Badger, B. Biedermann, and P. Uwer, *NGLuon: A Package to Calculate One-loop Multi-gluon Amplitudes*, *Comput.Phys.Commun.* **182** (2011) 1674–1692, [arXiv:1011.2900](#).
- [33] S. Badger, B. Biedermann, P. Uwer, and V. Yundin, *Numerical evaluation of virtual corrections to multi-jet production in massless QCD*, *Comput. Phys. Commun.* **184** (2013) 1981–1998, [arXiv:1209.0100](#).
- [34] H. van Deurzen et al., *Automated one-loop calculations with GoSam 2.0*, *PoS LL2014* (2014) 021, [arXiv:1407.0922](#).
- [35] P. Mastrolia and G. Ossola, *On the Integrand-Reduction Method for Two-Loop Scattering Amplitudes*, *JHEP* **11** (2011) 014, [arXiv:1107.6041](#).
- [36] S. Badger, H. Frellesvig, and Y. Zhang, *Hepta-Cuts of Two-Loop Scattering Amplitudes*, *JHEP* **1204** (2012) 055, [arXiv:1202.2019](#).
- [37] Y. Zhang, *Integrand-Level Reduction of Loop Amplitudes by Computational Algebraic Geometry Methods*, *JHEP* **09** (2012) 042, [arXiv:1205.5707](#).
- [38] P. Mastrolia, E. Mirabella, G. Ossola, and T. Peraro, *Scattering Amplitudes from Multivariate Polynomial Division*, *Phys. Lett. B* **718** (2012) 173–177, [arXiv:1205.7087](#).
- [39] P. Mastrolia, T. Peraro, and A. Primo, *Adaptive Integrand Decomposition in parallel and orthogonal space*, *JHEP* **08** (2016) 164, [arXiv:1605.03157](#).
- [40] W. J. Torres Bobadilla, *Interplay of colour kinematics duality and analytic calculation of multi-loop scattering amplitudes: one and two loops*, *PoS RADCOR2017* (2018) 082, [arXiv:1801.03010](#).
- [41] P. Mastrolia, T. Peraro, A. Primo, and W. J. Torres Bobadilla, *Adaptive Integrand Decomposition*, *PoS LL2016* (2016) 007, [arXiv:1607.05156](#).
- [42] A. Primo, *Cutting Feynman Amplitudes: from Adaptive Integrand Decomposition to Differential Equations on Maximal Cuts*. PhD thesis, Padua U., 2017.
- [43] S. Laporta, *High precision calculation of multiloop Feynman integrals by difference equations*, *Int. J. Mod. Phys. A* **15** (2000) 5087–5159, [hep-ph/0102033](#).
- [44] A. V. Kotikov, *Differential equations method: New technique for massive Feynman diagrams calculation*, *Phys. Lett. B* **254** (1991) 158–164.
- [45] E. Remiddi, *Differential equations for Feynman graph amplitudes*, *Nuovo Cim.* **A110** (1997) 1435–1452, [hep-th/9711188](#).
- [46] T. Gehrmann and E. Remiddi, *Differential equations for two loop four point functions*, *Nucl. Phys.* **B580** (2000) 485–518, [hep-ph/9912329](#).
- [47] M. Argeri and P. Mastrolia, *Feynman Diagrams and Differential Equations*, *Int. J. Mod. Phys. A* **22** (2007) 4375–4436, [arXiv:0707.4037](#).
- [48] J. M. Henn, *Dual conformal symmetry at loop level: massive regularization*, *J.Phys.A* **A44** (2011) 454011, [arXiv:1103.1016](#).
- [49] A. B. Goncharov, *Multiple polylogarithms, cyclotomy and modular complexes*, *Math. Res. Lett.* **5** (1998) 497–516, [arXiv:1105.2076](#).

- [50] M. Argeri, S. Di Vita, P. Mastrolia, E. Mirabella, J. Schlenk, U. Schubert, and L. Tancredi, *Magnus and Dyson Series for Master Integrals*, *JHEP* **03** (2014) 082, [arXiv:1401.2979](#).
- [51] P. Mastrolia, M. Passera, A. Primo, and U. Schubert, *Master integrals for the NNLO virtual corrections to  $\mu e$  scattering in QED: the planar graphs*, *JHEP* **11** (2017) 198, [arXiv:1709.07435](#).
- [52] S. Di Vita, S. Laporta, P. Mastrolia, A. Primo, and U. Schubert, *Master integrals for the NNLO virtual corrections to  $e$  scattering in QED: the non-planar graphs*, *JHEP* **09** (2018) 016, [arXiv:1806.08241](#).
- [53] M. K. Mandal, P. Mastrolia, J. Ronca, and W. J. Bobadilla Torres, *Two-loop scattering amplitude for heavy-quark pair production through light-quark annihilation in QCD*, [arXiv:2204.03466](#).
- [54] A. von Manteuffel and R. M. Schabinger, *A novel approach to integration by parts reduction*, *Phys. Lett. B* **744** (2015) 101–104, [arXiv:1406.4513](#).
- [55] T. Peraro, *Scattering amplitudes over finite fields and multivariate functional reconstruction*, *JHEP* **12** (2016) 030, [arXiv:1608.01902](#).
- [56] J. Böhm, A. Georgoudis, K. J. Larsen, H. Schönemann, and Y. Zhang, *Complete integration-by-parts reductions of the non-planar hexagon-box via module intersections*, *JHEP* **09** (2018) 024, [arXiv:1805.01873](#).
- [57] D. A. Kosower, *Direct Solution of Integration-by-Parts Systems*, *Phys. Rev.* **D98** (2018), no. 2 025008, [arXiv:1804.00131](#).
- [58] X. Liu and Y.-Q. Ma, *Determine Arbitrary Feynman Integrals by Vacuum Integrals*, [arXiv:1801.10523](#).
- [59] A. Kardos, *A new reduction strategy for special negative sectors of planar two-loop integrals without Laporta algorithm*, [arXiv:1812.05622](#).
- [60] H. A. Chawdhry, M. A. Lim, and A. Mitov, *Two-loop five-point massless QCD amplitudes within the IBP approach*, [arXiv:1805.09182](#).
- [61] A. von Manteuffel and C. Studerus, *Reduze 2 - Distributed Feynman Integral Reduction*, [arXiv:1201.4330](#).
- [62] R. N. Lee, *Presenting LiteRed: a tool for the Loop InTEgrals REDuction*, [arXiv:1212.2685](#).
- [63] A. V. Smirnov, *Algorithm FIRE – Feynman Integral REDuction*, *JHEP* **10** (2008) 107, [arXiv:0807.3243](#).
- [64] P. Maierhofer, J. Usovitsch, and P. Uwer, *KiraA Feynman integral reduction program*, *Comput. Phys. Commun.* **230** (2018) 99–112, [arXiv:1705.05610](#).
- [65] A. Georgoudis, K. J. Larsen, and Y. Zhang, *Azurite: An algebraic geometry based package for finding bases of loop integrals*, *Comput. Phys. Commun.* **221** (2017) 203–215, [arXiv:1612.04252](#).
- [66] P. Maierhöfer and J. Usovitsch, *Kira 1.2 Release Notes*, [arXiv:1812.01491](#).
- [67] A. V. Smirnov and F. S. Chuharev, *FIRE6: Feynman Integral REDuction with Modular Arithmetic*, [arXiv:1901.07808](#).



- [68] P. Mastrolia and S. Mizera, *Feynman Integrals and Intersection Theory*, *JHEP* **02** (2019) 139, [arXiv:1810.03818](#).
- [69] K. Aomoto and M. Kita, *Theory of Hypergeometric Functions*. Springer Monographs in Mathematics. Springer Japan, 2011.
- [70] M. Yoshida, *Hypergeometric Functions, My Love: Modular Interpretations of Configuration Spaces*. Aspects of Mathematics. Vieweg+Teubner Verlag, 2013.
- [71] K. Matsumoto, *Quadratic Identities for Hypergeometric Series of Type  $(k, l)$* , *Kyushu Journal of Mathematics* **48** (1994), no. 2 335–345.
- [72] K. Cho and K. Matsumoto, *Intersection theory for twisted cohomologies and twisted Riemann's period relations I*, *Nagoya Math. J.* **139** (1995) 67–86.
- [73] Y. Goto, *Twisted Cycles and Twisted Period Relations for Lauricella's Hypergeometric Function  $F_C$* , *International Journal of Mathematics* **24** (2013), no. 12 1350094, [arXiv:1308.5535](#).
- [74] Y. Goto and K. Matsumoto, *The monodromy representation and twisted period relations for Appell's hypergeometric function  $F_4$* , *Nagoya Math. J.* **217** (03, 2015) 61–94.
- [75] S. Mizera, *Scattering Amplitudes from Intersection Theory*, *Phys. Rev. Lett.* **120** (2018), no. 14 141602, [arXiv:1711.00469](#).
- [76] S.-J. Matsubara-Heo and N. Takayama, *An algorithm of computing cohomology intersection number of hypergeometric integrals*, [arXiv:1904.01253](#).
- [77] K. Aomoto and M. Ito, *Product of Hessians and Discriminant of Critical Points of Level Function for Hypergeometric Integrals*, *PoS MA2019* (2022) 009.
- [78] M. Yoshida, *Schwarz maps for the hypergeometric function*, *PoS MA2019* (2022) 011.
- [79] K. Matsumoto, *Introduction to the Intersection Theory for Twisted Homology and Cohomology Groups*, *PoS MA2019* (2022) 007.
- [80] Y. Goto, *Appell-Lauricella's hypergeometric functions and intersection theory*, *PoS MA2019* (2022) 008.
- [81] S. Mizera, *Aspects of Scattering Amplitudes and Moduli Space Localization*, [arXiv:1906.02099](#).
- [82] P. A. Baikov, *Explicit solutions of the multiloop integral recurrence relations and its application*, *Nucl. Instrum. Meth.* **A389** (1997) 347–349, [hep-ph/9611449](#).
- [83] A. G. Grozin, *Integration by parts: An Introduction*, *Int. J. Mod. Phys.* **A26** (2011) 2807–2854, [arXiv:1104.3993](#).
- [84] M. Harley, F. Moriello, and R. M. Schabinger, *Baikov-Lee Representations Of Cut Feynman Integrals*, *JHEP* **06** (2017) 049, [arXiv:1705.03478](#).
- [85] R. Sameshima, *On different parametrization of Feynman integrals*, *Master thesis CUNY university* (2019).
- [86] H. Frellesvig and C. G. Papadopoulos, *Cuts of Feynman Integrals in Baikov representation*, *JHEP* **04** (2017) 083, [arXiv:1701.07356](#).
- [87] S. Laporta, *High precision calculation of multiloop Feynman integrals by difference equations*, *Int. J. Mod. Phys.* **A15** (2000) 5087–5159, [hep-ph/0102033](#).

- [88] R. N. Lee, *LiteRed 1.4: a powerful tool for reduction of multiloop integrals*, *J. Phys. Conf. Ser.* **523** (2014) 012059, [arXiv:1310.1145](#).
- [89] J. Klappert, F. Lange, P. Maierhöfer, and J. Usovitsch, *Integral reduction with Kira 2.0 and finite field methods*, *Comput. Phys. Commun.* **266** (2021) 108024, [arXiv:2008.06494](#).
- [90] J. M. Henn, *Multiloop integrals in dimensional regularization made simple*, *Phys. Rev. Lett.* **110** (2013) 251601, [arXiv:1304.1806](#).
- [91] E. Remiddi and J. A. M. Vermaseren, *Harmonic polylogarithms*, *Int. J. Mod. Phys. A* **15** (2000) 725–754, [hep-ph/9905237](#).
- [92] J. Vollinga and S. Weinzierl, *Numerical evaluation of multiple polylogarithms*, *Comput. Phys. Commun.* **167** (2005) 177, [hep-ph/0410259](#).
- [93] O. V. Tarasov, *Connection between Feynman integrals having different values of the space-time dimension*, *Phys. Rev. D* **54** (1996) 6479–6490, [hep-th/9606018](#).
- [94] R. N. Lee, *DRA method: Powerful tool for the calculation of the loop integrals*, *J. Phys. Conf. Ser.* **368** (2012) 012050, [arXiv:1203.4868](#).
- [95] R. N. Lee, *Space-time dimensionality  $D$  as complex variable: Calculating loop integrals using dimensional recurrence relation and analytical properties with respect to  $D$* , *Nucl. Phys. B* **830** (2010) 474–492, [arXiv:0911.0252](#).
- [96] S. Laporta, *Calculation of master integrals by difference equations*, *Phys. Lett. B* **504** (2001) 188–194, [hep-ph/0102032](#).
- [97] T. Binoth and G. Heinrich, *Numerical evaluation of multiloop integrals by sector decomposition*, *Nucl. Phys. B* **680** (2004) 375–388, [hep-ph/0305234](#).
- [98] S. Borowka, G. Heinrich, S. P. Jones, M. Kerner, J. Schlenk, and T. Zirke, *SecDec-3.0: numerical evaluation of multi-scale integrals beyond one loop*, *Comput. Phys. Commun.* **196** (2015) 470–491, [arXiv:1502.06595](#).
- [99] A. V. Smirnov, *FIESTA4: Optimized Feynman integral calculations with GPU support*, *Comput. Phys. Commun.* **204** (2016) 189–199, [arXiv:1511.03614](#).
- [100] M. K. Mandal and X. Zhao, *Evaluating multi-loop Feynman integrals numerically through differential equations*, *JHEP* **03** (2019) 190, [arXiv:1812.03060](#).
- [101] F. Maltoni, M. K. Mandal, and X. Zhao, *Top-quark effects in diphoton production through gluon fusion at NLO in QCD*, [arXiv:1812.08703](#).
- [102] R. N. Lee and K. T. Mingulov, *Introducing SummerTime: a package for high-precision computation of sums appearing in DRA method*, *Comput. Phys. Commun.* **203** (2016) 255–267, [arXiv:1507.04256](#).
- [103] P. Kusch and H. M. Foley, *The Magnetic Moment of the Electron*, *Phys. Rev.* **74** (1948), no. 3 250.
- [104] J. S. Schwinger, *On Quantum electrodynamics and the magnetic moment of the electron*, *Phys. Rev.* **73** (1948) 416–417.
- [105] T. Aoyama, T. Kinoshita, and M. Nio, *Theory of the Anomalous Magnetic Moment of the Electron*, *Atoms* **7** (2019), no. 1 28.

- [106] D. Hanneke, S. Fogwell, and G. Gabrielse, *New Measurement of the Electron Magnetic Moment and the Fine Structure Constant*, *Phys. Rev. Lett.* **100** (2008) 120801, [arXiv:0801.1134](#).
- [107] **Muon g-2** Collaboration, B. Abi et al., *Measurement of the Positive Muon Anomalous Magnetic Moment to 0.46 ppm*, *Phys. Rev. Lett.* **126** (2021), no. 14 141801, [arXiv:2104.03281](#).
- [108] M. Fael and M. Passera, *Muon-Electron Scattering at Next-To-Next-To-Leading Order: The Hadronic Corrections*, *Phys. Rev. Lett.* **122** (2019), no. 19 192001, [arXiv:1901.03106](#).
- [109] D. Yu. Bardin and L. Kalinovskaya, *QED corrections for polarized elastic  $\mu e$  scattering*, [hep-ph/9712310](#).
- [110] N. Kaiser, *Radiative corrections to lepton-lepton scattering revisited*, *J. Phys.* **G37** (2010) 115005.
- [111] C. Gnendiger et al., *To d, or not to d: recent developments and comparisons of regularization schemes*, *Eur. Phys. J.* **C77** (2017), no. 7 471, [arXiv:1705.01827](#).
- [112] T. Hahn, *Generating Feynman diagrams and amplitudes with FeynArts 3*, *Comput. Phys. Commun.* **140** (2001) 418–431, [hep-ph/0012260](#).
- [113] R. Mertig, M. Bohm, and A. Denner, *FEYN CALC: Computer algebraic calculation of Feynman amplitudes*, *Comput. Phys. Commun.* **64** (1991) 345–359.
- [114] V. Shtabovenko, R. Mertig, and F. Orellana, *New Developments in FeynCalc 9.0*, *Comput. Phys. Commun.* **207** (2016) 432–444, [arXiv:1601.01167](#).
- [115] V. Shtabovenko, R. Mertig, and F. Orellana, *FeynCalc 9.3: New features and improvements*, *Comput. Phys. Commun.* **256** (2020) 107478, [arXiv:2001.04407](#).
- [116] P. Mastrolia, T. Peraro, A. Primo, J. Ronca, and W. J. Torres Bobadilla, *AIDA, Adaptive Integrand Decomposition Algorithm*, .
- [117] K. G. Chetyrkin and F. V. Tkachov, *Integration by Parts: The Algorithm to Calculate beta Functions in 4 Loops*, *Nucl. Phys.* **B192** (1981) 159–204.
- [118] R. Bonciani, P. Mastrolia, and E. Remiddi, *Vertex diagrams for the QED form-factors at the two loop level*, *Nucl. Phys. B* **661** (2003) 289–343, [hep-ph/0301170](#). [Erratum: *Nucl.Phys.B* 702, 359–363 (2004)].
- [119] R. Bonciani, P. Mastrolia, and E. Remiddi, *Master integrals for the two loop QCD virtual corrections to the forward backward asymmetry*, *Nucl. Phys. B* **690** (2004) 138–176, [hep-ph/0311145](#).
- [120] R. Bonciani, A. Ferroglia, T. Gehrmann, D. Maitre, and C. Studerus, *Two-Loop Fermionic Corrections to Heavy-Quark Pair Production: The Quark-Antiquark Channel*, *JHEP* **07** (2008) 129, [arXiv:0806.2301](#).
- [121] R. Bonciani, A. Ferroglia, T. Gehrmann, and C. Studerus, *Two-Loop Planar Corrections to Heavy-Quark Pair Production in the Quark-Antiquark Channel*, *JHEP* **08** (2009) 067, [arXiv:0906.3671](#).
- [122] M. Becchetti, R. Bonciani, V. Casconi, A. Ferroglia, S. Lavacca, and A. von Manteuffel, *Master Integrals for the two-loop, non-planar QCD corrections to top-quark pair production in the quark-annihilation channel*, *JHEP* **08** (2019) 071, [arXiv:1904.10834](#).

- [123] L. Naterop, A. Signer, and Y. Ulrich, *handyG —Rapid numerical evaluation of generalised polylogarithms in Fortran*, *Comput. Phys. Commun.* **253** (2020) 107165, [[arXiv:1909.01656](#)].
- [124] M. Czakon, *Tops from Light Quarks: Full Mass Dependence at Two-Loops in QCD*, *Phys. Lett. B* **664** (2008) 307–314, [[arXiv:0803.1400](#)].
- [125] P. Bärnreuther, M. Czakon, and P. Fiedler, *Virtual amplitudes and threshold behaviour of hadronic top-quark pair-production cross sections*, *JHEP* **02** (2014) 078, [[arXiv:1312.6279](#)].
- [126] A. Ferroglia, M. Neubert, B. D. Pecjak, and L. L. Yang, *Two-loop divergences of massive scattering amplitudes in non-abelian gauge theories*, *JHEP* **11** (2009) 062, [[arXiv:0908.3676](#)].
- [127] S. Mizera and A. Pokraka, *From Infinity to Four Dimensions: Higher Residue Pairings and Feynman Integrals*, [[arXiv:1910.11852](#)].
- [128] S. Weinzierl, *Correlation functions on the lattice and twisted cocycles*, *Phys. Lett. B* **805** (2020) 135449, [[arXiv:2003.05839](#)].
- [129] S. Weinzierl, *On the computation of intersection numbers for twisted cocycles*, [[arXiv:2002.01930](#)].
- [130] S. Caron-Huot and A. Pokraka, *Duals of Feynman integrals. Part I. Differential equations*, *JHEP* **12** (2021) 045, [[arXiv:2104.06898](#)].
- [131] S. Caron-Huot and A. Pokraka, *Duals of Feynman Integrals. Part II. Generalized unitarity*, *JHEP* **04** (2022) 078, [[arXiv:2112.00055](#)].
- [132] V. Chestnov, F. Gasparotto, M. K. Mandal, P. Mastrolia, S. J. Matsubara-Heo, H. J. Munch, and N. Takayama, *Macaulay Matrix for Feynman Integrals: Linear Relations and Intersection Numbers*, [[arXiv:2204.12983](#)].
- [133] P. Mastrolia, *From Diagrammar to Diagrammalgebra*, *PoS MA2019* (2022) 015.
- [134] S. Mizera, *Status of Intersection Theory and Feynman Integrals*, *PoS MA2019* (2022) 016.
- [135] M. K. Mandal and F. Gasparotto, *On the Application of Intersection Theory to Feynman Integrals: the multivariate case*, *PoS MA2019* (2022) 019.
- [136] S. L. Cacciatori, M. Conti, and S. Trevisan, *Co-Homology of Differential Forms and Feynman Diagrams*, *Universe* **7** (2021), no. 9 328, [[arXiv:2107.14721](#)].
- [137] P. Aluffi and M. Marcolli, *Feynman motives of banana graphs*, *Commun. Num. Theor. Phys.* **3** (2009) 1–57, [[arXiv:0807.1690](#)].
- [138] M. Marcolli, *Motivic renormalization and singularities*, *Clay Math. Proc.* **11** (2010) 409–458, [[arXiv:0804.4824](#)].
- [139] T. Bitoun, C. Bogner, R. P. Klausen, and E. Panzer, *Feynman integral relations from parametric annihilators*, *Lett. Math. Phys.* **109** (2019), no. 3 497–564, [[arXiv:1712.09215](#)].
- [140] R. N. Lee and A. A. Pomeransky, *Critical points and number of master integrals*, *JHEP* **11** (2013) 165, [[arXiv:1308.6676](#)].

- [141] M. Kreuzer and L. Robbiano, *Computational Commutative Algebra 1*. Computational Commutative Algebra. Springer Berlin Heidelberg, 2008.
- [142] K. Matsumoto, *Intersection numbers for logarithmic  $k$ -forms*, *Osaka J. Math.* **35** (1998), no. 4 873–893.
- [143] C. G. Papadopoulos, D. Tommasini, and C. Wever, *The Pentabox Master Integrals with the Simplified Differential Equations approach*, *JHEP* **04** (2016) 078, [arXiv:1511.09404](#).
- [144] T. Gehrmann, J. M. Henn, and N. A. Lo Presti, *Analytic form of the two-loop planar five-gluon all-plus-helicity amplitude in QCD*, *Phys. Rev. Lett.* **116** (2016), no. 6 062001, [arXiv:1511.05409](#). [Erratum: *Phys. Rev. Lett.*116,no.18,189903(2016)].
- [145] L. Mattiazzi, *Multiparticle scattering amplitudes at two-loop (Master thesis, Univ. of Padua, 2018)*, .
- [146] F. Gasparotto, *A modern approach to Feynman integrals and differential equations (Master thesis, Univ. of Padua, 2018)*, .
- [147] D. Chicherin, T. Gehrmann, J. M. Henn, N. A. Lo Presti, V. Mitev, and P. Wasser, *Analytic result for the nonplanar hexa-box integrals*, [arXiv:1809.06240](#).
- [148] K. J. Larsen and Y. Zhang, *Integration-by-parts reductions from unitarity cuts and algebraic geometry*, *Phys. Rev.* **D93** (2016), no. 4 041701, [arXiv:1511.01071](#).
- [149] A. Primo and L. Tancredi, *On the maximal cut of Feynman integrals and the solution of their differential equations*, *Nucl. Phys.* **B916** (2017) 94–116, [arXiv:1610.08397](#).
- [150] S. Badger, H. Frellesvig, and Y. Zhang, *A Two-Loop Five-Gluon Helicity Amplitude in QCD*, *JHEP* **12** (2013) 045, [arXiv:1310.1051](#).
- [151] A. V. Smirnov, *FIRE5: a C++ implementation of Feynman Integral REduction*, *Comput. Phys. Commun.* **189** (2015) 182–191, [arXiv:1408.2372](#).
- [152] T. Becher and M. Neubert, *On the Structure of Infrared Singularities of Gauge-Theory Amplitudes*, *JHEP* **06** (2009) 081, [arXiv:0903.1126](#). [Erratum: *JHEP* 11, 024 (2013)].
- [153] T. Becher and M. Neubert, *Infrared singularities of QCD amplitudes with massive partons*, *Phys. Rev. D* **79** (2009) 125004, [arXiv:0904.1021](#). [Erratum: *Phys.Rev.D* 80, 109901 (2009)].
- [154] R. J. Hill, *Effective field theory for large logarithms in radiative corrections to electron proton scattering*, *Phys. Rev. D* **95** (2017), no. 1 013001, [arXiv:1605.02613](#).